AN ABSTRACT OF A DISSERTATION

LOSS OF LIFE OF MEDIUM VOLTAGE OIL-IMMERSED CURRENT TRANSFORMERS UNDER THERMAL ACCELERATED AGEING

Diego M. Robalino Vanegas

Doctor of Philosophy in Engineering

The energy market faces great challenges derived from de-regulation process in North America. Operators are encouraged to minimize costs of operation while still keeping high indices of reliability and safety. Therefore, it is paramount for electrical operators to identify the best available tools to monitor and / or diagnose the condition of High-Voltage serial components within the electrical infrastructure, whether related to generation, transmission, or distribution of electrical energy.

Among High-Voltage serial components, High and Medium Voltage Current Transformers are seemingly simple electrical devices used for measurement and protection of other major electrical equipment and systems although their own protection has been disregarded so far. There is a growing interest in these components because their failure caused by electro-thermal breakdown of the high-voltage insulation may result in explosions whose intensity can damage nearby electrical apparatus, contaminate the surrounding soil, and cause serious injuries to on-site personnel.

This research work specifically investigates the ageing characteristics of Medium Voltage Oil-Immersed Current Transformers of the measurement type typically used in substations and proposes the use of thermal accelerated aging techniques by means of non-typical load profiles above rated specifications to age the combined insulation system and trace this aging process through state-of-the-art testing methods, capable of identifying changes in the physical, chemical, and dielectric properties of liquid and solid insulation.

The project started with the consideration of all factors involved in the aging process of the combined insulation. In this process, Pyrolysis was found to be the main one, which led the project into setting-up an experiment to replicate the thermal effect on the insulation system. A variety of sensors were strategically embedded in the Current Transformer to provide online information of the temperature variations on the transformer's hottest-spot within the insulation system. The thermal behavior turned out to be different for each type of Current Transformer, therefore, each type was independently modeled and its characteristics laid out.

Later on the research moved onto tracking the aging process and building the aging model by using electrical DC and AC techniques, dissolved in oil gas analysis, furanic compound concentration, and degree of polymerization. In particular, results showed the relevance of the furanic concentration for determining the life of the Current Transformer.

The final stage involved comparing the obtained values with previously published data and models. The results provided new models which, depending on the construction of the Current Transformer, can be used to estimate the age of the unit. The analysis of data determined that normal insulation life of Medium Voltage Oil-Immersed Current Transformers can go beyond standard limits to up to approximately 200,000 hours under a thermal acceleration factor equal to one.

LOSS OF LIFE OF MEDIUM VOLTAGE OIL-IMMERSED CURRENT TRANSFORMERS UNDER THERMAL ACCELERATED AGEING

A Dissertation

Presented to

The Faculty of the Graduate School

Tennessee Technological University

By

Diego M. Robalino Vanegas

In Partial Fulfillment

Of the Requirements of the Degree

DOCTOR OF PHILOSOPHY

Engineering

August 2009

ProQuest LLC
789 East Eisenhower Parkway
P.O. Box 1346
Ann Arbor, MI 48106-1346

CERTIFICATE OF APPROVAL OF DISSERTATION

LOSS OF LIFE OF MEDIUM VOLTAGE OIL-IMMERSED CURRENT TRANSFORMERS UNDER THERMAL ACCELERATED AGEING

By

Diego M. Robalino Vanegas

Graduate Advisory Committee:

_____	_____
Satish Mahajan, Chairperson	Date
_____	_____
Arun Sekar	Date
_____	_____
Ghadir Radman	Date
_____	_____
Sastry Munukutla	Date
_____	_____
David Smith	Date

Approved for the Faculty:

_____

Francis Otuonye
Associate Vice President for Research
and Graduate Studies

_____

Date

DEDICATION

I dedicate this dissertation work to my beloved wife Tatiana, whose charisma, love and strength inspire each and every day of my life; and, also to my daughters Cristina Elizabeth and Kathy Alexandra; they are my pride, my life and my passion.

ACKNOWLEDGEMENTS

First of all, I would like to thank God for giving me health, peace of mind, physical and spiritual strength to overcome all challenges faced during this stage of my academic development.

I would like to express my sincere and endless gratitude to Dr. Satish M. Mahajan, Chairperson of my Advisory Committee, for giving me this wonderful research project, for his confidence in my technical and academic abilities, for the many hours he spent supporting this research work, for his guidance, patience and encouragement during the entire path towards this final dissertation work.

I am deeply grateful to Dr. Arun Sekar, Dr. Sastry Munukutla, Dr. Ghadir Radman and Dr. David Smith for serving as members of my Advisory Committee, for their comments, recommendations and suggestions to the excellence of this work.

I emphasize my deep sense of gratitude to the Center for Energy Systems Research (CESR) for providing financial assistance throughout my Doctoral Program and to CESR's staff, Dr. Sastry Munukutla (Director), Sandra Garrison, Linda Lee, Etter Saggs, Tony Greenway and Robert Craven for their always friendly and professional support.

I take this opportunity to thank Dr. Stephen Parke, Chairperson of the Electrical and Computer Engineering (ECE) Department and all the faculty members who shared their knowledge throughout the various courses taken at Tennessee Technological University. I would also like to thank my classmates and friends for their support and motivation during this unique experience.

Finally, I would like to give special thanks to my father Miguel Angel (passed away), mother Maria Alicia, grandmother Marinita (passed away), sister Gladys Alicia and in-laws Alexander, Lyudmila, Vera and Oleg for their unconditional love, prayers and encouragement.

TABLE OF CONTENTS

Page

Page

Page

Page

LIST OF FIGURES

Page

Page

Page

Page

Page

Page

LIST OF TABLES

Page

Page

Page

CHAPTER 1

INTRODUCTION

1.1 Motivation for the Research Work

The Department of Energy (DOE) and the Tennessee Valley Authority (TVA), responsible and accountable for the reliability and security of Electric Energy Generation and Transmission in the State of Tennessee, have been concerned about the continuous growth of load and the reduced alternatives for physical upgrades of the system. Therefore, it is necessary to optimize performance of the existing equipment and provide additional operational alternatives for the utilities. Power lines are congested and the construction of new power corridors faces several challenges such as: right of way acquisition, planned power outages for system upgrades or maintenance, and equipment limiting ratings. The electrical industry, whether committed with the Generation, Transmission, or Distribution of Electrical Energy for public consumption, considers imperative the analysis of limiting factors for the operation of Transmission and Distribution systems under overloading conditions.

Overloading the Transmission and Distribution systems is one of the alternatives to compensate the existing imbalance between the growing electric power demand and the construction of new systems. It can also provide an alternative to optimize the use of installed existing assets and a base of study for practical solutions in the short and long term.

Electrical equipment is usually manufactured to withstand load levels that are slightly greater than the normal operating conditions. As a matter of fact, normal operation of electric power systems

includes overload operation due to Planned Loading beyond Nameplate (PLBN), Long-Time Emergency loading (LTE), and Short-Time Emergency loading (STE).

Current Transformers (CT) are Instrument Transformers intended to have their primary winding connected in series with the conductor carrying the current to be measured or controlled [1]. The proper application of current transformers within the electrical system implies the consideration of specific constructive requirements depending on the location for installation, surrounding environment, expected electrical and mechanical stresses to which the unit will be subjected. Great importance is given to the type of insulation (dry, liquid, or gas). The high voltage insulation, protecting the unit from breakdown during operation, must fully comply with the purpose of the device during the entire expected life of the unit.

"The life of a transformer is the life of the insulation and the life of the insulation is a controllable factor [2]."

The sentence above applies to all types of transformers: power, distribution, and instrument transformers that are affected by several internal and external factors capable of gradual degradation of the insulation. Under normal operating conditions, transformers are expected to remain in service for at least twenty years. The effect of loading beyond nameplate rating is described in depth in [3]. Nevertheless, IEEE Standard C57.91-1995 is mainly focused on 65° temperature rise insulation system used in distribution (Clause 8 of [3]) and power transformers (Clause 9 of [3]). Instrument Transformers used for this research work were built using 55° temperature rise insulation system and according to the general specification of [1]. The loading of transformers without thermally upgraded insulation (from an insulation ageing point of view) can be considered to be similar to transformers with thermally upgraded insulation (Appendix D of [3]).

Current Transformers are critical components of the electric power system. These electrical devices protect major electrical equipment from failure although they are not protected themselves. It is inevitable to operate Transmission and Distribution lines beyond nameplate ratings and the service condition of these devices is to be affected. Nevertheless, there is no general recommendation for loading 55°C temperature rise mineral-oil-immersed instrument transformers; neither has been proposed a model to estimate the age and loss of service life of this type of devices. The solution of this problem is interesting and pertinent nowadays.

1.2 Differences between this Research Work and Related Research

The subject of high voltage insulation is wide in content, covering areas of theory and experimental studies as well as technical and industrial applications. There is a vast amount of work published about loading guidelines, ageing estimation, and loss-of-life quantification for power and distribution transformers. This is because power transformers are one of the most expensive components of the electrical infrastructure and their failure involves power supply shortages, overloading of back-up units (if available), possible explosion, and contamination of the neighboring area. For these expensive units a series of testing procedures and condition assessment practices have been put in place. In addition, expensive remote and local monitoring devices, such as Top Oil Temperature (TOT) sensors, Dissolved Gas Concentration monitors, and pressure gages and sensors are mandatory. Electrical protection is part of the entire electrical system design wherein overvoltage, overcurrent, differential protection, and grounding protection relays are commonly used. Nevertheless, in order to electrically protect critical devices such as power transformers, high-accuracy instrument transformers are used. Current Transformers are not monitored in the field. Their construction does

not foresee installation of temperature or gas sensors and monitors. Therefore, in this work, state-of-the-art technology was used to monitor and test oil-immersed Current Transformers from factory acceptance to end-of-life (service life). This unique work explores all the variables capable of defining the aging process of Oil-Immersed Current Transformers.

The loading characteristics described for power and distribution transformers have been developed mainly based on scaled models where accelerated ageing test were used to determine the deterioration of whether liquid, solid, or composed insulation systems [4-11, 47]. It is a difficult task to bring into a laboratory such an expensive device to stress it up until end-of-service life. In this work, the experimental units were custom built for this research work so that the sensors strategically installed in the unit allowed a real-time reading of the temperature. Therefore, the test is based on real units under thermal accelerated ageing conditions, where the need of estimating TOT or Hot-Spot Temperature (HST) was avoided.

The work subject of this dissertation is unique in the way that tests were carried out from factory to end-of-life at different loading levels and different ageing stages without reclaiming or changing the liquid insulation. Most of the existing work related to ageing characteristics of current transformers does not have a historic trend of tests the same way it is to be described throughout this dissertation. Moreover, critical values are given in generic expressions that may not be applicable to instrument transformers. Condition assessment is based in this work on typical values more than critical values as addressed by other investigators [12] by developing a health index factor that finally is correlated to the chronological life of a transformer instead of the thermally calculated life or equivalent age based on ANSI/IEEE standards.

The work involves real devices instead of specifically fabricated models and provides a realistic approach to the loss-of-life evaluation not only by thermal parameters but also as a

cumulative consensus of other applicable technologies used for condition assessment and diagnostics of high voltage composite insulation systems of oil-immersed transformers.

1.3 Scope of the Research Work

This research work is limited to the application of Thermal Accelerated Ageing Procedures on 69kV Oil-Immersed Current Transformers (COF-350) of the Measurement Type with 55°C temperature rise insulation system. However, it can be applied to CTs and other devices having similar designs especially in the medium voltage range. Specific nameplate data of the experimental units are described in Chapter 4, Table 14.

The units are subjected to the locally available testing equipment to assess the condition of the experimental units throughout the ageing process. The tests carried out are limited to the following:

- DC Tests
    - Insulation Resistance
    - Polarization Index
    - Step Voltage Test
- AC Test
    - Dielectric Breakdown
    - Capacitance, Power Factor, Dissipation Factor (tan δ)

- Functional Test, including: burden measurement, winding resistance measurement, excitation characteristic recording, ratio measurement with consideration of connected burden and knee point VI curve. All tests were carried out in compliance with IEEE Std C57.13-1993.

- Specific Tests
  - Online Dissolved Gas Analysis
  - Furanic Compound Analysis (at DOBLE Engineering Laboratories)
  - Degree of Polymerization (at DOBLE Engineering Laboratories)

The research work was carried out at the High-Voltage / High-Current Laboratory at Tennessee Technological University from 2007 to 2009. The scope of the work includes the analysis of chemical, thermal, and dielectric characteristics of Oil-Immersed Current Transformers of the measurement type in the course of the thermal stress applied to these units, considering temperature to be the main enemy of the insulation system.

1.4 Contribution of Research

This research work explored a series of alternatives to define the ageing model of 69kV Oil-immersed Current Transformers and a possible common pattern between 1200:5 and 200:5 units which are very similar in construction of the secondary winding and insulation system with the difference in the primary winding size and construction.

From the alternatives explored, revised equations provide a better understanding of the thermal behavior of Oil-Immersed Current Transformers at normal operating levels and under extreme conditions. Results obtained provide a very good match between modeled and experimental results. The model shows the differences between both units and different factors were provided for each specific rating unit.

In addition, this research work captures the ageing process at different life intervals. The use of DC, AC, DGA, 2FAL and DP testing techniques in current transformers is unique and has not been presented in a chronological path as in this work. No one has previously been able to explore the changes in dielectric properties, physical and chemical composition of current transformers at this level.

Results obtained from the testing techniques were evaluated and ageing equations for Oil-Immersed Current Transformers are provided in the base of statistically significant variables.

In a final stage, it has been observed that normal insulation life of high and medium voltage oil-immersed current transformers goes beyond the stipulated values according to IEEE standards and it could be expected to be approximately 200,000 hours at an ageing acceleration factor equal to one.

1.5 Dissertation Organization

This dissertation compiles theoretical and experimental information. This final document has been arranged as follows:

Chapter 2 provides the fundamental concepts related to ageing of high voltage insulation systems in oil-immersed transformers. Concepts of ageing, loss-of-life, transformer thermal models, and formulae to quantify the remaining service life based on IEEE Standards are presented here.

Chapter 3 is a detailed literature review of the existing state-of-the-art technologies and testing techniques used to carry out High-Voltage insulation system condition assessment. Polarization De-polarization Current, Return Voltage Measurement, and Partial Discharge are not included.

Chapter 4 summarizes the experimental work carried out with CT1, CT2, CT3, and CT4. A complete description of the experimental setup and its components, thermal modeling results, ageing process of the units and obtained results, interpretation of test results, correlation with loss-of-life criterion DP 200, is presented, analyzed, and discussed.

Chapter 5 describes the statistical analysis of the experimental data obtained during the ageing process. Identified statistically significant variables are used to model Ageing of Oil-Immersed Current Transformers.

Chapter 6 provides conclusions and outcomes of this research work as well as recommendations for future research in this area.

CHAPTER 2

FUNDAMENTAL CONCEPTS

2.1 Background

An important aspect of the technology of dielectrics is ageing, especially under thermal and electrical stress in the context of electrical insulation [13]. Ageing[1] is an irreversible process applicable to all existing materials, substances and organisms known on the surface of the earth. A very comprehensive understanding of this concept is presented by T. J. Lewis [14]. In this publication ageing is defined as a gradual change of state and property that usually leads to a degree of malfunction and the ultimate failure, or at least an unacceptable loss of efficiency of an engineered element. *"The primal process in all cases is that the chemical and physical bonds between the atoms of the substance are repeatedly broken, reorganized and reformed in new configurations. Ageing is chemical kinetics."*

Two failure-modes have been typically observed in Oil-Immersed Current Transformers [15]:

- Electrical Breakdown or Ionization[2]-mode. Occurring predominantly under low temperature atmosphere conditions. Typically happen on the toroid shape design and are caused by de-impregnation of the condenser core, ingress of air and over-saturation.
- Thermal Breakdown or Ageing-mode. Failures occurred after 15-20 years of service also referred to as hot failures caused by increased losses, followed by thermal runaway and

[1] (Thermal classification of electric equipment and electrical insulation). The irreversible change (usually degradation) that takes place with time [16] .
[2] (outdoors apparatus bushings) The formation of limited avalanches of electrons developed in insulation due to an electric field.

subsequent ionization process. Ageing of the oil-paper bulk and localized moisture contamination have been observed as the most probable life-limiting factor.

In the context of this chapter, the fundamental concepts of the ageing process of power and distribution transformers are summarized. Moreover, the ageing factors affecting the life of the transformer are independently described and the Loss-of-Life criterion is introduced.

2.2 Ageing – Degradation of Transformer Insulation

Considering ageing to be a consequence of chemical kinetics, it is understood that there should be internal and/or external factors capable of accelerating or slowing down aging process. Of course, the factors to be contemplated are those whose effect on time is irreversible and lean towards breakdown of the insulation system, failure of the equipment, and subsequent removal from operation.

No insulation is perfect and it begins to degrade as soon as the device is put in operation or even before that during the manufacturing process. Similarly, as a consequence of acceptance tests (factory, commissioning, start-up, maintenance, etc.), the unit will stress therefore, deteriorate the insulation. Ageing of solid insulation is always in association with ageing of liquid insulation in combined insulation systems as it is the case of study. As insulation degrades, leakage current increases as a function of time; this modifies the dielectric loss characteristic and the degree of polarization of the material.

Insulation deterioration occurs on a power system when insulators are subjected to abnormal stresses and the final effect is the failure or breakdown of electrical apparatus. The fundamental factors interacting with each other and causing insulation degradation [17 – 19] are summarized in Fig. 1.

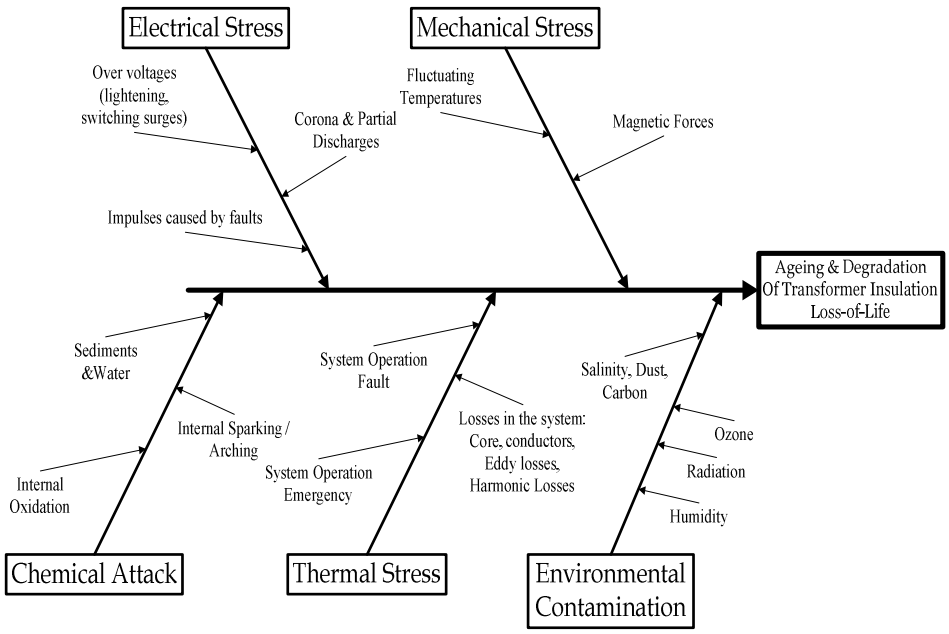

Fig. 1. Cause and Effect Diagram - Ageing Factors

2.2.1 Electrical Stress

Every piece of electrical equipment is designed and rated for a specific voltage application. Electrical stress comes in to play due to high voltage gradient, voltage surges, phase to ground faults, corona discharges, partial discharges, arcing with ground, or between phases and harmonics. High electric stress can accelerate the process of deterioration and chemical changes may take place.

When a high voltage is applied to any insulation material, the surface micro irregularities become traps in this material that will be filled up with fast or slow charges. Slow or trapped charges may cause adverse effect on the performance of the insulation [19]; thus, service life reduction. With increasing voltage and frequency, corona effects generate partial discharge (PD) phenomena [20, 21]. This partial discharge type of stress is not part of the scope of this research work.

2.2.2 Mechanical Stress

Mechanical stress arises due to moving parts in the electrical machinery, centrifugal forces, magnetic forces, vibration, and as a result of fluctuating temperature in winding with changes in load and differential expansion due to difference in thermal coefficient of components giving rise to abrasion [14, 19]. The magnitudes of the vibratory mechanical stresses produced by normal load current are insignificant when compared to those produced by system short-circuit currents [5]. The primary cause of transformer failure as the result of a short circuit is not because of the thermal damage of the insulation but rather the mechanical forces produced in the windings [2].

Thus, vibration in transformers radiates acoustical energy which is the nature of noise[3] which is continuous and largely confined to the medium range of audio frequencies disagreeable for the human ear [22]. Transportation of electrical equipment and its manipulation prior to installation might also produce lose contacts in the interior of the devices. This type of stress is typical in big power and sub-station type distribution transformers, because of the size of instrument transformers; these devices are not greatly affected by the mechanical stress.

2.2.3 Chemical Attack and Environmental Contamination

Effectiveness of insulation could also be affected by the external and/or internal corrosion, oil sediments and moisture. For units with liquid-solid insulation, it is imperative to determine the dielectric oil parameters separately; this will help define future ageing characteristics exclusive of the solid insulation or the oil itself [19]. Physical-chemical analysis and gas chromatography of the dielectric oil are typical tests adopted in the industry. Exposure to humidity (moisture), radiation,

[3] Sound which is undesired by the recipient – IEC 60050-801:1994, Glossary of Electrotechnical terms.

oxidation, ozone, salinity, chemical fumes, dust and carbon are some of the reasons for environmental stress.

2.2.4 Thermal Stress

As observed in Fig. 1, there are several factors that could bring an electrical device to a failure condition. With proper maintenance procedures in place and using oil preservation systems, moisture and oxygen presence can be minimized through dielectric oil dry-out or reclamation, leaving temperature as the major controlling parameter.

Thermal stress is produced in the active part of the transformer because of the electric load losses in the conductors, core losses due to hysteresis and eddy current, dielectric heating due to dipole movement, partial discharge activity, harmonic losses, and insulation defects. Generally insulating materials are poor conductors of heat which aggravates the problem further. Temperature distribution inside the transformer is not uniform and the hottest spot location is usually unpredictable and needs to be identified as this is the weakest point of the insulation system.

2.3 Thermal Ageing Principles

In 1948, Dakin defined insulation ageing rates by recognizing that ageing of cellulose is the result of a chemical reaction [3]; therefore, the property changes can be expressed through a constant K_0, which can be mathematically expressed as

$$K_0 = A' \cdot \exp^{\left[\frac{B}{\theta+273}\right]} \tag{2.1}$$

where

A′ and B – are empirical constants. B is the ageing rate constant for which a value of 15,000 is considered appropriate [3].

θ – is the temperature of insulation in °C.

The Dakin relationship is also known as the Arrhenius reaction rate equation and is widely accepted within the technical and scientific community. According to IEEE Std. 57-91-1995, for 65°C average winding temperature rise insulation systems, or usually called, thermally upgraded insulation, the ageing equations are

$$Per \quad unit \quad life = A \cdot \exp^{\left[\frac{B}{\theta_H + 273}\right]} = 9.80 \times 10^{-18} \cdot \exp^{\left[\frac{15000}{\theta_H + 273}\right]} \tag{2.2}$$

where

A - is the modified per unit constant, derived from the selection of 110 °C as the temperature established for “one per unit life” on 65°C temperature rise insulation systems.

B - is the same aging rate slope as in equation (2.1).

The reference hottest-spot temperature (θ_H) is 110 °C for 65 °C average winding rise (with thermally upgraded insulation). This value results from the addition of: reference ambient temperature of 30 °C, average winding rise of 65 °C and a hot-spot temperature allowance of 15 °C. The reference hottest-spot temperature (θ_H) is 95 °C for 55 °C average winding rise transformers (without thermally upgraded insulation). This value results from the addition of: reference ambient temperature of 30 °C, average winding rise of 55 °C and a hot-spot temperature allowance of 10 °C.

Ageing Acceleration Factor is found as

$$F_{AA} = \exp^{\left[\frac{15000}{383} - \frac{15000}{\theta_H + 273}\right]} \tag{2.3}$$

Equivalent Ageing Factor for the total life period is given as

$$F_{EQA} = \frac{\sum_{n=1}^{N} F_{AA_n} \cdot \Delta t_n}{\sum_{n=1}^{N} \Delta t_n} \tag{2.4}$$

Moreover, under the same standard in Appendix D and its Corrigendum 1 of 2002 [3], for transformers with 55°C average winding temperature rise insulation systems with a rated hottest-spot rise over ambient temperature of 65°C and a 30°C ambient, the reference temperature is 95°C, consequently, the ageing equations are

$$Per \quad unit \quad life = A \cdot \exp^{\left[\frac{B}{\theta_H + 273}\right]} = 2.00 \times 10^{-18} \cdot \exp^{\left[\frac{15000}{\theta_H + 273}\right]} \tag{2.5}$$

The Ageing Acceleration Factor is found as

$$F_{AA} = \exp^{\left[\frac{15000}{368} - \frac{15000}{\theta_H + 273}\right]} \tag{2.6}$$

The expression for the Equivalent Ageing Factor for the total life period is the same as (2.4). The percent loss of insulation life in the time period is equivalent to the hours of life consumed divided by the total normal insulation life (NIL). IEEE Std. 57.91 provides NIL criterions based on retained tensile strength[4] of insulation and degree of polymerization (DP). For the sake of reference, throughout the research work, NIL has been adopted based on the criterion of DP = 200 with estimated 150,000 hours of total service life. Therefore, percentage Loss-of-Life is given as

$$\%\ Loss\ of\ Life = \frac{F_{EQA} \cdot t \cdot 100}{NIL} \tag{2.7}$$

The standard does not provide reference information for time durations in hours for continuous operation above rated hottest-spot temperatures for different loss of life values based on a normal life

[4] Tensile strength of paper is the maximum tensile stress developed in a test specimen in a tension test carried to break under prescribed conditions, expressed for thin papers as force per unit original width of the test specimen [79] .

of 150,000 hours for 55°C temperature rise system. The data have been prepared and it is presented in Appendix A of this dissertation.

2.4 Transformer Thermal Models

In this research work, the formulae nomenclature is identical to that of [3]. Temperatures are indicated by θ and temperature rises by $\Delta\theta$.

2.4.1 Related Nomenclature

C is the thermal capacity of the transformer, $Watt-hours/^{\circ}C$

EXP is 2.71828 (base of natural logarithm)

I_R is rated current

K is the ratio of load L to rated load, per unit

L is the load under consideration, kVA or amperes

m is an empirically derived exponent used to calculate the variation of $\Delta\theta_H$ with changes in load depending on the cooling mode to account for effects of changes in resistance and viscosity

n is an empirically derived exponent used to calculate the variation of $\Delta\theta_{TO}$ with changes in load

$P_{T,R}$ is the total loss at rated load, watts

R is the ratio of load loss at rated load to no-load loss on the tap position to be studied

t is the duration of load, hours

θ is temperature, °C

θ_A is the average ambient temperature during the load cycle to be studied, °C

$\theta_{A,R}$ is the average ambient temperature at rated load, °C

θ_H is the winding hottest-spot temperature, °C

$\theta_{H,R}$ is the winding hottest-spot temperature at rated load, °C

$\theta_{H,U}$ is the ultimate winding hottest-spot temperature for load L, °C

θ_{TO} is the top-oil temperature, °C

$\Delta\theta_H$ is the winding hottest-spot rise over top-oil temperature, °C

$\Delta\theta_{H,i}$ is the initial winding hottest-spot rise over top-oil temperature for $t = 0$, °C

$\Delta\theta_{H,R}$ is the winding hottest-spot rise over top-oil temperature at rated load on the tap position to be studied, °C

$\Delta\theta_{H,U}$ is the ultimate winding hottest-spot rise over top-oil temperature for load L, °C

$\Delta\theta_{H/A,R}$ is the winding hot spot rise over ambient at rated load on the tap position to be studied, °C

$\Delta\theta_{TO}$ is the top-oil rise over ambient temperature, °C

$\Delta\theta_{TO,R}$ is the top-oil rise over ambient temperature at rated load on the tap position to be studied, °C

$\Delta\theta_{TO,i}$ is the initial top-oil rise over ambient temperature for $t = 0$, °C

$\Delta\theta_{TO,U}$ is the ultimate top-oil rise over ambient temperature for load L, °C

τ_{TO} is the oil time constant of transformer for any load L and for any specific temperature differential between the ultimate top-oil rise and the initial top-oil rise

$\tau_{TO,R}$ is the time constant for rated load beginning with initial top-oil temperature rise of 0°C, hours

τ_W is the winding time constant at hot spot location, hours

2.4.2 Hot-Spot and Top-Oil Temperature

The hottest-spot temperature (HST) is defined as the highest temperature inside the transformer winding. It is greater than the measured average temperature of the coil conductors [16] . It consists of three components and is defined in [3] by

$$\theta_H = \theta_A + \Delta\theta_{TO} + \Delta\theta_H \tag{2.7}$$

Equations follow the nomenclature introduced in 2.4.1. Top-oil temperature (TOT) is given by the expression

$$\theta_{TO} = \theta_A + \Delta\theta_{TO} \tag{2.8}$$

At this stage it is important to describe what rated values mean for the thermal models. Rated thermal current is the root-mean square current in amperes which the device is rated to carry under standard operated conditions for rated time without exceeding temperature limits [16]. A load variation derives in temperature changes where the initial value is considered at time t=0 and the ultimate value is considered at the point where temperature has reached steady values or said in other words, the process has reached thermal equilibrium $\left(\frac{dT}{dt} = 0\right)$.

After a step load change, TOT rise is given as

$$\Delta\theta_{TO} = \left(\Delta\theta_{TO,U} - \Delta\theta_{TO,i}\right)\cdot\left(1 - EXP^{\frac{1}{\tau_{TO}}}\right) + \Delta\theta_{TO,i} \tag{2.9}$$

where

$$\Delta\theta_{TO,U} = \Delta\theta_{TO,R} \cdot \left[\frac{\left(K_U^2 R + 1\right)}{R+1} \right]^n \tag{2.10}$$

For self cooled (OA) units, the thermal capacity is given as

$$\begin{aligned} C = {} & 0.0272\left(\text{weight of core and coil assembly in Kg}\right) \\ & + 0.01814\left(\text{weight of tank \& fittings in Kg}\right) \\ & + 5.034\left(\text{liters of oil}\right) \end{aligned} \tag{2.11}$$

Once the thermal capacity of the transformer is obtained, the top-oil time constant at rated load can be calculated as

$$\tau_{TO,R} = \frac{C \cdot \Delta\theta_{TO,R}}{P_{T,R}} \tag{2.12}$$

The top-oil time constant is then defined as

$$\tau_{TO} = \tau_{TO,R} \cdot \frac{\left(\frac{\Delta\theta_{TO,U}}{\Delta\theta_{TO,R}}\right) - \left(\frac{\Delta\theta_{TO,i}}{\Delta\theta_{TO,R}}\right)}{\left(\frac{\Delta\theta_{TO,U}}{\Delta\theta_{TO,R}}\right)^{1/n} - \left(\frac{\Delta\theta_{TO,i}}{\Delta\theta_{TO,R}}\right)^{1/n}} \tag{2.13}$$

If n is equal to 1.0, 63% of the temperature change occurs in a length of time equal to the time constant regardless of the relationship of initial temperature rise and ultimate temperature rise. If n is not unity, the temperature change in a similar time interval will be different, depending on both initial temperature rise and ultimate temperature rise.

The winding hottest-spot temperature rise over TOT in its transient form is given by an equation similar to (2.9) as follows:

$$\Delta\theta_H = \left(\Delta\theta_{H,U} - \Delta\theta_{H,i}\right) \cdot \left(1 - EXP^{\frac{1}{\tau_W}}\right) + \Delta\theta_{H,i} \tag{2.14}$$

The initial hot-spot temperature (HST) rise over TOT is given by

$$\Delta\theta_{H,i} = \Delta\theta_{H,R} \cdot K_i^{2m} \tag{2.15}$$

The ultimate HST rise over TOT is given by

$$\Delta\theta_{H,U} = \Delta\theta_{H,R} \cdot K_u^{2m} \tag{2.16}$$

The HST rated value over TOT is given by

$$\Delta\theta_{H,R} = \Delta\theta_{H/A,R} - \Delta\theta_{TO,R} \tag{2.17}$$

As indicated in the Standard of the reference [3], $\Delta\theta_{H/A,R}$ and $\Delta\theta_{TO,R}$ may be determined by actual test in accordance with IEEE Std C57.12.90-1993. Also, for type OA cooling systems, the standard suggests the following values for the empirically defined exponents:

$$\begin{cases} m = 0.8 \\ n = 0.8 \end{cases}$$

2.4.3 Top-Oil Temperature Model (TOTM)

A typical thermal model of a transformer can be thought of as two models working in series: a top oil temperature (oil to air) model and a hot-spot temperature (winding to oil) model.

The IEEE model is based on the following differential equation [3, 22 – 24]:

$$\tau_{TO,R} \frac{d\Delta\theta_{TO}}{dt} = -\Delta\theta_{TO} + \Delta\theta_{TO,U} \tag{2.18}$$

Substituting (2.10) in (2.18), using Euler's forward approximation, and discretizing (2.18) lead to:

$$\Delta\theta_{TO}[t] = K_1 \Delta\theta_{TO}[t-1] + K_2 (I[t])^{2n} \tag{2.19}$$

where K_1 and K_2 are parameters to be determined for a specific transformer, I(k) is the sample load current and k is the time step index.

Equations (2.8) and (2.19) represent IEEE model for estimation of TOT where ambient temperature (θ_A) is assumed constant.

A dynamic variation in the ambient temperature was then included in the IEEE model by Lesieutre et al. [25]. In addition, conditioning the model to n=1 (for directed FOA or FOW cooling system), the TOT could be estimated from the following equation [26, 27].

$$\theta_{TO}[t] = K_1\theta_{TO}[t-1] + (1-K_1)\theta_A[t] + K_2(I[t])^2 + K_3 \tag{2.20}$$

The factors K_1, K_2, and K_3 are described in [25] as a function of $\tau_{TO,R}$, Δt, R, and $\Delta\theta_{TO,R}$. Further development of (2.20) replacing (1-K_1) by another constant has been suggested in other publications [27], although replacement of $(1-K_1)$ is not required. The resulting equation (2.20) is given as the Top-Oil Temperature Model.

2.4.4 Oil-to-Air Model or Modified Top-Oil Temperature Model (MTOTM)

Using thermal-electrical analogy, a model that includes lumped thermal capacitance (C_{oil}) and thermal resistance (R_{oil}) was proposed [28, 29]. The differential equation pertaining to this model is given by

$$q_{fe} + q_{cu} = C_{oil}\frac{d\theta_{TO}}{dt} + \frac{1}{R_{oil,R}}(\theta_{TO} - \theta_A)^{1/n} \tag{2.21}$$

where

q_{fe} is the heat generated by iron losses

q_{cu} is the heat generated by copper losses

C_{oil} is the thermal capacitance of the oil

$R_{oil,R}$ is the thermal resistance of the oil under rated conditions.

By defining

$$\tau_{TO} = R_{oil,R} C_{oil},$$

$\Delta\theta_{TO,R} = \theta_{TO,R} - \theta_A$ and; $\beta = q_{Cu} / q_{Fe}$, at the rated load, Equation (2.10) becomes

$$\frac{K^2\beta + 1}{\beta + 1}\left(\Delta\theta_{TO,R}\right)^{\frac{1}{n}} = \tau_{TO,R}\frac{d\theta_{TO}}{dt} + \left(\theta_{TO} - \theta_A\right)^{\frac{1}{n}} \tag{2.22}$$

The differential equation corresponding to (2.22) is given by

$$\Delta\theta_{Top} = \frac{\Delta t}{\tau_{TO,R}}\left[\frac{K^2\beta + 1}{\beta + 1}\left(\Delta\theta_{TO,R}\right)^{\frac{1}{n}} - \left(\theta_{TO} - \theta_A\right)^{\frac{1}{n}}\right] \tag{2.23}$$

Parameters $\tau_{TO,R}$, $\Delta\theta_{TO,R}$, and n can be determined by using a nonlinear least square technique for the temperature data.

2.4.5 Hot-Spot Temperature Model (HSTM)

An equation corresponding to hot-spot temperature model could be obtained in a manner similar to that for top-oil temperature model [22 – 24]. The HST could be estimated from the following equation [3, 25 – 27]:

$$\theta_H[t] = K_1\theta_H[t-1] + (1 - K_1)\theta_{TO}[t] + K_2\left(I[t]\right)^{2m} + K_3 \tag{2.24}$$

where

$\theta_H[t]$ is the winding hot-spot temperature at time t.

The exponent m depends on the method of cooling. As indicated in 2.4.2, IEEE standard recommends m=0.8 for natural oil cooled system. K_1, K_2, and K_3 are parameters specific to a

transformer design and therefore, identical in TOTM (Eq. 2.20) and HSTM (Eq. 2.24).

2.4.6 Winding-to-Oil Model or Modified Hot-Spot Temperature Model (MHSTM)

A modified hot-spot temperature model was proposed on the lines similar to the modified top oil temperature model [28]. The equation for MHSTM was mentioned in [28] but it was not tested because of the lack of optical sensors in the windings of the transformer [29].

In the modified HSTM model, the surrounding environment is mineral oil, thus θ_{TO} calculated for the oil-to-air model becomes the ambient temperature. MHSTM was derived based on this analogy and is given by

$$\Delta\theta_H = \frac{\Delta t}{\tau_{w,R}}\left\{\frac{K^2\beta+1}{\beta+1}\cdot\left(\Delta\theta_{H,R}\right)^{\frac{1}{m}} - \left(\theta_H - \theta_{TO}\right)^{\frac{1}{m}}\right\} \tag{2.25}$$

where $\tau_W = R_W \cdot C_W$, and

$\Delta\theta_{H,R} = \theta_{H,R} - \theta_{TO,R}$, at the rated load.

C_w and R_w are the winding thermal capacitance and resistance, respectively, at the rated load. Values of τ_W, $\Delta\theta_{H,R}$, and m can be determined by using a nonlinear least square technique for the temperature data.

2.5 Thermal Breakdown Phenomena

Thermal Breakdown results from disruption of thermal equilibrium within the insulation (dielectric) system. In this case, the rate of heat generation exceeds the cooling properties of the surrounding environment. Temperature may rise continuously leaving the steady state condition and

increasing the dielectric losses. The continuous temperature raise will, at a certain point, set a runaway process leading towards breakdown. Therefore, it is important to understand and review the sources of heat and the construction of current transformers at medium and high-voltage levels from thermal point of view.

2.5.1 Transformer Losses

Medium and High Voltage transformers are built considering a minimum energy loss design. Apart from the core loss, the load loss begins when the transformer is loaded and increases with the square of the load that the transformer sees. The energy losses mentioned above turn into heat which has to be dissipated in order to prevent temperature rise above the limits defined by the manufacturer and described in IEEE[5], IEC[6], CSA[7], NETA, and BS[8] standards. All these standards provide reference values for winding temperatures and hot spot temperatures to be observed during operation [3 – 22].

The core material generally used by the manufacturers on CTs is high permeability iron or silicon steel. Core material has gone through different stages, from non-oriented silicon steel to cold rolled grain oriented (CRGO) silicon steel. Saturation flux density of CRGO is ~ 2.0 Tesla. Collette et al. [30] assume M4 grain-oriented silicon electrical steel to be the core material used in the same type of oil-immersed current transformers as the experimental units of this research work, with characteristics as shown in Fig. **2** and 3 below.

[5] The IEEE name was originally an acronym for the Institute of Electrical and Electronics Engineers, Inc. Today, the organization's scope of interest has expanded into so many related fields, that it is simply referred to by the letters I-E-E-E (pronounced Eye-triple-E).
[6] International Electrotechnical Commission
[7] Canadian Standard Association
[8] British Standards

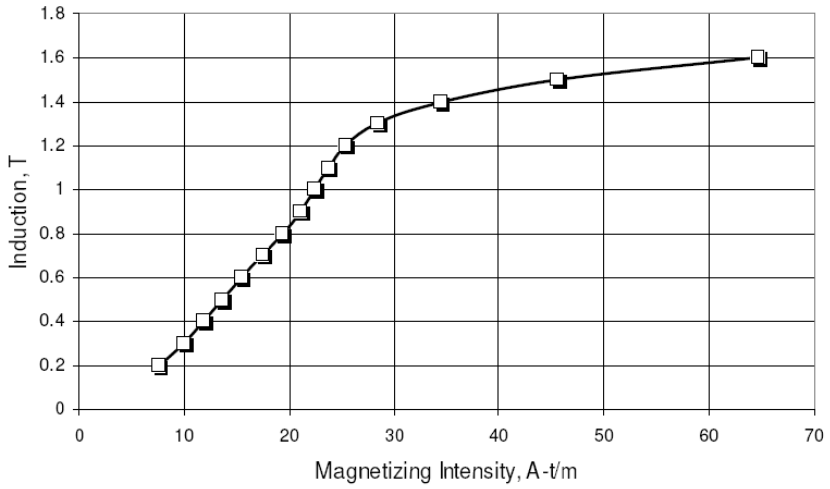

Fig. 2. Magnetization Curve of 0.011" M4 Steel [30]

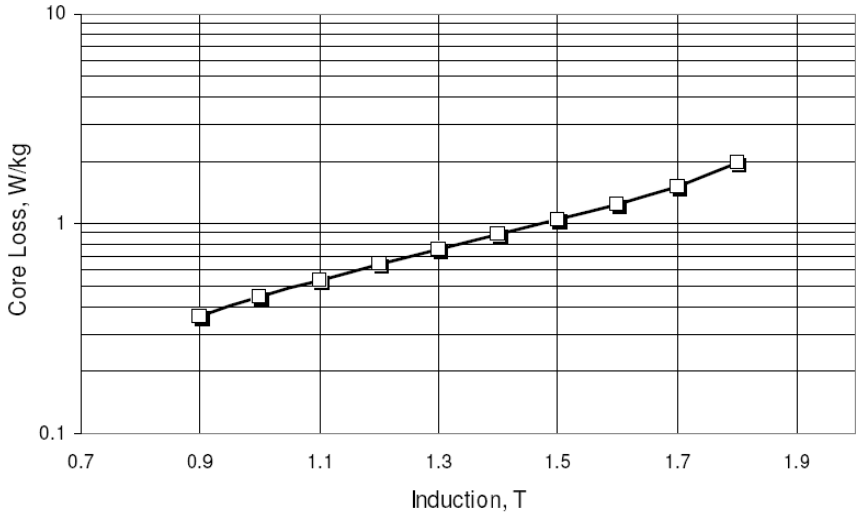

Fig. 3. Loss (Pc) versus Flux Density (B) for 0.011" M4 Steel [30]

The transformer core provides a low reluctance path for the magnetic flux linking primary and secondary windings, experiencing iron losses due to hysteresis and eddy currents which appear as heat from the core. Core losses represent energy loss in any type of transformer; therefore, instrument transformers are not an exception. The core design and the electrical steel used for construction are being investigated by manufacturers and researchers in order to minimize the core losses [31, 33]. There are continuous developments and introductions of better grades of core material. The core material has passed from non-mitred to mitred and then to the step-lap construction. Kulkarni [33]

indicated that better grades of core material reduce core loss and also help in reducing the vibration noise level by a few decibels [33].

Hysteresis loss is proportional to the frequency and dependent on the area of the hysteresis loop and it is defined by the following expression [30, 31]:

$$P_h = k_h f B_{\max}^n \left[Watt/Kg \right] \tag{2.26}$$

The eddy current loss is dependent on the square of the frequency and directly proportional to the square of the thickness of the material. Therefore, Eddy current loss is defined as [22, 31]:

$$P_e = k_e f^2 \frac{B_{eff}^2}{\rho} \left[Watt/Kg \right] \tag{2.27}$$

Or, as defined in [30] [31] :

$$P_e = k_e \left(B_{\max} \cdot f \cdot \delta \right)^2 \left[Watt/Kg \right] \tag{2.28}$$

where

f is the electrical power frequency in Hz,

δ is the skin depth of the core material in meters,

$B_{\max}$ is the maximum flux density in Tesla,

k_h, k_e are the core loss coefficients.

2.5.2 Current Transformer Construction

The two materials that are used most extensively as electric insulation in most of the transformers are Kraft Paper (as the solid insulation) and mineral oil (as the insulating liquid). The most important insulating medium – or dielectric – in the high-voltage equipment is actually neither

the liquid nor the solid. Rather, it is the combination of both materials [2]. Dry paper with low dielectric strength and low permittivity is impregnated with dielectric oil of high strength and permittivity, proper impregnation avoids differences in permittivity within the solid insulation. That way, there are no dry spots on which electrical stress may get enhanced. Both paper material and oil have limits on their dielectric withstand capabilities. Oil dielectric limits are used for the insulation design as this is the weakest material in the combination. The combination of oil soaked paper is a stronger dielectric that would be expected if the dielectric strength of the oil was added arithmetically to the dielectric strength of the paper. A good estimate is that the combination of Kraft Paper and mineral oil dielectric fluid has a dielectric strength that is about 20 to 25% greater than one would expect from just adding the dielectric breakdown strength of the two materials together [2].

Core construction from laminations increases resistance to the flow of eddy currents. The thinner the laminations, the more effective this is. Core losses exist immediately after applying voltage and are a constant value as long as the transformer is energized.

The construction of high-voltage current transformers based on the type of insulation media used is summarized in Table 1.

Table 1. Typical CT Designs for MV / HV Applications

Current Transformer Design	Rated Voltage (kV)													
	5	8.7	15	25	34.5	46	69	115	138	161	230	345	500	765
Outdoor Molded Epoxy, Wound Type			✓	✓	✓	✓	✓							
Outdoor Molded Resin, Window Type	✓	✓	✓	✓	✓									
COF Outdoor Oil-Filled, Wound Type			✓	✓	✓	✓	✓	✓	✓	✓				
CA Outdoor Oil-Filled, Wound Type (c/w bellows)											✓	✓	✓	✓
Oil-Filled, Wound Type, Single Phase Metering Combined CT/VT unit			✓	✓	✓									
IOSK Outdoors Oil-Paper (c/w bellows)							✓	✓	✓	✓	✓	✓	✓	
OSKF Outdoors Oil-Paper (c/w bellows)							✓	✓	✓	✓	✓	✓	✓	✓
IK5 Head-type Oil-Paper insulation				✓	✓	✓	✓	✓	✓	✓	✓			
Outdoors Gas-Insulated (SF_6)							✓	✓	✓	✓	✓	✓	✓	✓

2.5.3 Thermal Breakdown

Solid insulation breakdown may occur in the form of: Intrinsic Breakdown, streamer breakdown, electromechanical breakdown, edge breakdown, and treeing, thermal breakdown, erosion breakdown and finally, tracking. Energy loss in a solid insulation increases with increasing voltage, temperature, frequency, moisture content, impurities, etc., as previously described in Section 2.2 and shown in Fig. 1. Clearly the breakdown is a property of the dielectric material plus its electrode system, and not just the dielectric alone [34]. The effect of temperature increase in solid dielectrics is reflected in an increased electrical conductivity and a decreased thermal conductivity. For this reason, the breakdown phenomenon in solid dielectrics is ultimately thermal and breakdown at high temperatures tend to be thermal in nature.

According to ASTM[9] D 149 – 97a (2004), cumulative heating develops in local paths within many materials when they are subjected to high electric field intensities, causing dielectric and ionic conduction losses which generate heat more rapidly than can be dissipated. Breakdown may occur because of thermal instability of the material [35].

Thermal breakdown in the solid insulation is generated when the insulation material is continuously stressed by heat generated because of conduction currents and by dielectric losses due to polarization and ambient temperatures originating critical conditions when the insulation properties are lost. Thermal breakdown has been investigated both theoretically and experimentally by several researchers [36]. Since Wagner, Hayden and Steinmetz, and Gütherschulze proposed almost simultaneously that the electrical rupture of solid dielectrics is a phenomenon of overheating by current, the existence of a Thermal Breakdown has been recognized as one of the causes for the

[9] American Society for Testing and Materials

degradation of insulating materials [37]. The limitations on insulation and core operating temperatures ultimately determine the size of the magnetic components. There are three modes of operation [38]: Steady state in which the operating temperature is the final temperature under the heaviest continuous load and highest ambient temperature, short-term loading in which a heavy load is applied for an interval less than that required for the device to exceed the allowable insulation operating temperature, and adiabatic loading in which a very heavy load is applied for such a short interval that effectively no heat transfer occurs. Electrical conductivity is strongly dependent on temperature. In metals, electrical conductivity decreases with increasing temperature, whereas in semiconductors, electrical conductivity increases with increasing temperature. Over a limited temperature range, the electrical conductivity can be approximated as being directly proportional to temperature.

Whenever there is sufficient conductivity present in a dielectric to produce appreciable Joule heating, the possibility of thermal breakdown exists, for the accompanying rise in temperature will increase the conductivity still further. Thermal breakdown will also depend on the rate at which heat is conducted away to the surroundings. The heat balance equation can be expressed by the following continuity equation:

"Electric power dissipated in material per unit volume = rate of increase in heat content + rate at which heat is conducted away."

Therefore, the general power balance equation is given as [39]

$$\frac{dT}{dt} = \frac{1}{C_p \cdot D} \cdot \left(\sigma E^2 + \kappa \nabla^2 T\right) \tag{2.29}$$

where

C_p - is the specific heat,

D - is density,

κ - is the thermal conductivity,

σ – electrical conductivity.

This expression is better understood considering thermal equilibrium $\left(dT/dt = 0\right)$, then Equation (2.29) simplifies to

$$\sigma(T,E)E^2 + \kappa\nabla^2 T = 0 \tag{2.30}$$

It is convenient to consider the low-field case of field-independent electrical conductivity in a unidirectional 1-dimensional analysis where flux through the insulation follows an x-direction. The electrical conductivity is assumed to be only a function of temperature; therefore, thermal conductivity is constant, i.e. $\kappa(T) = \kappa_0$. Now Equation (2.30) is rearranged as

$$\sigma(T)\left(-\frac{\partial V}{\partial x}\right)^2 + \kappa_0 \frac{\partial^2 T}{\partial x^2} = 0 \tag{2.31}$$

The applied voltage (V_{app}) reaches the thermal breakdown voltage (V_{th}), when T_{max} reaches the critical temperature T_c. Considering the case of thermal runaway $T_c \to \infty \; as \; V_{app} \to V_{th}$, the maximum thermal voltage is given by

$$V_{th} = \left(8\int_{T_0}^{T_c=\infty} \frac{\kappa_0}{\sigma(T)} dT\right)^{1/2} \tag{2.32}$$

A complete derivation of Equation (2.32) is presented in Chapter 10 of [39].

CHAPTER 3

LITERATURE REVIEW - HV INSULATION DIAGNOSTIC TECHNIQUES

3.1 Background

The better the insulation condition is diagnosed; the sooner one can obtain advice for corrective actions to be taken. As a matter of fact, industry and researchers have worked together for many years looking for parameters to identify/measure active failure conditions and/or accelerated ageing processes in oil-immersed transformers. The IEEE C57 Standards series content guidelines, techniques, and models that have been used by manufacturers and operators to prevent power outages and unexpected failure of transformers. Research work is carried out at different scale levels. Some investigators have simulated failure conditions and ageing of transformers using different software applications while others have used insulation samples as reference to what could happen in a real unit under overload conditions.

There is a wide range of testing techniques being applied in the industry for the assessment and diagnostic of insulation condition on electrical equipment. The electrical tests could be divided into three major groups: DC Test, AC Tests, and Specific Device Test. The testing configurations are presented herein with a brief description of results obtained using state-of-the-art technology available at the High Voltage / High Current Laboratory at the Tennessee Technological University.

Experimental procedures applicable to our testing infrastructure follow NETA[10] Acceptance Testing Specifications [40] and IEEE Standards [1 - 3], as well as commonly applied industry testing practices described in [2, 41].

[10] InterNational Electrical Testing Association Inc.

Each test provides information on the dielectric condition from one only parameter [42]. Therefore, the information is more accurate and a better assessment is possible when greater amount of parameters are identified throughout the testing procedures.

In addition to the above described techniques, the industry and research entities provide insulation condition assessment of aged transformers by means of invasive and non-invasive procedures such as Degree of Polymerization (DP) and Furanic Compound Analysis by High Performance Liquid Chromatography (HPLC). Dissolved Gas Analysis (DGA) is used to identify active failure conditions that may bring the unit out of service.

3.2 DC Tests

The dielectrics have the property of both temporary and permanent absorption of electrical charges. DC Voltage tests are the oldest type of testing applied to high-voltage electric apparatus. The current injected is large at the beginning in order to provide the required charging energy, decreasing due to continuous leakage or watt loss through the insulation. Charged particles capable of traveling through the dielectric from one electrode to the other constitute the leakage current and are not part of the polarization phenomena as shown in Fig. 4, which is characterized by the material properties such as structure and condition of the insulation system.

The losses from the dielectric absorption process are much higher than the leakage losses. Small increases in moisture content within the insulation system produce a large increase in the dielectric absorption.

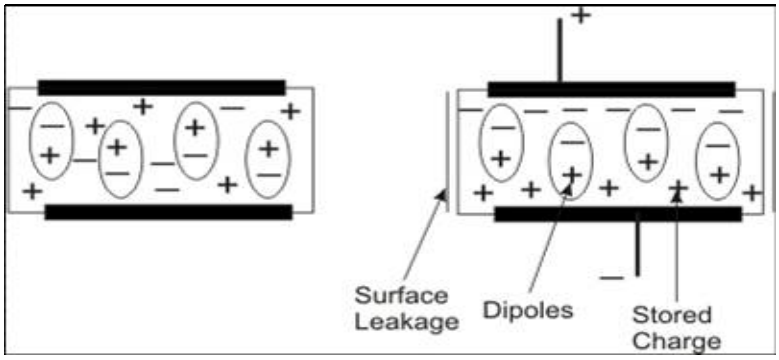

Fig. 4. Polarization Phenomena in Dielectrics [19]

3.2.1 Insulation Resistance Test

If a perfect insulation material did exist, there would be no flow of electrical current through the insulation to ground or between the windings, but since no insulation has infinite resistance, there is always some leakage current flowing through it [41, 43]. Therefore, if the insulation ages and degrades then the leakage current flowing through the system tends to increase. The test measures the resistance of the insulation material to the flow of leakage current.

The test is performed connecting a DC supply to the insulation sample. A standard Megger testing equipment (Fig. 5) is used, the 'line' terminal of which is connected to the winding or core bolt under test [22]. There is a time relationship for three currents: Capacitive (I_c), Dielectric Absorption (I_{da}), and Resistive or Leakage (I_r) [44] as it is shown in Fig. 6.

Thus, it can be said then that

$$I_t = I_c + I_{da} + I_r \tag{3.1}$$

where

I_t – Total Current

I_C – Capacitive Charging Current

I_{da} – Dielectric Absorption Current

I_r – Resistive (Leakage) Current

A detailed description of each of these current components is provided in [2, 4]. A graphical representation of these currents during the polarization process is shown in Fig. 7.

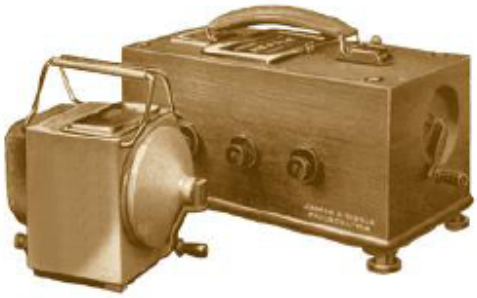

Early Biddle-Brand Insulation Test Sets
(Source: Megger)

Modern Insulation Test Sets
(Source: Megger)

Fig. 5. Insulation Test Sets - Past and Present (Source: Megger ®)

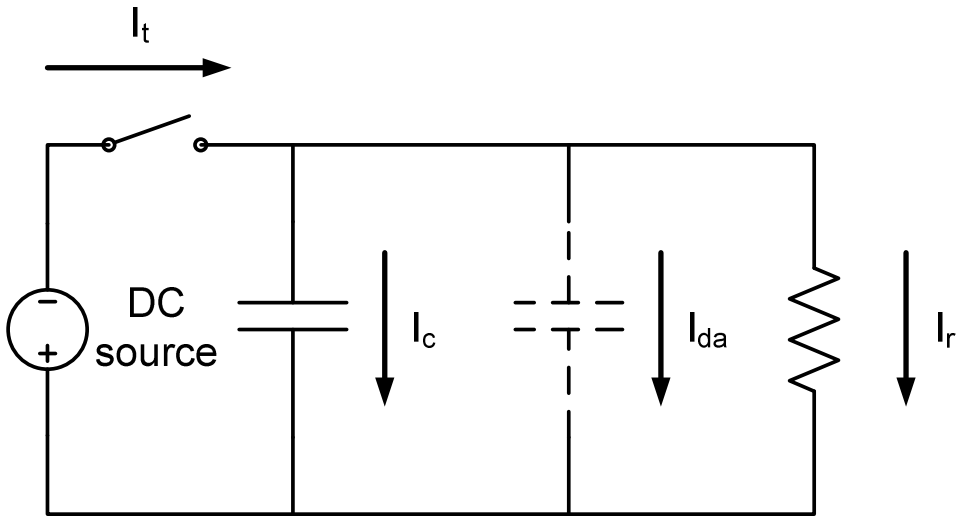

Fig. 6. DC Test - Typical Configuration

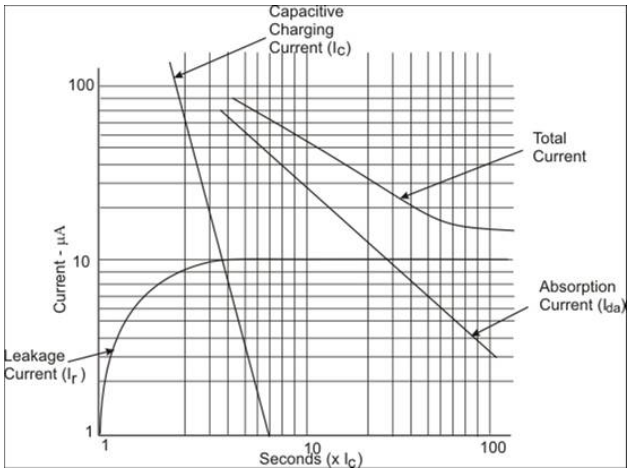

Fig. 7. Currents Flowing Through the Dielectric [19]

Insulation Resistance test helps in the assessment of the insulation condition with a capacitance low enough to detect any gradual variation in the insulation resistance. The test is to be performed on a regular basis in order to track any parameter changes with respect to time.

Insulation resistance values decrease with increasing temperature and vice versa. For more accurate readings, measurement should be carried out at temperatures close to 20°C. Of course this is not an option in the field where temperatures could be over or below this mark. There are, though, some rough corrections that can be applied based on halving or doubling the resistance measurement for every 10°C above or below the base temperature of 20°C. Although, this rough calculation is not accurate because each type of dielectric has a different reaction to temperature variation and a temperature coefficient should be obtained from the manufacturer. If the information is not available from the manufacturer, a practical way to establish temperature coefficients is provided in Appendix A of [43] or in Table 2 reproduced as published in [2].

The insulation resistance measurement is an old testing technique. The megohmmeter or Megger® has a built-in current generator with both current and voltage coils, developing a high DC voltage that causes a small current to flow through and over the insulation of the Unit under Test (UUT).

Table 2. Temperature Correction Factors
for Oil-Filled Transformers [2]

Base Temperature 20°C		
°C	**°F**	**Correction Factor**
0	32	0.25
5	41	0.36
10	50	0.5
15	59	0.720
20	68	1
30	86	1.98
40	104	3.95
50	122	7.85

Oil-filled high-voltage equipment has a wide range of leakage current values depending on the quality and volume of oil, as well as solid insulation. The concept of 'Minimum Insulation Resistance' (MIR) for specific acceptance tests is defined in [2] as

$$R_{\min} = \frac{C \cdot E}{\sqrt{kVA}} \tag{3.2}$$

where

kVA is the rated capacity of the winding under test

$C = 0.8$ for oil-filled transformers at 20°C (testing w/o guard terminal)

$C = 1.5$ for oil-filled transformers at 20°C (testing with guard terminal)

E is the voltage rating of one of the single phase windings under test

Applying (3.2) on the 69kV CTs used for this experimental work, the MIR expected is

$$R_{\min\,(1200,69)} = \frac{C \cdot E}{\sqrt{kVA}} = \frac{0.8 \cdot 69000}{\sqrt{82800}} = 191.83\ M\Omega$$

$$R_{\min\,(200,69)} = \frac{C \cdot E}{\sqrt{kVA}} = \frac{0.8 \cdot 69000}{\sqrt{13800}} = 469.89\ M\Omega$$

A good insulation system will draw a continued increase in its insulation resistance value over time which implies that the effect of absorption current decreases as time increases. A common ratio used for condition assessment is the dielectric absorption ratio (DAR):

$$DAR = \frac{R_{60s}}{R_{30s}} \tag{3.3}$$

where

R_{60s} - is the insulation resistance value measured at 60 seconds; and

R_{30s} - is the insulation resistance value measured at 30 seconds.

Further investigation and/or repair is suggested when DAR ratio is below 1.25.

3.2.2 Polarization Index Test

Polarization Index (PI) Test is used mainly for high capacitance equipment such as large motors, generators or apparatus with complex insulation systems. The test measures the ratio between insulation resistance tests measured at ten (10) and one (1) minutes after applying the voltage. This ratio allows judgment of the rate at which the capacitance and absorption currents disappear thereby indicating if the insulation is damp or dirty. Moisture and dirt have a flattening effect on the PI curve since the leakage current increases at a faster rate with contamination or damaged insulation than the absorption current. One of the advantages of the PI test is that the results are independent of the surrounding temperature as the purpose is to look at the trend and not at one specific reading.

$$PI = \frac{R_{10\,\min}}{R_{1\,\min}} \tag{3.4}$$

A fair value of PI usually lies between 1.25 and 2.0. Oil-filled transformers have typical PI values of 1.1 to 1.3 [43]. In any case, a value of PI below 1.1 is considered as indicative of surface conductive dirt and surface moisture films.

3.2.3 Step Voltage Test

Also known as the DC Voltage Tip-up Test, this technique is based on the application of voltage in increasing steps. Increasing insulation resistance shows that the leakage currents are very low compared to the normal charging current values. Nearly constant or constant insulation resistance indicates that the insulation is probably good. However, if the insulation resistance decreases with increasing steps of voltage and has a constant down slope, the insulation system is probably damp with dirty surfaces.

Even though the highest available voltage may not stress the insulation beyond its rating, at least a two-voltage step test can normally reveal the presence of harmful contaminants [2]. Modern automated equipment exceeds that minimum requirement and run a five (5) minute five-voltage test.

3.3 AC Tests

AC testing is becoming more and more popular within the power industry. Capacitance, Power Factor, and Dissipation Factor (tanδ) are commonly used as part of factory, commissioning, and maintenance acceptance procedures. These testing techniques detect any increase of moisture content in the insulation which accelerates the degradation process of the solid or the combined insulation.

Earlier AC tests were not as common as DC tests because the procedures carried out at power frequency (50 or 60 Hz) implied the use of a somewhat bulky equipment. Nowadays, very low frequency (VLF) equipment is available in the market. VLF is generally considered to be 0.1 Hz and lower. The only way to field test high capacitance loads like cables and motors/generators with AC voltage is to use a VLF AC hipot. The lower the frequency, the less current and power are needed to test high capacitance loads, hence the reduction in size.

$$Xc_{(\text{capacitance reactance})} = \frac{1}{2\pi fC} \tag{3.5}$$

If a 15 kV cable with approximately 1μF of capacitance was to be tested, the capacitive reactance at 60 Hz would be ~ 2650 Ω. To apply the IEEE recommended 22 kV test voltage, it would require a power supply rated for 8.3 amps, or 183 kVA. At 0.1 Hz, the capacitive reactance is ~ 1.6 MΩ. The same 22 kV would draw only 14 mA, or only 0.302 kVA, or 600 times less than at 60 Hz. Moreover, at 60 Hz a cable must be charged to its test voltage every 4.2 milliseconds, 0 – 90 degrees of the waveform. It takes a lot of power to charge a cable that fast. At 0.1 Hz, 2.5 seconds are available to charge the cable. It takes 600 times less power than 60 Hz and 500 times less than at 50 Hz.

In the context of this research work, typical acceptance tests and newly-developed techniques related to diagnostic and ageing estimation of the insulation of oil-filled transformers are discussed.

3.3.1 Dielectric Breakdown Voltage

As per ATS-2003[11] 7.2.2.2.11 acceptance of liquid-filled transformers requires removal of sample of insulating liquid as per ASTM[12] standard D923 and be tested for dielectric breakdown voltage (DBV) [40]. As normally applied, dielectric breakdown voltage test is an empirical test

[11] Acceptance Testing Specifications – developed by NETA for Electrical Power Distribution Equipment and Systems
[12] American Society for Testing and Materials

procedure intended to identify the presence of contaminants and to evaluate the oil's ability to withstand electrical stress [45]. There are two ASTM Standards for DBV test of insulating oil: D 877 and D 1816, both methods use an increasing AC electrical field by means of a constant rate of voltage rise until breakdown occurs. Incremental increases should not exceed 2% of the expected breakdown voltage. The voltage applied to the electrodes of the liquid-filled cell shall have an approximately sinusoidal waveform, such that the peak factor is within the following limits: 1.41 ± 0.07.

Method D 877 uses square-edged electrodes spaced at 0.1 in. The use of this test gap results in a uniform electrostatic field at the center line of the test discs and a highly nonuniform field at the edges of the disc [41]. Laboratories and owners have practically eliminated the use of D 877 test as the test has limited sensitivity to moisture content (unless it exceeds 60%), and the test is not sensitive to oxidation products in service aged insulating oil [2]. ASTM Standard Method D 1816 uses spherical VDE (Verband Deutscher Elektrotechniker) electrodes to attain uniform field strength at all points which are set-up at 1 or 2 mm gap (0.04 or 0.08 inches). In 2002, the revision of IEEE Std C57.106 included D 1816 limits for new and in-service oil. D 1816 limits are summarized in Table 3.

Table 3. D 1816 Dielectric Breakdown Voltage Limits [2]

VOLTAGE CLASS	**1 MM GAP SETTING**			**2 MM GAP SETTING**		
	Acceptable	**Questionable**	**Unacceptable**	**Acceptable**	**Questionable**	**Unacceptable**
≤ 69 kV	≥ 23 kV	< 23 kV ≥ 18 kV	< 18 kV	≥ 40 kV	< 40 kV ≥ 35 kV	< 35 kV
> 69 kV < 230 kV	≥ 28 kV	< 28 kV ≥ 23 kV	< 23 kV	≥ 47 kV	< 47 kV ≥ 42 kV	< 42 kV
≥ 230 kV	≥ 30 kV	< 30 kV ≥ 25 kV	< 25 kV	≥ 50 kV	< 50 kV ≥ 45 kV	< 45 kV

The test device is composed of a voltage regulator, step-up transformer, switching system, and energy limiting devices. The voltage applied to the electrodes increases form zero at the rate of $0.5\,kV\,s^{-1}$ until breakdown occurs.

3.3.2 Capacitance, Power Factor (PF), and Dissipation Factor (tanδ)

As a transformer ages, the moisture content in the solid and liquid insulation tends to rise. This moisture level increase has an adverse effect on electrical and thermal degradation and the moisture development in a transformer needs to be monitored as part of the routine tests.

The loading process is complex in most of the utilities and load variability will be reflected in a non-stable condition of moisture equilibrium as the moisture is extracted from the paper insulation at higher temperatures, but it returns to the paper when the transformer cools down. For paper degradation analysis identification of the hot-spot location is critical because the paper in this region will be drier than the bulk insulation [46].

Dielectric Spectroscopy is becoming popular for moisture evaluation in insulation and it is not dependent on moisture equilibrium between the paper and the oil [46, 47]. Of the few variations of this test technique, frequency domain loss factor measurements are found to be convenient.

Capacitance of a system is defined by the magnitude of charge that it can store at a given voltage. The charge is proportional to the area of the conductive plates, the dielectric constant of the insulating material between the plates, and inversely proportional to the distance between them.

$$C \approx \frac{A}{d} \cdot \varepsilon \tag{3.6}$$

Vacuum and air have a relative dielectric constant of 1 and all other insulating materials have a relative dielectric constant larger than 1. The Power Factor (PF) in a circuit is defined as the ratio of

active power to volt-amperes (W/VA). Power factor is also defined as the cosine of the angle between the voltage and current in a circuit (Theta θ). This angle is typically very close to 90 degrees for capacitive circuits.

Dissipation Factor is defined as the ratio of active power to reactive volt-amperes (W/VAr) in a circuit. The Dissipation Factor is equal to the tangent of Delta, where δ is the angle of 90°-θ. For practical insulation circuits, where θ > 85°, the power factor and the dissipation factor at the power frequency are numerically the same.

ASTM D 150 defines dissipation factor as the ratio of the loss index (ε") to the relative permittivity (ε') which is equal to the tangent of its loss angle (δ) or the cotangent of its phase angle (θ). Therefore, dissipation factor is expressed as [48]

$$D = \frac{\varepsilon''}{\varepsilon'} = \tan\delta = \cot\theta = \frac{X_p}{R_p} = \frac{G}{\omega C_p} = \frac{1}{\omega C_p R_p} \tag{3.7}$$

where

G – equivalent AC conductance

X_p – parallel reactance

R_p – equivalent ac parallel resistance

C_p – parallel capacitance

ω - $2\pi f$ (sinusoidal wave shape assumed)

The reciprocal of the dissipation factor is the quality factor, Q, sometimes called the storage factor. The dissipation factor of the capacitor is the same for both the parallel (Fig. 8) and the series (Fig. 9) representations as follows:

$$D = \omega R_s C_s = {}^{1}\!\!\diagup\!\!_{\omega R_p C_p} \tag{3.8}$$

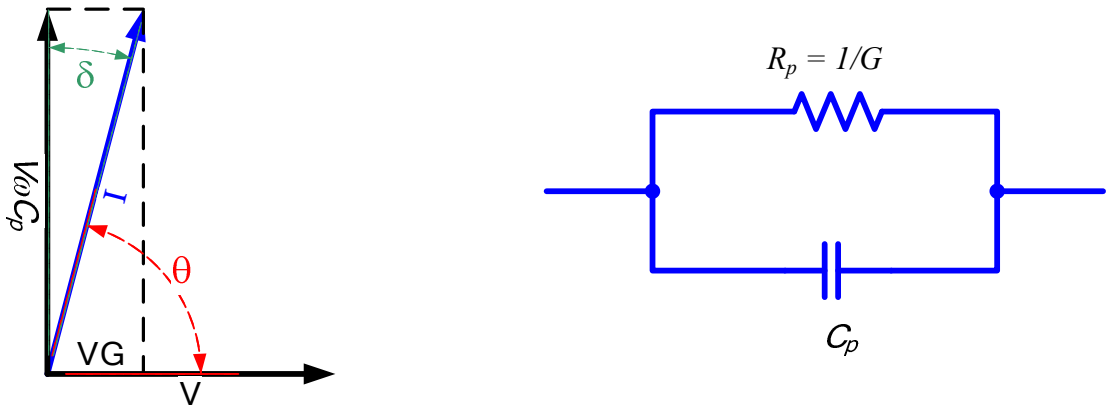

Fig. 8. Power and Dissipation Factor angle components. Vector Diagram for Parallel Circuit

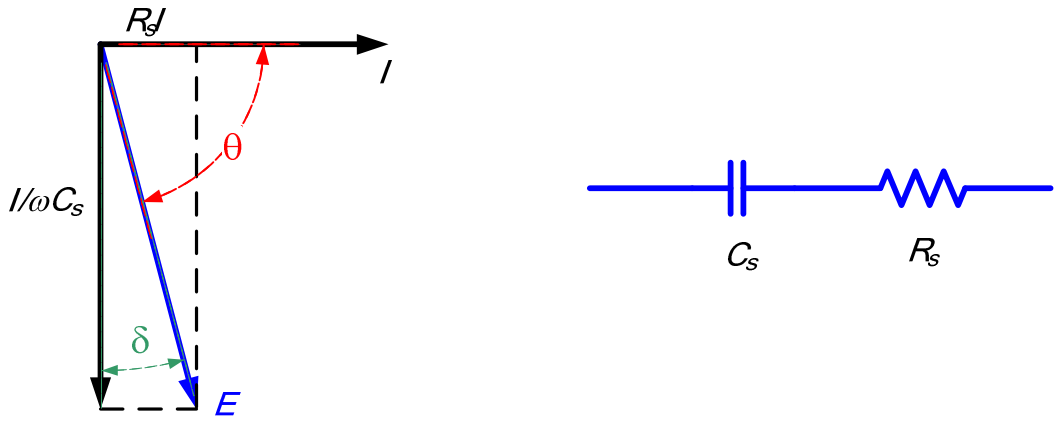

Fig. 9. Power and Dissipation Factor angle components. Vector Diagram for Series Circuit

When the dissipation factor is less than 0.1, the power factor differs from the dissipation factor by less than 0.5%. Their exact relationship may be found from the following:

$$PF = D \Big/ \sqrt{1 + D^2} \tag{3.9}$$

The AC loss should be small, both in order to reduce the heating of the material and to minimize its effect on the rest of the network. The dielectric loss increases directly with frequency; therefore, high frequency applications should show a very low value of loss index.

The dynamic properties of dielectric materials can be measured in the time and/or frequency

domain. The fundamentals of dielectric response functions and the theory of dynamic properties of dielectrics are well described in [47 – 49]. The aim of this work is the specific application of this theory on oil-paper insulation systems, using a mechanism capable of identifying the ageing process of the insulation measuring the changes in the chemical and dielectric properties of the tested unit. The approach to such mechanism is through measurements of capacitance (C) and dielectric loss quantified by the loss or dissipation factor $(\tan\delta)$. This type of test is part of many manufacturing quality control procedures and it is normally carried out at power frequency only.

On a frequency spectrum, power factor (PF) and dissipation factor (tanδ), both curves draw similar paths as long as they are on the high frequency spectrum range. Below 0.07Hz in the low frequency spectrum, curves draw different paths, depending on the condition of the experimental unit. This will be observed in the curves obtained form the experimental work detailed in Chapter 4.

The relation between complex electric displacement and complex dielectric permittivity is given by

$$D^*(\omega) = \varepsilon_0 \varepsilon^*(\omega) E^*(\omega) \tag{3.10}$$

where the complex dielectric permittivity can be expressed as

$$\varepsilon^*(\omega) = \varepsilon'(\omega) - j\varepsilon''(\omega) \tag{3.11}$$

The instrument used to measure capacitance and dissipation factor can cover a wide frequency range (spectrum) from 0.0001 to 1000 Hz. The device measures the dielectric response function $f(t)$ with the tested unit offline. In the industry practice this is a disadvantage to the method especially if low frequency readings are required. This test could then take several hours and those may not be available for a normally-operational device. Nevertheless, the low and very low frequency range are most prone to the ageing effects. Very low frequency readings are also important because those define the capacitance of the paper insulation alone. Oil conductivity is dominant in the medium frequency.

A single point measurement at power frequency is not usually enough to determine if the liquid insulation is to be reclaimed or just dried.

Due to the low volume of liquid insulation contained, instrument transformers are not considered for a dry-out process; instead, a possible reclamation is always feasible and easy to do.

The instrument measures the insulation impedance based on the complex capacitance model described as

$$Z = \frac{1}{j\omega C^*} \tag{3.12}$$

where

$$C^* = C' - jC'' \tag{3.13}$$

$$C' = \mathrm{Re}\left\{\frac{1}{j\omega Z}\right\} \tag{3.14}$$

$$C'' = -\mathrm{Im}\left\{\frac{1}{j\omega Z}\right\} \tag{3.15}$$

Once the impedance of the dielectric is obtained, power factor and $\tan\delta$ can be calculated. Then,

$$PF = \cos\varphi = \frac{\mathrm{Re}\{Z\}}{|Z|} \tag{3.16}$$

$$\tan\delta = -\frac{\mathrm{Re}\{Z\}}{\mathrm{Im}\{Z\}} \tag{3.17}$$

The imaginary part of the complex capacitance expressed in (3.15) represents the losses. In insulation materials or dielectrics, the permittivity is the complex function describing capacitance and losses. Thus, (3.13) can be expressed as

$$C^* = C_0\left(\varepsilon' - j\varepsilon''\right) \tag{3.18}$$

where

C_0 - is the geometrical capacitance

Therefore, the permittivity components of the dielectric model become

$$\varepsilon' = \mathrm{Re}\left\{\frac{1}{j\omega C_0 Z}\right\} \tag{3.19}$$

$$\varepsilon'' = -\mathrm{Im}\left\{\frac{1}{j\omega C_0 Z}\right\} \tag{3.20}$$

The instrument is not capable of distinguishing between pure dc conductivity and the dielectric loss. Therefore, the measured relative permittivity is different form the permittivity in (3.11) and is expressed in [47] as

$$\varepsilon^*_{mr}(\omega) = \varepsilon'_r(\omega) - j\varepsilon''_r(\omega) = \varepsilon'(\omega) - j\left[\varepsilon''(\omega) + \frac{\sigma_0}{\varepsilon_0\omega}\right] = 1 + \chi'(\omega) - j\left[\chi''(\omega) + \frac{\sigma_0}{\varepsilon_0\omega}\right] \tag{3.21}$$

A physical background of dielectric loss and a complete derivation of these equations can be found in [50]. Now, the tested unit is represented in (3.21) by the real part (capacitance) and the imaginary part (losses), both frequency dependant. This leads to a more convenient expression for (3.17) when the dielectric model is applied:

$$\tan\delta(\omega) = \frac{\varepsilon''_r(\omega)}{\varepsilon'_r(\omega)} = \frac{\varepsilon''(\omega) + \sigma_0 / \varepsilon_0\omega}{\varepsilon'_r(\omega)} \tag{3.22}$$

From Equations (3.13) – (3.19), the dissipation factor can also be expressed as

$$\tan\delta(\omega) = \frac{C''(\omega)}{C'(\omega)} \tag{3.23}$$

The factors affecting permittivity and loss characteristics during the measurement process are frequency, temperature, voltage, humidity, water immersion, weathering, and deterioration. The frequency at which loss index is a maximum is called the relaxation frequency for that polarization

which is also the frequency at which the permittivity is increasing at the greatest rate. Temperature will increase the relaxation frequencies. The temperature coefficient of permittivity is positive at the lower frequencies and negative at high frequencies. The temperature coefficient of loss index and dissipation factor may be either positive (for frequencies higher than relaxation frequency) or negative (for lower frequencies). The major electrical effect of humidity is to increase greatly the magnitude of its interfacial polarization, thus increasing permittivity and loss index as well as dc conductance on an insulating material. The observed changes in any dielectric property, particularly dissipation factor, can be looked at as a measure of deterioration and hence a measure of decrease in the dielectric strength. The dissipation factor is a very sensitive measure of the purity of raw materials, of chemicals used in the manufacturing process, and of cleanliness in the manufacturing process.

Moisture content in the solid insulation is a major concern in the life of electrical apparatus and because the volume of solid insulation is minor in this type of units, the percentage of moisture content should vary from standard accepted values to empirically recognized trough investigation critical values where operation may be considered to be risky. Transformers are dried during the manufacturing process until measurements yield moisture content in the cellulosic insulation from 0.5 to 1% or less. For moisture in cellulose the measure is percent of weight (%) and for moisture in oil it is parts per million of weight (ppm). IEC 60814 defines moisture for oil-impregnated paper and board as [51]

$$W = \frac{m_{as} - m_d}{m_d} \cdot 100\% \tag{3.24}$$

where m_{as} - mass as sampled

m_d - mass when dry

Local excessive moisture can be detected because it causes the insulation power factor to be high, particularly at elevated temperatures.

3.3.3 CT Analysis of Functional Parameters

Each type of equipment requires its own unique testing procedure, conforming to different test standards. CT analysis of functional parameters may be carried out with testing equipment which is mainly used by manufacturers and utilities for acceptance, pre-commissioning and/or commissioning tests, overall monitoring, and inspection.

The CT Analyzer is a testing device capable of providing a set of parameters indicating complete performance analysis of these units. In a simple and quick test, the nameplate parameters as well as the construction integrity of the device can be verified. The testing device complies with ANSI/IEEE [1] and IEC standards. The analysis provides the following parameters:

- Primary and Secondary Current values
- Knee points (ANSI 30, ANSI 45, IEC 60044-1, IEC 60044-6)
- Burden measurement
- CT winding resistance measurement
- CT excitation characteristic recording (V-I curve)
- CT ratio measurement with consideration of connected burden
- CT phase and polarity measurement
- Remanence factor (Kr)
- Saturated (Ls) and non-saturated (Lu) inductivity

3.4 Specific Tests

3.4.1 Dissolved Gas Analysis (DGA)

Dissolved gas concentration in oil varies when an active fault condition exists. The interpretation of Dissolved Gas Analysis (DGA) for transformers is provided in IEC Standard 60599-1999 and IEEE Std. C57.104-1991.

The condition assessment of oil-immersed transformers using the DGA technique is effective for diagnosis of active fault conditions affecting the normal operation of the unit or generating accelerated ageing of the transformers. Moreover, DGA is one of the most important tools available to the maintenance engineer concerned about the condition and life expectancy of transformers [22]. It is important to highlight any change in the dielectric oil during the operation of the unit as if it will change the dissolved gas concentration. Although, completely changing oil in an instrument transformer will re-confirm the existence of an active failure condition if the rate of increase of the gases in the DGA analysis presents similar characteristics to those before changing.

The process of gas evolution during normal operation of a transformer has been discussed by different authors [52 – 60]. Dielectric oil is a complex composition of hydrocarbon molecules refined from the crude oil. This mixture, under the influence of thermal or electrical stress, discharges gas molecules such as Acetylene, Hydrogen, Methane, Ethane, and Ethylene. The solid insulation (Kraft paper) is composed of cellulosic molecules. From the solid insulation, Carbon Monoxide and Carbon Dioxide will evolve at low energy and temperature levels.

The fault indicator gases are summarized in Table 4 as presented in [59].

Table 4. Fault Indicator Gases [59]

Fault Gas	Key Indicator	Secondary Indicator
Hydrogen (H_2)	Corona	Arcing, overheated oil
Methane (CH_4)		Corona, Arcing and Overheated oil
Ethane (C_2H_6)		Corona, Overheated Oil
Ethylene (C_2H_4)	Overheated oil	Corona, Arcing
Acetylene (C_2H_2)	Arcing	Severely overheated oil
Carbon Monoxide (CO)	Overheated Cellulose	Arcing if the fault involves cellulose
Carbon Dioxide (CO_2)		Overheated Cellulose, Arcing if the fault involves cellulose
Oxygen (O_2)		System leaks, over-pressure
Nitrogen (N_2)		System leaks, over-pressure

DGA interpretation is complex and critical for proper condition assessment of the unit under observation. The continuous analysis provides important data related to the gas evolution inside the transformer, possible approach to critical values or an unexpected behavior of the gas evolution (rate of increase) that may suggest additional testing by other techniques or repeated chromatography.

The most commonly used gas-in-oil diagnostic methods include the following [54]:

Table 5. IEEE Maximum Dissolved Gas Concentrations and Standard Limits [55]

Gas	Condition 1	Condition 2	Condition 3	Condition 4
H_2	100	101 - 700	701 – 1,800	>1,800
CH_4	120	121-400	401-1,000	>1,000
C_2H_2	35	36-50	51-80	>80
C_2H_4	50	51-100	101-200	>200
C_2H_6	65	66-100	101-150	>150
CO	350	351-570	571-1,400	>1,400
CO_2	2500	2,500-4,000	4,001 – 10,000	>10,000
TDCG	720	721-1,920	1,921-4,630	>4,630

3.4.1.1. IEEE C57.104-1991 [55].

The standard provides values for norms in relation to the total dissolved combustible gas content (TDCG) for the transformers and these are set out in Table 5. The criterion for classification of risks is described in Table 6.

Table 6. IEEE Criteria for classification of Risks based on DGA sample analysis

Risk Condition	Description
1	TDCG below this level indicates the transformer is operating satisfactorily. Any individual combustible gas exceeding specified levels should prompt additional investigation.
2	TDCG within this range indicates greater than normal combustible gas level. Any individual combustible gas exceeding specified levels should prompt additional investigation. Action should be taken to establish a trend. Fault(s) may be present.
3	TDCG within this range indicates a high level of decomposition. Any individual combustible gas exceeding specified levels should prompt additional investigation. Immediate action should be taken to establish a trend. Fault(s) are probably present.
4	TDCG within this range indicates excessive decomposition. Continued operation could result in failure of the transformer.

3.4.1.2. Rogers' Method (IEEE PC57.104 D11d).

IEEE considers three ratios for the condition analysis using DGA data. In addition to the three Rogers ratios, the standard contemplates the CO_2/CO ratio with the interpretation similar to CIGRE SC15 K_4. The Roger's Ratios are

$$R_1 = \frac{Methane(CH_4)}{Hydrogen(H_2)} \tag{3.25}$$

$$R_2 = \frac{Acetylene\left(C_2H_2\right)}{Ethylene\left(C_2H_4\right)} \tag{3.26}$$

$$R_3 = \frac{Ethylene\left(C_2H_4\right)}{Ethane\left(C_2H_6\right)} \tag{3.27}$$

3.4.1.3. CIGRE[13] SC15.

Five key ratios are given for transformer condition diagnostic. These key ratios are listed below.

$$K_1 = \frac{Acetylene\left(C_2H_2\right)}{Ethane\left(C_2H_6\right)} \tag{3.28}$$

$$K_2 = \frac{Hydrogen\left(H_2\right)}{Methane\left(CH_4\right)} \tag{3.29}$$

$$K_3 = \frac{Ethylene\left(C_2H_4\right)}{Ethane\left(C_2H_6\right)} \tag{3.30}$$

$$K_4 = \frac{Carbon\ Dioxide\left(CO_2\right)}{Carbon\ Monoxide\left(CO\right)} \tag{3.31}$$

$$K_5 = \frac{Acetylene\left(C_2H_2\right)}{Hydrogen\left(H_2\right)} \tag{3.32}$$

Table 7. Interpretation of Roger's Ratios

Suggested Fault Type	R1	R2	R3
Case 0: NORMAL	< 0.1	< 0.01	< 1.0
Case 1: Discharge of Low Energy	≥0.1, <0.5	≥1.0	≥1.0
Case 2: Discharge of High Energy	≥0.1, <1.0	≥0.6, <3.0	≥2.0
Case 3: Thermal fault, low temp < 300°C	≥1.0	<0.01	<1.0
Case 4: Thermal fault, temp < 700°C	≥1.0	<0.1	≥1.0, <4.0
Case 5: Thermal fault, temp > 700°C	≥1.0	<0.2	≥4.0

[13] International Council on Large Electric Systems

Table 8. Interpretation of CIGRE SC15 Key Ratios

Key Ratio	Value Significance	Interpretation
K_1	>1	Discharge
K_2	>10	Partial Discharge
K_3	>1	Thermal fault in Oil
K_4	> 10	Overheating of Cellulose
	< 3	Degradation of cellulose by electrical fault
K_5	> 2	In Tank Load tap Changer

3.4.1.4. The Duval Triangle (IEC 60599-1999).

The interpretation method developed by M. Duval[14] provides codes of gas ratios for fault diagnosis as published in [55 – 58]. The Duval Triangle method was developed empirically in the early 1970s, and is used by the IEC. It is based on the use of three gases (CH_4, C_2H_4, and C_2H_2) corresponding to the increasing energy levels of gas formation. This information is reproduced in Table 9 [22, 59].

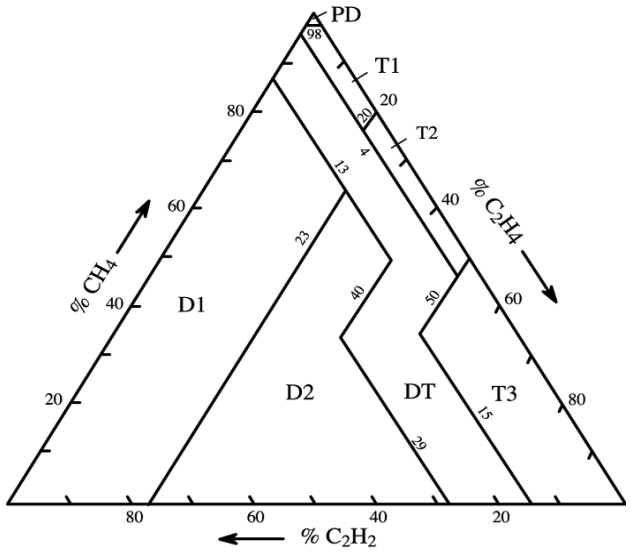

Fig. 10. Duval Triangle - Zones

[14] Michel Duval, PhD. A Fellow Member of IEEE and the Chemical Institute of Canada.

Table 9. Fault Diagnosis [22, 59]

	Ratios of Gases	Codes of gas ratios		
		$\frac{C_2H_2}{C_2H_4}$	$\frac{CH_4}{H_2}$	$\frac{C_2H_4}{C_2H_6}$
	< 0.1	0	1	0
	0.1 – 1	1	0	0
	1 – 3	1	2	1
	> 3	2	2	2
Case	**Fault Type**			
0	No Fault	0	0	0
1	Low Energy Partial Discharges	0	1	0
2	High Energy Partial Discharges	1	1	0
3	Discharge of Low Energy	1→2	0	1→2
4	Discharge of High Energy	1	0	2
5	Thermal fault T < 150°C	0	0	1
6	Thermal fault 150°C<T< 300°C	0	2	0
7	Thermal fault 300°C<T< 700°C	0	2	1
8	Thermal fault T > 700°C	0	0	2

The Duval triangle method plots the relative % of the three gases on each side of the triangle, from 0% to 100%. The six main zones of faults are indicated in the triangle in Fig. 10, plus a DT zone (mixture of thermal and electrical faults).

Transformers in-service will always have some degree of fault gases dissolved in the liquid insulation. The possibility of a fault condition comes into picture when the concentration of one or more of these gases over goes the safety recommended values.

3.4.2 Degree of Polymerization

The solid insulation in transformers is mainly built up of paper and pressboard, where cellulose is the fundamental component. Cellulose is a polymer of alpha-D-glucose units linked to one another in a special manner as shown in Fig. 11 . It may be represented simply as $\left[C_5H_{10}O_5\right]_n$, ignoring the

extra atoms on the end groups, where *n* is the Degree of Polymerization (DP) [60]. The number of monomer glucose units is the DP. The DP of Kraft pulps ranges from 1100 to 1200 and it can be determined by ASTM D-4243 testing method, but the number will reduce at least by 10% when the transformer undergoes factory testing, dry-out and oil impregnation in the manufacturing process are the main factors reducing the initial DP value. The DP of fresh and site samples indicated that fresh paper was having a DP ranging from 800 to 950 [61].

The ageing process and cellulose degradation are complex processes under normal operation of transformers where different factors interact lowering the DP by depolymerization and accelerating these processes, which involve the breakage of the linkage by hydrolytic decomposition, and by breakup of the ring structure that would give CO, CO2, and water as ultimate products and also lowering the mechanical strength properties of the paper which gets darker and brittle [46].

At this point and for further understanding of the ageing characteristics, it is important to mention that water and carbon dioxide (CO_2) are the main by-products of the thermal degradation of cellulose. Furans and carbonyl derivatives are the second major degradation by-products [62].

A DP value of 200 is currently accepted as the end of life [3, 46, 63] for power and distribution transformers. At this point the life of the transformer is estimated to be 150,000 hours at an ageing acceleration factor equal to 1 ($F_{AA} = 1$).

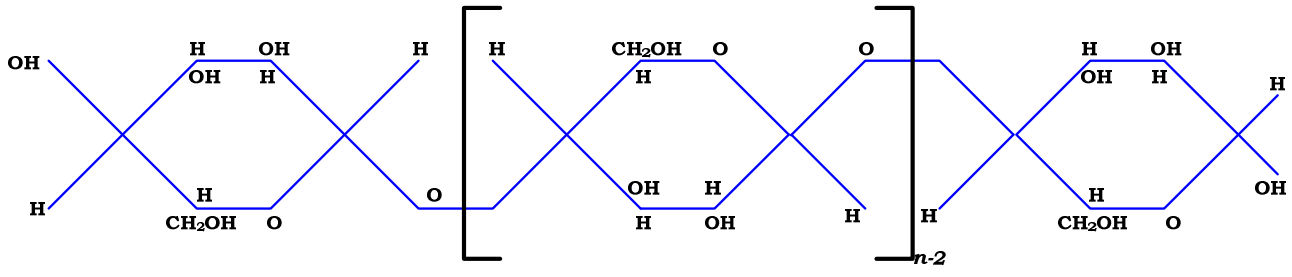

Fig. 11. Cellulose Polymer

The most direct method to determine the DP of paper insulation requires taking a sample of the paper and submitting it to the lab for a DP test. The DP proves to be the most informative and reliable parameter for assessing the cellulose ageing process [62 – 64]. This method is the most accurate way to assess the condition of the paper insulation but it is impractical. The test is intrusive and the transformer must be offline. In addition to that, removing the sample can have a negative effect on the transformer. The major weakness is the uncertainty of getting representative results from top-layer samples versus results from inner part of the paper insulation.

Emsley et al. [65] obtained an equation from an extensive literature review for a "thermally activated" paper ageing process. The interpretation of DP is given for life prediction from cellulose degradation kinetics. The life estimates are based on a theoretical model where knowledge of the initial value of DP is critical. The obtained expression is

$$\frac{1}{DP_t} - \frac{1}{DP_0} = k \cdot t \tag{3.33}$$

where

DP_t – Degree of Polymerization after ageing

DP_0 – Degree of Polymerization before ageing

k – Constant

t – Equivalent ageing [hours]

In order to correlate DP with life it is necessary to relate k to temperature of the system via the Arrhenius relationship. The experimental results yield to the following expression for k:

$$k = A \cdot \exp\left(- \frac{E}{R \cdot (T + 273)} \right) \tag{3.34}$$

T – Measured temperature in Celsius. In the context of this work, this temperature represents the hottest-spot temperature within the insulation system and will be indicated as θ_H as initially described in the nomenclature section.

E – Activation energy of the chemical process, 111 kJ/mole with 95% confidence interval [105:117]

R – Molar gas constant = 8.314 J/mole/K

A – Pre-exponential factor of Equation (3.34) dependent on operating conditions such as chemical environment, moisture in paper, acidity.

Subtituting (3.34) in (3.33) gives a correlation between DP and ageing of the insulation system (or electrical apparatus) expressed in hours. Thus,

$$t = \left(\frac{DP_0 - DP_t}{DP_0 \cdot DP_t \cdot A} \right) \cdot \exp^{\left(\frac{E}{R \cdot (\theta_H + 273)} \right)} \tag{3.35}$$

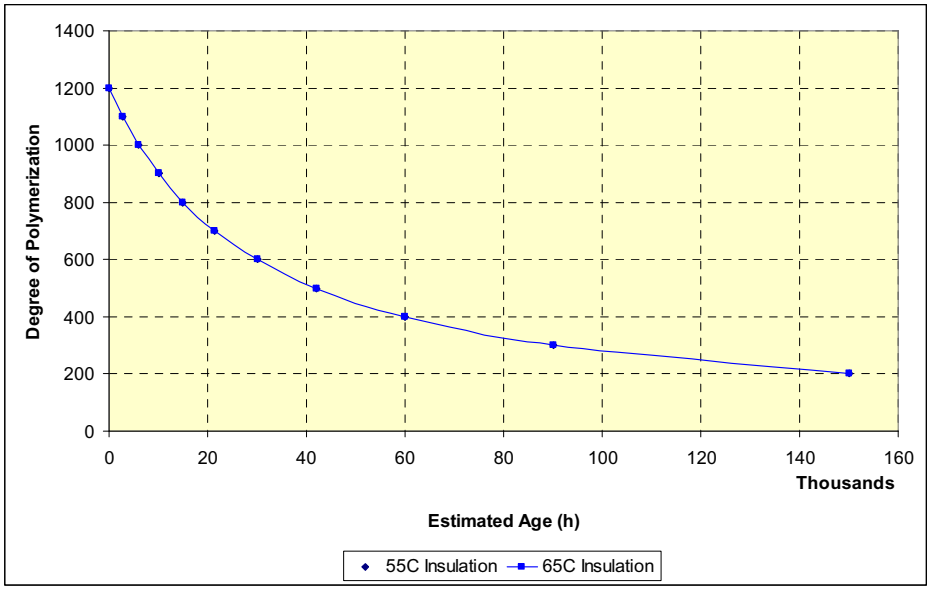

Fig. 12. Equivalent ageing calculated for thermally upgraded and non-upgraded insulation

Application of (3.35) was validated against standard DP_0 and DP_t reference values provided in the Standards. Therefore, with $DP_0 = 1000$ and including the end-of-life criterion where at $DP_t = 200$ the life of the unit equals 150,000 hours. Substituting these values into (3.35) and considering three different values for HST, the relationship between DP vs. equivalent age is presented in Fig. 12.

$$\text{Calculated factor A}\begin{cases} A_{65°C} = 3.83\times10^{7} \\ A_{55°C} = 1.58\times10^{8} \end{cases}$$

Calculated value of A based on standard parameters are in good agreement and within 95% confidence limits with the values of A given in [65] from the Analysis of Covariance for different Kraft paper conditions. These values are presented in Table 10.

Stebbins et al. in [63] suggest a predictive expression based on a wide experimental base, comparing a *"general expression"* to calculate %LOL as a function of DP (3.36) against an empirically developed expression (3.37) for which initial value of DP_t is 800.

$$\%LOL = \left(\frac{1200 - DP_t}{1000}\right)\times100\% \tag{3.36}$$

Equation (3.36) considers DP_0=1200 and end of life definition with DP_t=200.

Table 10. Values of "A" from analysis of Covariance of Degradation Rates [65]

Data Set	**A**	**95% Confidence Limits**	
Upgraded paper in oil	3.65 x 10^7	7.93 x 10^6	1.68 x 10^8
Dry Kraft Paper in oil	1.07 x 10^8	2.41 x 10^7	4.71 x 10^8
Kraft paper +1% H_2O in oil (or paper or cotton in vacuum)	3.50 x 10^8	8.41 x 10^7	1.46 x 10^9
Kraft paper +2% H_2O in oil (or paper or cotton in air)	7.78 x 10^8	1.83 x 10^8	3.30 x 10^9
Kraft paper +4% moisture in oil H_2O in oil (or paper or cotton in oxygen)	3.47 x 10^9	7.66 x 10^8	1.57 x 10^{10}

$$\%LOL = \frac{\log_{10}(DP_t) - 2.903}{-0.006021} \tag{3.37}$$

The samples sent for DP analysis to DOBLE laboratories taken from the experimental units used for this research work gave an average DP value of 915. In addition to the baseline samples taken from each transformer, a factory paper sample registered a DP value of 838. Therefore, an initial value of DP=900 will modify (3.37) to

$$\%LOL = \frac{\log_{10}(DP_t) - 2.954}{-0.0065321} \tag{3.38}$$

3.4.3 Furanic Compounds Analysis

An alternative method used to indirectly determine the DP value of an aged transformer is based on Furanic Compound Analysis. When cellulose degrades, the glycosidic bonds[15] that hold the glucose molecules together break apart, shortening the cellulose chains and releasing glucose into the oil. Glucose is an unstable molecule quickly converting into intermediate products of paper degradation including five-membered heterocyclic compounds known as furanic compounds of which 2-furaldehyde is the most important [46] and by far the most abundant. These furan derivatives found in the oil sample taken from factory and corresponding concentrations are presented in Table 11.

Furan is soluble in oil and only produced in a transformer by the degradation of cellulose. Taking a sample for furan analysis is a non-destructive technique, requiring about 40ml of oil per sample which can make it a part of routine testing procedure.

[15] In chemistry, a glycosidic bond is a certain type of functional group that joins a carbohydrate (sugar) molecule to another, which may be another carbohydrate

Table 11. Furanic Derivatives and Concentrations from Factory Oil Sample

Description	Abbrev.	Concentration (ppb)
2-furaldehyde	(2FAL)	5
Furfuryl alcohol	(FOL)	<1
2-acetylfuran	(2AF)	<1
5-methyl-2-furaldehyde	(5M2F)	<1
hydroxymethyl-2-furfural	(HMF)	<1

The oil sample is prepared and analyzed with high-performance liquid chromatography (HPLC) following ASTM D5837 or IEC 61198. The sample is injected into the chromatograph flowing into the column. The molecules of stronger polarity are weaker and elute first. The concentration signals of various components including furfurals are obtained by the UV detector and then changed into chromatogram by the Intergraph.

S. D. Myers, Inc., found the distribution of the five furanic compounds in several years of worth furan data [63] as described in Table 12.

Table 12. Relative Abundance of five Furanic Compounds [63]

Compound	% of All Data Sets
5H2F	2.8
2FOL	1.0
2FAL	98.7
2ACF	1.2
5M2F	8.3

Several studies derived from both laboratory experiments and field measurements have attempted to correlate furanic content to DP indicating a close approximation of estimated DP against the measured DP [62 – 64]. A brief review of those studies is presented below.

From the approach presented by De Pablo and CIGRE Task Force 15.01.03 [62], the amount of furfural dissolved in the oil is defined by

$$2FAL\left[\mu g/g_{paper}\right] = \frac{10^6}{162 \times DP_0} \times N \times 96 \times 0.3 = 222 \times N \tag{3.39}$$

where DP_0 is the initial DP (assumed to be 800), 162 is the molecular weight of the glucose units constituting the cellulose, N is the number of chain scissions, 96 is the molecular weight of furfural, and 0.3 is the reaction yield.

$$N = \frac{DP_0}{DP} - 1 \tag{3.40}$$

Assuming a ratio (R) oil to paper of 25, (3.40) can be expressed in terms of oil mass as

$$2FAL\left[mg/kg_{OIL}\right] = \frac{222 \times N}{R} = 8.88 \times N \tag{3.41}$$

Combining (3.40) and (3.41), the proposed correlation between 2FAL and DP made by De Pablo is

$$DP_t = \frac{8.88 \times DP_0}{8.88 + 2FAL} = \frac{7100}{8.88 + 2FAL} \tag{3.42}$$

In another work X. Chendong applied regression analysis to the gathered data and gave the following relationship between furfural content and DP [64]

$Log_{10}\left(2FAL\left[mg/l\right]\right) = 1.51 - 0.0035 \cdot DP$, or

$$DP = \frac{1.51 - Log_{10}(2FAL)}{0.0035} \tag{3.43}$$

The original reference uses "Fur" to define the furfural content of 2FAL and "D" for DP. Equation (3.43) has been altered to follow common nomenclature. The different units to measure 2FAL must be observed for proper evaluation or comparison between Equations (3.42) and (3.43). Of course, these are not the only documented relationships. There are also other applicable equations to be evaluated further. The research team of S. D. Myers suggested the following expression:

$$DP = \frac{1.17 - Log_{10}(2FAL))}{0.00288} \tag{3.44}$$

Pahlavanpour proposed other relationship[16] [46] :

$$DP_t = \frac{DP_0}{(0.186 \times 2FAL) + 1} \tag{3.45}$$

The equations described above have one limitation. The experimental work is specifically meant for thermally upgraded insulation (65°C temperature rise). Therefore, these equations may mislead the investigation and data as the Oil-Immersed CTs are of non-thermally upgraded insulation as per IEEE C57.13.

The work of Stebbins, et al. in [63] included the study of non-thermally upgraded paper. In the conclusions authors indicate that thermally upgraded paper generated substantially lower furanic compounds concentrations and that furanic compounds demonstrated lower stability in insulating liquids spiked with dicyandiamide. Furthermore, a revised equation for predicted DP from Total Furanic Compounds for transformers with thermally upgraded paper is given by

[16] B. Pahlavanpour, "Power Transformer Insulation Ageing," CIGRE SC 15 Symp., Sydney, Australia, 1995.

$$DP = \frac{Log_{10}\left(Total\ Furans\right) - 4.0355}{-0.002908} \tag{3.46}$$

In the same reference a modification of the Chendong equation (3.43) is given for transformers without thermally upgraded paper, using 2FAL content in ppb by weight (µg/kg) becomes

$$DP = \frac{Log_{10}\left(2FAL_{\left[\mu g/Kg_{OIL}\right]} \times 0.88\right) - 4.51}{-0.0035} \tag{3.47}$$

Equation (3.47) needs to be modified to address parts per billion, weight to volume (µg/L). For the dielectric oil used in the experimental units, $1\left[\mu g/L_{OIL}\right] = 1.11544\left[\mu g/Kg_{OIL}\right]$. Thus, the equation applicable for the quantities reported by DOBLE Laboratory is

$$DP = \frac{Log_{10}\left(2FAL_{\left[\mu g/L_{OIL}\right]} \times 0.88 \times 1.11544\right) - 4.51}{-0.0035} = \frac{Log_{10}\left(2FAL_{\left[\mu g/L_{OIL}\right]} \times 0.981587\right) - 4.51}{-0.0035} \tag{3.48}$$

The analysis of Equation (3.48) indicates that $DP_0 = 1200$ was used for DP estimation.

M. Dong et al. in [66] reviewed the relationship between 2FAL and DP, but also provide an additional expression correlating furfural content with water content (w) and the time of operation (a) expressed in years. The relationship is given as

$$Log_{10}\left(furfural\right) = -0.148 + 0.01w + 0.02a \tag{3.49}$$

Water is a product of degradation and so the moisture level in the paper increases with ageing by 0.5% every time the DP of the cellulose is halved by degradation [65], resulting in a decrease in electrical strength.

$$water\ concentration = \frac{0.5 \cdot \log\left(\frac{DP_0}{DP_t}\right)}{\log 2} \tag{3.50}$$

For further verification of the values obtained during experimentation, it is important to indicate that the 2FAL values provided by the third party laboratory were expressed in (ppb) or (μg/L). Therefore, careful analysis is required when using these equations as units may differ from one author to another. The dielectric oil used in the experimental units is CrossTrans 206. Specific information regarding weight and conductivity were addressed to the manufacturer who confirmed the following:

"CrossTrans 206 is not a pure compound so the density will vary. Average specific gravity at 60F/60F was 0.8966 with a range of 0.8961 to 0.8984. Average lbs/gal was 7.466 with a range of 7.448 to 7.481. Relative Permittivity [Dielectric Constant] per ASTM D924 at 2.2 @ 25C. CrossTrans 206 would be around 2.2 - 2.3."

Based on the information above, $1\left[\frac{\mu g}{L_{OIL}}\right] = 0.001115\left[\frac{mg}{Kg_{OIL}}\right]$.

Life prediction from DP measurements can be empirically related to insulation condition. Nevertheless, the procedure involves a series of problems.

- The unit should be offline and the sampling procedure requires draining the dielectric oil.
- The sampling procedure may be destructive to the integrity of the solid insulation.
- The rates of hydrolytic and oxidative degradation of paper depend on accessibility of the reactants to the interior of the insulation. It has been demonstrated that the rate of degradation varies across the thickness and is greatest in the inner layers [65].

By using nondestructive and non-invasive Furanic Compound Analysis, whose procedure does not require offline conditions, DP can be estimated and therefore, age predicted.

CHAPTER 4

EXPERIMENTAL WORK

4.1 Background

In the context of this research work, thermal stress was the only fundamental ageing acceleration factor which was to be generated by means of typical and non-typical load profiles and long-term overloading conditions. To carryout the accelerated ageing process under laboratory conditions by means of thermal stress, a heat run load bed configuration was designed and put in place. Part of the implementation of this test set up was to modify the factory typical current transformer design, adding top entry threaded fittings on the tank cover and additional piping and fittings to the drain valve for the addition of DGA instrumentation. The secondary terminal box had to be modified to incorporate a set of terminal for the internally located thermocouples and using wall penetrators, the fiber-optic sensors were connected to the external interface.

The same technical approach was used for all experimental units. Age of the units reached different values to be compared against Normal Insualtion Life defined as per IEEE standards [3].

In this chapter, a complete description of the experimental setup, testing procedures carried out on the experimental units and the obtained results are presented independently for each specific unit. Results of each test are summarized and compared against the loss-of-life values.

4.2 Experimental Setup

The equipment specifically designed under project specifications was installed in the designated area at the High Voltage / High Current Lab at Tennessee Technological University where a monitoring area and the testing area were prepared to provide safe operation of the devices during experimentation.

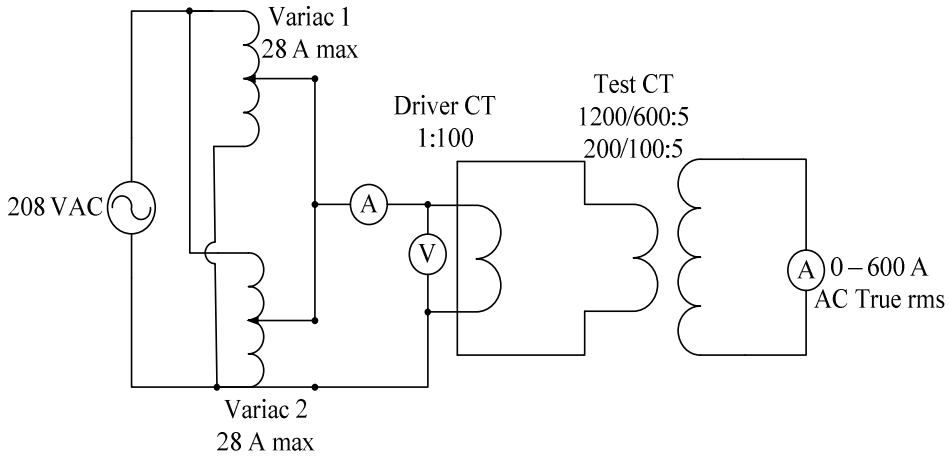

Fig. 13. CT Loading Bed (Experimental Setup) - Connection Diagram

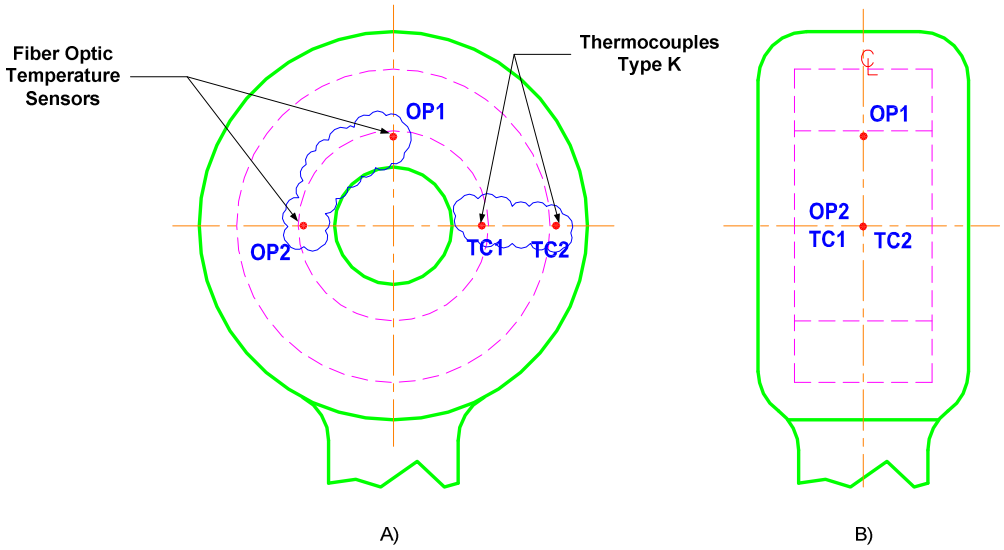

Fig. 14. Location of Temperature Sensors. (A) Front View Cross Section, (B) Side View Cross Section

The experimental setup shown in a simplified connection diagram in Fig. 13 provided a simple though accurate way to thermally stress the unit under test (UUT) according to selected profiles that will be presented later in this chapter.

The analysis of thermal parameters was conducted in accordance with IEEE standards [1, 3]. Therefore, the technical requirements submitted to the CT manufacturer included the addition of temperature sensors surrounding the core of the CT. The location of these sensors is shown in Fig. 14.

In Fig. 14, OP1 and OP2 represent the Optical Fiber sensors and, TC1 and TC2 represent the thermocouples embedeed between the core and the secondary winding of the Current Transformer, and TOT corresponds to the thermocouple measuring the Top-Oil temperature on the liquid insulation. In the context of the dissertation the sensors description (OP1, OP2, TC1, TC2, TOT) will be used to represent that measured values presented in figures or tables were obtained by the use of these specific sensors.

In order to visualize the thermal dynamics of the system under different load levels, state-of-the-art technology was used for online monitoring of the temperature variations. The fiber-optic system manufactured by Luxtron – Lumasense interfaces with the ThermAsset2 Controller. ThermAsset2 most important system specifications are summarized in Table 13.

Table 13. ThermAsset2 Specifications

Feature	**Enumeration**
Number of Channels	4
Temperature Range	-30 to +200 °C
Accuracy	± 2 °C
Serial output	RS-232
Temperature Data Storage	Retains 90 days at 1 reading/minute and max Temperature each channel retained until reset by user
Probes	Luxtron Ruggedized Probes

Temperature measurement is based on the fluorescence decay time of a special phosphor sensor, located at the end of a fiber-optic cable as shown in Fig. 15. Light generated by an excitation LED is routed through a probe extension and connectors, where it falls on the phosphor material at the probe tip.

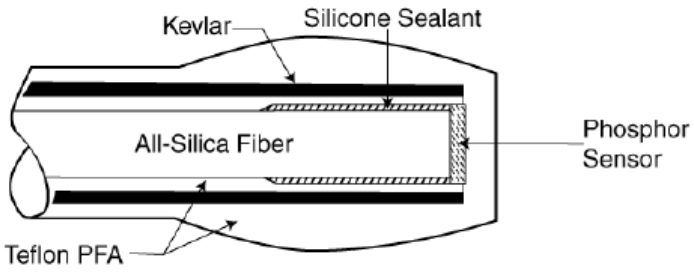

Fig. 15. Fiber-optic Probe Design [67]

The way the system was connected to the CT is shown in Fig. 16.

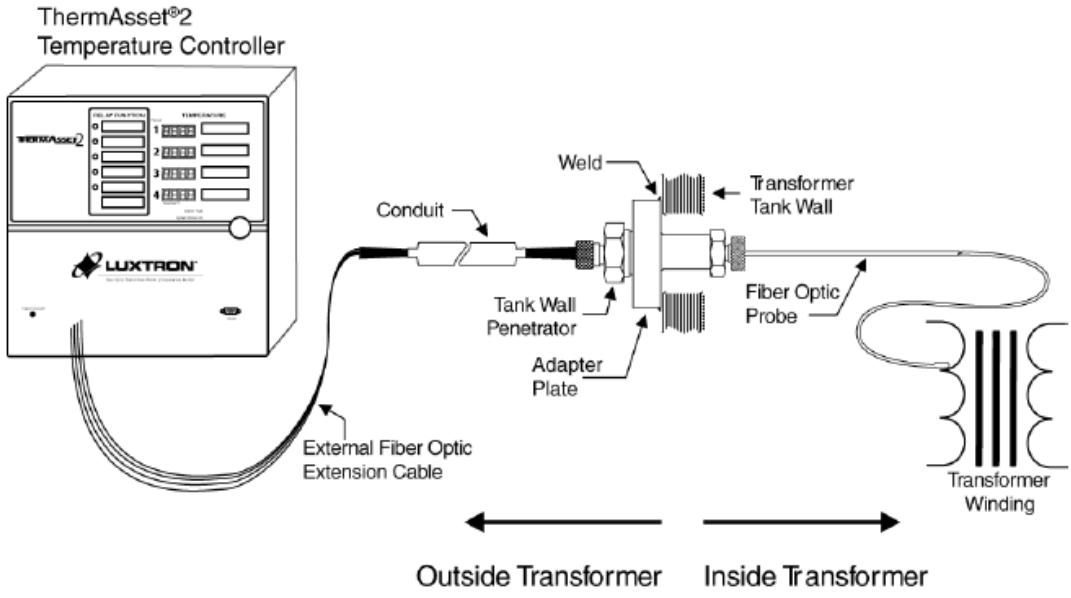

Fig. 16. ThermAsset2 System Assembly Diagram [67]

When stimulated with red light, the phosphor emits radiation over a broad spectrum in the near infrared region. The time required for the fluorescence to decay is dependent upon the phosphor temperature. After the LED is turned off, the decaying fluorescent signal continues to transmit through the fiber to the instrument, where it is focused onto a detector. The signal from the detector is amplified and sampled after the LED is turned off. The measured decay time is then converted to temperature, using the built-in instrument lookup table. The other sensors used for temperature recording were Type K thermocouples, manufactured by RTD Company, having the following specifications.

Temperature Range	Standard Limits of Error	Special Limits of Error
0 to 1250 °C	+/-2.2°C or 0.75%	+/-1.1°C or 0.4%

The above described thermocouples were connected to a PC via a National Instruments data acquisition system using NI 9211 4-Ch ±80 mV, 14 S/s modules. A simplified diagram of the temperature monitoring system is shown below in Fig. 17.

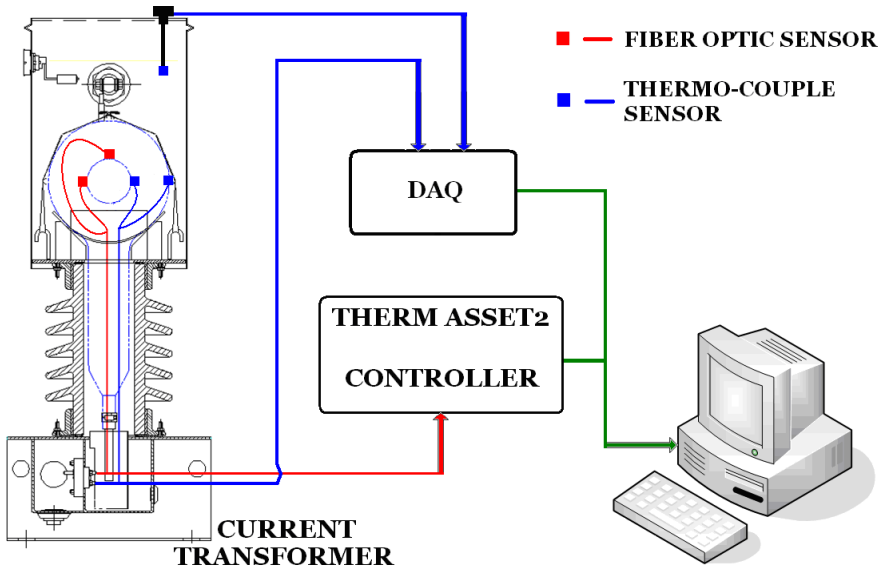

Fig. 17. Temperature Data Acquisition System – Simplified Diagram

The load on CT was manually set by means of regulating the output voltage of the autotransformers (Variacs) which allowed voltage regulation of the input power supply and control of the driver CT's current output, therefore, of the current at the high voltage terminals of the UUT. The experimental setup description, its operation and the readings obtained during a 24-hour loading profile were presented during the 39th North American Power Symposium [68]. Characteristics of the Oil-immersed Current Transformers and Driver CTs are summarized in Table 14.

Technical specifications of all the equipment used to carry out testing procedures on the CTs are not described within the context of this Chapter, but are included in Appendix B. Accuracy of the testing equipment used for this work was certified by the manufacturer's calibration certification.

Table 14. Instrument Transformers Nameplate Data

	OIL IMMERSED CURRENT TRANSFORMERS TYPE COF-350											
Parameters	**I_{pr} (A)**	**I_{sec} (A)**	**Connection**	**Ratio**	**NSV (kV)**	**R.F.**	**BIL (kV)**	**Acc.**	**Freq. (Hz)**	**Tot. WT. (lb)**	**Oil Vol. (Gal)**	**Rise °C**
CT1 & CT2	1200	5	X1 – X3	240:1	69	1.5	350	0.3B1.8	60	450	15	55
	600	5	X2 – X3	120:1		2.0						
CT3 & CT4	200	5	X1 – X3	40:1	69	1.5	350	0.3B1.8	60	450	15	55
	100	5	X2 – X3	20:1		2.0						
	DRIVER CURRENT TRANSFORMERS TYPE RM-D1											
Parameters	**I_{IN_MAX} (A)**	**I_{OUT_MAX} (A)**	**Connection**	**Ratio**	**NSV (kV)**		**BIL (kV)**		**Freq. (Hz)**		**Rated Voltage (VAC)**	
DCT	35	3500	X1 – X2	1:100	0.6		10		60		240	

4.3 Thermal Modeling Experimental Results

Four CTs were subjected to step load changes, one 24-hour load profile, and two ramp load profiles (2.0 p.u. and 3.0 p.u.) on full-turns ratio. Tests consisted of a start-up period during which rated current was passed for duration sufficient to bring TOT and HST to steady state such that their measured values stopped changing for over an hour.

The equipment connected as shown in Fig. 13 was used as a heat run test bed, operating as described in Section 4.2. The outcome of this experimental and analytical work [69] was recently submitted for approval for publication in the IEEE Transactions on Power Delivery.

4.3.1 Step Profiles

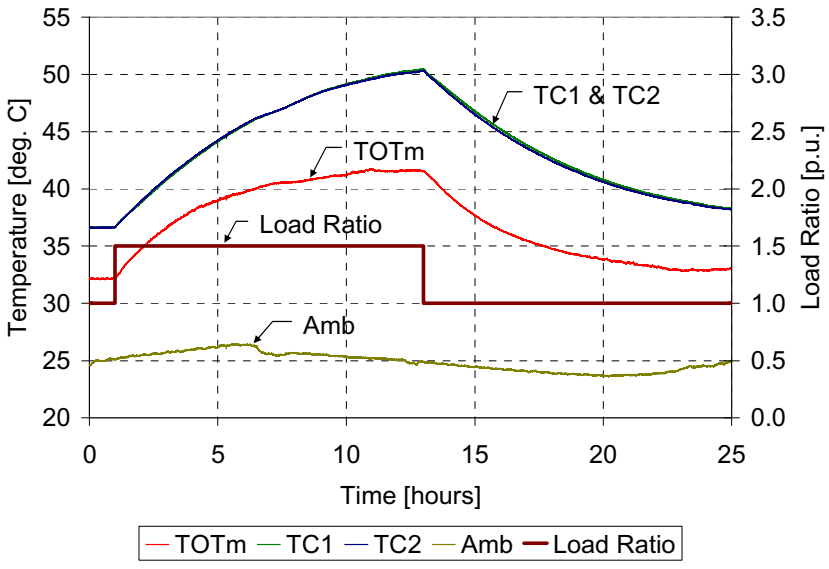

Fig. 18. 200/5A CT, Step Load Profile - Measured HST and TOT

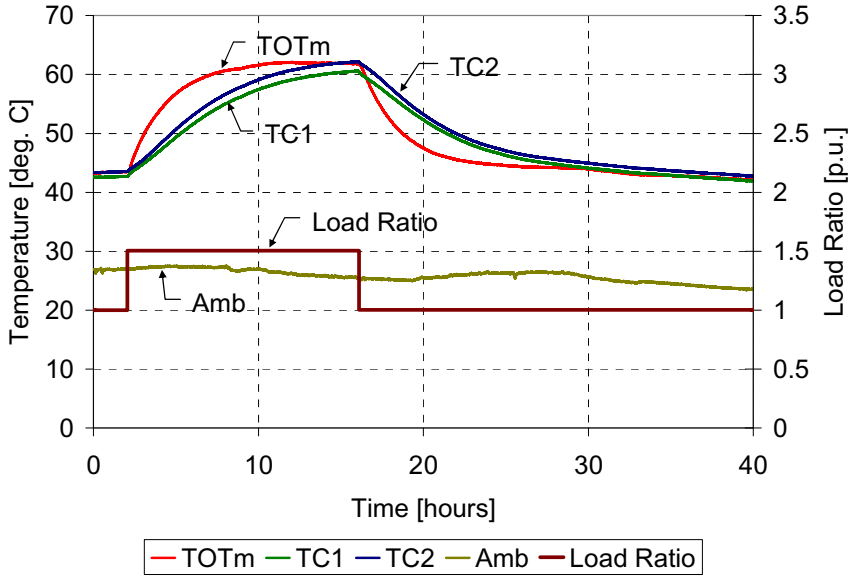

Fig. 19. 1200/5A CT, Step Load Profile - Measured HST and TOT

Figures 18 and 19 show the measured TOT (TOTm) and HST step load profiles for a 200/5A and for a 1200/5A CT, respectively. The step load profiles were used to determine the input parameters for modeling. Equations (2.20) and (2.24) were used to model TOT and HST, respectively. In the following figures measured HST by thermocouples is shown as TC1 and TC2 (see Fig. 14) and measured TOT by thermocouple is TOTm.

4.3.2 Twenty-four Hour and Ramp Profiles

The 24-hour load profile defined in Table 15 and two different ramp profiles defined in Table 16 and Table 17 were used for the predictive tests. Temperature profiles as a function of time for these three current profiles were recorded from all the embedded sensors and are presented in Figures 20 to 23.

Table 15. 1.5 p.u. max 24-hour Load Profile used for CT Testing

Load (p.u)	1.1	1.5	1.1	1.4	1.3	1.1	1.0	1.1
Time (Hrs)	0-3	3-4	4-9	9-10	10-17	17-19	19-22	22-24

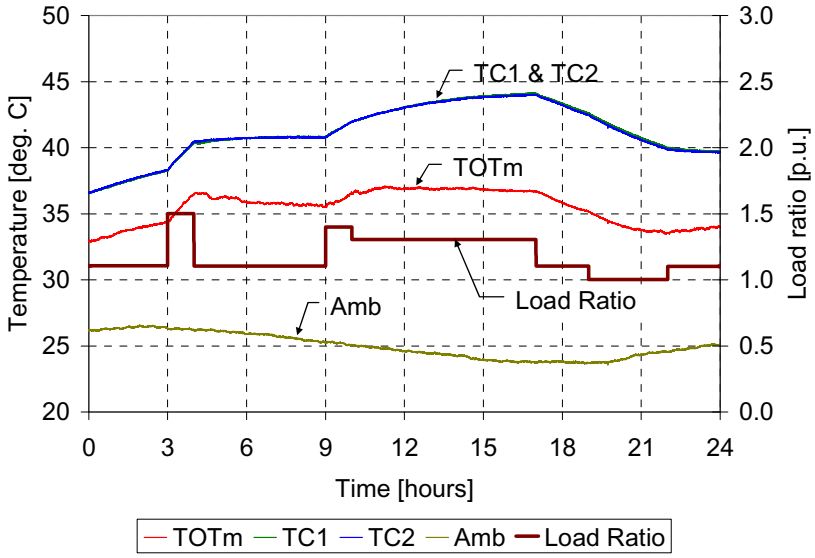

Fig. 20. 200/5A CT, 24-hour Load and Temperature Profile

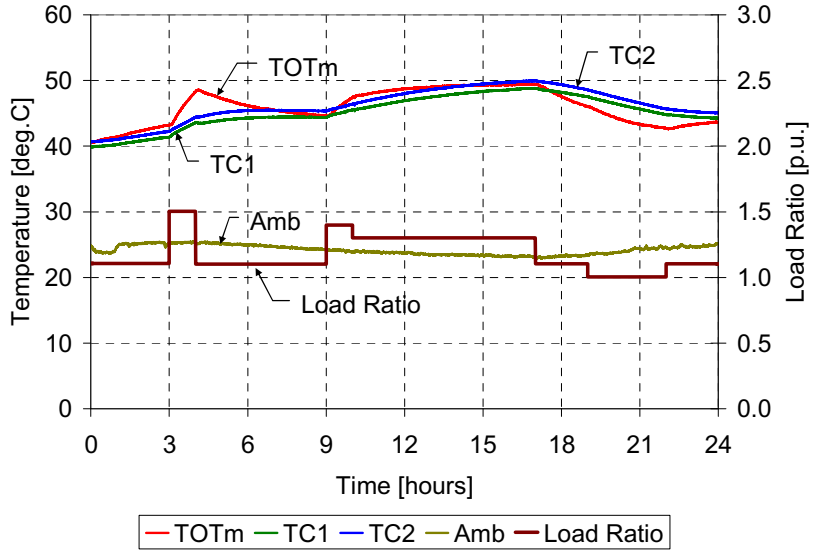

Fig. 21. 1200/5A CT, 24-hour Load and Temperature Profile

Table 16. 2.0 p.u. Max Ramp Load Profile used for CT testing

Load (p.u)	0.5	0.8	0.7	0.9	1.1	1.2	1.4	1.6
Time (Hrs)	0-1	1-4	4-8	8-10	10-17	17-18	18-19	19-20
Load (p.u)	1.8	2.0	1.8	1.6	1.4	1.2	1.0	
Time (Hrs)	20-21	21-22	22-23	23-24	24-25	25-26	26-40	

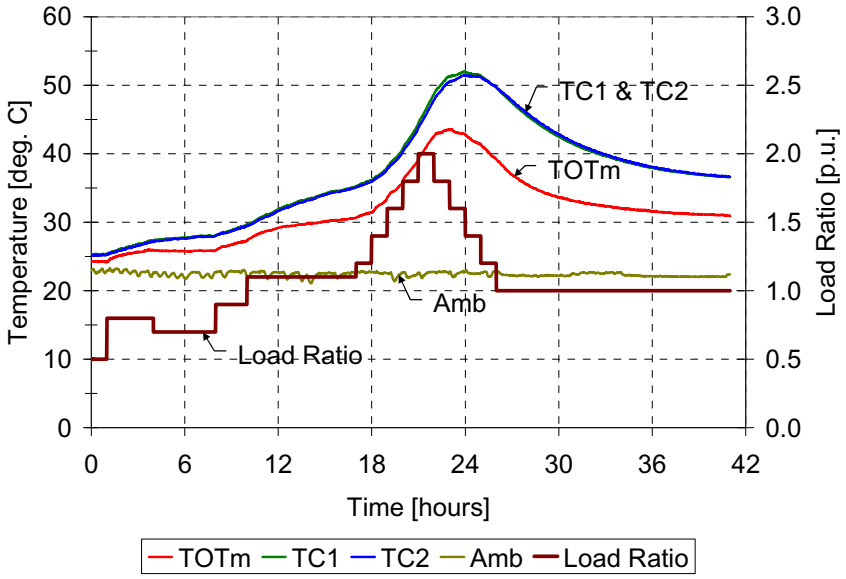

Fig. 22. 200/5A CT, 2.0 max Ramp Load and Temperature Profile

Table 17. 3.0 p.u. Max Ramp Load Profile used for CT testing

Load (p.u)	0.0	0.5	1.0	1.5	2.0	2.5	3.0
Time (Hrs)	0-3	3-6	6-9	9-12	12-15	15-18	18-21
Load (p.u)	2.5	2.0	1.5	1.0	0.5	0.0	
Time (Hrs)	21-24	24-27	27-30	30-33	33-36	36-50	

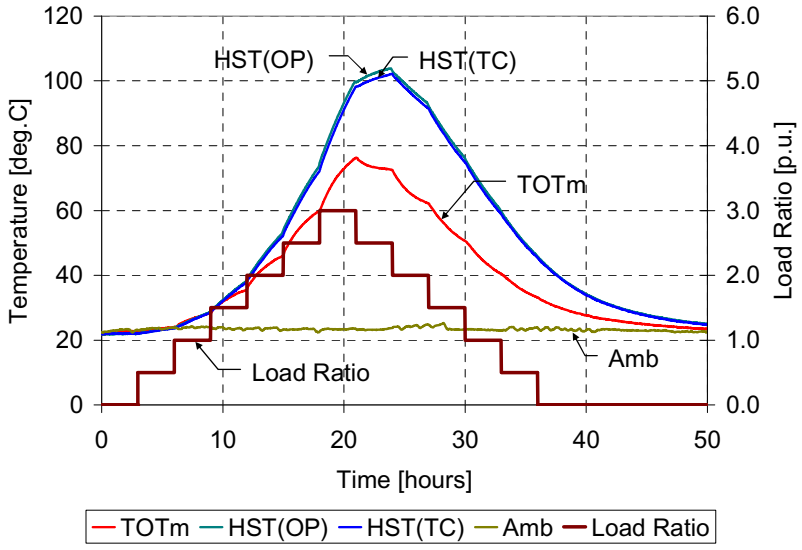

Fig. 23. 200/5A CT, 3.0 max Ramp Load and Temperature Profile

It can be observed from Figures 20 to 23 that the HSTm (Hot-Spot Temperature measured, represented by TC1 and TC2) remained above TOTm (Top-Oil Temperature measured) at all values of load current. However, in the higher ratio CT (1200/5) the TOTm rises faster than the HSTm (Fig. 19, Fig. 21). This thermal behavior where TOT stays above HST is similar to that observed in the power transformers [70]. It can be attributed to the presence of relatively higher copper losses in the primary winding as compared to the core losses. Therefore, Hot-Spot seems to lie closer to the region where primary winding touches the secondary winding in the inner window of the toroid. This observation may require further investigation. In lower ratio (200/5) CT, the HST is definitely deep inside the winding and much closer to the core of the transformer, as expected.

4.3.3 Estimation of TOTM Parameters and Predicted Values

Temperature profiles shown in Figures 18 and 19 (i.e. step load profile) were used for the estimation of parameters for this model. Table 18 shows the estimated TOTM parameters derived from Equation (2.20).

The required parameters in the TOT model (TOTM) were estimated by nonlinear least square technique using the following objective function:

$$Minimize: \sum_{t=1}^{p} \frac{1}{2}\left[F\left(\bar{z}\right)_t - \theta_m(t)\right]^2 \tag{4.1}$$

Where $F\left(\bar{z}\right)_t$ is the calculated temperature using equation (2.20), $\bar{z}$ is a vector whose elements are the parameters being estimated, p is the total number of temperature samples and $\theta_m(t)$ is the measured temperature at time t. A temperature sample was collected at different time intervals over at least 24 hours.

Table 18. Top-Oil Temperature Model Parameters

CT Ratio	$\tau_{TO,R}$	R	$\Delta\theta_{TO,R}$	n	K_1	K_2	K_3
200/5A	4.25	3.875	7.75	1.135	0.996	0.024	0.006
1200/5A	2.88	5500	16.9	0.92	0.999	0.009	1.7E-06

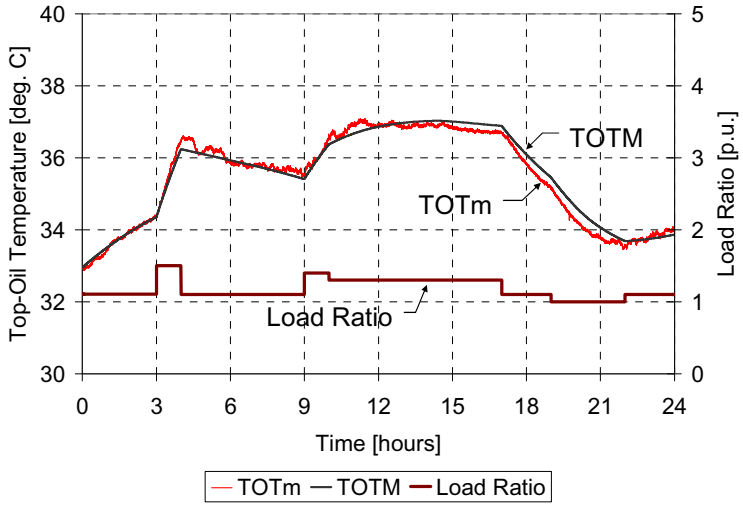

Fig. 24. 200/5A CT, TOT measured vs. TOT Model for 24-hour load profile

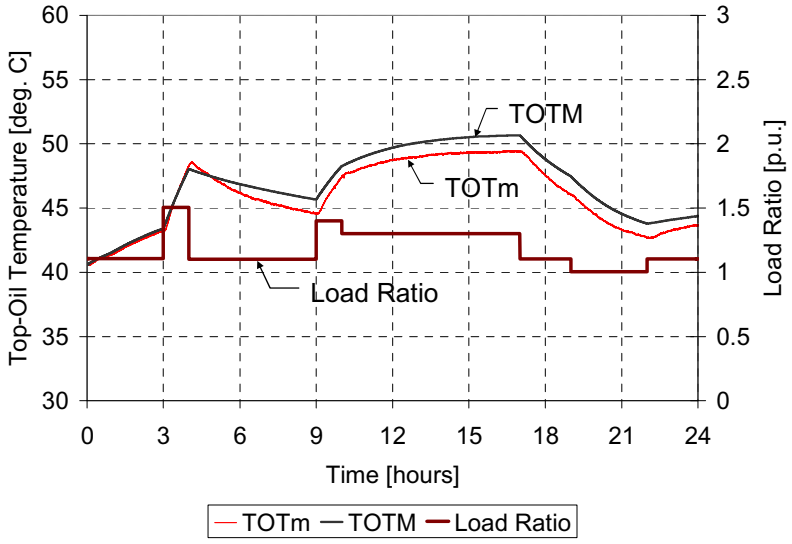

Fig. 25. 1200/5A CT, TOT measured vs. TOT Model for 24-hour load profile

Figures 24 to 27 show results of the model after applying the parameters indicated in Table 18 to the 24-hour load Profile, 2.0 p.u. max, and 3.0 p.u. max ramp profiles.

The ramp profiles were used exclusively on 200/5A CTs. Measured values of temperature (TOTm) for a particular load profile are also shown in each figure for quick comparison. A reasonably good agreement between measured and modeled values of TOT can be observed at these overload profiles.

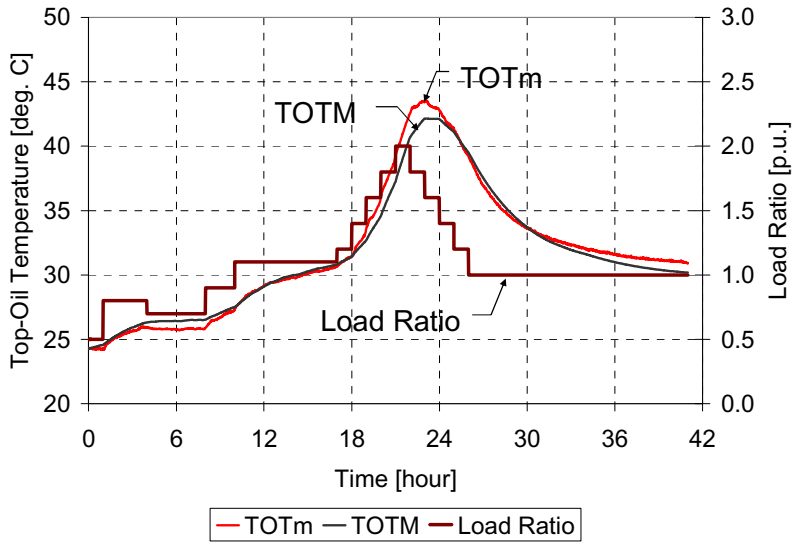

Fig. 26. 200/5A CT, TOT measured vs. TOT Model for 2.0 p.u. max ramp profile

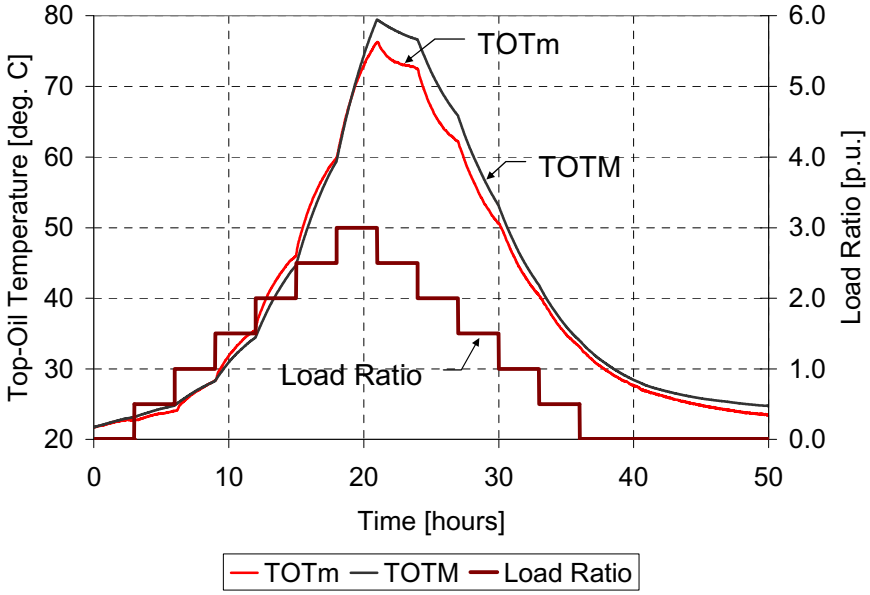

Fig. 27. 200/5A CT, TOT measured vs. TOT Model for 3.0 p.u. max ramp profile

Table 19. Top-Oil Temperature Model Maximum Variation (°C)

Load Profile		1.5 p.u. 24-hour	2.0 p.u. Ramp	3.0 p.u. Ramp
CT Ratio	200/5A	0.566	2.091	5.107
	1200/5A	1.514	-	-

Maximum variation in the value of the Top-Oil Temperature model against measured value is presented in Table 19.

4.3.4 Estimation of HSTM Parameters and Predicted Values

Temperature profiles shown in Figures 18 and 19 were used to estimate HSTM parameters. Table 20 shows the estimated parameters for this model for 200/5A and 1200/5A CTs as per Equation (2.24).

The required parameters in the HST model (HSTM) were estimated by nonlinear least square technique using the same objective function as for TOTM parameter estimation (4.1).

For power or distribution transformers (sub-station type), TOT is normally obtained from the temperature sensors located in the units, but this is not the case for CTs. Normally Oil-Immersed CTs are not installed with any thermal sensors. Therefore, it is important to validate these parameters obtained from the step load profile against two scenarios: (a) HSTM as a function of measured TOT i.e. TOTm, and (b) HSTM as a function of the previously modeled TOT i.e. TOTM. The results of these scenarios are presented in Figures 28 to 31.

Table 20. Hot-Spot Temperature Model Parameters

CT Ratio	$\tau_{W,R}$	R	$\Delta\theta_{H,R}$	m	K_1	K_2	K_3
200/5A	2.8	3.875	5.15	0.955	0.994	0.024	0.006
1200/5A	2.5	5500	0.05	0.9	0.999	3.3E-05	6.0E-09

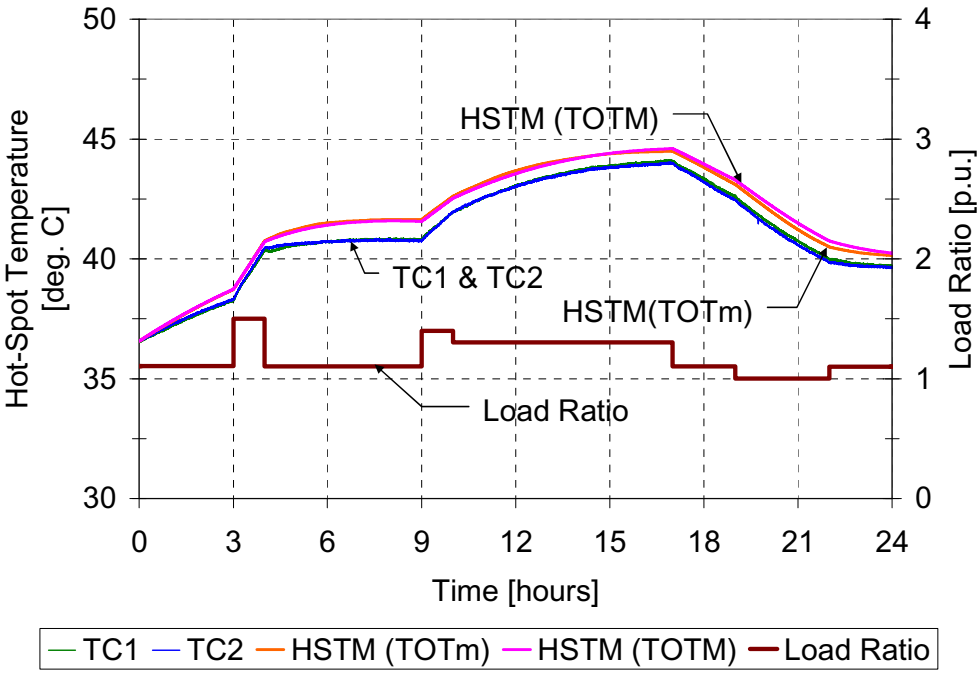

Fig. 28. 200/5A CT, HST measured vs. HST Model 24-hour load profile

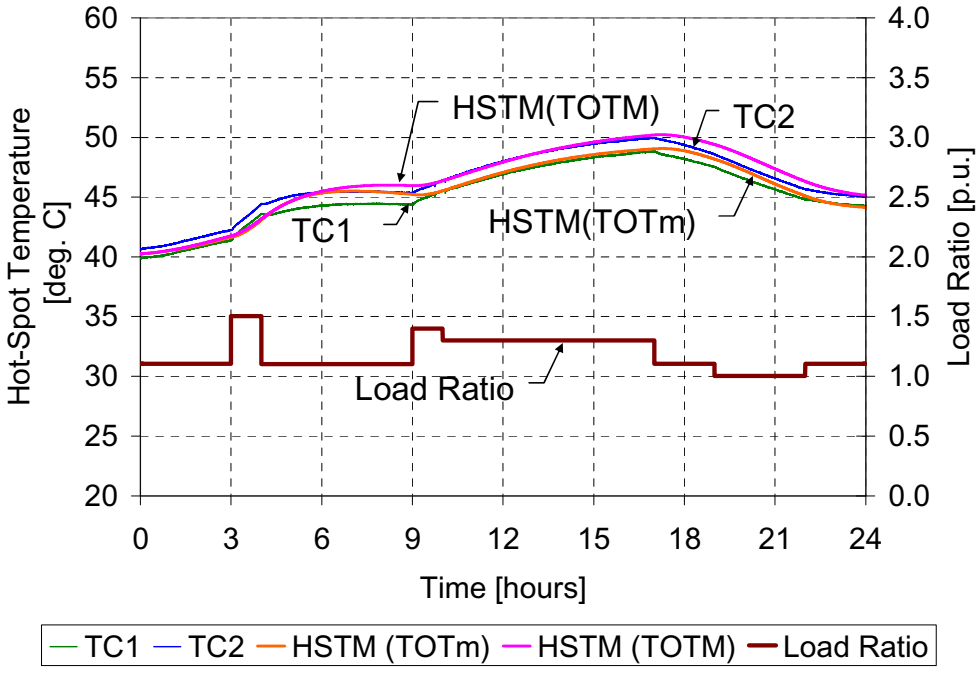

Fig. 29. 1200/5 CT, HST measured vs. HST Model for 24-hour load profile

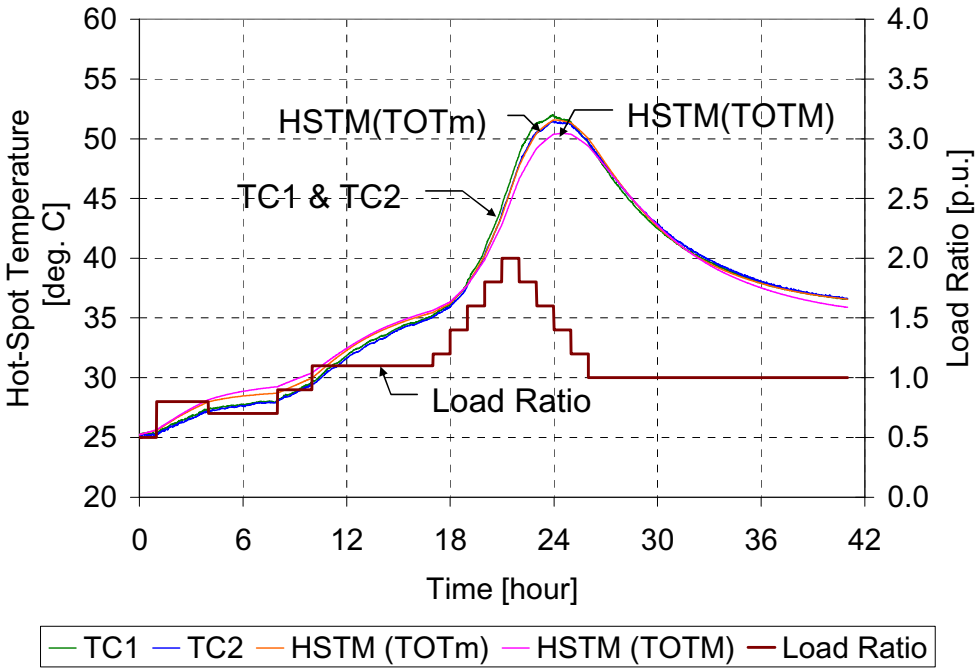

Fig. 30. 200/5A CT, HST measured vs. HST Model for 2.0 max ramp profile

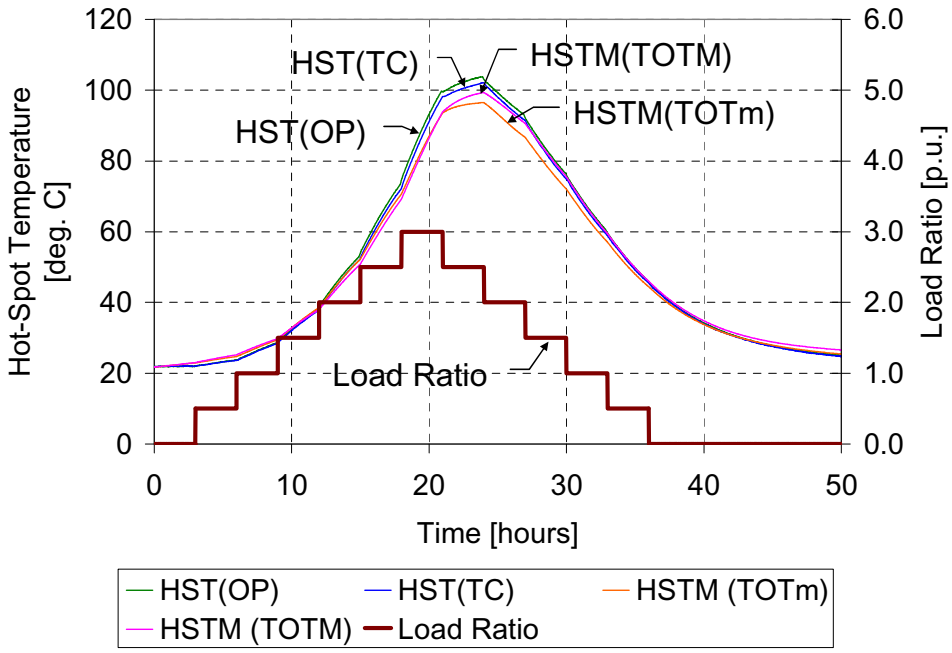

Fig. 31. 200/5A CT, HST measured by fiber-optic sensors (OP) and thermocouples (TC) vs. HST Model for 3.0 max ramp profile

Table 21. Hot-Spot Temperature Model Maximum Variation (°C)

		HSTM (TOTm)			HSTM (TOTM)		
Load Profile		1.5 p.u. 24-hour	2.0 p.u. Ramp	3.0 p.u. Ramp	1.5 p.u. 24-hour	2.0 p.u. Ramp	3.0 p.u. Ramp
CT Ratio	200/5	0.901	0.820	5.652	1.053	1.909	4.722
	1200/5	0.943			1.485		

Once again, a reasonably good agreement between HST obtained from a TOT measurement, HST obtained from a TOT model, and actual measurement of HST can be observed in all these figures at overloads ranging from 1.5 p.u. to 3.0 p.u. in different current profiles.

Maximum variation in the two modeled values of Hot-Spot Temperature against measured value is presented in Table 21.

4.4 Ageing CT2 - Experimental Work, Results, and Discussion

The first unit put under thermal accelerated ageing was CT2 (1200/600:5, 69kV) whose technical characteristics are described in Table 14. Typical load profiles provide a daily average load of 85% of the loading rate as illustrated in [3]. Note that non-typical profiles used for thermal accelerated life testing will maintain an average load greater than 100%.

The technical approach considered in this work involved the application of constant non-typical load profiles to thermally stress the UUT. CT2 was loaded @ 300% rated load (I_p = 3600 A) for 169 hours. The work was presented during the International Symposium on Electrical Insulation (ISEI) 2008 Conference in Vancouver [71].

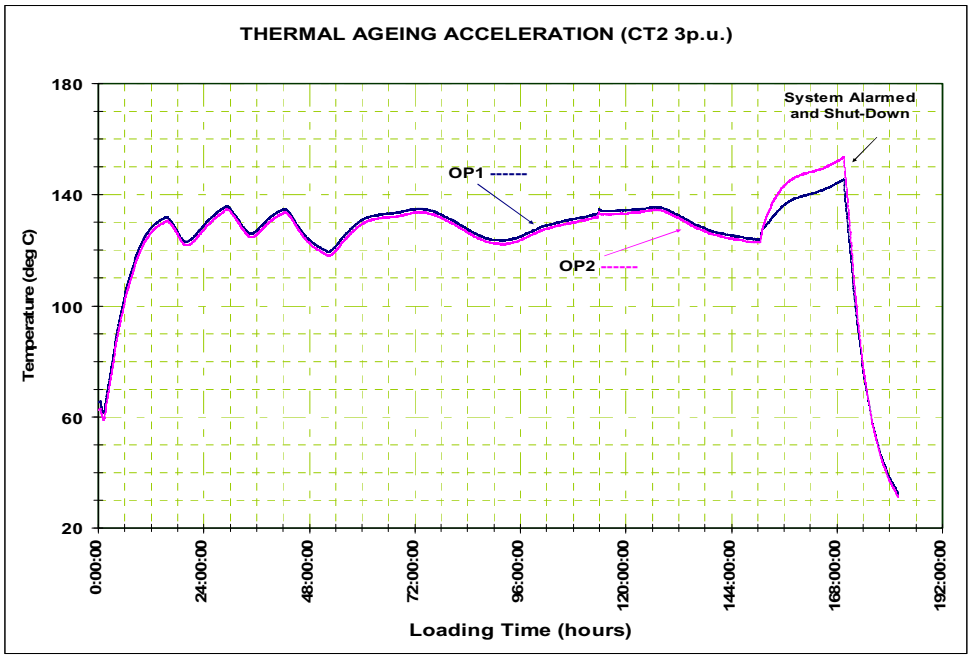

Fig. 32. CT2 Hot-Spot readings at 300% load

The simulated load was the controllable variable to stress the sample. Each of the profiles used for experimentation provided valuable data by means of uncontrolled observed variables (Ambient Temperature, TOT and HST). Temperature curves presented in [68] did not include the non-typical 300% load profile, which is presented in Fig. 32.

In order to avoid emergency conditions, the system was monitored 24/7 and shut down when θ_H reached the critical temperature of 150ºC. The observed temperature fluctuation was mainly due to variation of ambient temperature in the laboratory.

To visualize the effect of each loading profile on the condition of the CT, the following tests were carried out: Complete CT Functional, DC Insulation Tests, Furanic Compound Analysis (ASTM D 5837), Degree of Polymerization, Online Hot-Spot Temperature monitoring, and Online Dissolved Gas Analysis.

Each test provided information on one specific parameter, as described below.

4.4.1 DC Testing on CT2

A summary of all data obtained from DC tests carried out with the MEGGER S1-1052 tester is presented in

.

The simplest Insulation Test, Insulation Resistance (IR), or Spot Test indicated a clear variation of the resistance value after loading the unit at 300% rated load. The Insulation Resistance became approximately 20% of the initial value. The Polarization Index (PI) values were computed according to Equation (3.4).

4.4.2 Analysis of the Functional Parameters on CT2

The OMICRON CT Analyzer was used to run a complete functional test of the unit. The readings obtained are shown in Table 23.

Table 22. CT2 Summary of Insulation DC Tests Data

	I R (TΩ)	**P I**
Before Loading	1.14	1.88
After 169h @ 300% load	0.22	2.55

Table 23. CT2 Functional Parameters Analysis

Parameter	**Before Loading**	**After 169h @ 300% load**
Knee Point excitation	194.4V; 69.20mA	195.1V; 68.95mA
Ratio	1200:5.0011	1200:5.0023
RCF	0.99978	0.99953
Phase displacement	1.43 min	1.42min

4.4.3 Dissolved Gas Analysis on CT2

The loading process was recorded using the SERVERON TM-8 Dissolved Gas Analysis (DGA) online monitor. Its closed loop repeatable oil collection process is used in Oil-Immersed Instrument Transformers for the first time. The readings obtained from this device are presented in Fig. 33.

At 300% load, there is a clear increase of CO and CO_2 in the oil. The increase in CO and CO_2 is typical for insulation that has aged in service. Other gases such as Methane, Ethylene and Ethane came into picture in small amounts. These are so-called "hot-metal" gases (produced in the surrounding oil).

Hydrogen was never observed alone during the loading process. Therefore, only temperature-dependant Key Ratios (KR) were worth calculations following CIGRE SC15 equations (See Section 3.4.1).

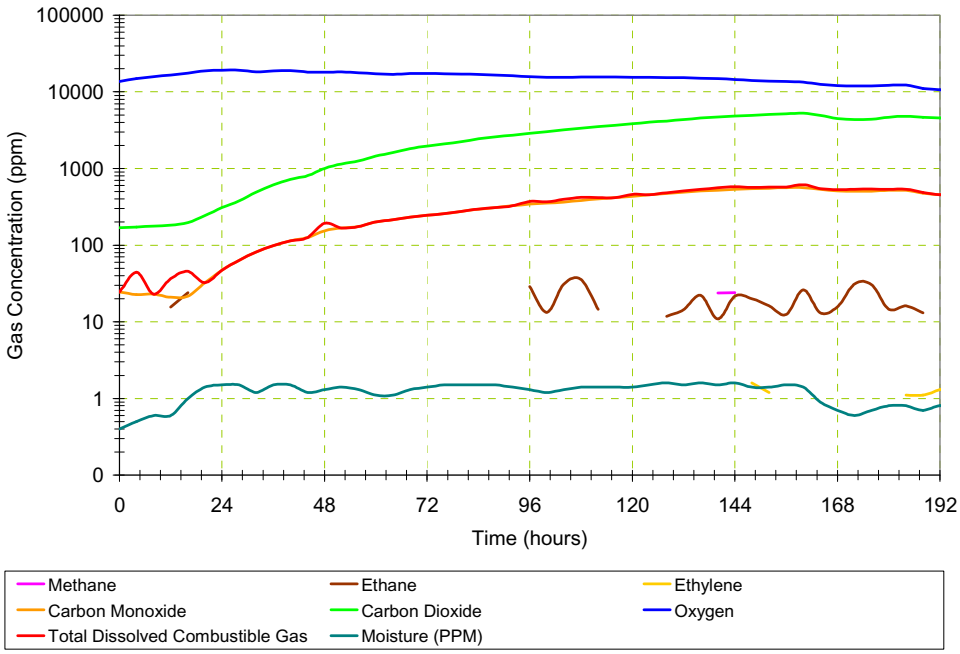

Fig. 33. CT2 Gas evolution during the 300% Load Profile

$$KR_3 = \frac{C_2H_4}{C_2H_6} = \frac{1.5}{16.2} = 0.0926$$

$$KR_4 = \frac{CO_2}{CO} = \frac{4499.8}{448.2} = 10.04$$

The values obtained for KR_3 and KR_4 are indicative of the thermal process in the transformer since $KR_3<1$ is interpreted as thermal fault < 300°C (as per IEC 60599-1999) and KR_4 >10 indicates cellulosic degradation (as per CIGRE SC15).

4.4.4 Degree of Polymerization and Furanic Compound Analysis on CT2

The Furan compound analysis is an industry standard test which allows a comparative value of the various tests carried out in the laboratory. Oil and insulation paper samples were taken and analyzed in a third party laboratory. The results are shown in Table 24.

The estimated DP and % remaining life value obtained from the D 5837 analysis from the laboratory only uses the Chendong equation (3.43). As a practical rule in sealed power transformers with thermally upgraded insulation, 2FAL accumulation greater than 20 μg/L/year is indicative of accelerated ageing.

The functional parameters do not present significant variation. The average Hot-Spot Temperature calculated for the 300% loading profile from Fig. 32 was $\overline{\theta}_H = 128.3\,^oC$. Substituting this measured value of HST in (2.6), F_{AA} was obtained as

$$F_{AA} = \exp^{\left[\frac{15000}{368} - \frac{15000}{128.3+273}\right]} = 29.42$$

Table 24. Laboratory Analysis of Furanic Compounds and Degree of Polymerization CT2

TEST DESCRIPTION		Before Loading	After 169h @ 300%
Furanic Compounds Analysis ASTM D 5837 IEC 61198	Hydroxymethyl-2-furfural (HMF) (µg/L)	< 1	3
	Furfuryl Alcohol (FOL) (µg/L)	< 1	< 1
	2-furaldehyde (FAL) (µg/L)	2	67
	2-acetylfuran (AF) (µg/L)	< 1	< 1
	5-methyl-2-furfural (MF) (µg/L)	< 1	< 1
	Estimated DP	1200	764
	Estimated Remaining Life to DP 200 (%)	100	90
Degree of Polymerization	DP	893	1067[a]
	Estimated Remaining Life to DP 200 (%)	97	100 [a]

[a] Paper sample was taken from the bottom of the tank

Finally, substituting the calculated value of F_{AA} into (2.7), %LOL was found. Note that for a DP = 200, the Normal Insulation Life (NIL) is estimated to be 150,000 hours [3]. Thus,

$$\%LOL = \frac{29.42 \times 169 \times 100}{150{,}000} = 3.3146\,\%$$

The Online Dissolved Gas Analysis clearly identified the effect of heat on the chemical composition of the oil. The increase of CO and CO_2 is an indication of thermal degradation of the cellulose material. Key ratios 3 and 4 were calculated and estimated for prolonged load conditions. Resulting values are indicative of thermal fault and cellulosic degradation.

The DC Test indicated a variation of the insulation resistance to approximately 20% of the original value. Nevertheless, the readings indicate an acceptable value of insulation resistance to continue with the unit in operation.

Degree of Polymerization is the criterion used to predict the remaining life of the unit, although ageing of the cellulosic insulation within a current transformer may not be uniform, and the DP test confirms this statement. The location where the paper sample was taken showed no degradation during the process.

From the furan compound analysis, the concentration of 2-furaldehyde (2FAL) is indicative of thermal stress and cellulosic degradation. Laboratory results show an estimated 10% decrease of the Estimated Remaining Life. This value is approximately three times greater than the %Loss-Of-Life calculated in accordance with the Arrhenius expression with the ANSI/IEEE proposed constants. This discrepancy in the results calls for a possible revision of the F_{AA} calculation, or the relationship between DP and Furanic compound.

4.5 Ageing CT1 - Experimental Work, Results, and Discussion

The overall testing / ageing process with CT1 took approximately 8 months. Delays in the experimentation process were subjected to failure of the monitoring devices forcing the test to be put on standby for repair or maintenance. The thermal acceleration ageing process applied to CT1 implied the use of non-typical load profiles in time intervals of 168 hours or greater. After the experience gained from CT2 where a rapid temperature increase suggested thermal runaway, the decision was taken to load the transformer in steps initially of 0.5 p.u. to later reduce those steps to 0.1 p.u. intervals. The unit was connected to the DGA monitoring system that caused cooling; therefore, TOT readings may be somewhat misleading. This is explained in detail later.

In order to provide a thermal profile of the unit based on applicable loads (Rating Factor ± 1 p.u), the unit was loaded *without the DGA system* for approximately 120 hours. The results of this loading process are presented in Fig. 34.

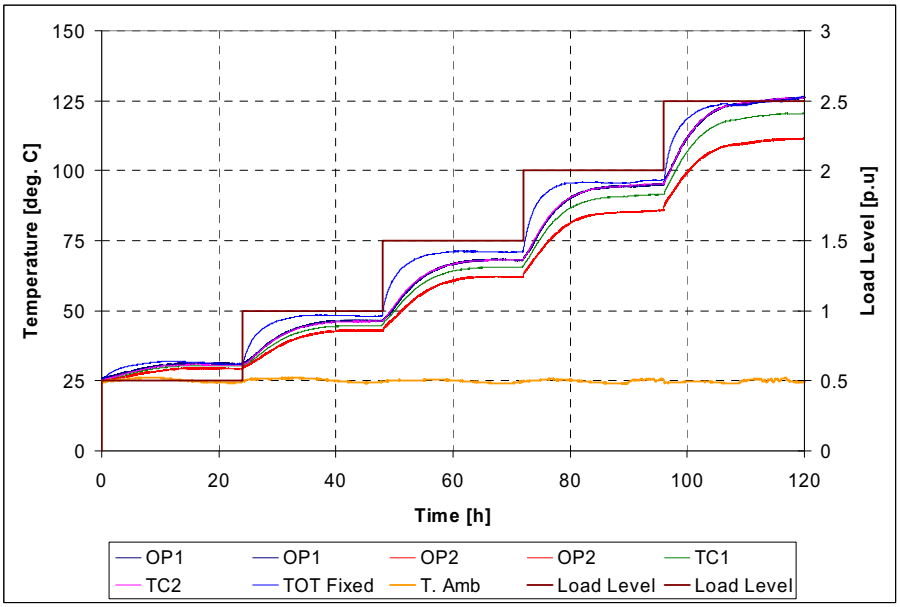

Fig. 34. Thermal Profile of CT1 - Optical Sensors and Thermocouples

It is important to highlight the behavior of TOT. The reaction to load changes is much faster than HST (recorded by OP1-2 and TC1-2) within a 12-hour time interval. This clearly indicates that for this type of transformer, thermal control under real operation could be made by means of TOT data and there will be no need for embedded sensors in the core and secondary winding insulation system. TOT in a long-term operation (over 24 hours) under extreme loading conditions (over 2.5 p.u. load) will not provide the maximum temperature value deep inside the CT structure.

Looking for a solution to the temperature distortion on TOT because of the DGA monitor connection, the idea of a floating sensor came into picture and the results can be observed in Fig. 35, comparing "TOT Fixed" against "TOT Floating" when the unit was loaded at 2.5 p.u.

The idea of defining a continuous correlation between the experimental data and the ageing of the paper insulation was always a priority. Factory-supplied paper samples were added to the core/secondary winding solid insulation structure, as shown in Fig. 36. These samples were removed later during the scheduled testing profiles and sent to the laboratory for DP analysis. The unit

remained in standby until results from the laboratory were received. A detailed description of the experimentation work follows.

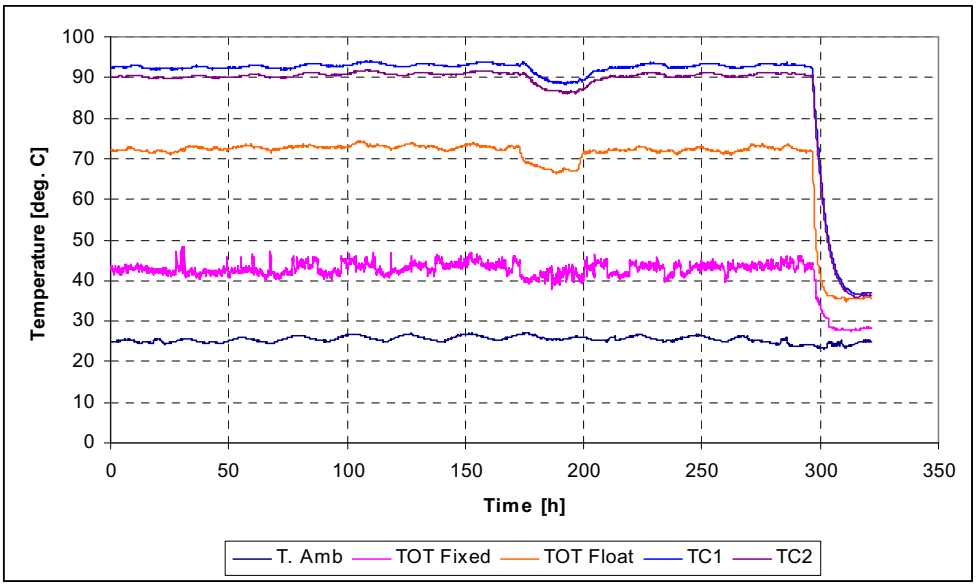

Fig. 35. Observed differences between TOT fixed and TOT floating when loading CT1 @ 2.5 p.u.

Fig. 36. Paper samples located on the top surface of the core/2-ry winding insulation of CT1

4.5.1 DC Testing on CT1

DC tests as described in Chapter 3 were carried out on CT1. The insulation resistance (IR) test was repeated at least twice at each scheduled testing procedure. This allowed obtaining an average reliable value of IR.

Tests were carried out always at 5kV. Laboratory conditions were 23°C ± 3°, and 55 % RH ± 15%. Baseline characteristics are shown in Figures 37 to 40.

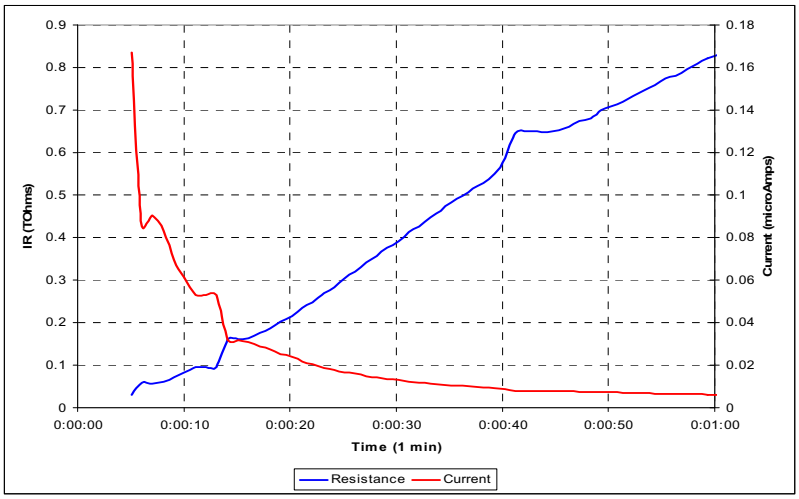

Fig. 37. Insulation Resistance test on CT1 - Baseline Curve

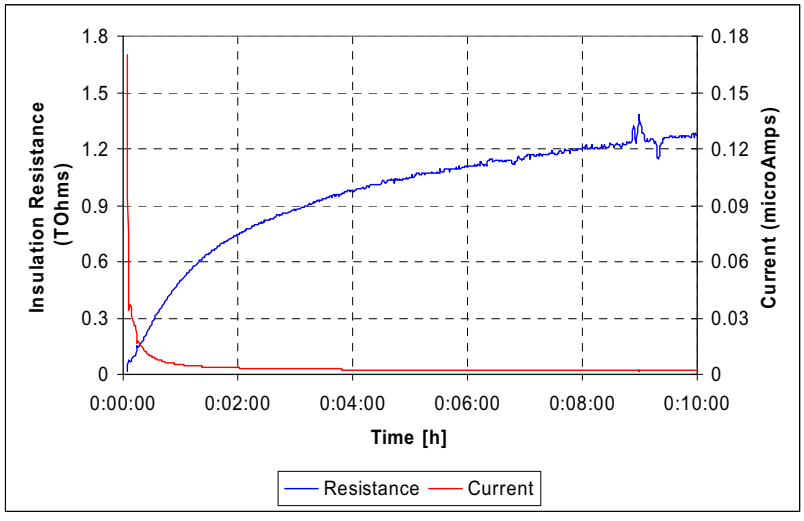

Fig. 38. Polarization Index test on CT1 - Baseline Curve

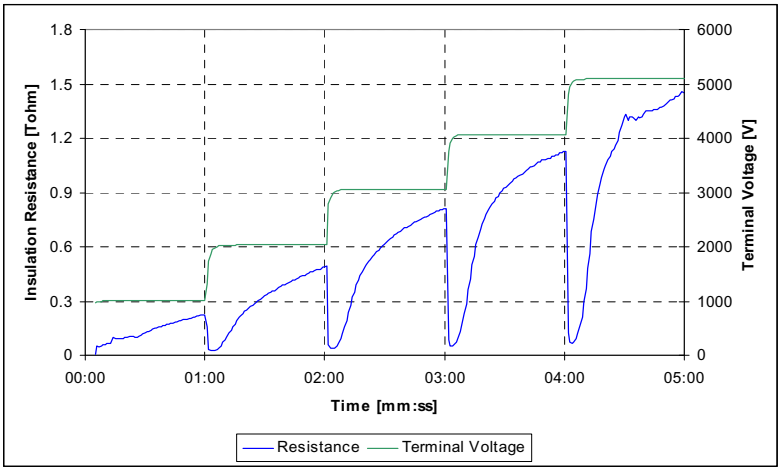

Fig. 39. Step Voltage test on CT1 - Baseline Curve

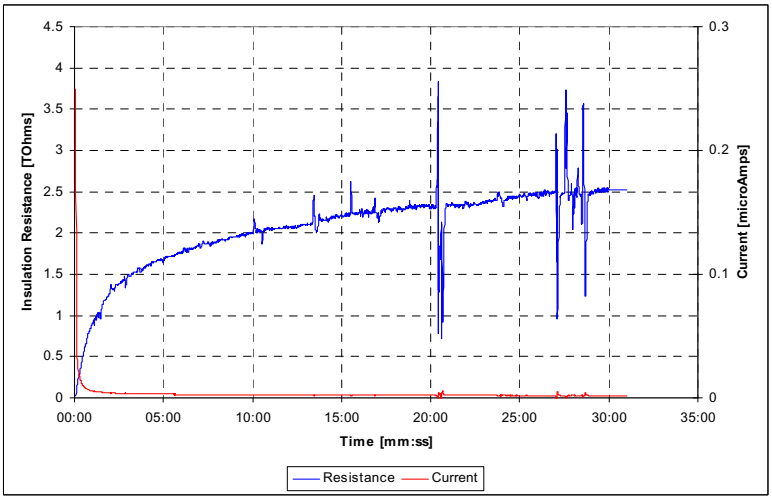

Fig. 40. Dielectric Discharge test on CT1 - Baseline Curve

The baseline tests indicated a robust insulation system between the high voltage primary winding and the ground connection terminal. Baseline values by itself may not have great significance unless these values are tracked in future tests as ageing is monitored on the unit. Insulation resistance and polarization index will be tracked and recorded at every stage and compared against ageing estimation based on Arrhenius equation. The baseline curves shown above indicate that the insulation system in CT1 is in good conditions and capable to operate according to the nameplate specifications.

Step Voltage Test is more a yes/no test where the obtained values of insulation resistance should draw an exponential increasing curve as the one in Fig. 39. A continuous peak value or a decreasing value may represent damages in the insulation of the unit.

For CT1 the Normal Insulation Life was determined strictly as per IEEE standards expecting a DP value of 200 after an accelerated ageing process ending at 150,000 ageing hours. Further testing was not performed as the unit was removed from the load bed for a conscious investigation and complete dissection of the solid insulation. More information regarding this part of the research work will be presented in 4.5.5.

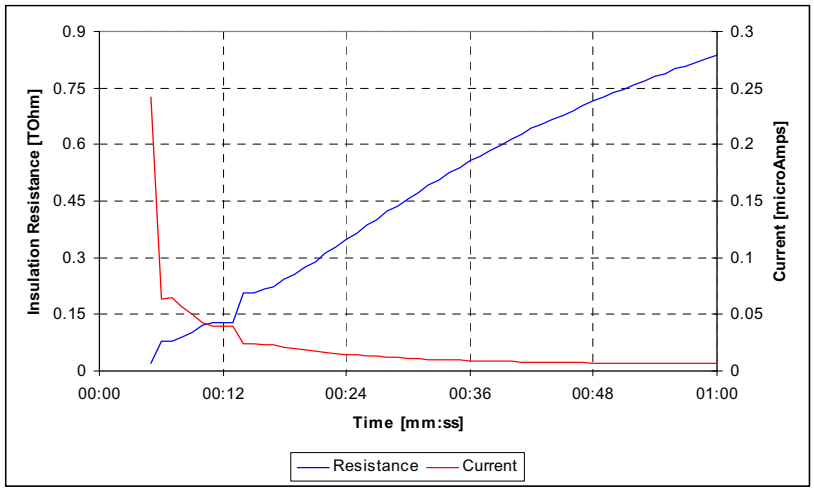

Fig. 41. Insulation Resistance test on CT1 - After 150,000 ageing hours

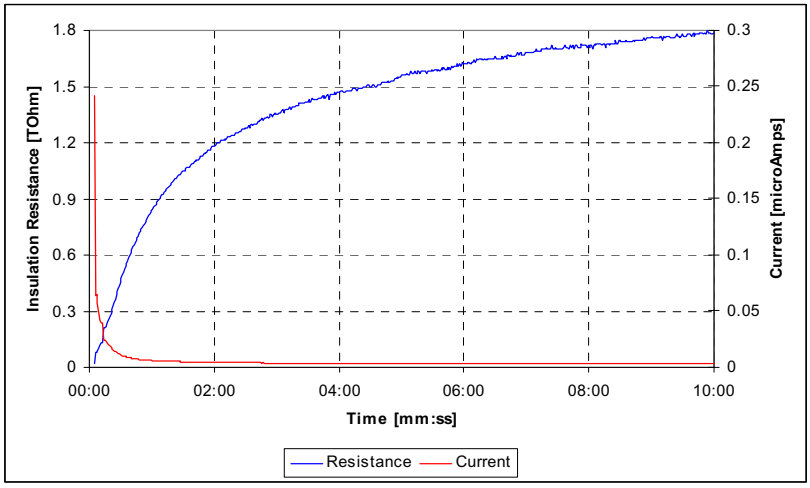

Fig. 42. Polarization Index test on CT1 - After 150,000 ageing hours

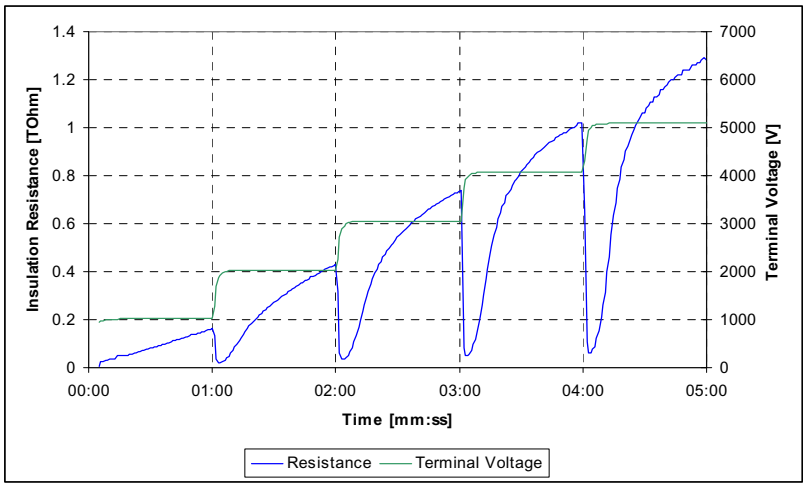

Fig. 43. Step Voltage test on CT1 - After 150,000 ageing hours

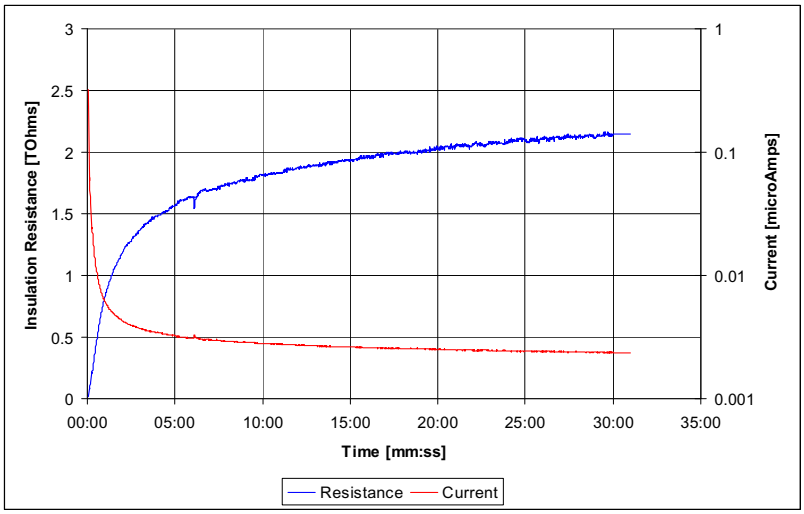

Fig. 44. Dielectric Discharge test on CT1 - After 150,000 ageing hours

After completion of the expected ageing process (150,000 h), the DC testing results obtained on CT1 are presented in Figures 41 to 44.

At first glance, the DC tests after 150,000 ageing hours seem to describe characteristics almost as good as the baseline test values. Nevertheless, during the experimental process, data of the DC tests were recorded and it is shown in Fig. 45.

After the post-factory test, the unit presented on the initial life stages (~1000 hours) IR values very close to be considered unacceptable for operation. The accelerated ageing experimental work continued because the process is purely thermal and high voltage was never applied.

The recorded data indicated an improvement of the insulation characteristics. As ageing of CT1 passed over the 50,000 hours, the IR value started increasing. The simple explanation to this phenomenon is a contamination of the internal environment due to the placement of paper samples in the system and the continuous extraction of the samples for laboratory analysis. Final testing stages were characterized by oil leaks from the top sealing of the unit and the extreme thermal stress applied to the unit worked as a thermal filter. In any case, these values should be compared with other testing results.

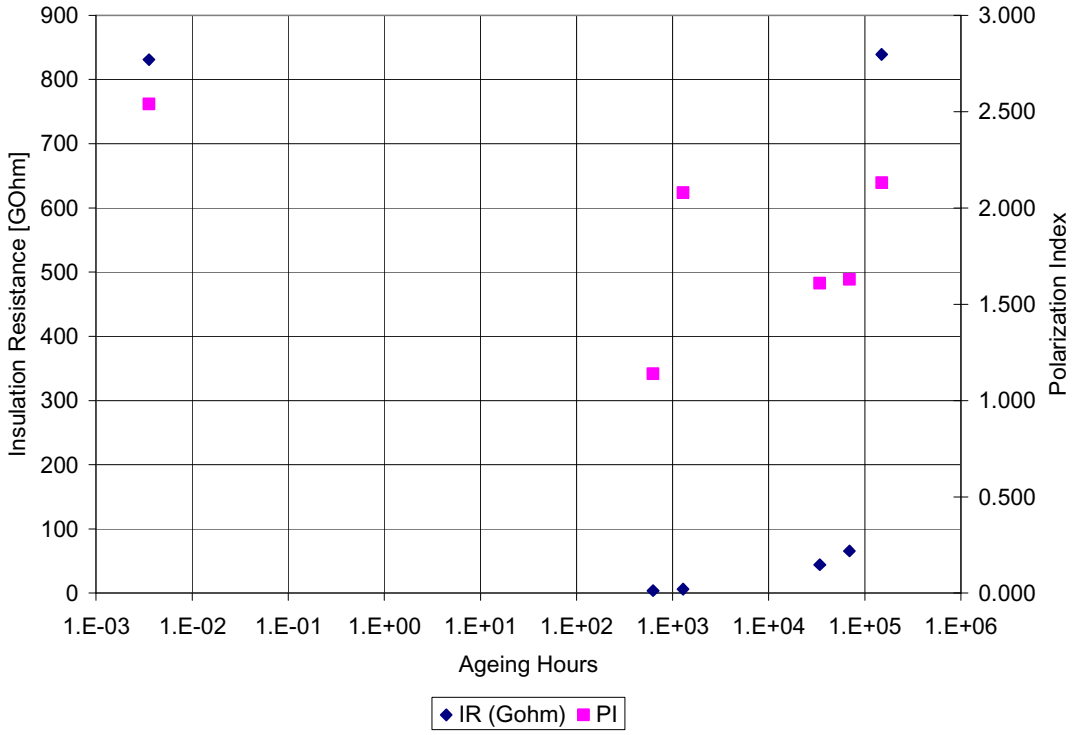

Fig. 45. DC Tests on CT1 - Data Trend for Insulation Resistance and Polarization Index

4.5.2 AC Testing on CT1

Dielectric Spectroscopy in the Frequency Domain using the IDAX-206 device was used to evaluate the condition of the mixed insulation system in CT1. Baseline characteristics of Power Factor, Dissipation Factor (tanδ), Capacitance, and Complex Permittivity components are presented in Fig. 46. The curves presented have not been corrected for temperature variation over the testing span of approximately 2 hours. Temperature correction is carried out for final data analysis setting all results to a common 20°C base.

Dissipation Factor values in the baseline figure draw identical characteristics with Power Factor curve in the high frequency range down to 0.22 Hz. The frequency sweep analysis was performed at every scheduled testing procedure and the data were stored for future ageing analysis. The last test at a calculated ageing of 150,000 hours is shown below in Fig. 47. The analysis, after estimated 100% LOL, was performed at full equipment frequency sweep capacity the range from 1000 Hz to 0.0001 Hz.

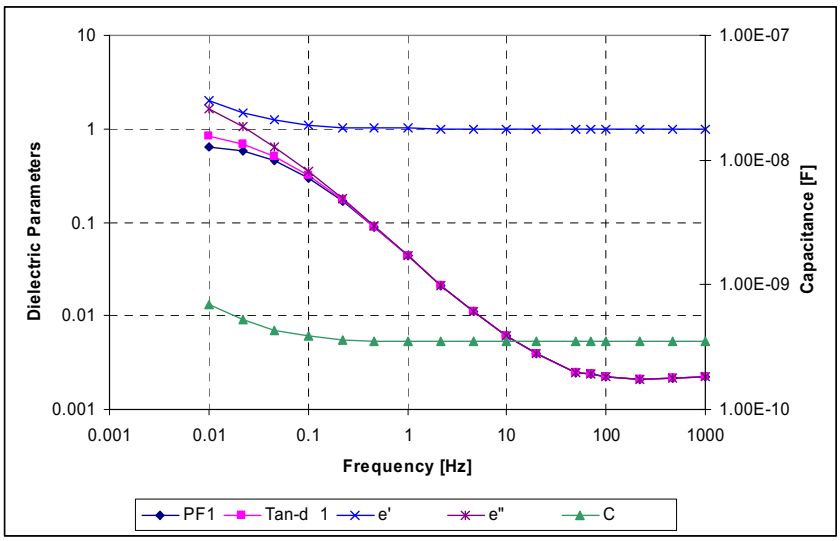

Fig. 46. Dielectric Spectroscopy test on CT1 – Baseline Curve

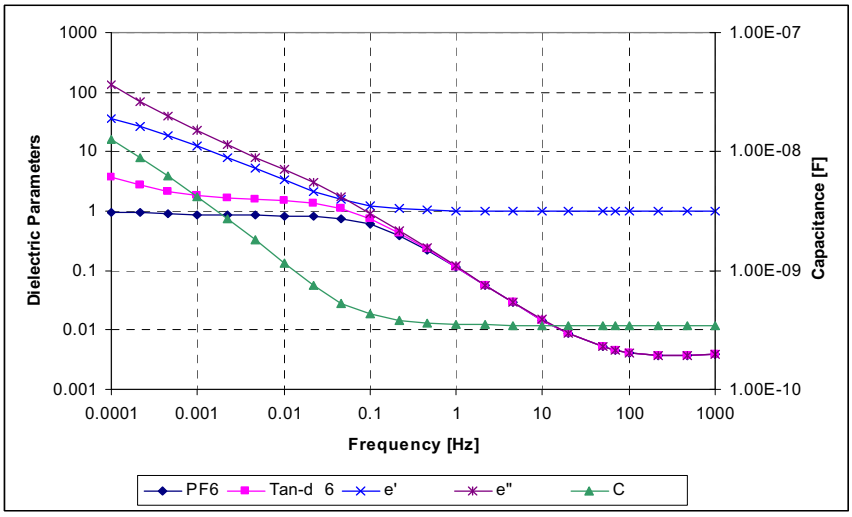

Fig. 47. Dielectric Spectroscopy test on CT1 - After 150,000 Ageing Hours

After 150,000 ageing hours, the shape of the curves is quite similar to the baseline curves, but some differences can be observed in the power frequency range. Power factor and dissipation factor are a little bit higher as well as the Capacitance value. Just looking at the baseline and last tests, there is not a big difference that could be used for evaluation of the system. A more detailed analysis is required looking at the data trend as shown in Figures 48 and 49 where the sequence is given from 1 to 6. The baseline curve is 1 and the last measurement is 6 after 150,000h.

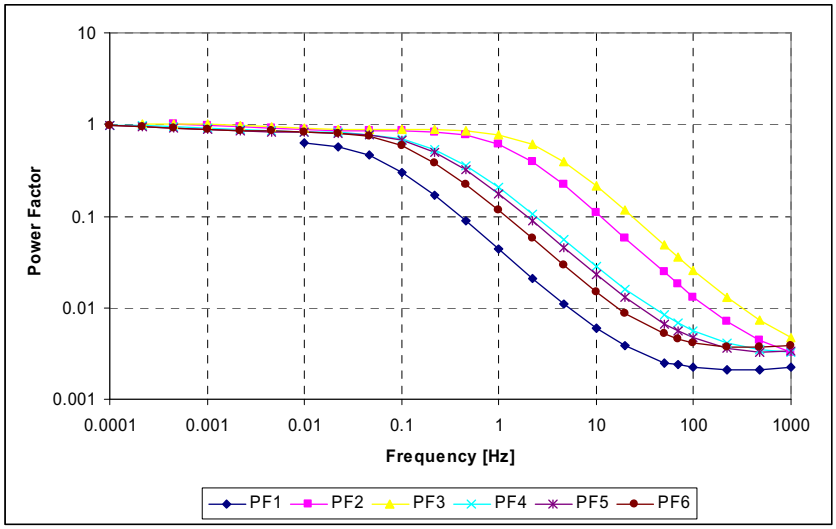

Fig. 48. Ageing CT1 - Power Factor Frequency Sweep trend data

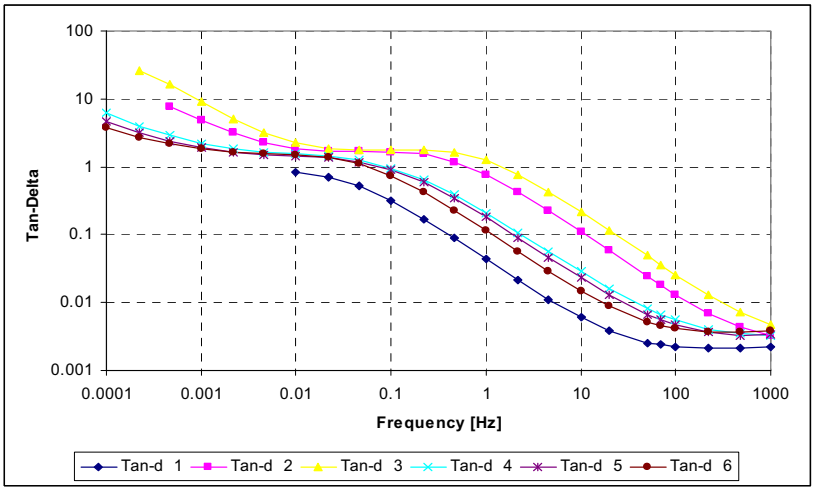

Fig. 49. Ageing CT1 - tan δ Frequency Sweep trend data

A similar behavior as observed with the DC test results was observed here. The worst characteristic is represented by curve 3 because dissipation factor tan δ is the greatest as compared to other curves and the last test (curve 6) gets closer to the original baseline curve. Therefore, DC tests and FDS (Frequency Domain Spectroscopy) confirm the initial contamination of the insulation system with external moisture and an unexpected improvement due to the thermal stress. Moreover, both types of tests indicate that CT1 can continue working under normal conditions. This implies that the end-of-life time of CT1 was not reached. A summary of the data collected with the IDAX 206 is shown below in Fig. 50. The values presented in this chart are the result of the evaluation using the MODS software and setting the data for a of 20°C temperature base.

4.5.3 Analysis of the Functional Parameters on CT1

The operation of CT1 under overload conditions did not affect the physical characteristics of the unit. This is clearly observed on the summary of values recorded using the CT Analyzer on the corresponding chart on Fig. 51 and in Table 58 in Appendix C.

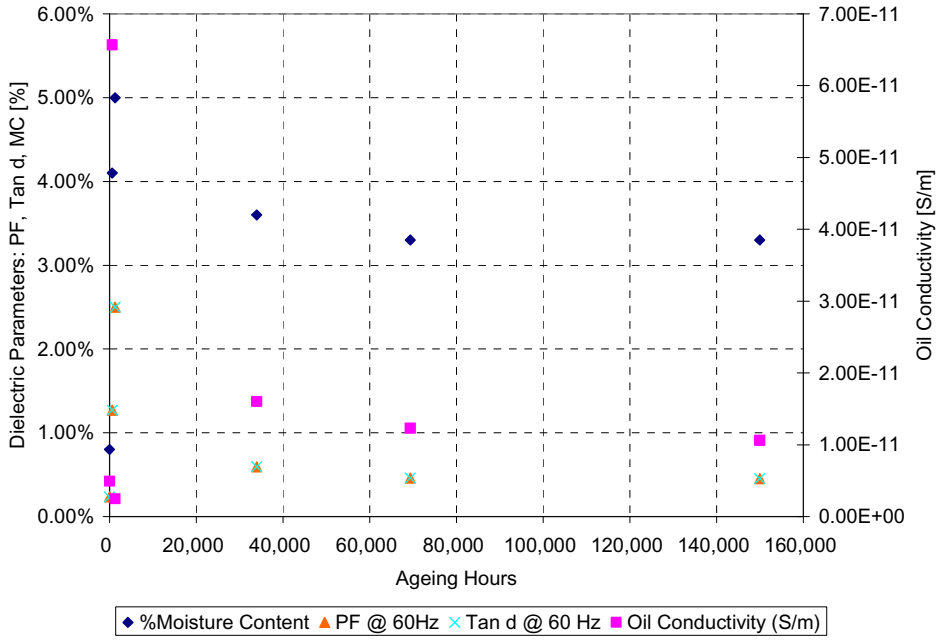

Fig. 50. Dielectric Spectroscopy Data Trend on CT1 - PF, tan δ, MC, and Oil Conductivity

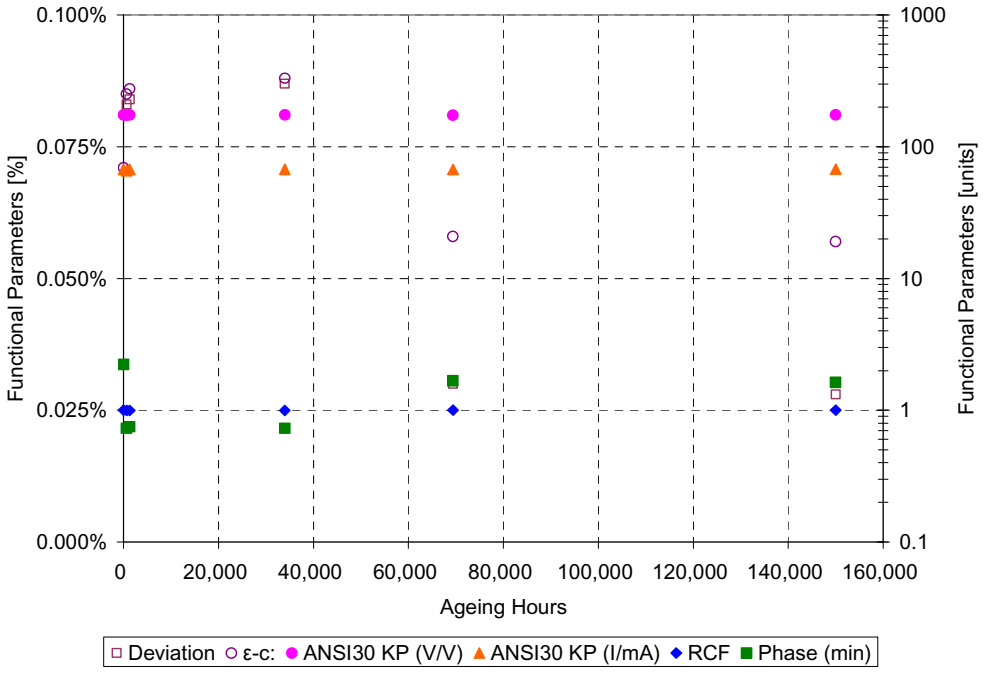

Fig. 51. Functional Parameters recorded for CT1 – Data Trend up to 150,000 h

The integrity of the physical components of the unit was not deteriorated due to the thermal ageing process. Even though, at a later day, some charring on the primary winding was observed. The functional test did not provide any evidence of ageing of the CT1. The transformer passed the functional test confirming the specifications as per manufacturer's nameplate.

4.5.4 Dissolved Gas Analysis on CT1

DGA results are presented in the form of loading profiles. Non-typical load levels used to thermally age and stress the unit were used to monitor the behavior of gases under extreme conditions. Long term loading provides an estimated rate of increase that could be used for emergency conditions where the system must operate above ratings.

4.5.4.1. Long-Term Loading Process at 200% of Rated Load.

The unit was kept at 200% load level for over 300 hours. During this time, temperature, dissolved-in-oil gases' concentration, and moisture in oil were monitored online.

- Oxygen and Carbon Dioxide: These two gases behave in different way. Oxygen reduces its concentration due to the temperature increase in the unit. A linear function is good to describe the oxygen concentration decrease. On the other hand, CO_2 increases its concentration at this load level. Oxygen's molecules contribute to the increasing concentration of CO_2. The rate of increase of these gases shown in Fig. 52 is numerically described as

$$O_{2(200\%)}(t) = -6.2898t + O_2(t_0) \tag{4.1}$$

$$CO_{2(200\%)}(t) = 0.0226t^2 - 2.679t + CO_2(t_0) \tag{4.2}$$

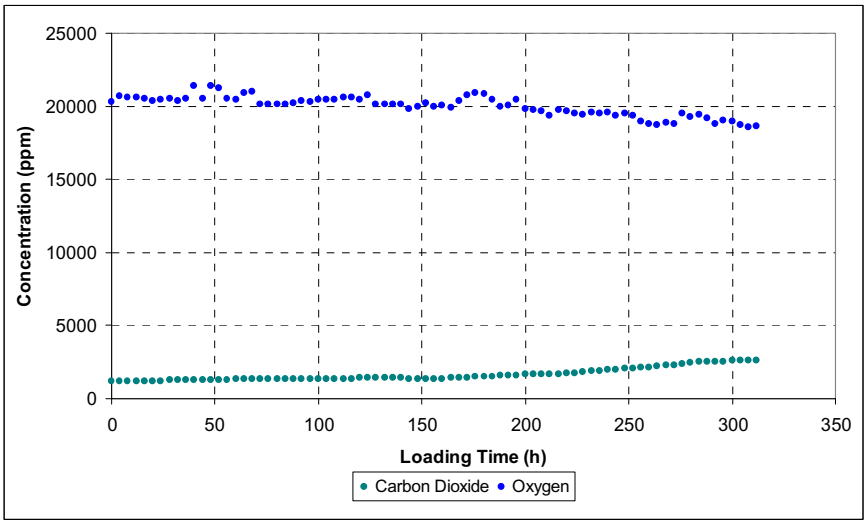

Fig. 52. Behavior of O_2 and CO_2 in CT1 under 200% load

- Carbon Monoxide and TDCG (Total Dissolved Combustible Gas): At a lower level, CO also obtains Oxygen's molecules and presents a continuous increase as shown in Fig. 53. CO is the main contributor of TDCG and other gases had sporadic presence. Therefore, CO and TDCG can describe the same rate of increase in time at 200% load.

$$CO_{(200\%)}(t) = 0.0034t^2 - 0.4925t + CO(t_0) \tag{4.3}$$

$$TDCG_{(200\%)}(t) = 0.0034t^2 - 0.4925t + TDCG(t_0) \tag{4.4}$$

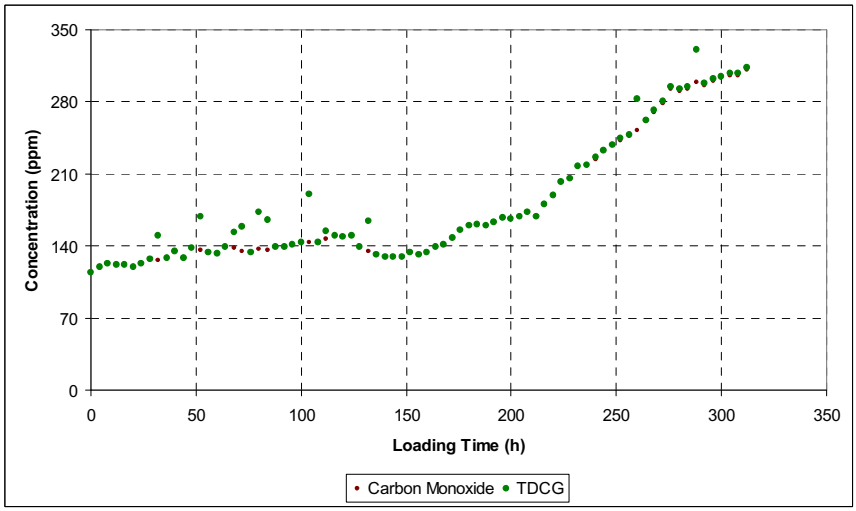

Fig. 53. Behavior of CO and TDCG in CT1 under 200% load

- Moisture: It is important to mention that the tested current transformer had never been in service before. The remaining moisture inside the unit after the manufacturing process as well as certain time in storage was reduced initially due to the thermal stress inside the unit. Once the moisture level became stable the thermal stress extracted the moisture of the solid insulation generating a minimum increase. The moisture content (MC) variation (in ppm) is presented in Fig. 54 and described as

$$MC_{ppm(200\%)}(t) = 2\times10^{-5}t^2 - 0.00047t + MC_{ppm}(t_0) \tag{4.5}$$

- Other Gases: Other hydrocarbon gases were detected by the online monitor. Their presence in some cases was seldom; in other cases it originated after certain time. Mainly Hydrogen and Ethane appeared during the process. Methane, Ethylene, and Acetylene were not present at this stage. Data are presented in Fig. 55.

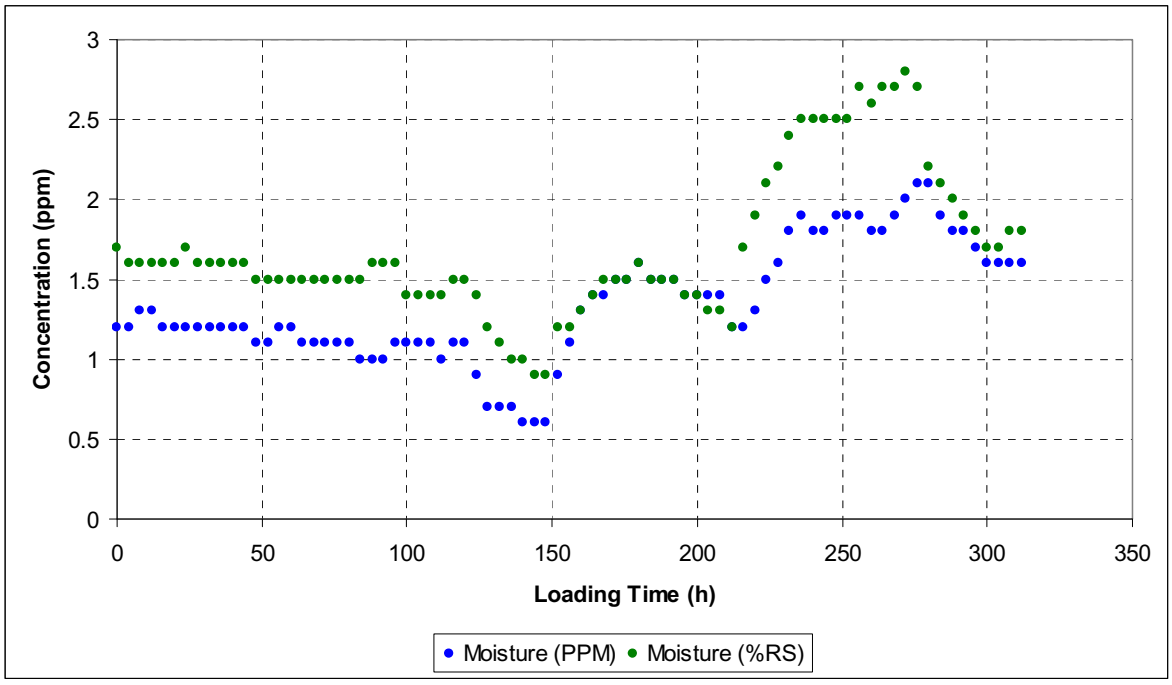

Fig. 54. Behavior of Moisture concentration in CT1 under 200% load

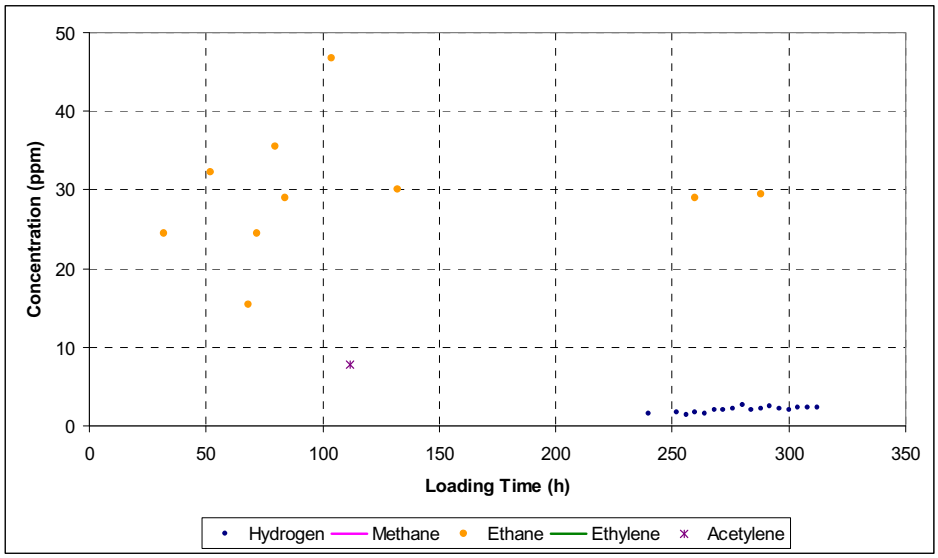

Fig. 55. Concentration of other gases in CT1 under 200% load

4.5.4.2. Long-Term Loading Process at 250% of Rated Load.

Right after loading the unit at 200% of rated load, the experimental work continued increasing the load up to 250% (I_p=3,000 A) for over 168 hours. Significant variation was observed as a result of the thermal stress.

- Oxygen and Carbon Dioxide: The behavior is similar to the 200% loading level; of course, faster evolution of these gases is confirmed as shown in Fig. 56 and described by the following expressions:

$$O_{2(250\%)}(t) = -15.37t + O_2(t_0) \tag{4.6}$$

$$CO_{2(250\%)}(t) = 8.56t + CO_2(t_0) \tag{4.7}$$

- Carbon Monoxide and TDCG: At this level of stress and because other combustible gases increase their concentration, the characteristics of CO and TDCG are different. It is also clear that the gas evolution is in a faster process as presented in Fig. 57.

$$CO_{(250\%)}(t) = 1.041t + CO(t_0) \tag{4.8}$$

$$TDCG_{(250\%)}(t) = 1.588t + TDCG(t_0) \tag{4.9}$$

- Moisture: Moisture content is also presented as part of this work. The data obtained from the humidity sensor installed in the unit are presented in Fig. 58:

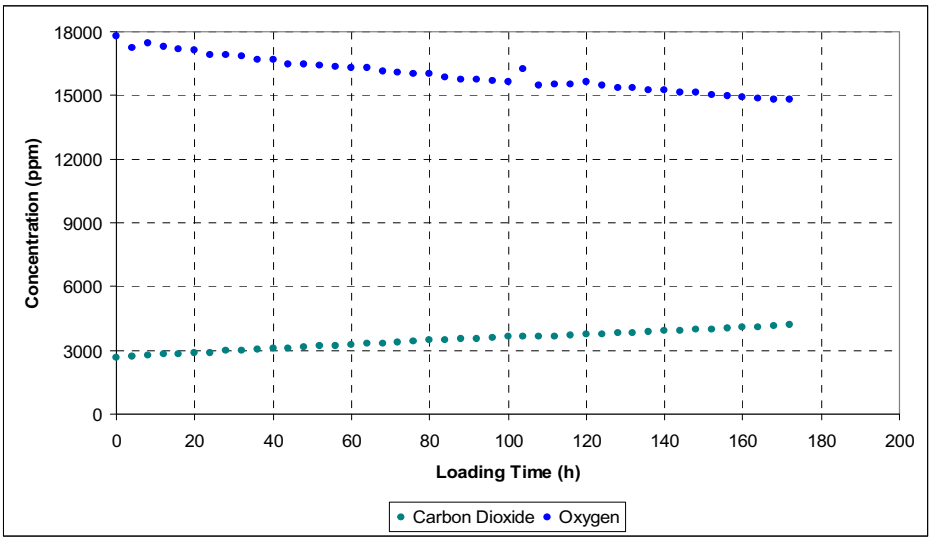

Fig. 56. Behavior of O_2 and CO_2 in CT1 under 250% load

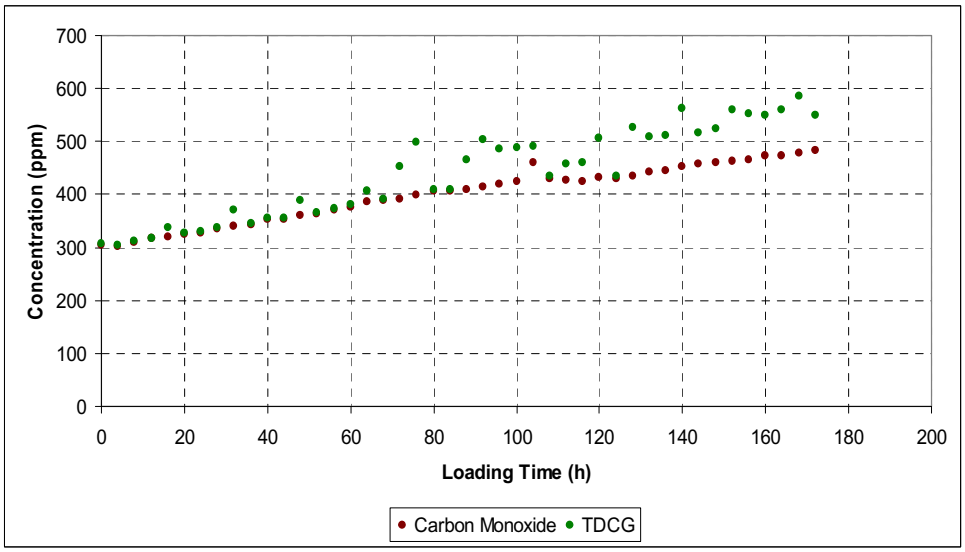

Fig. 57. Behavior of CO and TDCG in CT1 at 250% Load

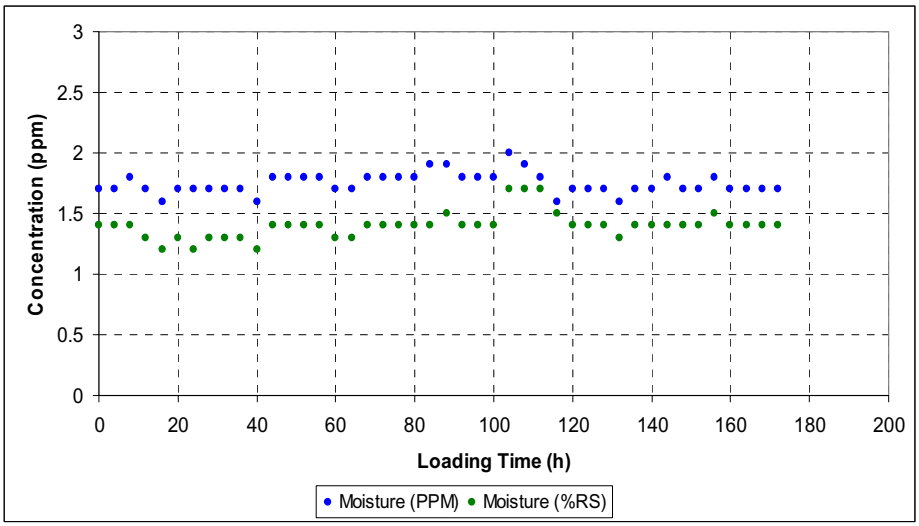

Fig. 58. Moisture behavior in CT1 at 250% Load

At this point and after the previous loading processes, the moisture concentration remains mostly constant. This indicates that there is no external contamination or filtration and that a higher energy level will be required to extract additional moisture from the solid insulation. Moisture Content at this loading level is expressed as

$$MC_{ppm(250\%)}(t) = 5\times10^{-5}t + MC_{ppm}(t_0) \tag{4.10}$$

Therefore, moisture content in the current transformer had reached stable condition and its increase was minor at this specific thermal and energy level.

- Other Gases: Two gases were previously identified during the process. Presence of Hydrogen remained almost constant with a minimum increase. Ethane had a more disperse presence and Methane appeared as part of this process. Ethylene and Acetylene were not present during this process. The concentration of these gases during the process is shown in Fig. 59.

The rate of increase of Hydrogen and Ethane during the process can be expressed as

$$H_{2(250\%)} = 0.0124t + H_2(t_0) \tag{4.11}$$

$$C_2H_{6(250\%)} = 0.0135t + C_6H_6(t_0) \tag{4.12}$$

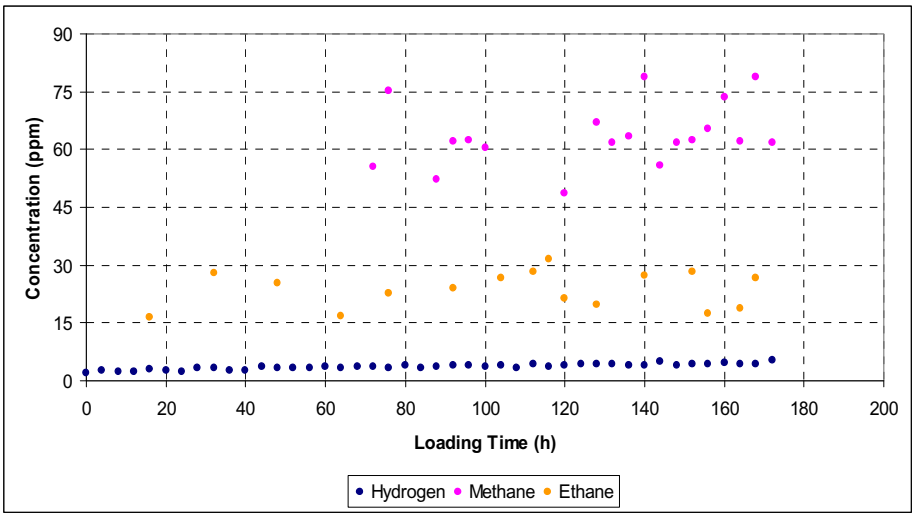

Fig. 59. Other gases with lower concentration levels in CT1 at 250% Load

4.5.4.3. Long-Term Loading Process at 300% of Rated Load.

The data obtained from the temperature sensors indicated that the expected temperature at 300% loading level will be at the edge of the critical values (~150°). The loading process was initiated and the recorded values are presented below.

- Oxygen and Carbon Dioxide: These two gases repeated the behavior presented before. The concentration values are presented in Fig. 60 and described by the following expressions:

$$O_{2(300\%)}(t) = -0.16t^2 - 70.67t + O_2(t_0) \tag{4.13}$$

$$CO_{2(300\%)}(t) = -0.153t^2 + 95.217t + CO_2(t_0) \tag{4.14}$$

Oxygen was consumed rapidly. This indicates a fast increase in CO and CO_2 which ratio was analyzed separately.

- Carbon Monoxide and TDCG: As can be observed from Fig. 61, the high level of stress originated a rapid increase in the value of CO and, consequently, of TDCG as well. The high concentrations observed need to be analyzed in order to determine if a failure condition became active during the process.

$$CO_{(300\%)}(t) = -0.001t^2 + 5.16t + CO(t_0) \tag{4.15}$$

$$TDCG_{(300\%)}(t) = -0.01t^2 + 5.87t + TDCG(t_0) \tag{4.16}$$

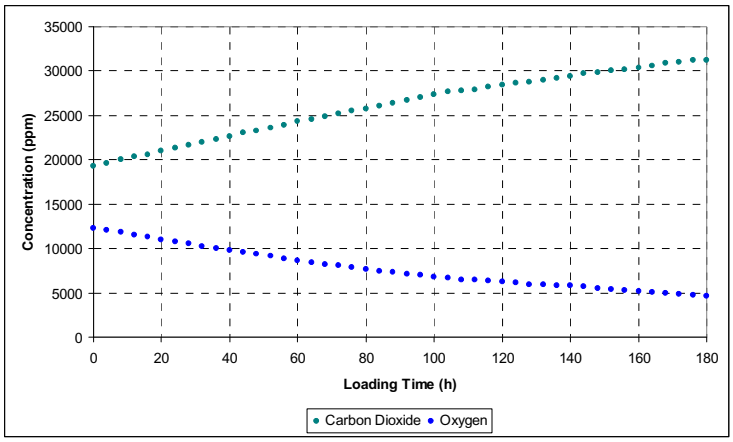

Fig. 60. Oxygen and CO_2 behavior in CT1 at 300% Load

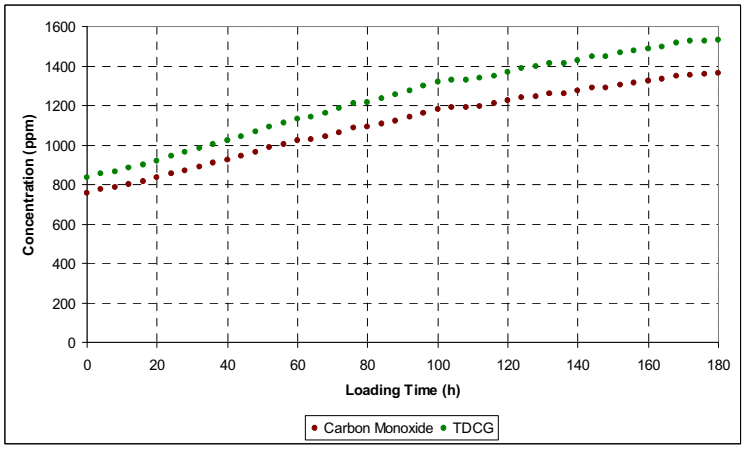

Fig. 61. CO and TDCG behavior in CT1 at 300% Load

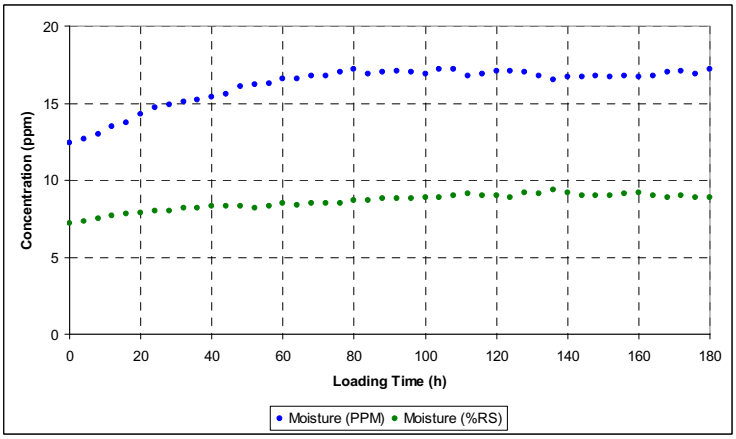

Fig. 62. Moisture behavior in CT1 at 300% Load

- Moisture: The high temperature of the process and, thus, the greater energy level of this loading stage caused an increase in the moisture concentration with a tendency to become stable as far as the thermal stress remains constant. The data obtained form the humidity sensor installed in the unit are presented in Fig. 62. Moisture had increased at this loading stage, due to the thermal effect on the solid insulation of the current transformer. Moisture Content at this loading level is expressed as

$$MC_{ppm(300\%)}(t) = 3\times10^{-6}t^3 - 0.001t^2 + 0.124t + MC_{ppm}(t_0) \tag{4.17}$$

- Other Gases: At this stage of the loading process, the only gas that was not present during the thermal accelerated ageing process applied to CT1 was Acetylene (C_2H_2). The concentration of Hydrogen, Ethane, Methane, and Ethylene during the process is shown in Fig. 63. The rate of increase of these gases during the process can be expressed as

$$H_{2(300\%)}(t) = 0.0278t + H_2(t_0) \tag{4.18}$$

$$C_2H_{6(300\%)}(t) = 0.042t + C_2H_6(t_0) \tag{4.19}$$

$$CH_{4(300\%)}(t) = 0.206t + CH_4(t_0) \tag{4.20}$$

$$C_2H_{4(300\%)}(t) = 0.0243t + C_2H_4(t_0) \tag{4.21}$$

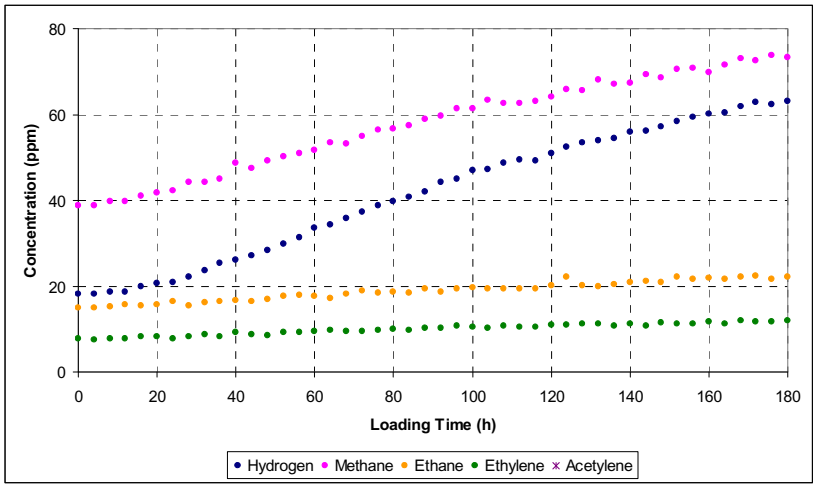

Fig. 63. Other gases behavior in CT1 at 300% Load

Technical diagnosis for condition assessment of the transformer needs to be performed based on existing standards as described in Chapter 3, section 3.4.1. Therefore, standard interpretation is used and presented below.

CIGRE SC15: Out of the five ratios, those related to any Acetylene concentrations are disregarded (K_1 and K_5) as none of the loading stages encountered this gas during the process. At 200% load the only key ratio to be analyzed is K_4 because significant concentrations were given only by CO and CO_2. Using Equations (4.2) and (4.3) to estimate this ratio, it is observed in Fig. 64 that at all times the ratio will be within limits ($3<K_4<10$) at any positive value of time; therefore, there is no active fault condition in the operation of this CT at 200% rated load. It can also be observed in the same figure that these two gases reach steady sate at different time spans, according to the rate of increase expressions provided for CO_2 and CO at 200% load (4.2) and (4.3), respectively. At this load level, CO reaches stability at approximately 200 hours and CO_2 after approximately 800 hours.

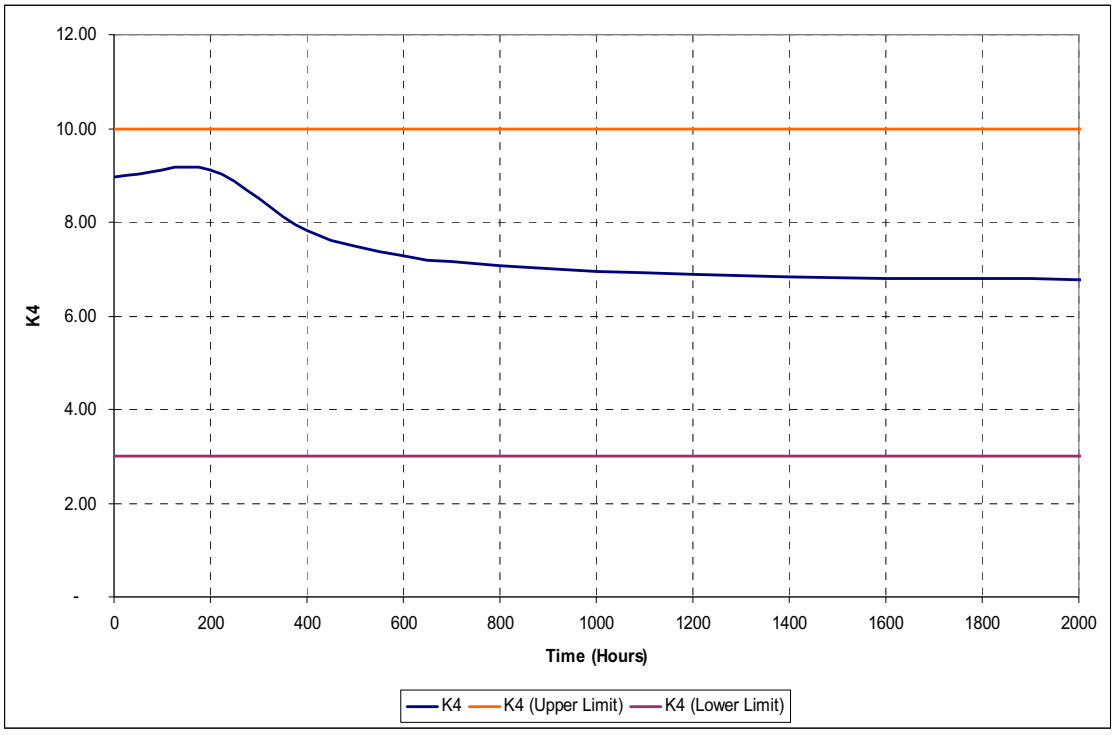

Fig. 64. Evaluation of Key Ratio # 4 using Rate of Increase equations for CT1 @ 200% load

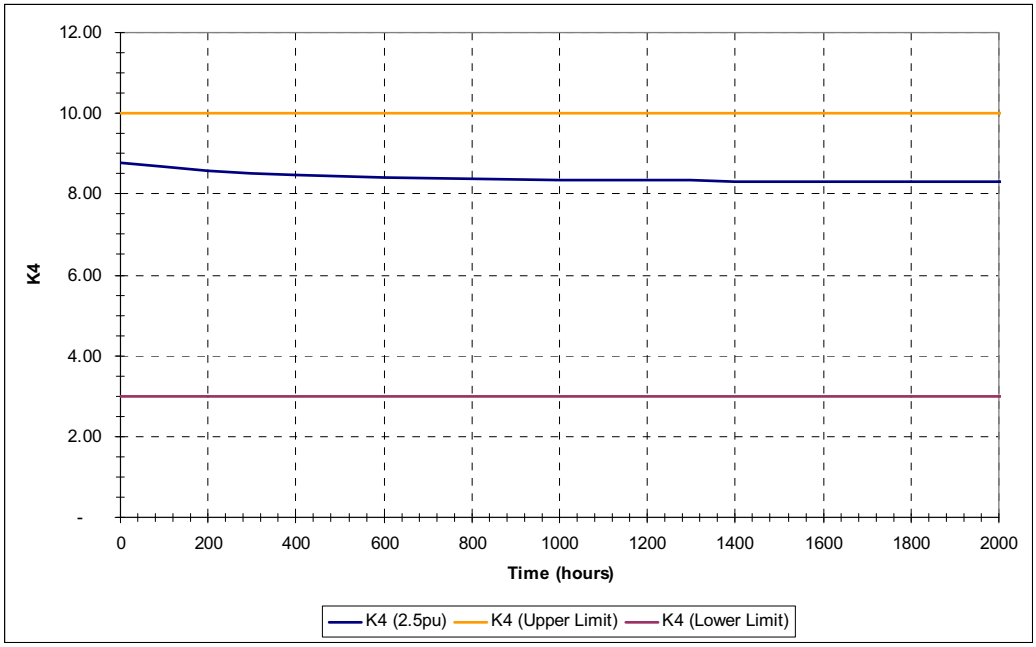

Fig. 65. Evaluation of Key Ratio #4 using Rate of Increase equations for CT1 @ 250% load

At 250% load, again, the only key ratio to be analyzed is K_4 because Methane's presence was sporadic and Ethylene was not present during the process. Significant concentrations were given only by CO and CO_2. Using Equations (4.7) and (4.8) to estimate K_4 ratio, it is observed in Fig. 65 that for any time value, the ratio will be within limits ($3<K_4<10$). Therefore, at 250% load K_4 ratio indicates a proximity to its upper boundary (indicative of overheating of cellulose), but the values show normal condition and no active fault condition in the operation of the CT.

At 300% load, the analysis becomes more complex. Three key ratios were calculated K_2, K_3, and K_4 as shown in Fig. 66. Calculated values of K_2 using Equations (4.18) and (4.20) are all less than 1.4 confirming that the stress is purely thermal and not electrical. K_2 shows that H_2 rises faster than CH_4 for the first 200 hours of operation and the applied load or the thermal effect do not derive into values where Partial Discharge activity could be contemplated in the CT. K_3 is calculated using Equations (4.21) and (4.19) and the values obtained are all within the range $1.7<K_3<2$, which indicates thermal fault in oil. K_4 is calculated using Equations (4.14) and (4.15). Most of calculated values are

greater than 10, which is an indicative of overheating of cellulose, with the exception of the time span between 700 to 1000 hours. Special attention is given to the time span 780 to 860 hours where K_4 reports degradation of cellulose by electrical fault.

Roger Ratios and CO_2/CO ratio: The outcome of CO_2/CO ratio (K_4) has already been discussed in the CIGRE SC15 – Key Ratios analysis in this Section. R_2 is not applicable in this analysis because of the absence of Acetylene in the loading process. At 200% load, Rogers Ratios can not be used for analysis. Only sporadic values of Hydrogen and Ethane were registered. At 250% load, Methane's presence was sporadic and Ethylene was not present during the process. Thus, neither R_1 nor R_3 could be used for further analysis. At 300% load, most fault gases are present in the liquid insulation and ratios R_1 (which is the inverse value of K_2) and R_3 (which is the same value of K_3) can be computed using the following expressions:

$$R_1 = 1/K_2 \tag{4.22}$$

$$R_3 = K_3 \tag{4.23}$$

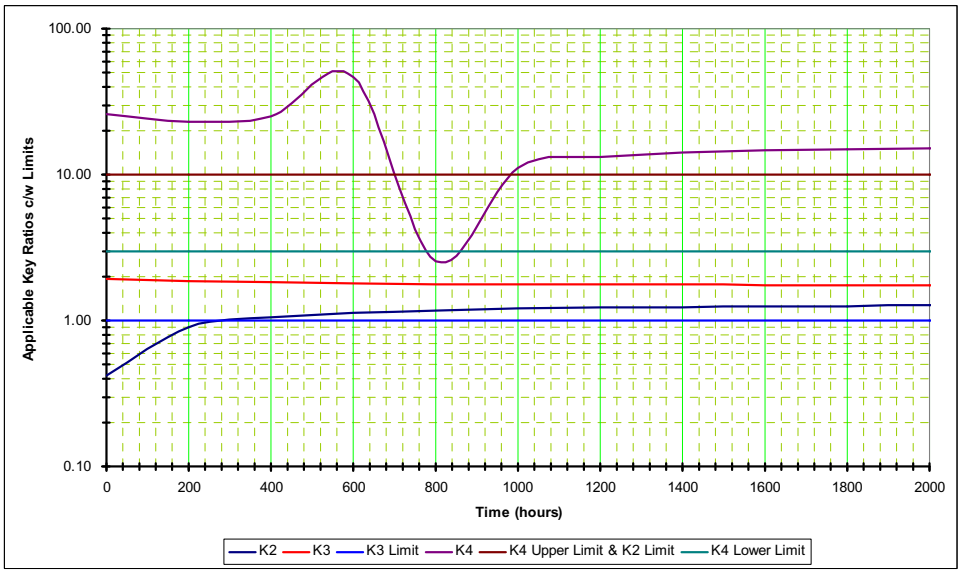

Fig. 66. Evaluation of Key Ratios # 2, 3, and 4 using Rate of Increase expressions for CT1 @ 300% load

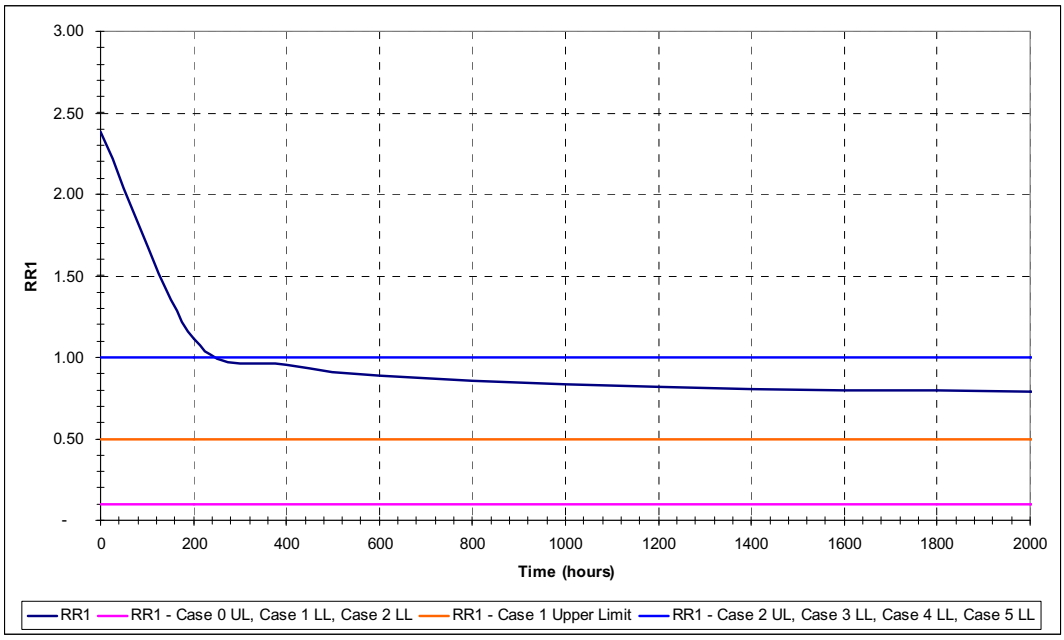

Fig. 67. Roger Ratio #1 Evaluation using Rate of Increase equations for CT1 @ 300% load

In order to predict a possible fault condition, the values of R_1 and R_3 were forecast based on the corresponding rates of increase of each of their components. Results of this analysis for R_1 and R_3 are shown in Figures 67 and 68, respectively.

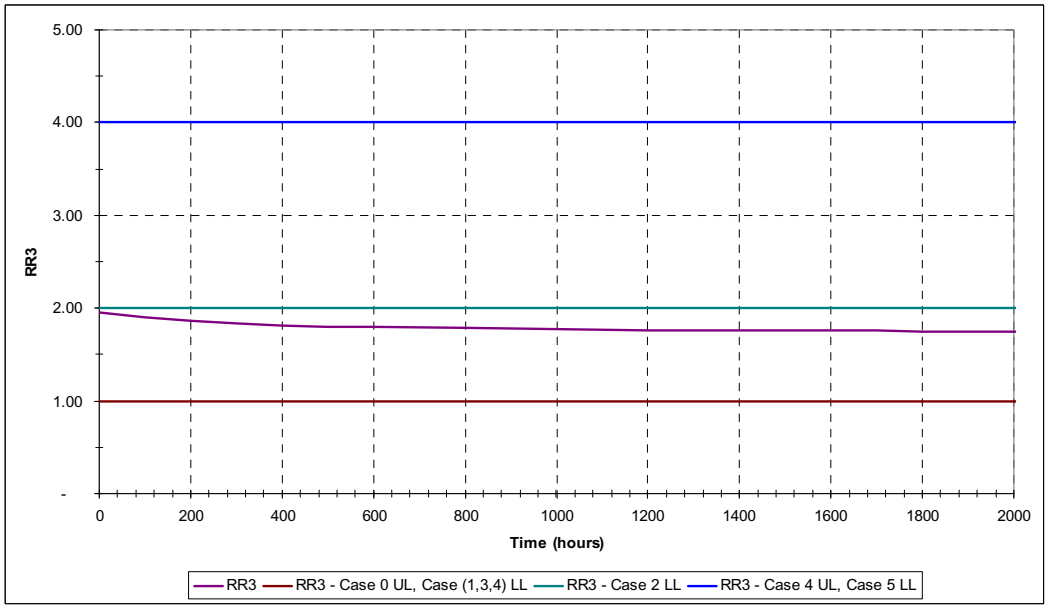

Fig. 68. Roger Ratio #3 Evaluation using Rate of Increase equations for CT1 @ 300% load

For R_1, the first 250 hours suggest thermal fault condition, later the decreasing value of R_1 crosses the unit value falling within the range $0.7 \geq R_1 \leq 1$ suggesting high energy discharge, but R_2 does not support this condition and; therefore, it cannot be assumed a high energy discharge fault condition. Some values obtained within the range $1.0 \geq R_1 \leq 2.5$ suggest a thermal fault as well. The calculated values of R_3 are located within the range $1.7 \geq R_3 \leq 2$ as shown in Fig. 68. This indicates low energy discharge and a thermal fault with temperatures less than 700°C. For overall evaluation, R_2 is considered to be equal to zero; otherwise the Rogers Ratios method would not be applicable as the combination of results of these three ratios suggests the fault type.

The Duval Triangle method of interpretation suggested a thermal fault during the experimental profile of CT1 as it can be observed in Fig. 69 .

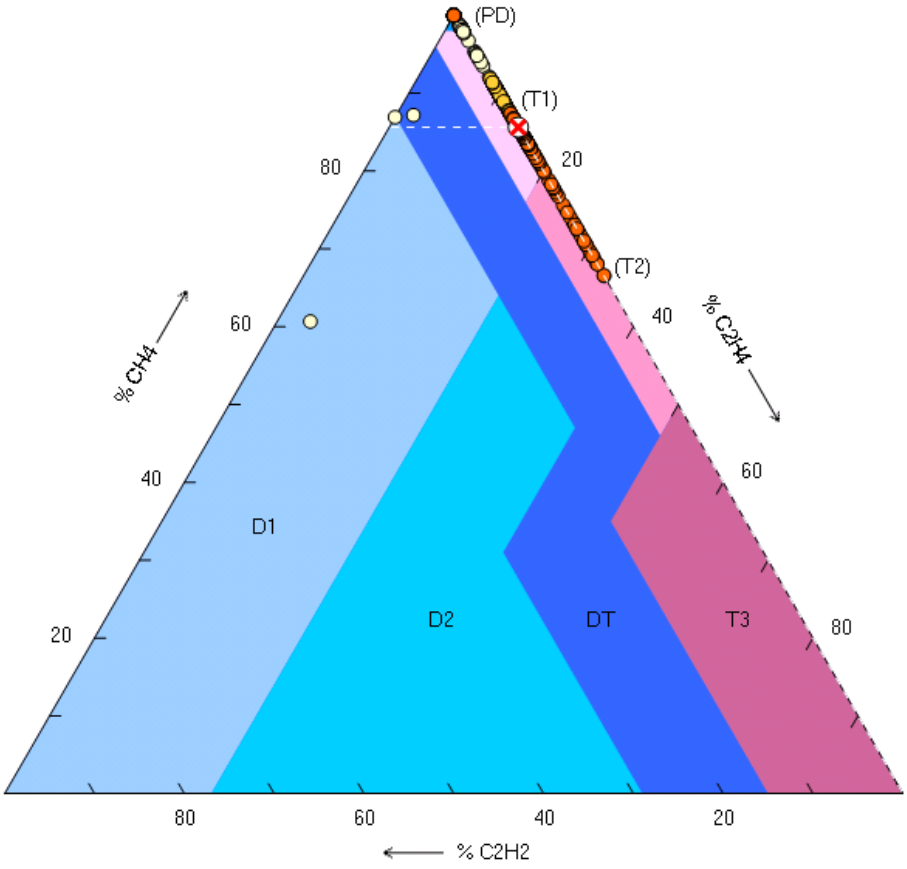

Fig. 69. Graphical interpretation of Gases Behavior in CT1 during its experimental profile

Table 25. Typical Dissolved Gas Concentration Values for CT1

DISSOLVED GAS	TYPICAL VALUES FOR INSTRUMENT TRANSFORMERS [72]	TYPICAL CALCULATED CONCENTRATION (PPM) [58]
Hydrogen	6-300	14.6
Methane	11-120	65.3
Ethane	7-130	21.8
Ethylene	3-40	7.3
Acetylene	1-5	0
Carbon Monoxide	250-1,100	1,166
Carbon Dioxide	800-4,000	25,161.2

Based on the guidelines given in [58], typical dissolved gas concentrations have been estimated for the complete life cycle of CT1. The obtained values are congruent with those presented in [72] based on IEC-60599 (Appendix A1) and are presented in Table 25.

Instrument Transformers in-service will always have some degree of fault gases dissolved in the liquid insulation. The possibility of a fault condition comes into picture when the concentration of one or more of these gases over goes the safety recommended values. Dissolved key gas concentration limits (ppm) as presented in [41, 58, 73] are compared to the maximum values registered during the accelerated ageing process in Table 26.

Calculated typical concentration of CO_2 is the only value exceeding the numbers presented in [72]. Moreover, CO and CO_2 maximum values exceed the safety suggested concentration limits. This is explained due to the thermal acceleration process applied to the experimental unit, but even that extreme thermal stress did not lead to a complete unit failure. The progressive thermal stress applied to CT1 and the gas behavior during the complete experimentation process is illustrated in Fig. 165 in Appendix D of this dissertation.

Table 26. CT1 Maximum Dissolved Gas Concentrations and Standard Limits

Gas	Condition 1	Condition 2	Condition 3	Condition 4	Bureau of Reclamation	Pre-Failure Concentration	Max. Recorded Values CT1
H_2	100	101 - 700	701 – 1,800	>1,800	500	725	64.2
CH_4	120	121-400	401-1,000	>1,000	125	400	91.9
C_2H_2	35	36-50	51-80	>80	7	450	12.4
C_2H_4	50	51-100	101-200	>200	175	800	12.1
C_2H_6	65	66-100	101-150	>150	75	900	46.7
CO	350	351-570	571-1,400	>1,400	750	2,100	1,372.6
CO_2	2500	2,500-4,000	4,001 – 10,000	>10,000	10,000	50,000	31,621
TDCG	720	721-1,920	1,921-4,630	>4,630	-	5,380	1,543.4

4.5.5 Degree of Polymerization and Furanic Compound Analysis on CT1

This CT was the first one to complete the entire life cycle considering Normal Insulation Life under the expected DP 200 criterion at 150,000 ageing hours. Since the furanic compound concentration was recorded during the ageing process, it is possible to correlate 2FAL with the ageing Arrhenius equation. Although, ageing hours do not reflect the DP value as established to be the end-of-life criterion. Estimation of DP based on the models proposed in Chapter 3 is detailed below.

The values obtained from the laboratory at different ageing stages are summarized below in Table 27 and graphically presented in Fig. 70.

Table 27. CT1 Furanic Compound Concentration [ppb] - Data Trend

Arrhenius Ageing	HMF	FOL	2FAL	2AF	5M2F	Total Furan Content
0.00	2	0	2	0	0	4
1,283.06	3	0	7	0	0	10
2,793.27	4	0	47	0	2	53
5,333.47	6	0	133	0	3	142
17,453.65	10	0	411	0	12	433
33,955.35	20	0	796	0	62	878
69,357.48	109	0	2723	16	43	2891
104,726.23	130	0	4050	17	82	4279
149,990.53	310	0	6331	10	133	6784

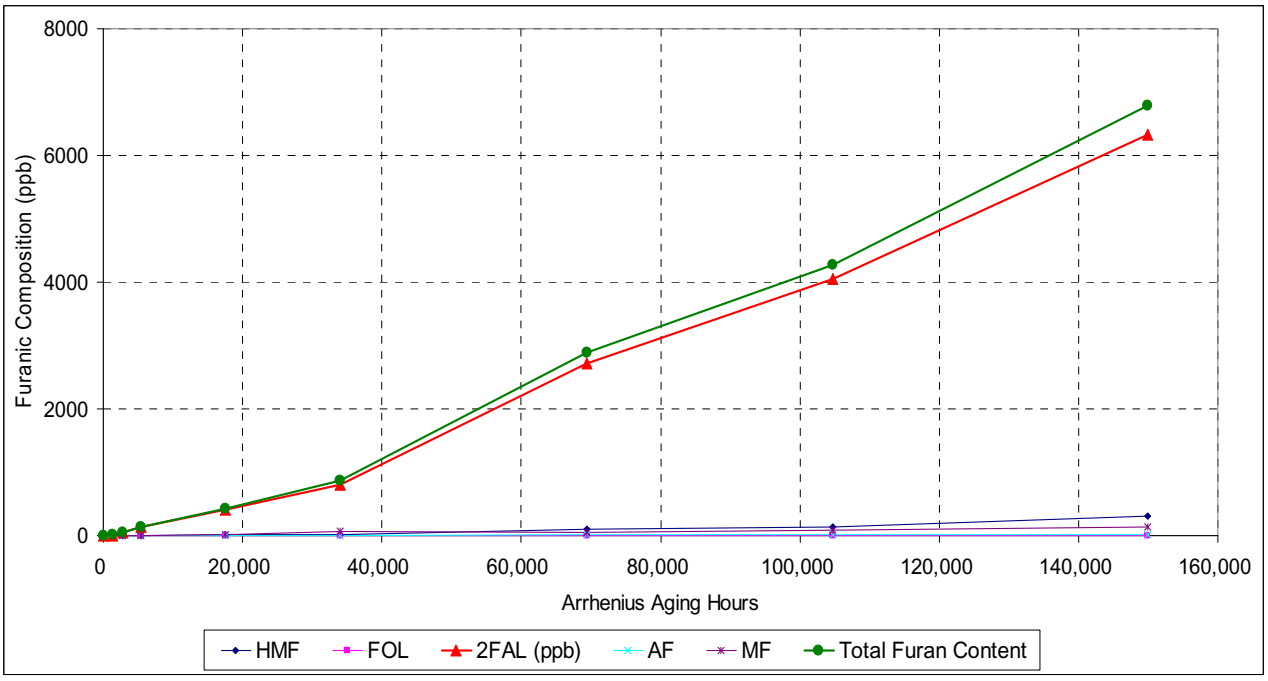

Fig. 70. Evolution of Furanic Compounds in CT1 during Thermal Ageing process

The Laboratory reported the following estimated values for DP, as shown in Table 28, which was correlated to the estimated ageing as shown in Fig. 71.

Table 28. DP Estimated by DOBLE and % LOL Models for CT1

Arrhenius Ageing	DOBLE Estimated DP	% LOL Emsley for DOBLE DP	% LOL General for DOBLE DP	% LOL Stebbins for DOBLE DP
0.00	1200	0%	0%	0%
1,283.06	1044	3%	16%	0%
2,793.27	808	10%	39%	7%
5,333.47	679	15%	52%	19%
17,453.65	539	25%	66%	34%
33,955.35	457	33%	74%	45%
69,357.48	304	59%	90%	72%
104,726.23	255	74%	95%	84%
149,990.53	200	100%	100%	100%

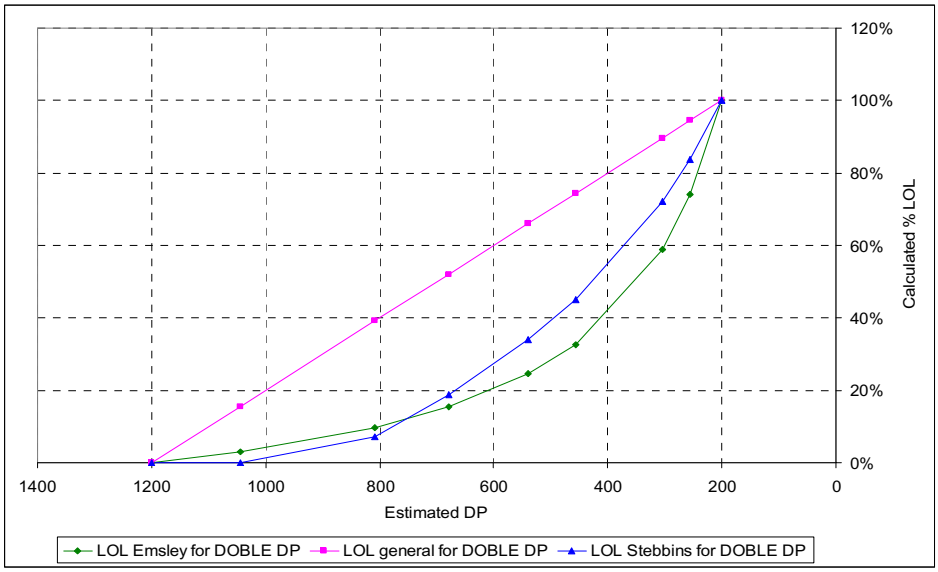

Fig. 71. DOBLE Estimated DP based on Furanic Concentration - Calculated % LOL for CT1

DOBLE Laboratory suggests a perfect match between Furanic Compounds content and thermal ageing as per the Arrhenius equation in IEEE standard. After ageing the unit up to 150,000 hours, the concentration of 2FAL estimates a DP value of 200, thereby implying a loss-of-life of 100%.

DePablo model as per (3.41) was used to calculate DP values and correlate with the estimated ageing of CT1 as shown in Table 29 and Fig. 72.

Table 29. DP Estimated by DePablo CIGRE and % LOL Models for CT1

Arrhenius Ageing	DePablo CIGRE Estimated DP	% LOL Emsley for DePablo DP	% LOL General for DePablo DP	% LOL Stebbins for DePablo DP
0.00	899.77	7%	30%	0%
1,283.06	899.21	7%	30%	0%
2,793.27	894.72	7%	31%	0%
5,333.47	885.22	7%	31%	1%
17,453.65	855.83	8%	34%	3%
33,955.35	818.22	9%	38%	6%
69,357.48	670.69	16%	53%	20%
104,726.23	596.61	20%	60%	27%
149,990.53	501.41	28%	70%	39%

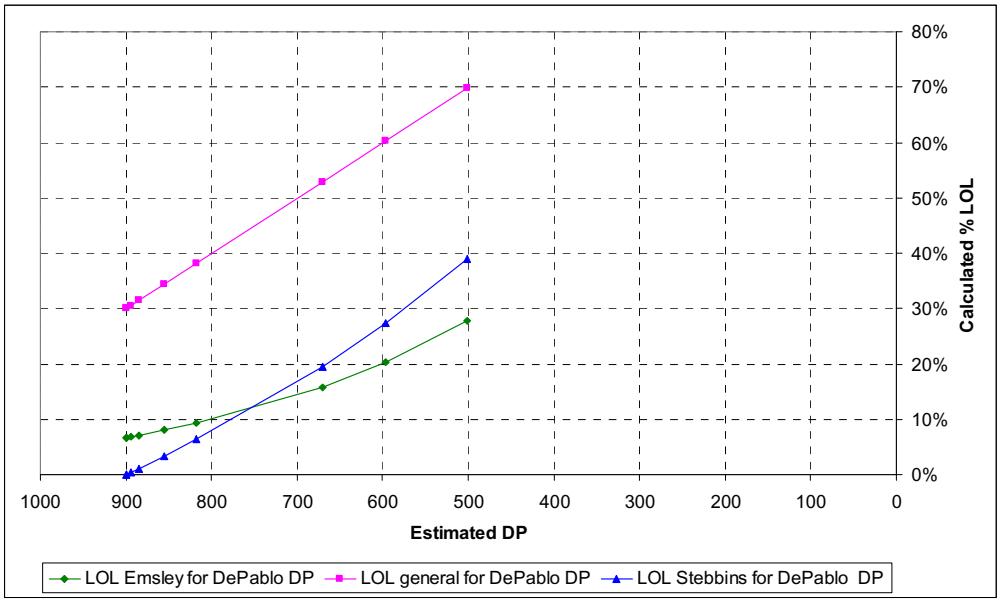

Fig. 72. DePablo CIGRE Estimated DP based on Furanic Concentration - Calculated % LOL for CT1

A great difference can be observed between the first two methods of estimating DP value. Applying DePablo's correlation, the furanic concentration values indicate still a strong characteristic of DP after the loading process and thus, a small % LOL. Because the initial DP value is less than 1200, the equation suggests a lower quality material from the beginning of the process.

At first glance, DePablo's equation appears to be extremely conservative bearing in mind the long thermal stress applied to the unit. Table 30 shows the estimated values of DP using equation

(3.48) as reported by the Transformer Maintenance Institute. The estimated DP values suggest complete deterioration of the solid insulation and possible end-of-life at approximately 70,000 ageing hours. This is a greater contradiction as compared with DePablo's obtained values and even with DOBLE's estimates. Again, validation of the data via DP analysis becomes imperative for a definitive correlation between furanic compound – DP and real ageing of the CT.

Table 30. DP Estimated by Stebbins / Myers and % LOL Models for CT1

Arrhenius Ageing	Stebbins/Myers Estimated DP	% LOL Emsley for Stebbins DP	% LOL General for Stebbins DP	% LOL Stebbins for Stebbins DP
0.00	840.05	9%	36%	5%
1,283.06	731.67	13%	47%	14%
2,793.27	566.93	22%	63%	31%
5,333.47	476.94	30%	72%	42%
17,453.65	379.33	43%	82%	57%
33,955.35	322.14	55%	88%	68%
69,357.48	215.74	91%	98%	95%
104,726.23	181.40	112%	102%	106%
149,990.53	142.75	148%	106%	122%

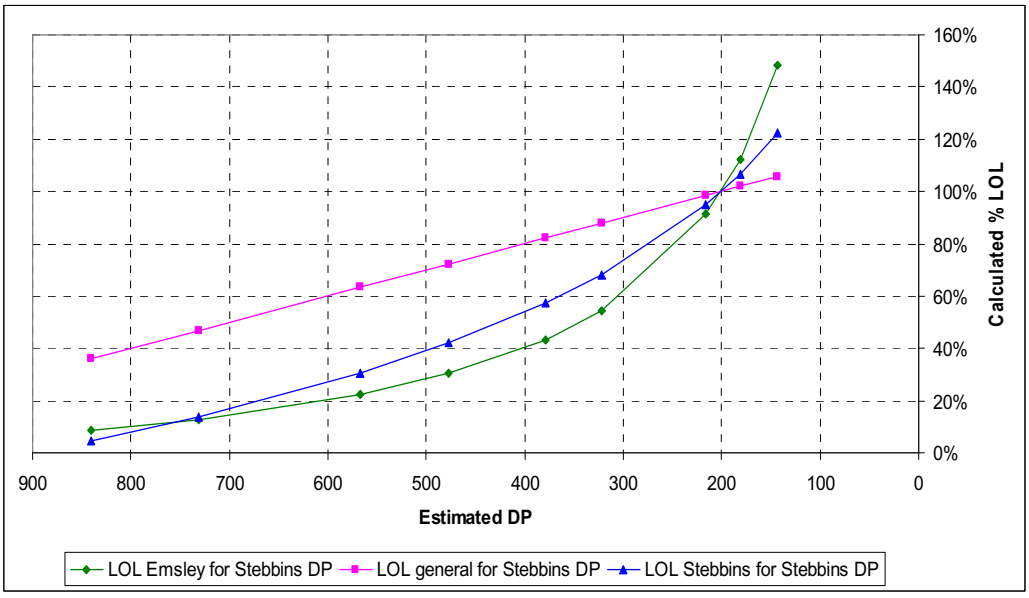

Fig. 73. Stebbins Estimated DP based on Furanic Concentration - Calculated % LOL for CT1

Equation (3.42) introduced by X. Chendong has been used widely in industry and research. The estimated DP values as per (3.42) are presented in Table 31 with the corresponding percentages LOL calculated by the techniques presented in Chapter 3.

The obtained DP values reflect almost similar values as the ones provided by DOBLE. The problem with using this equation is that it was empirically developed for thermally upgraded paper.

Table 31. DP Estimated by Chendong and % LOL Models for CT1

Arrhenius Ageing	Chendong Estimated DP	% LOL Emsley for Chendong DP	% LOL General for Chendong DP	% LOL Stebbins for Chendong DP
0.00	1202.56	0%	0%	0%
1,283.06	1047.11	3%	15%	0%
2,793.27	810.83	10%	39%	7%
5,333.47	681.76	15%	52%	18%
17,453.65	541.76	24%	66%	34%
33,955.35	459.74	32%	74%	45%
69,357.48	307.13	58%	89%	71%
104,726.23	257.87	73%	94%	83%
149,990.53	202.44	99%	100%	99%

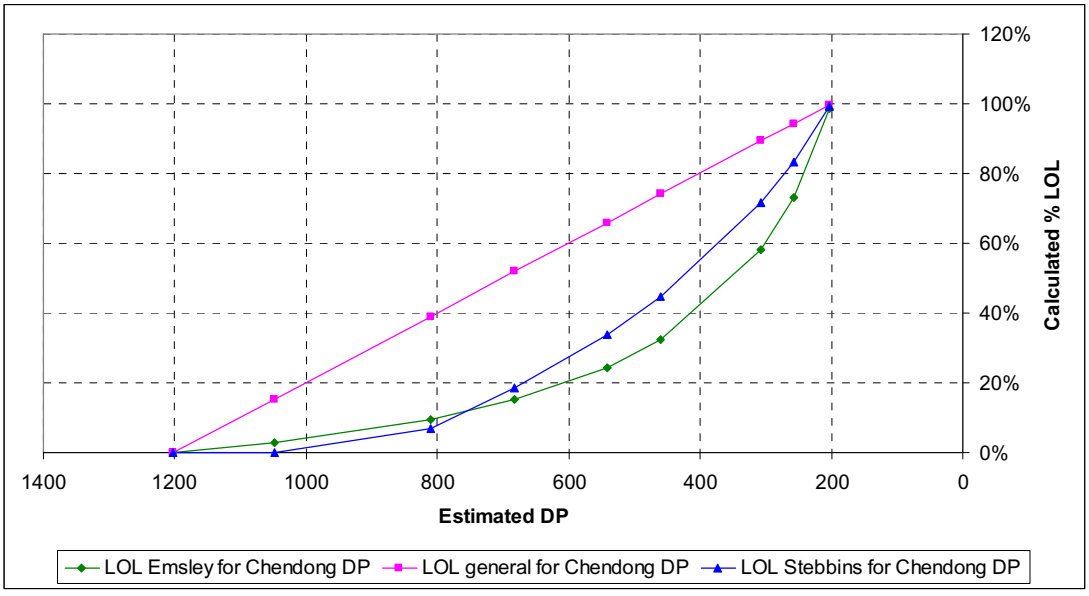

Fig. 74. Chendong Estimated DP based on Furanic Concentration - Calculated % LOL for CT1

One more DP estimation equation is to be reviewed. The expression given by Pahlavanpour (3.45) using $DP_0 = 900$ is applied to the furanic concentration values and the resulting DP estimates are summarized in Table 32 and shown in Fig. 75.

By just visual inspection, and following the "expected" logical result, one would think that DOBLE and Chendong estimated values for DP with any of the %LOL models would apply to define the thermal ageing of the unit reaching the DP 200 criterion and ageing of 150,000 hours according to the Arrhenius equation. The only way to verify the validity of the data is to extract a sample of the solid insulation and perform the corresponding DP analysis.

Therefore, CT1 was removed from the load bank, drained, and put for dissection. This intrusive inspection had the following objectives:

- Visual inspection of the solid insulation
- Remove paper samples from the core paper wrap
- Remove paper samples at different layers of the paper insulation

Table 32. DP Estimated by Pahlavanpour and % LOL Models for CT1

Arrhenius Ageing	**Pahlavanpour**	**LOL Emsley for Pahlavanpour DP**	**LOL general for Pahlavanpour DP**	**LOL Stebbins for Pahlavanpour DP**
0.00	899.63	7%	30%	0%
1,283.06	898.70	7%	30%	0%
2,793.27	891.31	7%	31%	1%
5,333.47	875.84	7%	32%	2%
17,453.65	829.31	9%	37%	5%
33,955.35	772.48	11%	43%	10%
69,357.48	575.18	22%	62%	30%
104,726.23	489.15	29%	71%	41%
149,990.53	389.11	42%	81%	56%

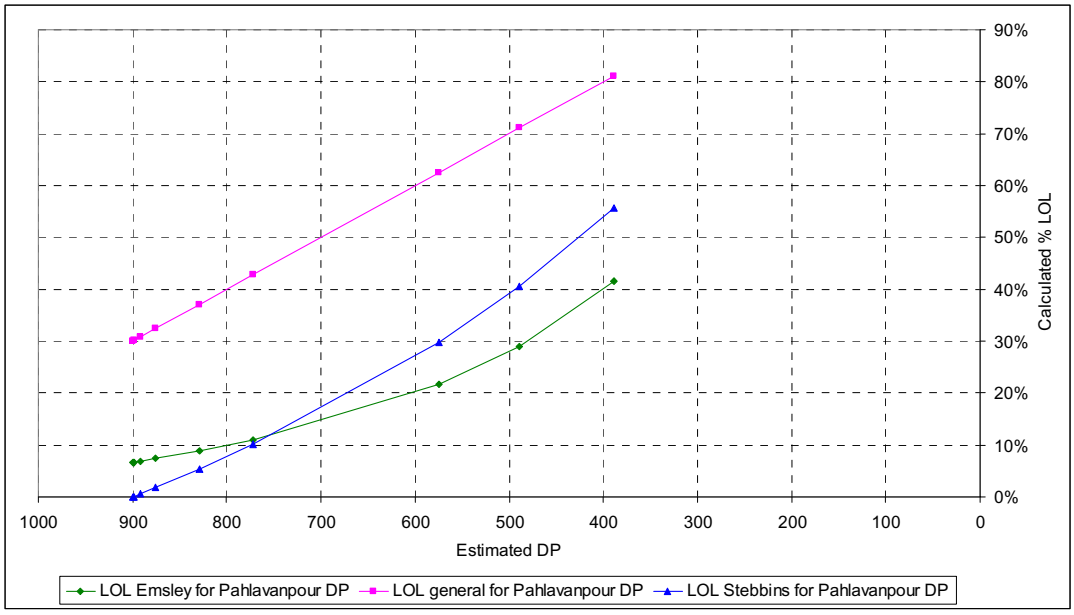

Fig. 75. Pahlavanpour Estimated DP based on Furanic Concentration - Calculated % LOL for CT1

Paper samples sent to the DOBLE laboratory for DP analysis reported all values close to 95% estimated remaining life, even at stages where the furanic compound analysis reported ageing above 50% LOL. This discrepancy required additional investigation and great expectations were given to the CT1 dissection. Some pictures taken during the dissection activity show the core and secondary winding in Fig. 76.

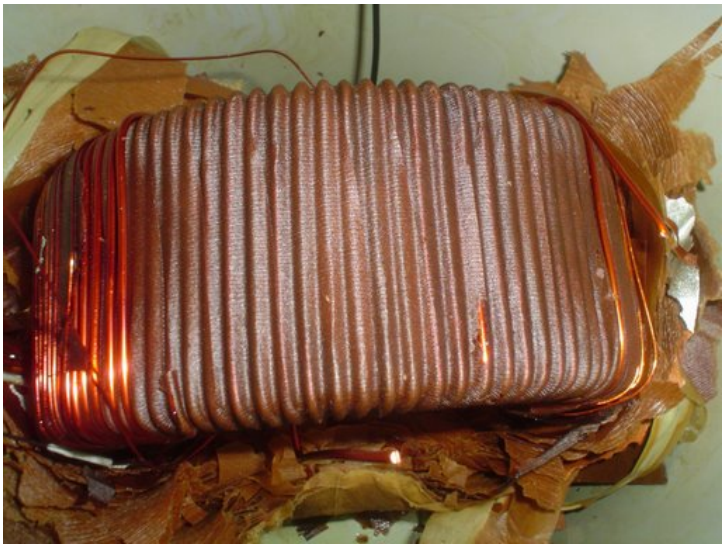

Fig. 76. CT1 Dissection - Paper insulation layer between secondary winding and core

Fig. 77. CT1 Dissection – Temperature Sensors

The location of the fiber-optic temperature sensor as well as of the thermocouples is visualized in Fig. 77.

These pictures do not show the core itself. There is still a thin layer of solid insulation between this level and the core. The dissection had to reach the lowest layer of paper insulation. Removal of the secondary winding from the core was the most difficult part in this procedure and finally, the core is shown in Fig. 78. As it can be observed here, the secondary winding and the core do not show any evidence of charring.

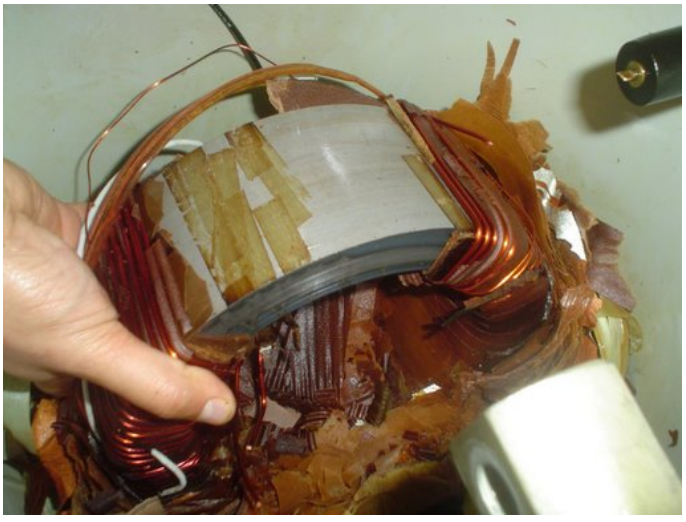

Fig. 78. CT1 Dissection - Core

Table 33. CT1 DP Values Obtained from DOBLE Laboratory after Dissection

Dissection Secondary - Core and Primary winding				
Layer	**DP Value**	**LOL Emsley for Lab DP value**	**LOL general for Lab DP value**	**LOL Stebbins for Lab DP value**
Top Surface (1)	690.00	15%	51%	18%
5	596.00	20%	60%	27%
10	607.00	20%	59%	26%
25	500.00	28%	70%	39%
2-ry winding wrap	426.00	36%	77%	50%
Core wrap	302.00	59%	90%	73%
1-ry winding	644.00	17%	56%	22%

The solid insulation samples taken during the dissection procedure were submitted to DOBLE Laboratory for DP analysis. The obtained results are summarized in Table 33.

The primary winding was the only component in the assembly presenting evidence of charring as it can be clearly observed in Fig. 79. Because the primary winding conductors were wrapped in paper insulation as well, a sample was additionally taken and sent for DP analysis. The obtained values reported in Table 33 confirm that ageing of the paper insulation in the primary winding is relatively close to the ageing of the top surface paper insulation of the secondary winding / core insulation. The analysis also reflects an important factor: the hottest spot within the CT assembly is localized as originally expected on the top angle of the solid insulation between the core and the secondary winding and that DP sampling from the top surface layer is worthless. Under failure conditions or reconditioning of the unit, samples should be taken from the zone between the core and the secondary winding; this is the weakest insulation point identified for CT1 during this experimental work.

Fig. 79. CT1 dissection after 150,000 ageing hours - Primary Winding

A summary of the data obtained from DOBLE laboratory is presented in Fig. 80. Estimated % LOL and Calculated %LOL to DP200 reached maximum value after 150,000 ageing hours.

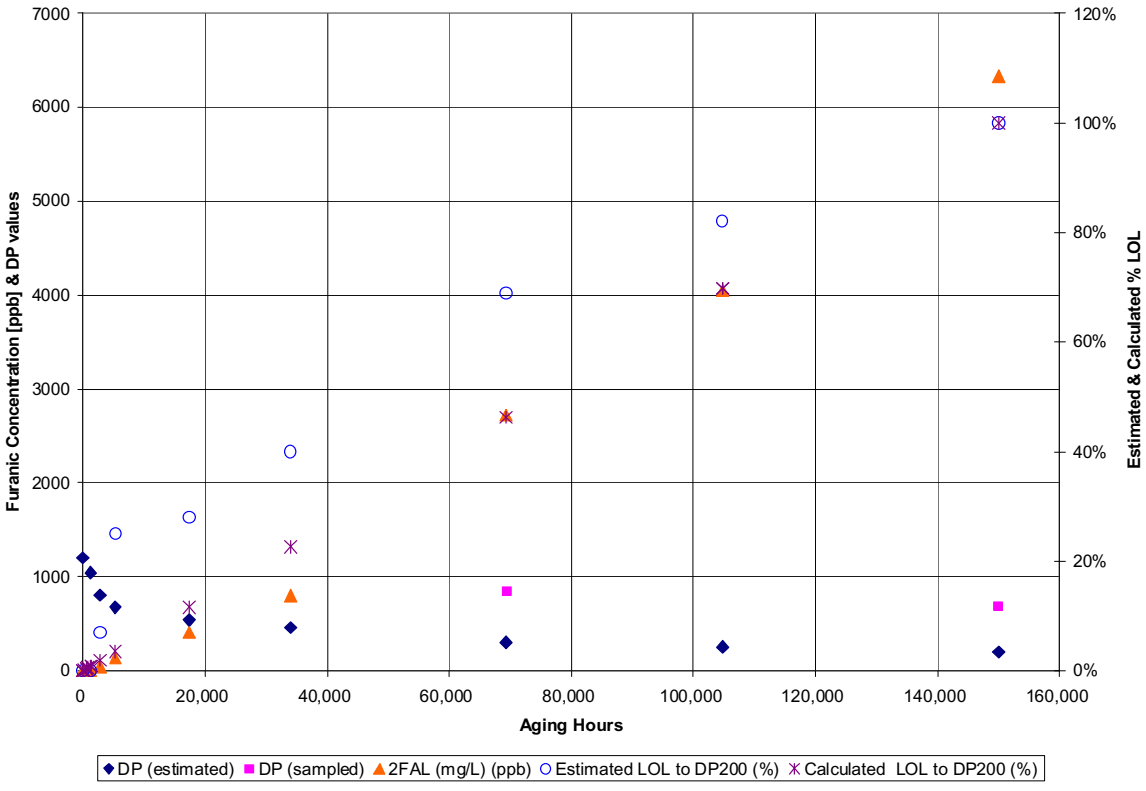

Fig. 80. Furanic Compound evolution and Estimated DP Laboratory Data for CT1

The data indicates that the DP estimation, based on furanic concentration, proposed by Pahlavanpour (see Table 32) is the closest approximation to the laboratory results. The difference between the top surface sample and the core-wrapping sample is in the range of 40% - 50% of the estimated loss-of-life. Another good reason to avoid judgment of the transformer age based on the top-surface paper sample.

4.6 Ageing CT3 - Experimental Work, Results, and Discussion

After a thorough review of the results obtained from thermally ageing CT1 and CT2 and in order to minimize intrusive activities that interfere with the inner environment of the CT, it was decided to continue the thermal stress process in steps up to reaching a load level that will give a measured value of HST close to 150°C. CT3 was not connected to the DGA monitor and no DP sampling was carried out during the ageing process.

The loading process for CT3 was initiated in November 2008 with 200A on the primary winding. The previous experience indicated that the Oil-Immersed transformer needs to pass through an initial endurance stage. Otherwise, the CT will not be able to handle future loads above the nameplate rating. Therefore, a gradual increase of load, starting from 1 p.u. (200A), was initiated up to the maximum safe level at 3.0 p.u. where temperatures recorded were close to 150° C.

A summary of the ageing process and the recorded thermal and load profiles is presented in Fig. 163 in Appendix C. The chart shows average temperature values recorded during the process by fiber-optic temperature sensors and Thermocouples embedded in CT3. These values were used to estimate the percentage Loss-of-Life of CT3.

The initial loading process recorded by the DAQ system is shown in Fig. 81.

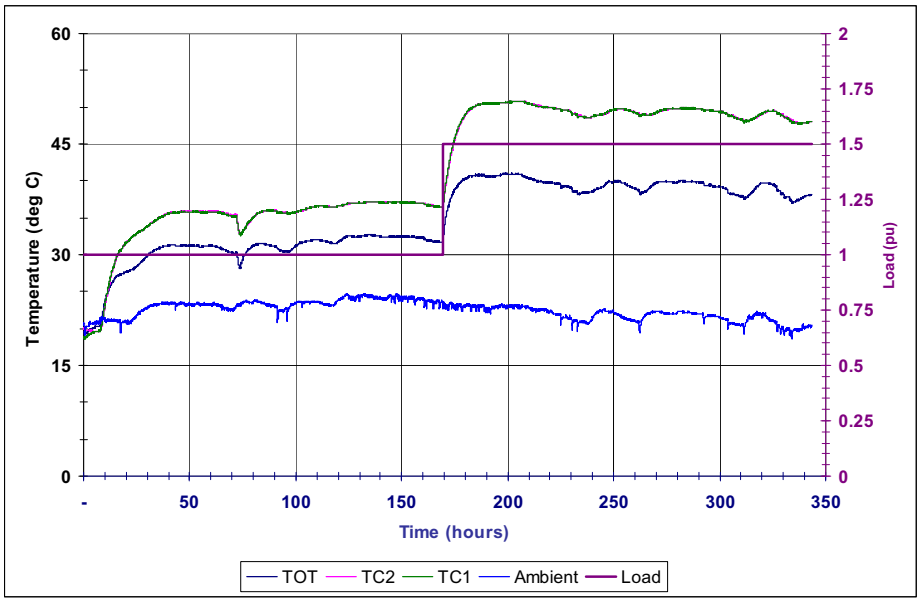

Fig. 81. Accelerated Ageing of CT3. Thermal profile at 1 and 1.5 p.u. load

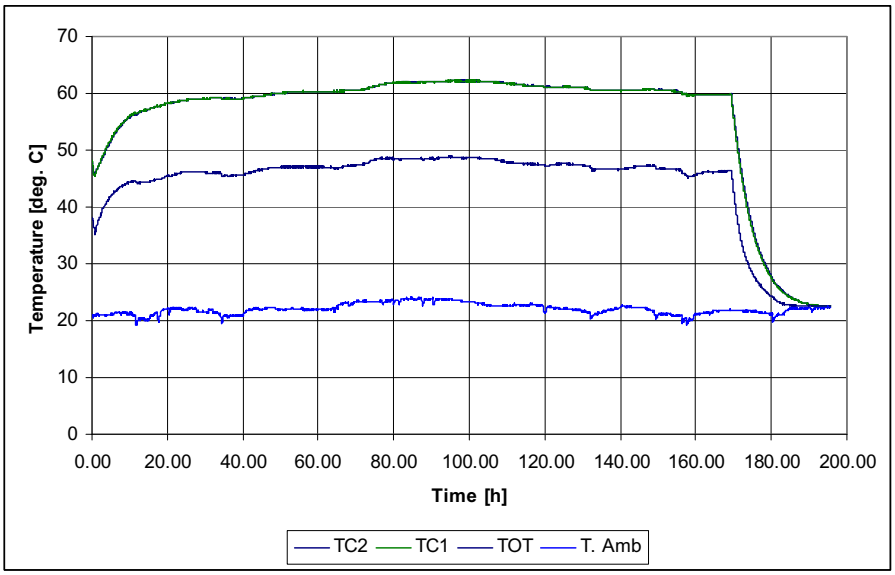

Fig. 82. Accelerated Ageing of CT3. Thermal profile at 1.75 p.u.

The values recorded by thermocouples (TC1, TC2) and optical sensors (OP1, OP2) do not reflect representative differences at load values close to nameplate ratings (1, 1.5 and 1.75 p.u.) (see Figures 81 and 82).

At higher levels of thermal stress, differences will be more evident and thus the curves of all sensors will be included. Up to 1.75 p.u., the sensors did not identify a significant difference between

fiber-optic thermal data and the data collected by the Thermocouples, this difference starts becoming observable at 2 p.u. load as presented in Fig. 83. As can be observed in Fig. 83, three additional curves are introduced: CT3 BOT (Bottom Oil Temperature), OP1, and OP2 (representing the fiber-optic sensors). OP1 shows the highest recorded average temperature and that is the value used for HST in further analysis at that load level, and OP2 drawing a very close path together with TC1 and TC2 curves.

The initial loading values do not represent significant stress in the life of the unit, for the purpose of thermal reference; the unit was loaded for extended periods of at least 168 hours. This is reflected in Figures 81 to 85. It may have been interesting for the overall temperature monitoring process to observe any thermal changes during the ageing process through the BOT. Some results indicate temperatures lower than the ambient even at the increased load imposed on the primary winding. Therefore, BOT did not contribute with valuable data to this research project and will be not included in the rest of the figures.

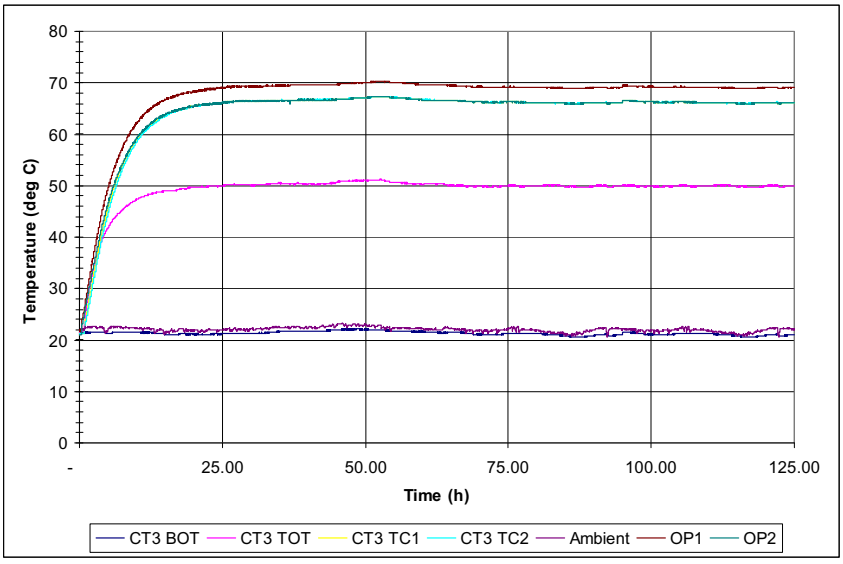

Fig. 83. Thermal Accelerated Ageing of CT3. Thermal Profile at 2 p.u.

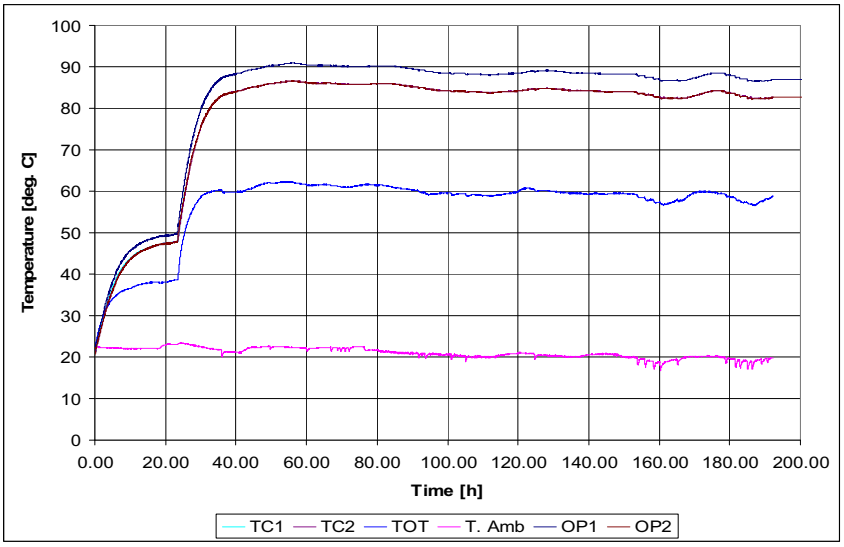

Fig. 84. Thermal Accelerated Ageing of CT3. Thermal profile at 2.25 p.u.

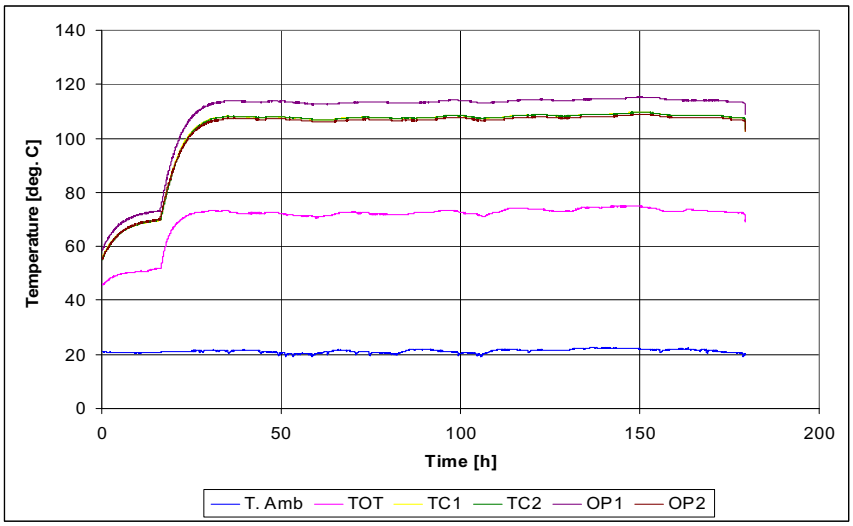

Fig. 85. Thermal Accelerated Ageing of CT3. Thermal profile at 2.75 p.u.

One of the reasons for not using temperature sensors in current transformers of this type is because of the relative proximity to the high voltage compartment.

After loading the unit at 2.75 p.u., CT3 presented an estimated ageing of approximately 1,500 hours. The next decided step was to stress the unit at 2.9 p.u. up to a value close to 10,000 ageing hours as shown in Fig. 86.

After the first 10,000 ageing hours, the experimental process was defined such that loading will be carried out at levels where the safety of personnel and equipment will not be compromised. Therefore, maximum temperature should be kept at approximately 150°C. This was achieved by loading the unit between 3.05 – 3.1 p.u and performing the planned testing every approximately 30,000 ageing hours. Recorded thermal profiles are shown in Fig. 87.

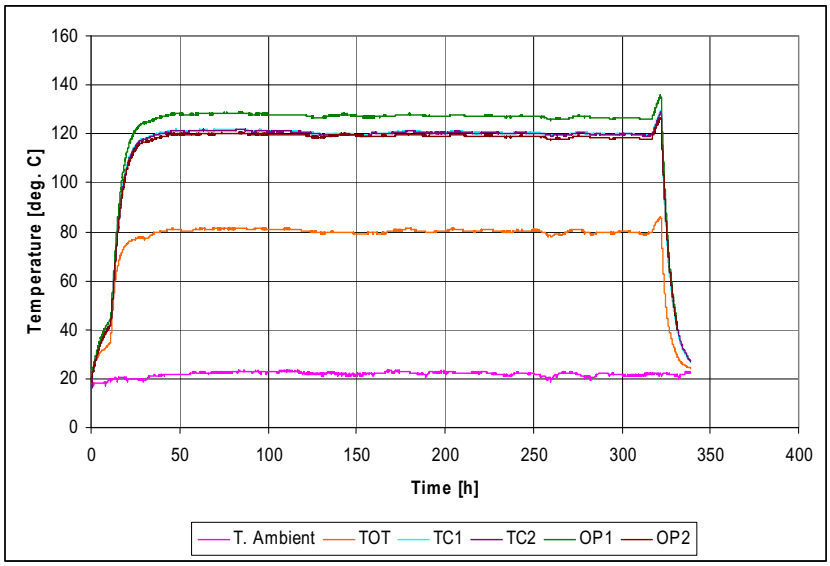

Fig. 86. Thermal Accelerated Ageing of CT3. 10,000 Arrhenius hours captured in 340 h Real Time

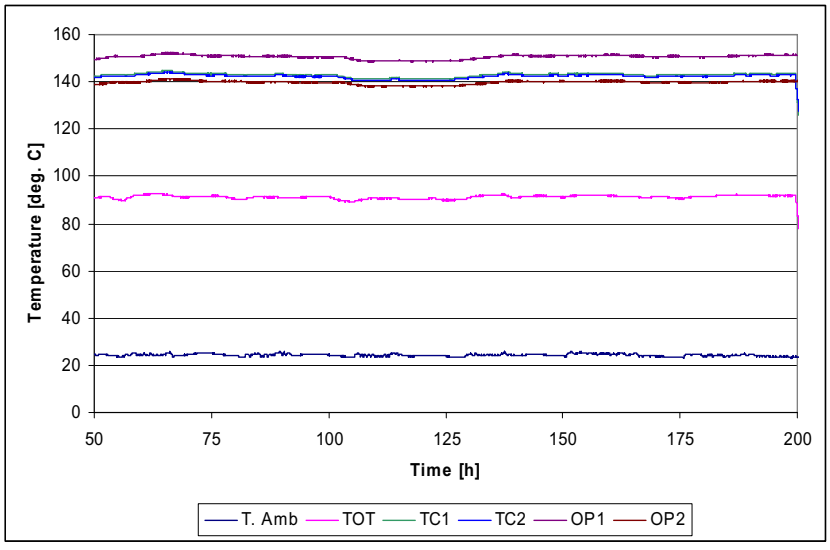

Fig. 87. Typical 30,000 hours ageing profile for CT3

The continuous thermal stress applied to CT3 brought the unit up to a calculated Arrhenius age of 300,000 hours. Thus, the process passed above the DP200 criterion and also the complete Loss-Of-Life limit stipulated at 180,000 ageing hours. After completion of 240,000 ageing hours, the unit was left at ~ 150°C constant thermal stress expecting thermal runaway. The overall testing / ageing process with CT3 took approximately 8 months. During this time each specific test was recorded and included in a database for future correlation with DP analysis and ageing evaluation. Details of the experimental process, obtained results and analysis of the gathered data are presented herein.

4.6.1 DC Testing on CT3

DC tests as described in Chapter 3 were carried out on CT3. The insulation resistance (IR) test was repeated at least five times during each scheduled testing cycle. This allowed obtaining an average reliable value of IR.

Tests were always conducted at 5kV under laboratory conditions where temperature fluctuated around 23°C ± 3°, and a relative humidity of 55 % ± 10%. Baseline characteristics of the DC tests carried out for CT3 are shown in Figures 88 to 91.

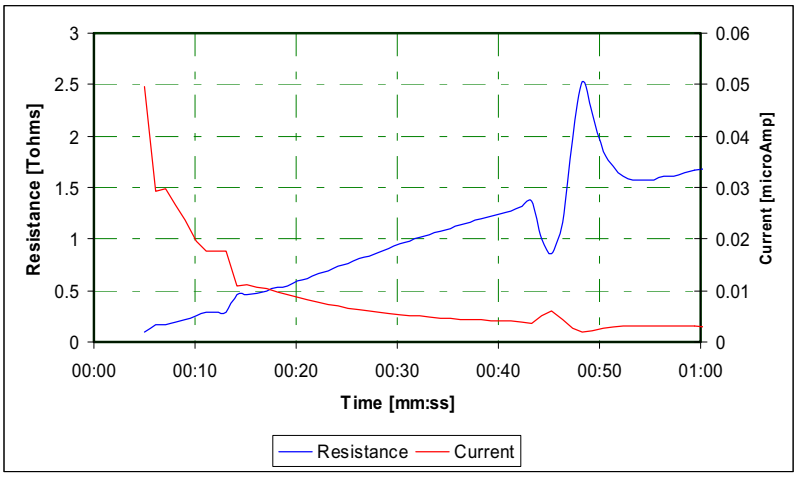

Fig. 88. Insulation Resistance test on CT3 – Baseline Curve

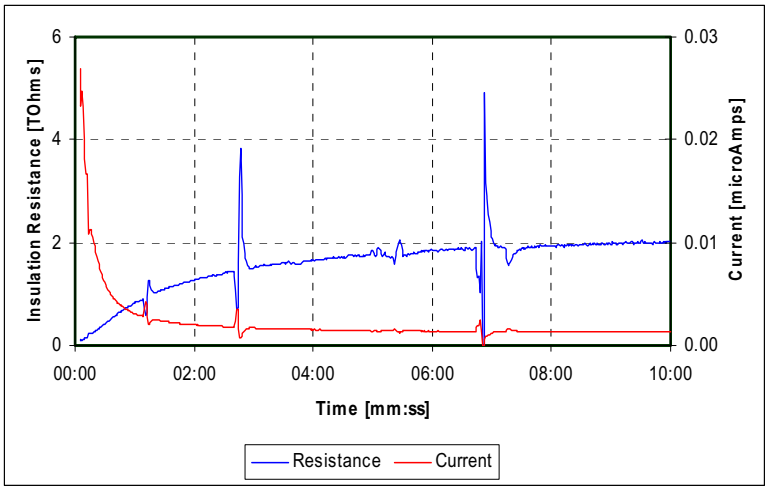

Fig. 89. Polarization Index test on CT3 - Baseline Curve

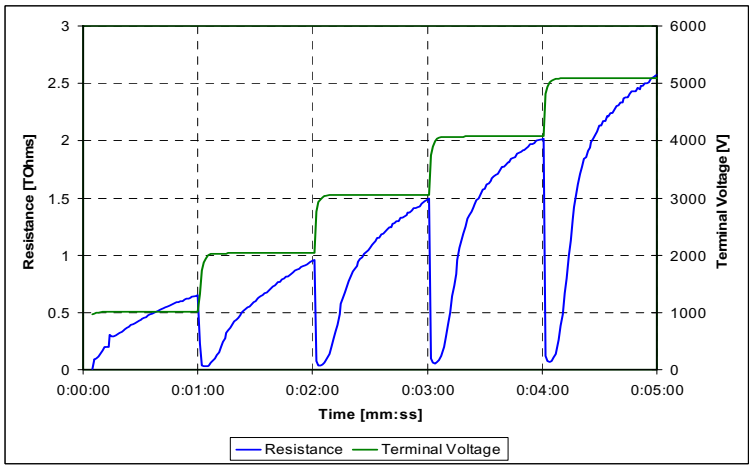

Fig. 90. Step Voltage Test on CT3 - Baseline Curve

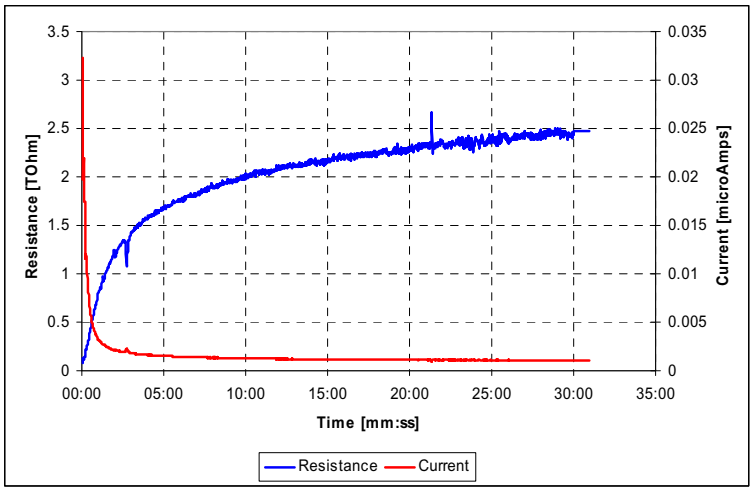

Fig. 91. Dielectric Discharge Test on CT3 - Baseline Curve

The baseline curves indicate that the insulation system in CT3 is in good conditions and capable of operating according to the nameplate specifications.

For CT3 the definition of Normal Insulation Life was left open to be determined by the experimental process and not strictly as per IEEE standards expecting a DP value of 200 after an accelerated ageing process ending at 150,000 ageing hours or complete end-of-life after 180,000 hours. The characteristics obtained after 180,000 ageing hours are presented in Figures 92 to 95.

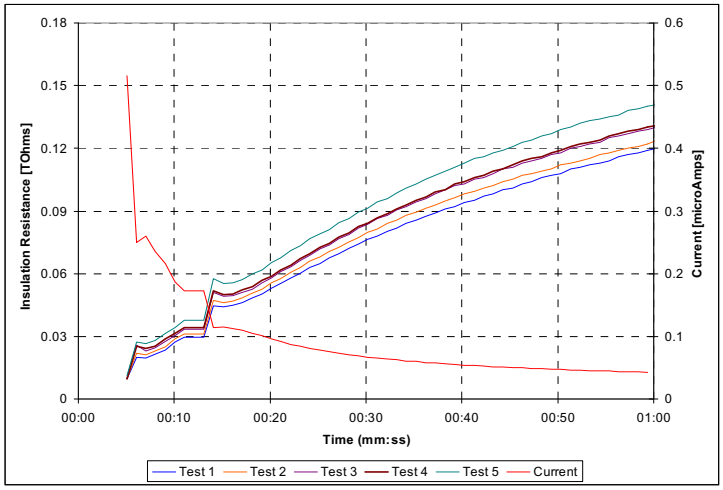

Fig. 92. Insulation Resistance Test on CT3 - Unit after 180,000 Ageing Hours

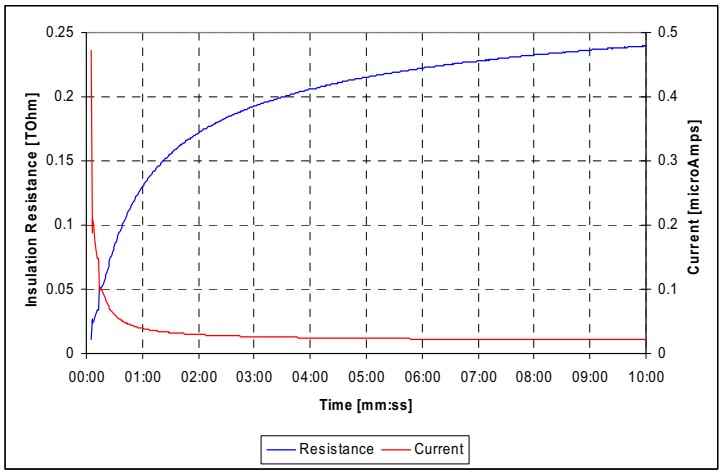

Fig. 93. Polarization Index Test on CT3 - Unit after 180,000 Ageing Hours

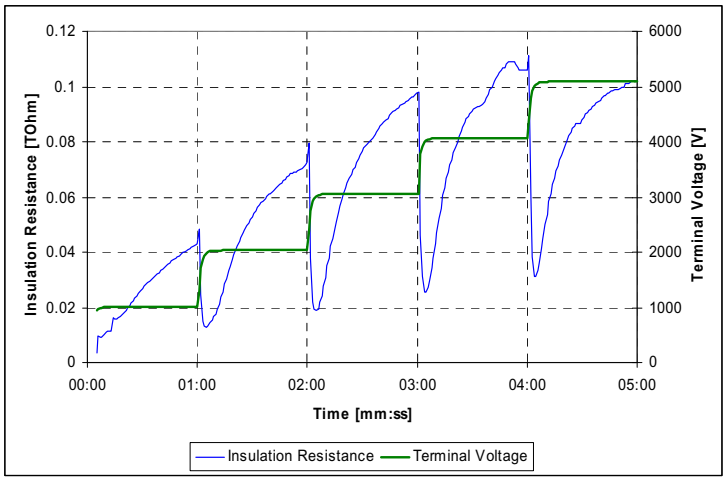

Fig. 94. Step Voltage test on CT3 - Unit after 180,000 Ageing Hours

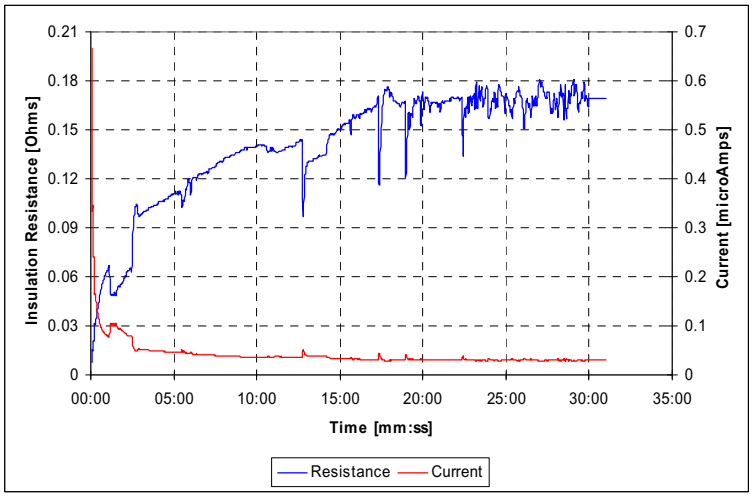

Fig. 95. Dielectric Discharge Test on CT3 - Unit after 180,000 Ageing Hours

The obtained curves after 180,000 ageing hours indicate minor resistance variation of the insulation. Only the step-voltage characteristics suggest the need for additional testing as the final step at 5kV showed a resistance decay as compared against the one at 4kV. Further testing was performed as CT3 continued to be thermally stressed and aged up to 300,000 hours. It was not expected to see CT3 surviving such a continuous high thermal stress, in fact, thermal runaway was expected even before reaching 240,000 ageing hours.

The characteristics obtained after 300,000 ageing hours are presented in Figures 96 to 99.

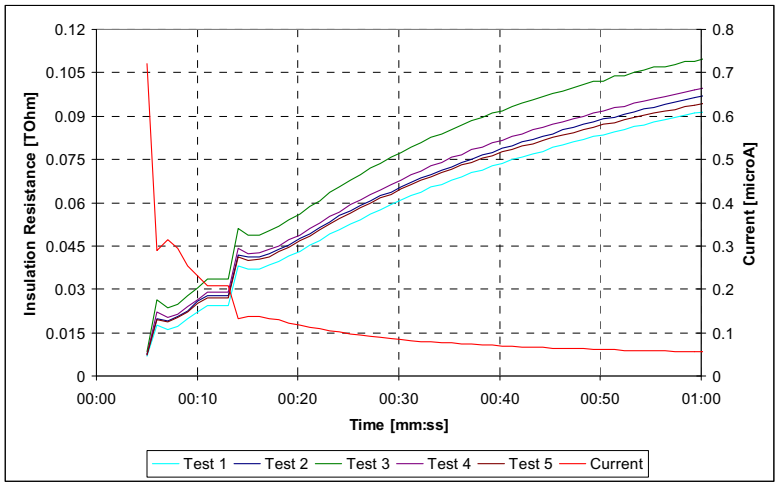

Fig. 96. Insulation Resistance Test on CT3 - Unit after 300,000 Ageing Hours

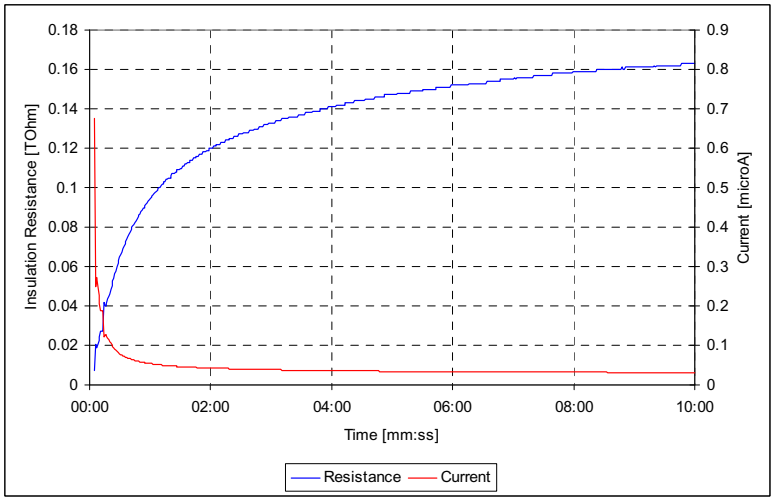

Fig. 97. Polarization Index Test on CT3 - Unit after 300,000 Ageing Hours

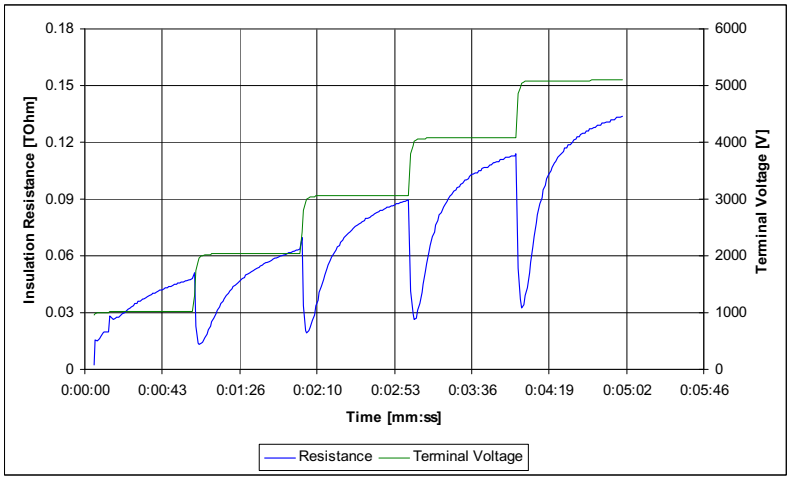

Fig. 98. Step Voltage Test on CT3 - Unit after 300,000 Ageing Hours

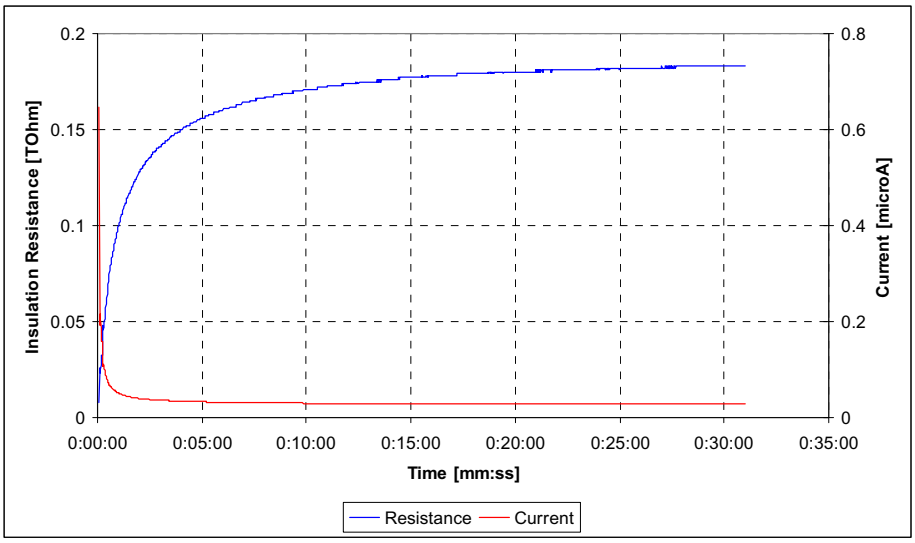

Fig. 99. Dielectric Discharge Test on CT3 - Unit after 300,000 Ageing Hours

In summary, the changes in insulation resistance and polarization index were tracked numerically and the trend data up to 300,000 ageing hours is presented in Fig. 100.

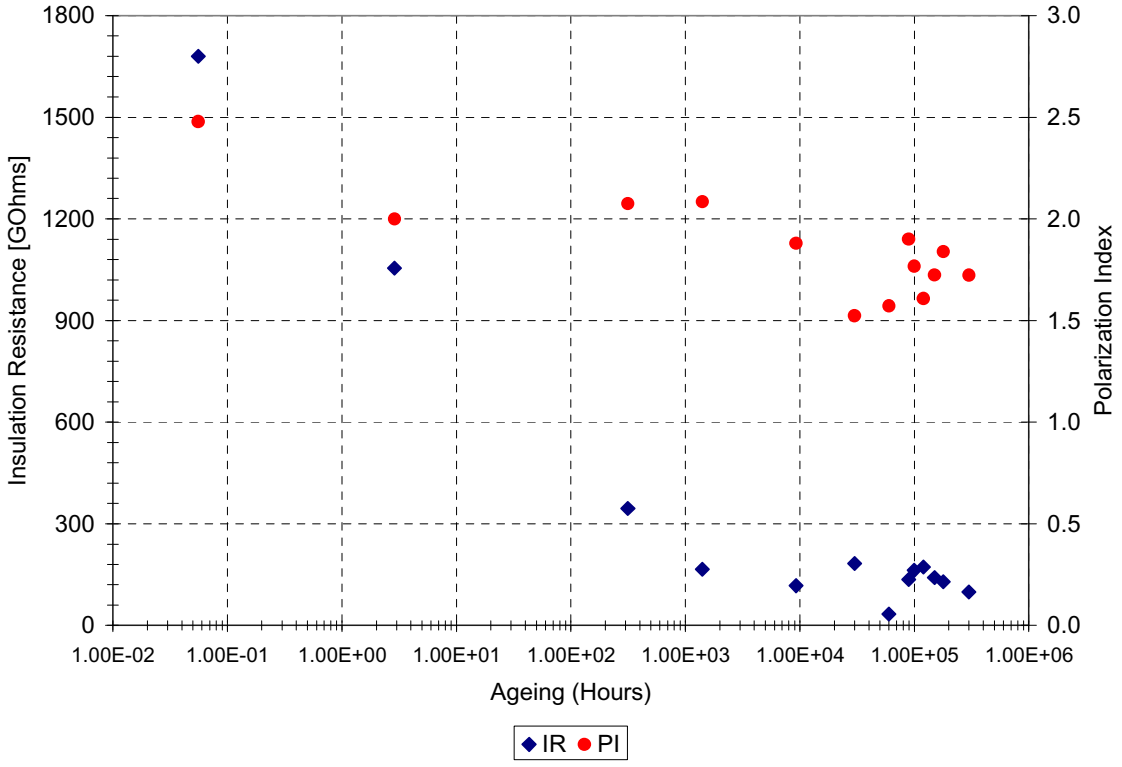

Fig. 100. Data Trend DC Test on CT3 - Insulation Resistance and Polarization Index up to 300KH

From the curves obtained during the testing process, it can be concluded that the insulation resistance of the unit reached stable values after approximately 2,000 ageing hours. Insulation resistance was recorded within the range of 50 and 200 GΩ. Polarization index value lay in the range between 1.5 and 2.0. Tests up to 300,000 ageing hours indicate that the insulation system of CT3 was still in good conditions and capable of operating under normal conditions.

After 300,000 ageing hours, CT3 was removed from the load bed for inspection and complete dissection of the solid insulation surrounding the core/secondary winding assembly. More information regarding this part of the experimental work will be presented later in Section 4.6.4.

4.6.2 AC Testing on CT3

Dielectric Spectroscopy in the Frequency Domain was used for the analysis of dielectric parameters in CT3 as described in Chapter 3. Post-factory baseline curves obtained are presented below in Fig. 101.

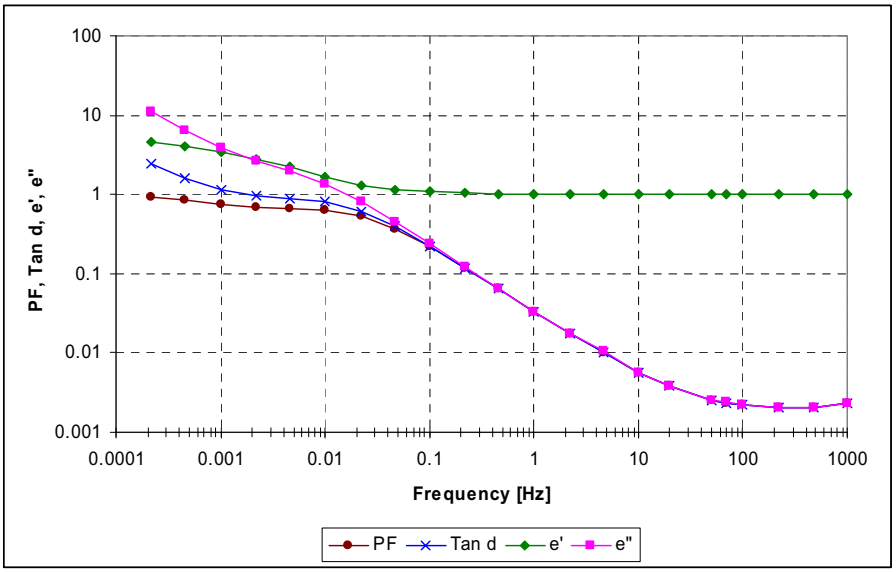

Fig. 101. Dielectric Spectroscopy Test on CT3 - Baseline Curves PF, tan δ, and Complex ε

The observed dielectric properties at the power frequency value appear acceptable for operation as previously discussed in Chapter 3. All dielectric parameters were continuously recorded and evaluated. The characteristics recorded after 300,000 ageing hours are shown in Fig. 102.

The progressive deterioration of the liquid-solid insulation system is difficult to visualize only from Figures 101 and 102. The next figures, representing Power Factor trend (Fig. 103) and tan δ trend (Fig. 104) can be used to visualize the changes of dielectric characteristics during the ageing process using the frequency sweep response.

In the field the common Power factor Test carried out at power frequency exclusively may not lead to an accurate analysis. The figures below indicate a very close match of values for frequencies equal and / or above 1 Hz.

Similar to what was observed in the DC Tests, the insulation system on the baseline curve presents stronger dielectric characteristics. The characteristics are very similar from 30,000 to 300,000 hours.

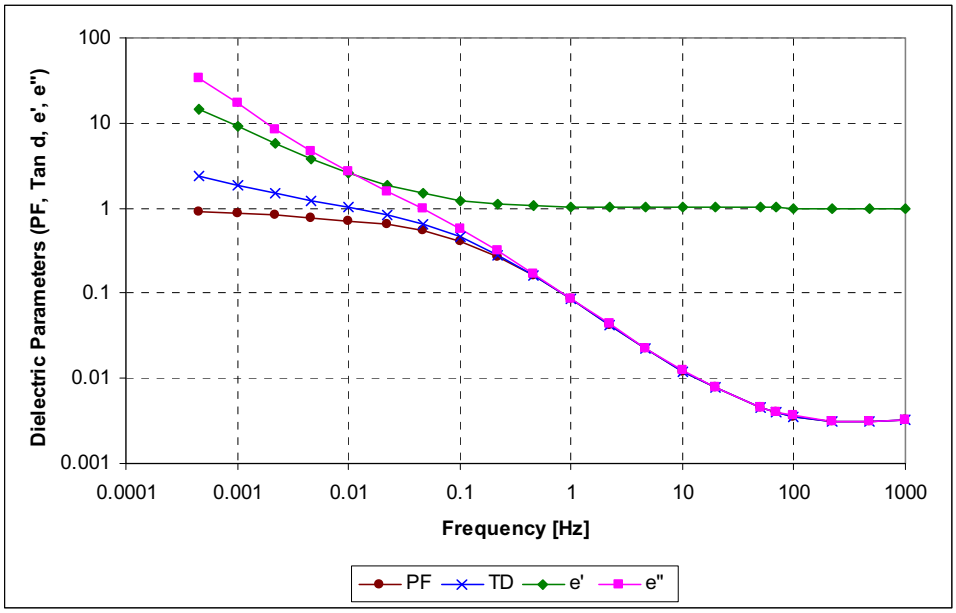

Fig. 102. Dielectric Spectroscopy Test on CT3 - Unit after 300,000 Ageing Hours

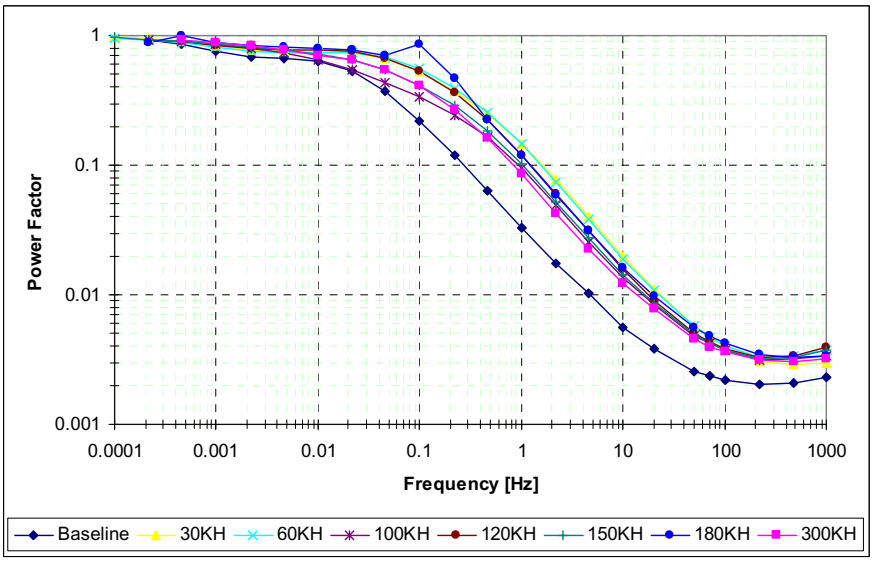

Fig. 103. Thermal Ageing of CT3 - Power Factor, Frequency Sweep Trend Data

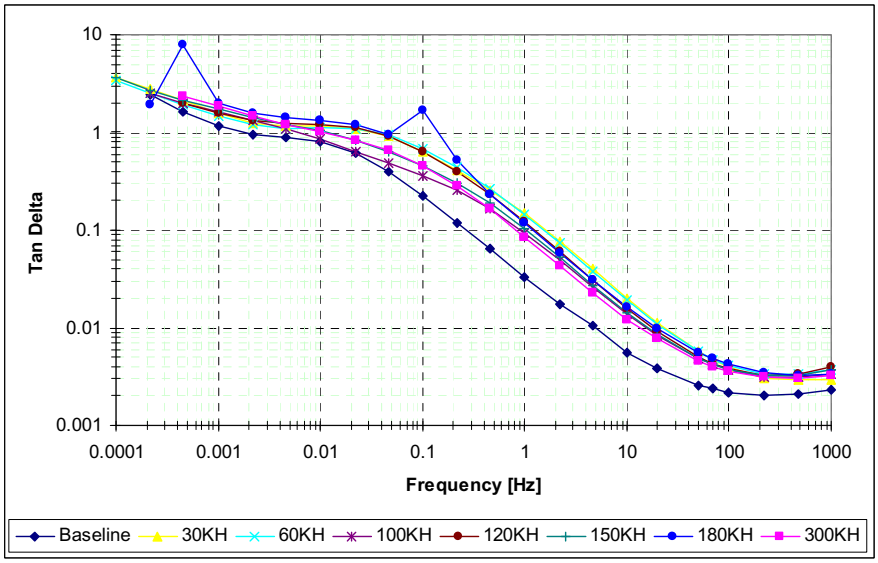

Fig. 104. Ageing of CT3 - tan δ, Frequency Sweep Trend Data

For CT3 the moisture content reported is not a typical value. The unit after the manufacturing process had to go through additional modifications that allowed moisture ingress at levels not critical for the type of experimentation work carried out. Some values may not be acceptable in the industry for normal operation under high voltage conditions. The acceptance value at power frequency (60Hz) for PF is < 0.5%.

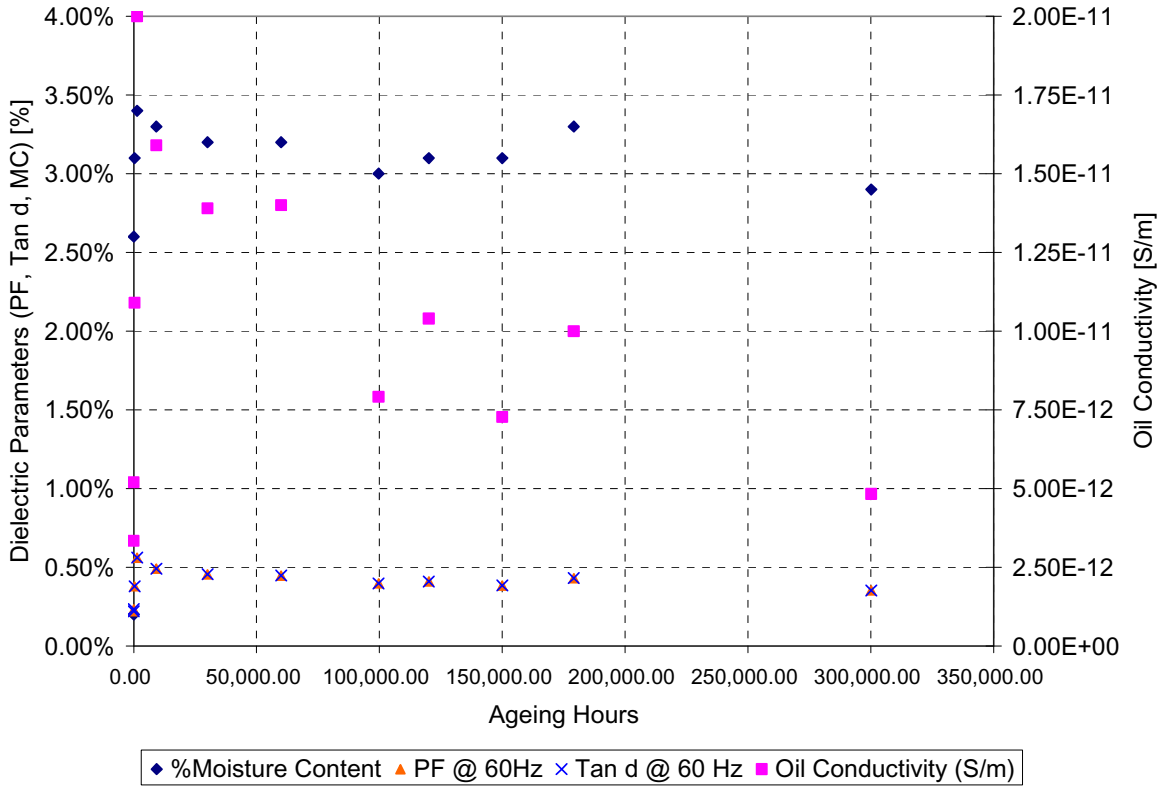

Fig. 105. Dielectric Spectroscopy Data Trend on CT3- PF, tan δ, MC, and Oil Conductivity up to 300,000 h

A summary of the result of the dielectric spectroscopy test in the frequency domain for CT3 is presented in Fig. 105.

4.6.3 Analysis of Functional Parameters on CT3

The operation of CT3 under overload conditions did not affect the physical characteristics of the unit. This is clearly observed on the summary of values recorded using the CT Analyzer on the corresponding chart on Fig. 106 and in Table 60 in Appendix C.

It is demonstrated that the integrity of the physical components of the unit were not deteriorated due to the thermal ageing process. The quality of operation sustained according to the specifications and manufacturer's nameplate until 300,000 Arrhenius age hours.

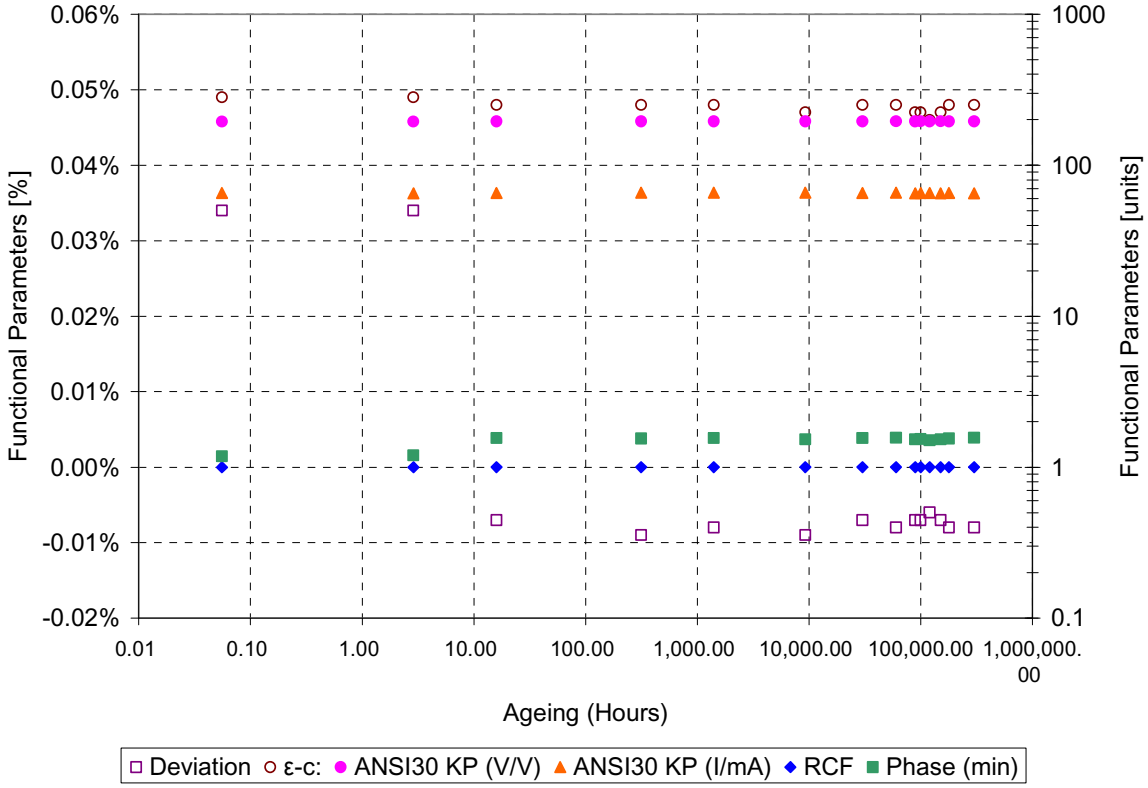

Fig. 106. Functional Parameters recorded for CT3 – Data Trend up to 300,000 h

4.6.4 Degree of Polymerization and Furanic Compound Analysis on CT3

Previous experience indicated the existence of a direct relation between furanic compounds evolution in the liquid insulation and degradation of the solid insulation reflected in the decreasing value of Degree of Polymerization.

The results obtained from the laboratory at different ageing stages during the process are presented in Table 34 and Fig. 107.

The Laboratory reported the following estimated values for DP, as shown in Table 35, which was correlated to the estimated ageing as shown in Fig. 108.

Table 34. CT3 Furanic Compound Concentration - Data Trend

Arrhenius Ageing (h)	HMF (ppb)	FOL (ppb)	2FAL (ppb)	2AF (ppb)	5M2F (ppb)	Total Furan Content (ppb)
0.06	0	0	1	0	0	1
0.6	0	0	1	0	0	1
2.88	0	0	1	0	0	1
9,279.41	0	0	42	0	0	42
30,025.97	0	0	100	3	0	103
60,012.93	0	0	358	7	6	371
89,016.98	0	0	845	9	16	870
120,085.63	13	0	1279	11	26	1329
150,031.81	39	0	1966	17	47	2069
179,094.89	1	92	2651	13	60	2817
240,169.55	10	124	3277	16	76	3503
270,113.06	26	0	3711	19	97	3853
300,191.28	36	50	4509	16	122	4733

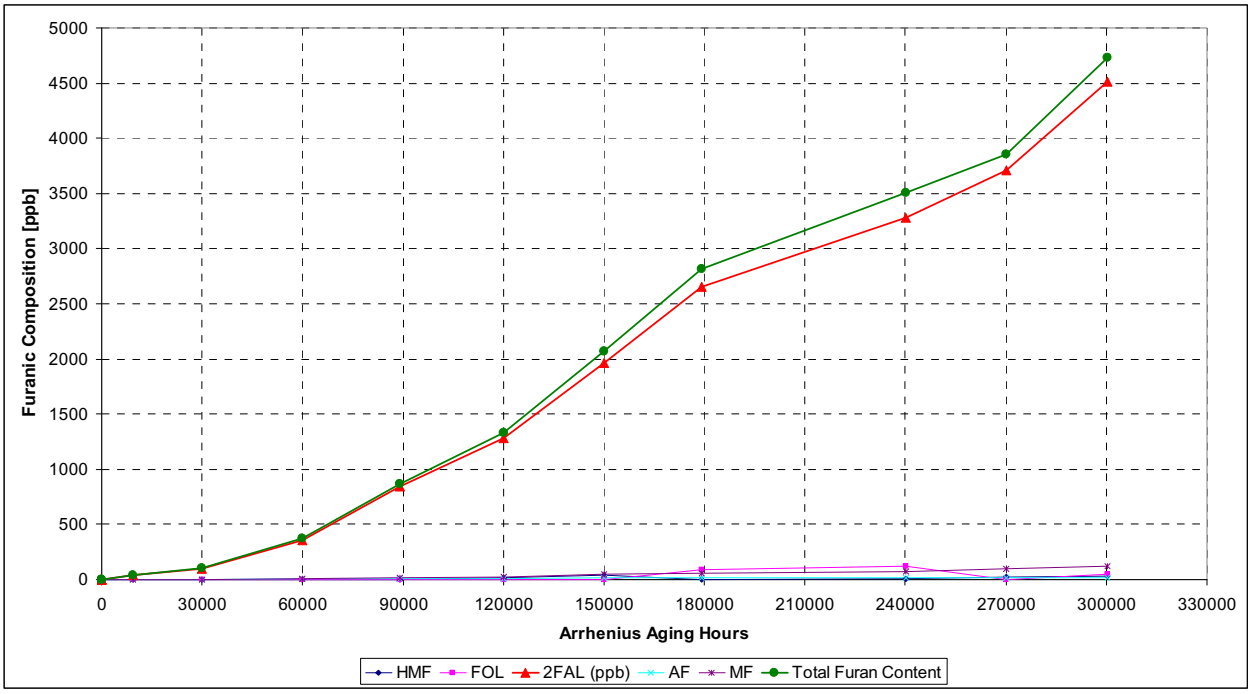

Fig. 107. Furanic Content Evolution during the ageing process of CT3

Table 35. DP Estimated by DOBLE and % LOL Models for CT3

Arrhenius Ageing (h)	DOBLE Estimated DP	% LOL Emsley for DOBLE DP	% LOL General for DOBLE DP	% LOL Stebbins for DOBLE DP
0.06	1286	0%	0%	0%
0.6	1286	0%	0%	0%
2.88	1286	0%	0%	0%
9,279.41	822	9%	38%	6%
30,025.97	714	14%	49%	15%
60,012.93	556	23%	64%	32%
89,016.98	449	33%	75%	46%
120,085.63	398	40%	80%	54%
150,031.81	345	50%	86%	64%
179,094.89	308	58%	89%	71%
240,169.55	281	65%	92%	77%
270,113.06	266	70%	93%	81%
300,191.28	242	79%	96%	87%

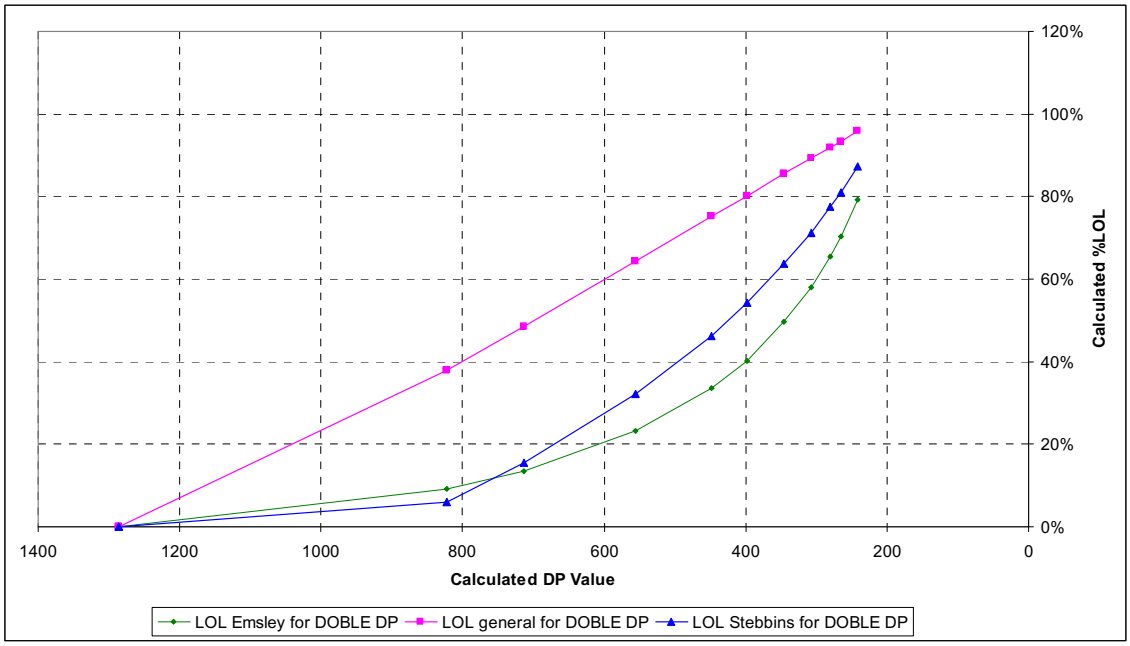

Fig. 108. DOBLE Estimated DP based on Furanic Concentration - Calculated % LOL for CT3

DOBLE Laboratory estimates LOL to be 86%. This first analysis results are of great interest because CT3 passed by far the 150,000 ageing hours. At 300,000 ageing hours the furanic composition was expected to be much higher. Nevertheless, all the data will be compared against DP results.

DePablo model as per (3.41) was used to calculate DP values and correlate with the estimated ageing of CT1 as shown in Table 36 and Fig. 109.

A great difference can be observed between the first two methods of estimating DP value. Applying DePablo's correlation, the furanic concentration values still indicate a strong DP characteristic even after such a long loading process and thus a small % LOL. Because the initial DP value is less than 1200, the equation suggests a lower quality material from the beginning of the process. At first glance, DePablo's equation appears to be extremely conservative bearing in mind the long thermal stress applied to the unit.

Table 36. DP Estimated by DePablo CIGRE and % LOL Models for CT3

Arrhenius Ageing	DePablo CIGRE Estimated DP	% LOL Emsley for DePablo DP	% LOL General for DePablo DP	% LOL Stebbins for DePablo DP
0.06	899.89	7%	30%	0%
0.6	899.89	7%	30%	0%
2.88	899.89	7%	30%	0%
9,279.41	895.28	7%	30%	0%
30,025.97	888.84	7%	31%	1%
60,012.93	861.28	8%	34%	3%
89,016.98	813.67	9%	39%	7%
120,085.63	775.46	11%	42%	10%
150,031.81	721.81	13%	48%	15%
179,094.89	675.24	16%	52%	19%
240,169.55	637.63	18%	56%	23%
270,113.06	613.93	19%	59%	25%
300,191.28	574.65	22%	63%	30%

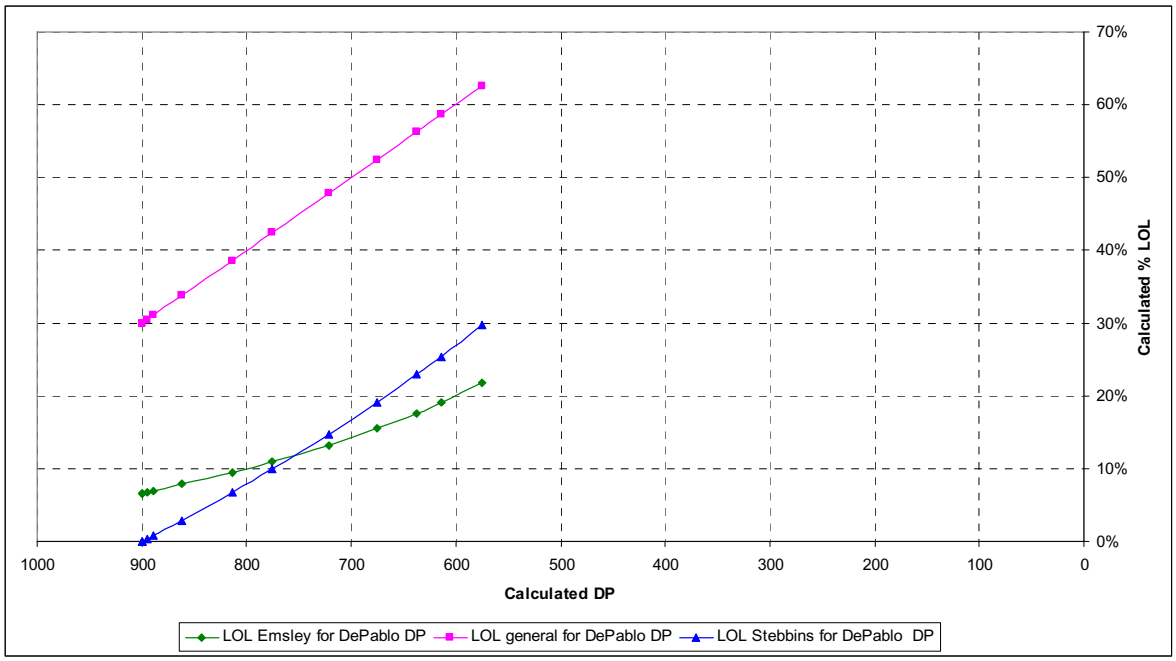

Fig. 109. DePablo CIGRE Estimated DP based on Furanic Concentration - Calculated % LOL for CT3

Table 37. DP Estimated by Stebbins / Myers and % LOL Models for CT3

Arrhenius Ageing	Stebbins/Myers Estimated DP	% LOL Emsley for Stebbins DP	% LOL General for Stebbins DP	% LOL Stebbins for Stebbins DP
0.06	900.01	7%	30%	0%
0.6	900.01	7%	30%	0%
2.88	900.01	7%	30%	0%
9,279.41	576.66	22%	62%	30%
30,025.97	501.61	28%	70%	39%
60,012.93	391.27	41%	81%	55%
89,016.98	316.97	56%	88%	69%
120,085.63	281.12	65%	92%	77%
150,031.81	243.92	78%	96%	87%
179,094.89	218.06	90%	98%	94%
240,169.55	199.72	100%	100%	100%
270,113.06	188.96	107%	101%	104%
300,191.28	172.11	119%	103%	110%

Table 37 shows the estimated values of DP using Equation (3.48) as reported by the Transformer Maintenance Institute. The estimated DP values suggest reaching the DP200 criterion and possible end-of-life at approximately 240,000 ageing hours as clearly visualized in Fig. 110. This is a great contradiction as compared to DePablo's values and even with DOBLE's estimates. Again, validation of the data via DP analysis becomes imperative for a definitive correlation between furanic compound – DP and real ageing of the CT.

The estimated DP values using Chendong's expression (3.42) are presented in Table 38 with the corresponding percentages LOL calculated by the techniques presented in Chapter 3 and graphically presented in Fig. 111.

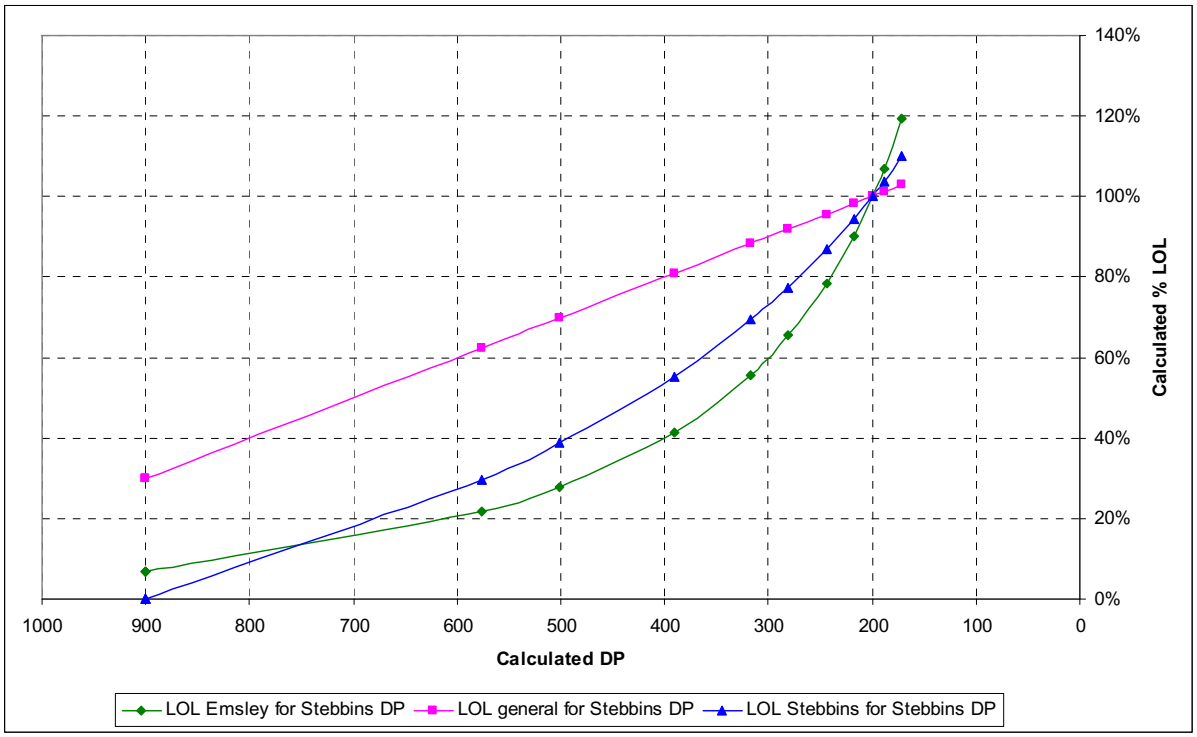

Fig. 110. Stebbins Estimated DP based on Furanic Concentration - Calculated % LOL for CT3

Table 38. DP Estimated by Chendong and % LOL Models for CT3

Arrhenius Ageing	Chendong Estimated DP	% LOL Emsley for Chendong DP	% LOL General for Chendong DP	% LOL Stebbins for Chendong DP
0.06	1288.57	0%	0%	0%
0.6	1288.57	0%	0%	0%
2.88	1288.57	0%	0%	0%
9,279.41	824.79	9%	38%	6%
30,025.97	717.14	13%	48%	15%
60,012.93	558.89	23%	64%	32%
89,016.98	452.33	33%	75%	46%
120,085.63	400.89	40%	80%	54%
150,031.81	347.55	49%	85%	63%
179,094.89	310.45	57%	89%	71%
240,169.55	284.15	64%	92%	77%
270,113.06	268.72	69%	93%	80%
300,191.28	244.55	78%	96%	87%

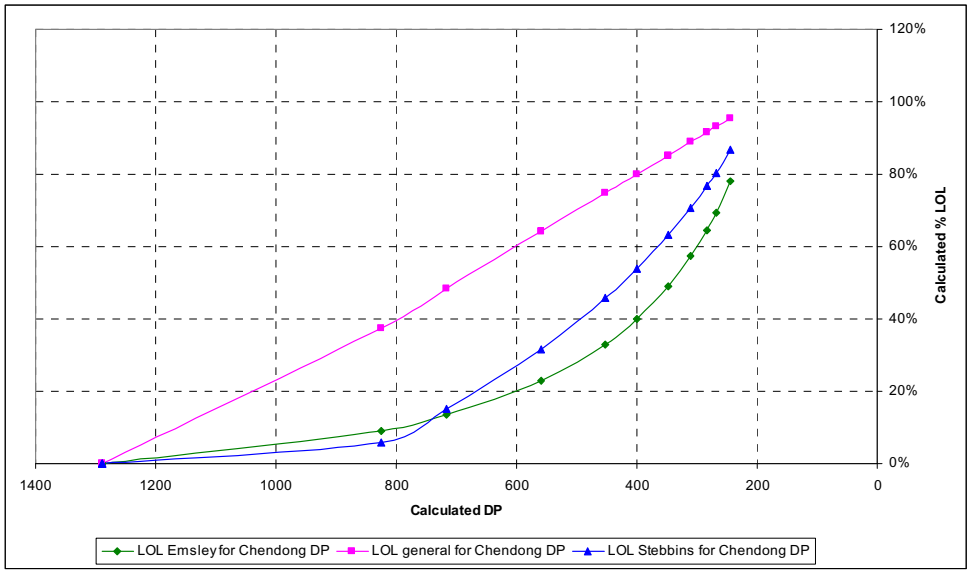

Fig. 111. Chendong Estimated DP based on Furanic Concentration - Calculated % LOL for CT3

The obtained DP values reflect almost similar values as the ones provided by DOBLE. The problem with using Chendong equation is that it was empirically developed for thermally upgraded paper.

Another DP expression given by Pahlavanpour (3.44) using $DP_0 = 900$ was then applied to the furanic concentration values and the resulting DP estimates are summarized in Table 39 and shown in Fig. 112.

By just visual inspection, it is not possible to define the most accurate result to estimate DP. All the models reviewed present different values which lead to a sparse probability of %LOL. One thing is clear from this experimental unit, NIL is much higher than 150,000 hours. The only way to verify the validity of the data is to extract a sample of the solid insulation and perform the corresponding DP analysis.

Table 39. DP Estimated by Pahlavanpour and % LOL Models for CT3

Arrhenius Ageing	Pahlavanpour Estimated DP	LOL Emsley for Pahlavanpour DP	LOL general for Pahlavanpour DP	LOL Stebbins for Pahlavanpour DP
0.06	899.81	7%	30%	0%
0.6	899.81	7%	30%	0%
2.88	899.81	7%	30%	0%
9,279.41	892.23	7%	31%	1%
30,025.97	881.71	7%	32%	1%
60,012.93	837.80	9%	36%	5%
89,016.98	765.80	11%	43%	11%
120,085.63	711.32	14%	49%	16%
150,031.81	639.33	18%	56%	23%
179,094.89	580.72	21%	62%	29%
240,169.55	535.84	25%	66%	34%
270,113.06	508.58	27%	69%	38%
300,191.28	465.09	32%	73%	44%

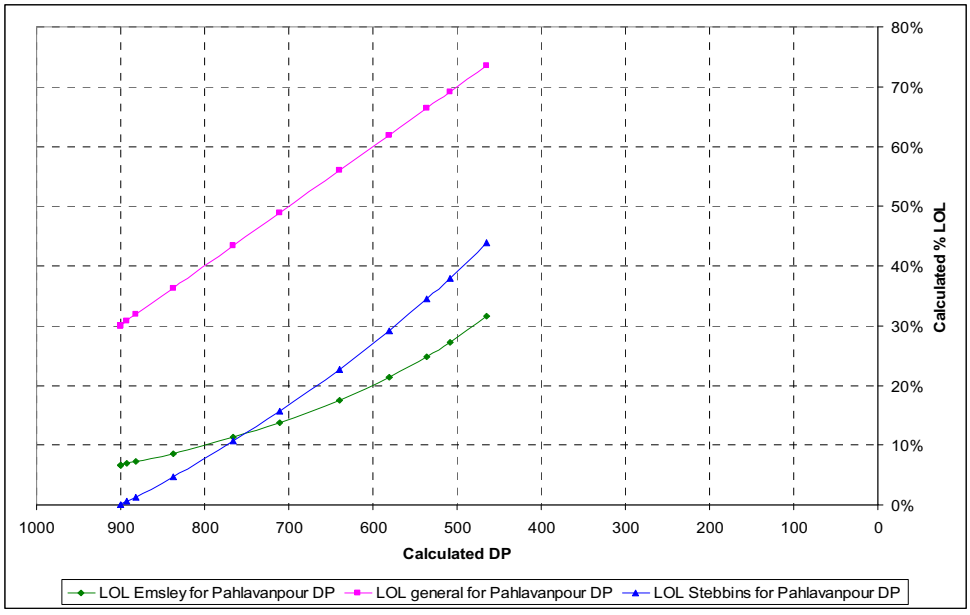

Fig. 112. Pahlavanpour Estimated DP based on Furanic Concentration - Calculated % LOL for CT3

Therefore, CT3 was removed from the load bank after being stressed for a continuous thermal process resulting in an estimated ageing of 300,000 hours. The unit was drained and opened for dissection. This intrusive inspection had the following objectives:

- Visual inspection of the solid insulation and windings
- Remove paper samples from the core paper wrap
- Remove paper samples at different layers of the paper insulation

The discrepancies observed in the analysis of CT1 between DP estimated and sampled were, respectively, analyzed in 4.5.5. The analysis of CT3 leads to an increasing interest of verifying the DP samples. Again, great expectations were given to the CT3 dissection and the results of the DP analysis taken at different layers of the solid insulation, same as it was taken for CT1. During the dissection process, the core and both primary and secondary windings can be observed with their complete insulation in Fig. 113. The dark color of the liquid insulation is due to the high thermal stress applied to the unit and charring of the primary conductor as it will be shown later. The location of the

aluminum shield wrap is visualized in Fig. 114 and the secondary winding in Fig. 115. Constructive differences are observed only in the primary winding installation.

Fig. 113. CT3 Dissection – Draining Oil, observed primary, secondary, and core insulation

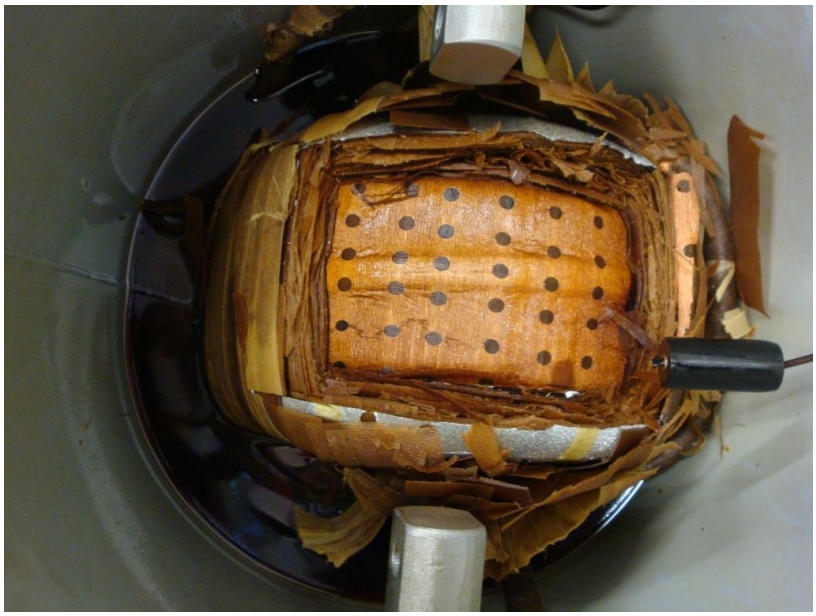

Fig. 114. CT3 Dissection – Second Layer Shield

The dissection had to reach the most inner layer of paper insulation surrounding the core. Finally, the core is shown in Fig. 116. As can be observed here, the secondary winding and the core do not show any evidence of charring.

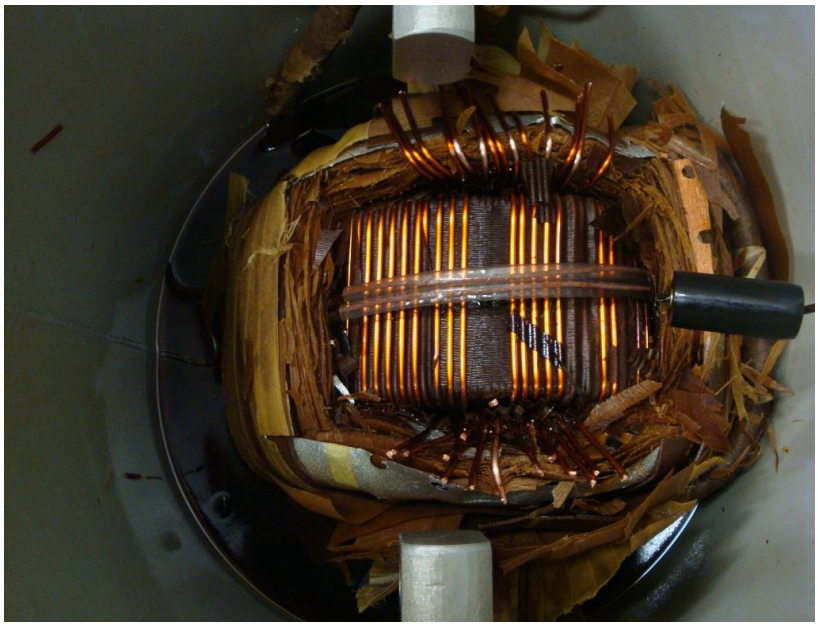

Fig. 115. CT3 Dissection – Secondary Winding

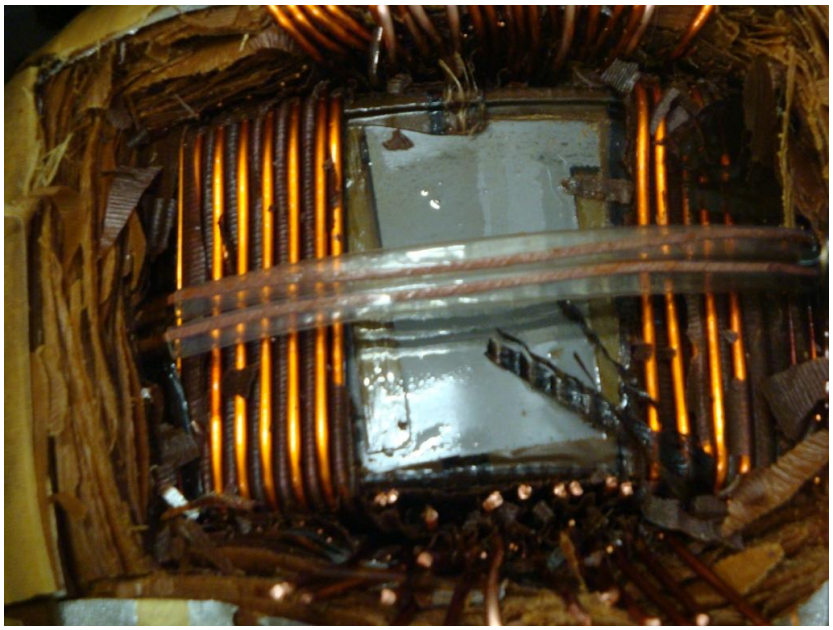

Fig. 116. CT3 Dissection – Core

The solid insulation samples taken during the dissection procedure were submitted to DOBLE Laboratory for DP analysis. The reported results are summarized in Table 40.

Table 40. CT3 DP Values Obtained from DOBLE Laboratory after Dissection

Dissection Secondary - Core and Primary winding				
Layer	**DP Value**	**LOL Emsley for Lab DP value**	**LOL general for Lab DP value**	**LOL Stebbins for Lab DP value**
Top Surface (1)	748.00	12%	45%	12%
20	690.00	15%	51%	18%
2-ry winding wrap	276.00	67%	92%	79%
Core wrap	302.00	59%	90%	73%
1-ry winding	667.00	16%	53%	20%

The primary winding, as observed previously in Section 4.5.5 for CT1, was the only component in the assembly presenting evidence of charring as it is shown in Fig. 117. Because the primary winding conductors were wrapped in paper insulation as well, a sample was additionally taken and sent for DP analysis. The obtained values reported in Table 40 confirm that ageing of the paper insulation in the primary winding is relatively close to the ageing of the top surface paper insulation of the secondary winding / core insulation. The analysis confirms the location of the hottest spot in the CT between the secondary winding and the core. Therefore, DP sampling from the top surface layer is worthless for ageing evaluation. Similar observation was also described in the earlier literature [65]. Under failure conditions or reconditioning of the unit, samples should be taken from the zone between the core and the secondary winding; this is the weakest insulation point identified for CT3 and previously for CT1 during this experimental work. A summary of the data obtained from DOBLE laboratory is presented in Fig. 118. Estimated % LOL and Calculated %LOL to DP200 reached maximum value after 300,000 ageing hours.

Fig. 117. CT3 dissection after 300,000 ageing hours - Primary Winding

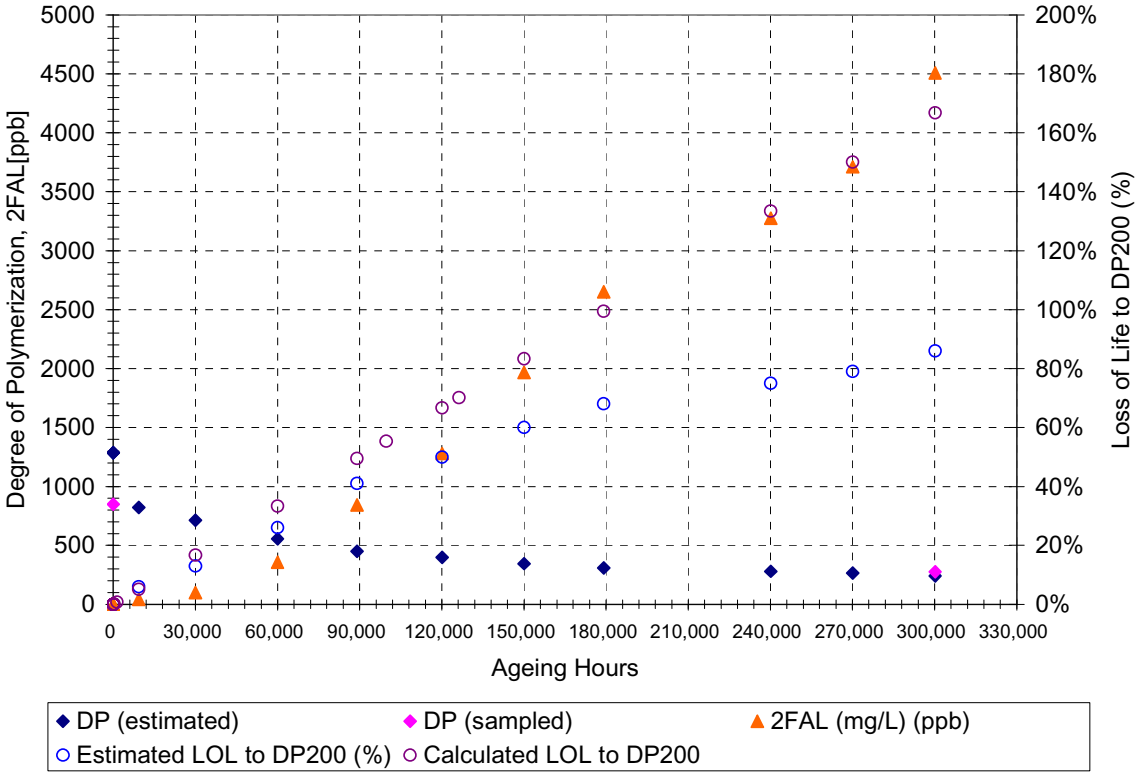

Fig. 118. Furanic Compound evolution and Estimated DP Laboratory Data for CT3

The data indicate that the DP estimation, based on furanic concentration, of all reviewed models do not provide a close approximation to the laboratory results. The difference between the top surface sample and the core-wrapping sample is in the range of 40% - 60% of the estimated loss-of-life. This is good reason to avoid judgment of the transformer age based on the top-surface paper sample.

4.7 Ageing CT4 - Experimental Work, Results, and Discussion

CT3 and CT4 were thermally stressed simultaneously for most of the time. The difference between both units is that the resources for the test allowed only one unit to be attached to the DGA monitoring system and this was CT4. The continuous sampling of dissolved gas concentration by the TM8 monitor originates a continuous oil recirculation in CT4 taking cold (ambient temperature) oil from the bottom of the unit, cooling it before the chromatography, and injecting it back into CT4 through the top connection as it is shown in Fig. 160. This un-common Forced-Oil Natural-Air cooling effect creates a difference of HST values as compared against the same loading values on CT3 without the DGA monitor. Therefore, the ageing process was properly accomplished based on temperature control. Load requirements are higher to match similar HST temperatures with the twin unit CT3. The loading process for accelerated ageing was completed in steps up to reaching a load level (approximately 3.5 p.u.) that will give a measured value of HST close to 150°C. CT4 was connected to the DGA monitor and no DP sampling was carried out during the ageing process.

The loading process in this unit initiated on December 2008 with minor load on the primary winding. The previous experience indicated that the unit needs to pass through an initial endurance stage in order to be able to handle future loads above the nameplate rating. Therefore, a gradual

increase of load, starting from 1 p.u. (200A), was initiated up to the maximum safe level at 3.5 p.u. where hot-spot temperatures recorded were close to 150° C.

A summary of the ageing process and the obtained thermal results are shown in Fig. 164 in Appendix C. Average Hot-Spot temperature values were used to calculate the ageing acceleration factor and to estimate the percentage Loss-of-Life. Top-Oil Temperature is not presented in this study because the oil recirculation process interfered with the accuracy of the sensor.

4.7.1 DC Testing on CT4

DC tests as described in Chapter 3 were carried out on CT4. The insulation resistance (IR) test was repeated at least five times during each scheduled testing cycle. This allowed obtaining an average reliable value of IR. Tests were carried out always at 5kV. Laboratory conditions were 23°C ± 3° and 55 % RH ± 10%. Baseline characteristics are shown in Figures 119 to 121.

The baseline curves shown above indicate that the insulation system in CT4 was in good conditions and capable to operate according to the nameplate specifications.

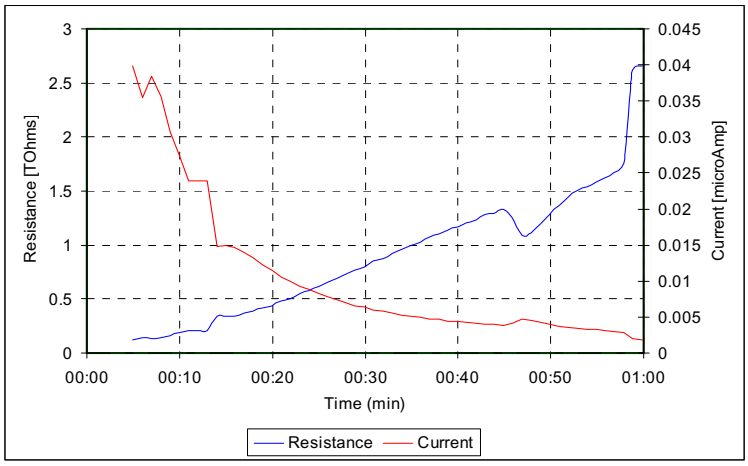

Fig. 119. Insulation Resistance test on CT4 - Baseline Curve

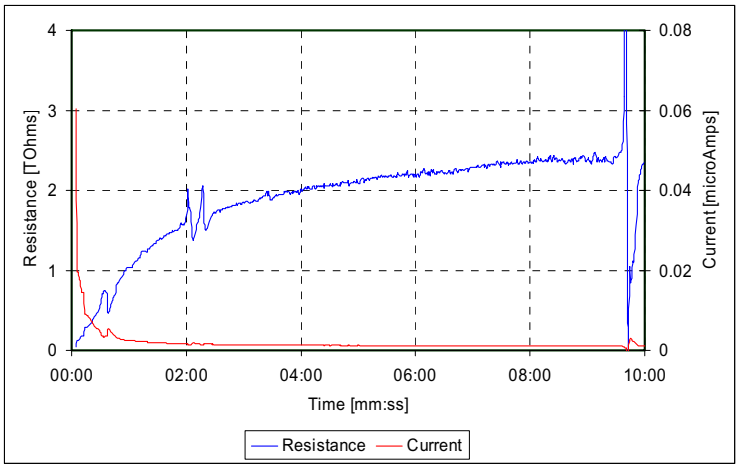

Fig. 120. Polarization Index test on CT4 - Baseline Curve

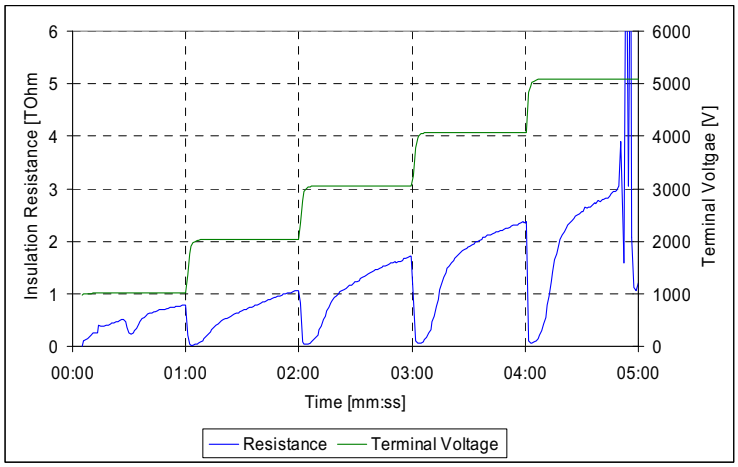

Fig. 121. Step Voltage test on CT4 - Baseline Curve

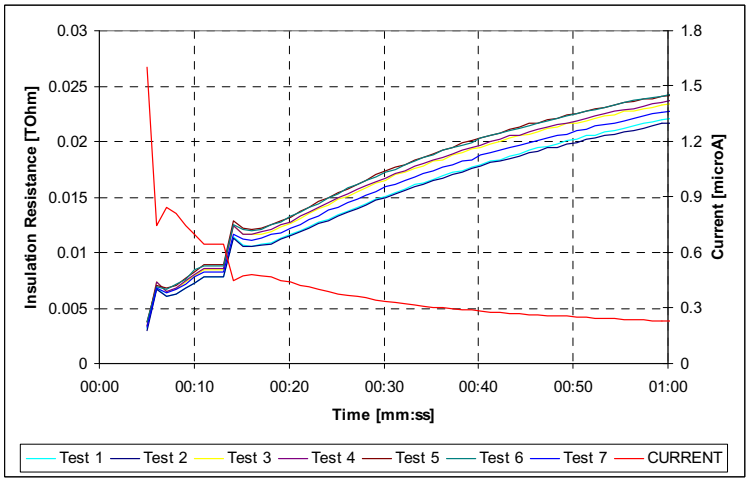

Fig. 122. Insulation Resistance test on CT4 – After 210,000 ageing hours

For CT4 as well as for CT3, the definition of Normal Insulation Life was left open since CT3 continued to operate normally even after 300,000 ageing hours. In order to match with the experimental schedule, the decision was taken to age the CT4 transformer up to 210,000 hours. Results of the DC testing after 210,000 ageing hours are presented in Figures 122 to 125.

From the curves obtained during the testing process, it can be concluded that the insulation resistance of the unit reached stable values after approximately 10,000 ageing hours. Insulation resistance was recorded within the range of 10 and 25 GΩ. Polarization index value lay in the range between 1.3 and 1.8. Tests up to 210,000 ageing hours indicate that the insulation system of CT4 was still in good conditions and capable to operate under normal conditions as observed in Fig. 126.

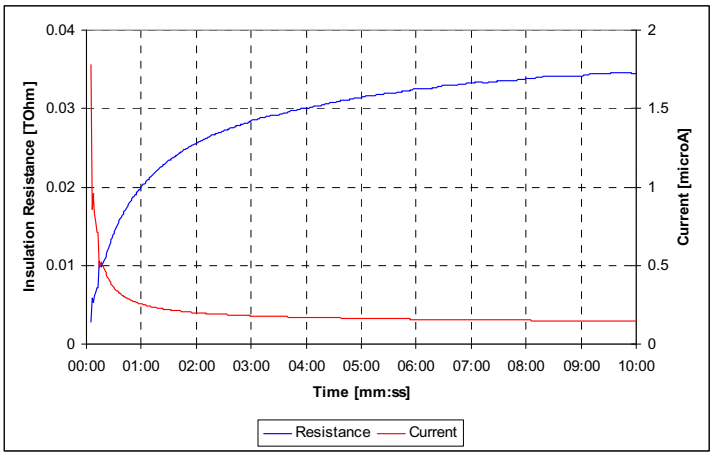

Fig. 123. Polarization Index test on CT4 – After 210,000 ageing hours

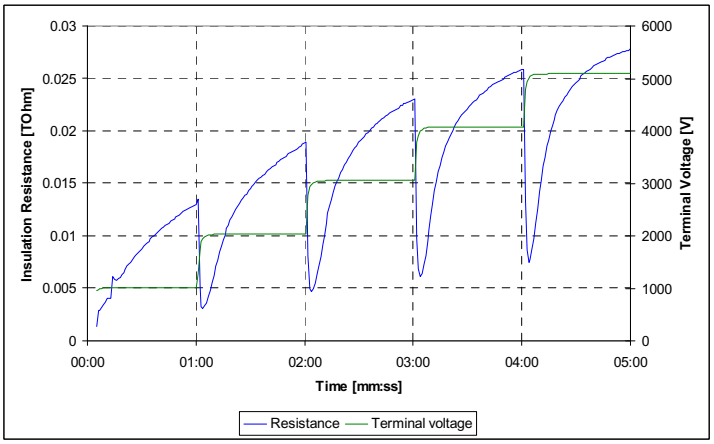

Fig. 124. Step Voltage test on CT4 – After 210,000 ageing hours

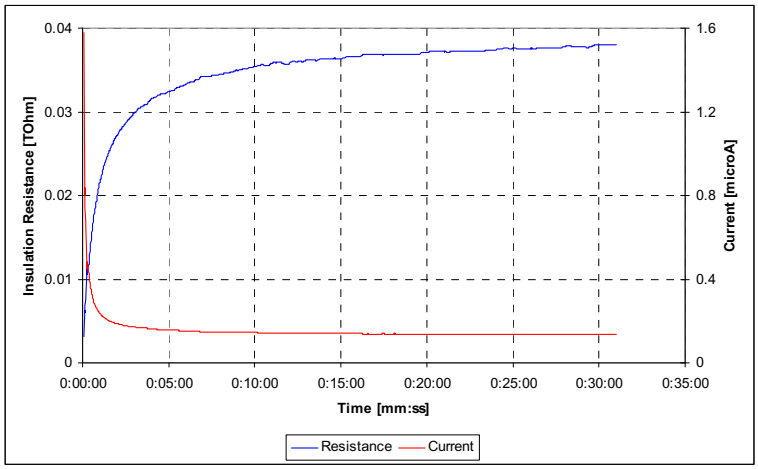

Fig. 125. Insulation Resistance test on CT4 – After 210,000 ageing hours

After 210,000 ageing hours, CT4 was left for future research and possible future loading under more conservative parameters.

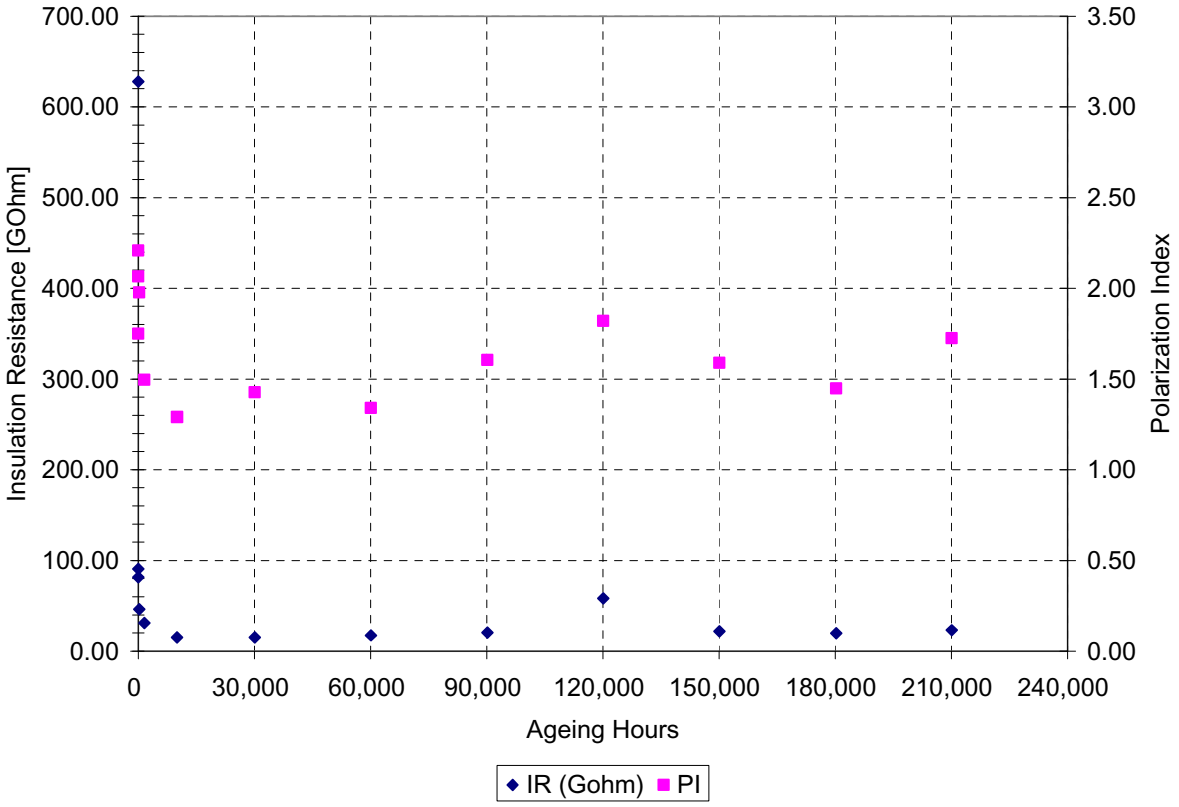

Fig. 126. Insulation Resistance and Polarization Index - Trend Data for CT4

4.7.2 AC Testing on CT4

Dielectric Spectroscopy in the Frequency Domain was used for the analysis of dielectric parameters in CT4 as described in Chapter 3. Post-factory baseline curves are presented below in Fig. 127. The observed dielectric properties at the power frequency value are acceptable for operation as previously discussed in Chapter 3.

All dielectric parameters were continuously recorded and evaluated as described below. The characteristics recorded after 210,000 ageing hours are shown in Fig. 128.

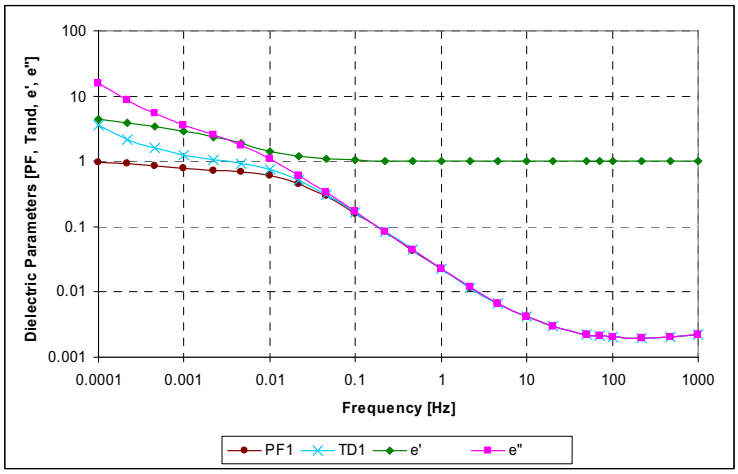

Fig. 127. Dielectric Spectroscopy Test on CT4 - Baseline Curves PF, tan δ, and Complex ε

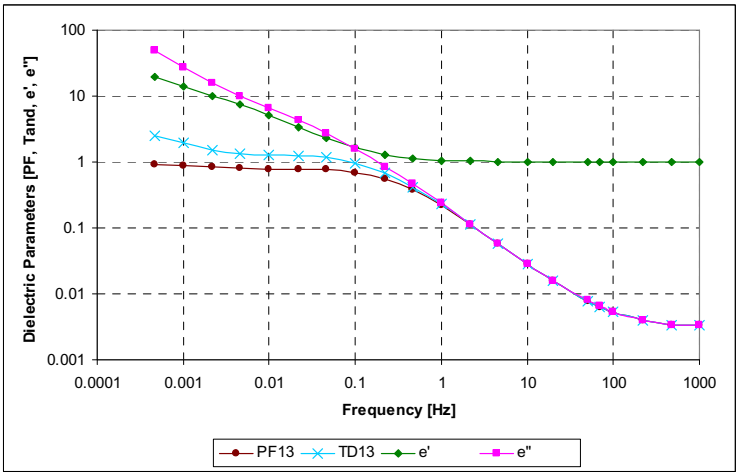

Fig. 128. Dielectric Spectroscopy Test on CT4 – Unit after 210,000 Ageing Hours

The progressive deterioration of the liquid-solid insulation system can be visualized better in the data collected from CT4 as it is clear that the dielectric properties have changed. The next figures, representing the Power Factor trend (Fig. 129) and tan δ trend (Fig. 130) can be used to visualize the changes of dielectric characteristics during the ageing process using the frequency sweep response. Power Factor values recorded at the power frequency did differentiate from the baseline value, but all consecutive readings were reported in a very small range as can be observed in Fig. 129.

Similar to what was observed in the DC Tests, the insulation system on the baseline curve presents stronger dielectric characteristics. From 30,000 to 180,000 hours, the characteristics are very similar and do not present major variation in the moisture content in cellulose and oil conductivity. The curves obtained up to 210,000 ageing hours show the typical shape characteristics of Power Factor and tan δ for this specific unit in the low frequency range.

The software tool MODS used for interpretation of the measured parameters reflected the importance of the frequency sweep. The characteristics of all the investigated units are different in the overall frequency sweep range (0.0001 – 1000Hz), but they are all very similar at the 60Hz value. As mentioned before, readings of Power Factor and tan δ only at the power frequency value do not provide localized insulation diagnostics. A summary of the result of the dielectric spectroscopy test in the frequency domain for CT4 is presented in Fig. 131.

Baseline data obtained in the post-factory test for CT4 is a typical value. This was confirmed with additional investigation carried out in the factory. The unit after the manufacturing process had to go through additional modifications that allowed moisture ingress at levels not critical for exclusively thermal acceleration of the ageing of the unit. Some values would not be acceptable for normal high voltage operation conditions.

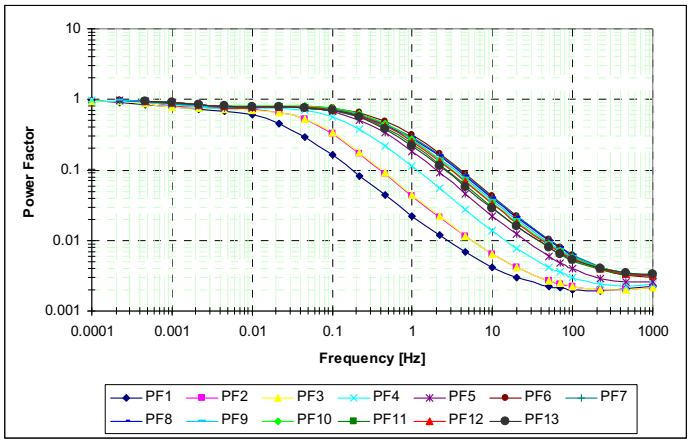

Fig. 129. Thermal Ageing of CT4 - Power Factor, Frequency Sweep Trend Data

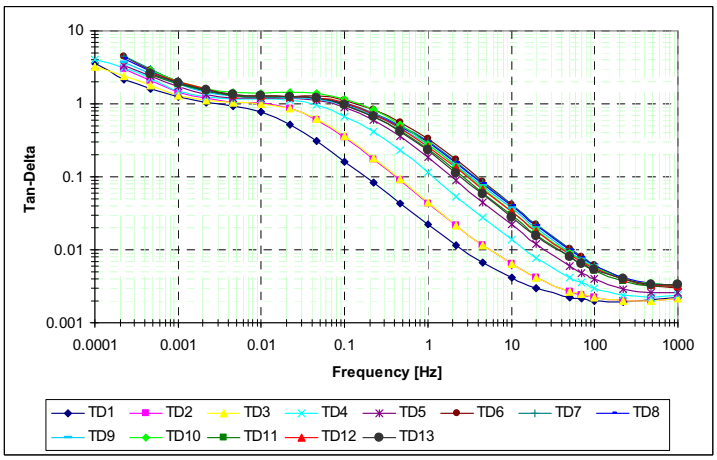

Fig. 130. Thermal Ageing of CT4 – tan δ, Frequency Sweep Trend Data

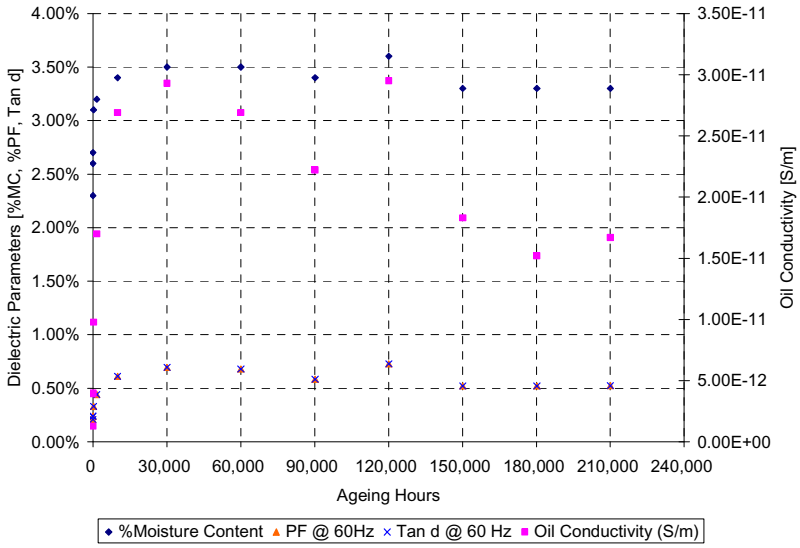

Fig. 131. Dielectric Spectroscopy Test on CT4 - Data Trend PF, tan δ, MC, and Oil Conductivity up to 210,000h

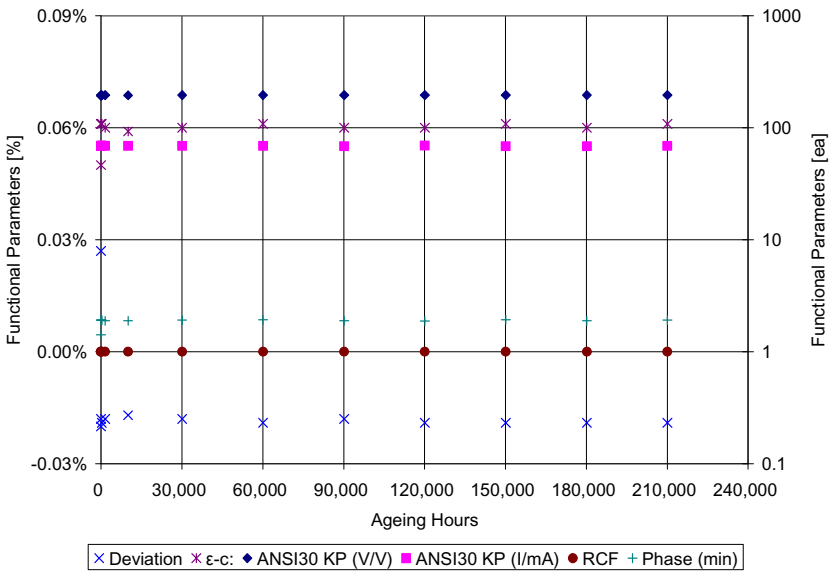

Fig. 132. Functional Parameters recorded for CT4 – Data Trend up to 210,000 h

4.7.3 Analysis of Functional Parameters on CT4

The operation of CT4 under different load conditions did not affect the physical characteristics of the unit. This is clearly observed on the summary of values recorded using the CT Analyzer on the corresponding chart shown in Fig. 132 and in Table 61 in Appendix C.

It was demonstrated that the integrity of the physical components of the unit were not deteriorated due to the thermal ageing process. The quality of operation is according to the specifications and manufacturer's nameplate.

4.7.4 Dissolved Gas Analysis on CT4

The experimental work conducted with CT2 and CT1 did not provide a clear approach to correlate the evolution of gases within the insulation system of the CTs and the estimated or calculated

ageing of the units. CT1 provided valuable information regarding the rate of increase (or decrease) of these chemical components as a function of the thermal stress applied to these units which is directly proportional to the load applied and the surrounding ambient temperature. The removal of paper samples from CT1 for DP analysis produced gas mixing with atmospheric components and exposure to outside moisture level.

The conditions set for CT4 clearly avoided any interaction of the insulation system with external environments and no oil leaks were reported during the experimental process. This allowed a continuous evaluation of the increasing concentration of gases in the liquid insulation. The values used to estimate the concentration at different age stages were obtained after leaving CT4 offloaded for at least 96 hours. This time was necessary to cool down the unit and let it internally to reach equilibrium, in other words, stabilize the extraction/absorption process of chemical components between the solid and liquid insulations.

Once the concentrations reached stable values, readings were taken from the TM8 online monitoring system and added to the log book. The data added to the DGA log book are to be used for the analysis of gas evolution and risk during the operation of the unit. The data trend is summarized and presented in Fig. 133 below and the full DGA record obtained in real-time from CT4 is included in Appendix D together with the evaluation of active fault conditions prepared to avoid emergency conditions during the monitoring process.

It can be seen from Fig. 133 that gas evolution in CT4 provides additional information to this research work, such as

- Oxygen, Carbon Monoxide, and Carbon Dioxide are present since manufacturing in the gas composition of the dielectric oil.

- Hydrogen and Methane appear in the early life of the transformer after approximately 1,500 ageing hours.
- Ethane came into picture after 30,000 ageing hours.
- Ethylene appeared as part of the chemical components only after 60,000 ageing hours.

This information gives a good an idea of what gas and what concentration may be expected in the life of an oil-immersed current transformer under normal ageing conditions.

Technical diagnosis for condition assessment of the transformer needs to be performed based on existing standards as described in Chapter 3, section 3.4.1. Therefore, the fault condition analysis based on the calculation of Key Ratios and Roger ratios is presented in Table 62 in Appendix D and in Fig. 134.

CIGRE SC15: Out of the five ratios, those related to any Acetylene concentrations are disregarded (K_1 and K_5) as none of the loading stages encountered this gas during the process. K_2 and K_3 did not provide any warning during the loading process, and only K_4 indicated the condition of overheated cellulose in the very early life of the transformer and later after approximately 30,000 ageing hours. A detailed description can be reviewed in Table 62 in Appendix D.

Roger Ratios and CO_2/CO ratio: R_2 is not applicable in this analysis because of the absence of Acetylene in the loading process. The condition analysis proposed in IEEE standards gave more accurate results. As observed in Table 62 and Fig. 134, the analysis indicates an initial "Condition 0 – Normal" for the first 1,500 ageing hours and later "Thermal Fault < 300°C." This is true as compared to the loading profiles applied to the unit and presented in Fig. 164.

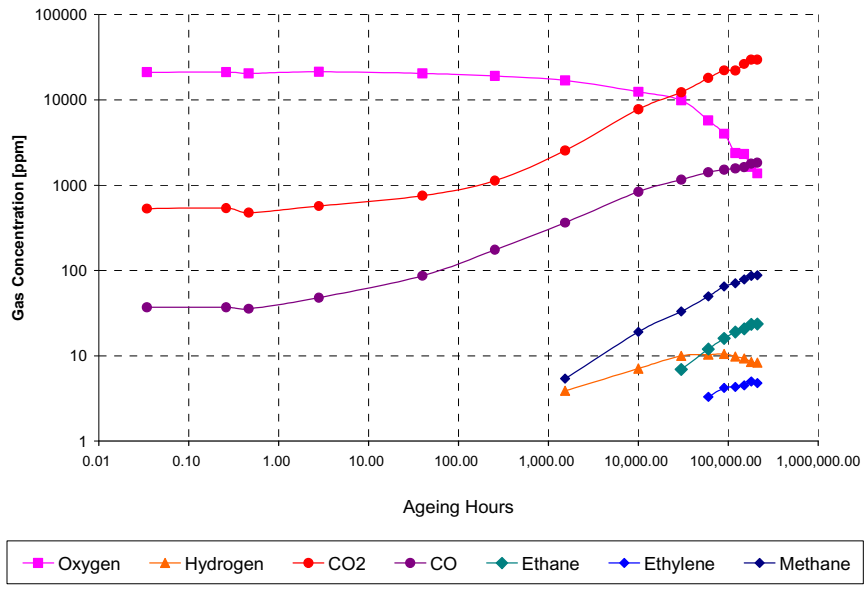

Fig. 133. Dynamic Gas Evolution in CT4 – Correlation with Ageing Data

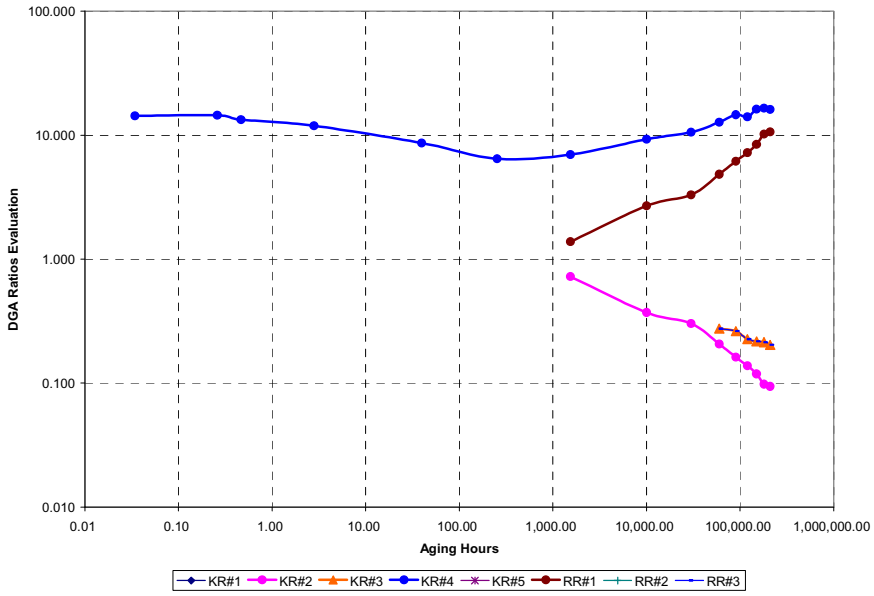

Fig. 134. Monitoring of Critical Fault Conditions during Ageing Process of CT4

The Duval Triangle method of interpretation suggested a "Thermal Fault < 300°C" – Zone T1, during the ageing process of CT4 as it can be observed in Fig. 135 .

Therefore, Rogers Ratios analysis and the Duval Triangle Method provided similar results and realistic interpretation of the gas concentration data.

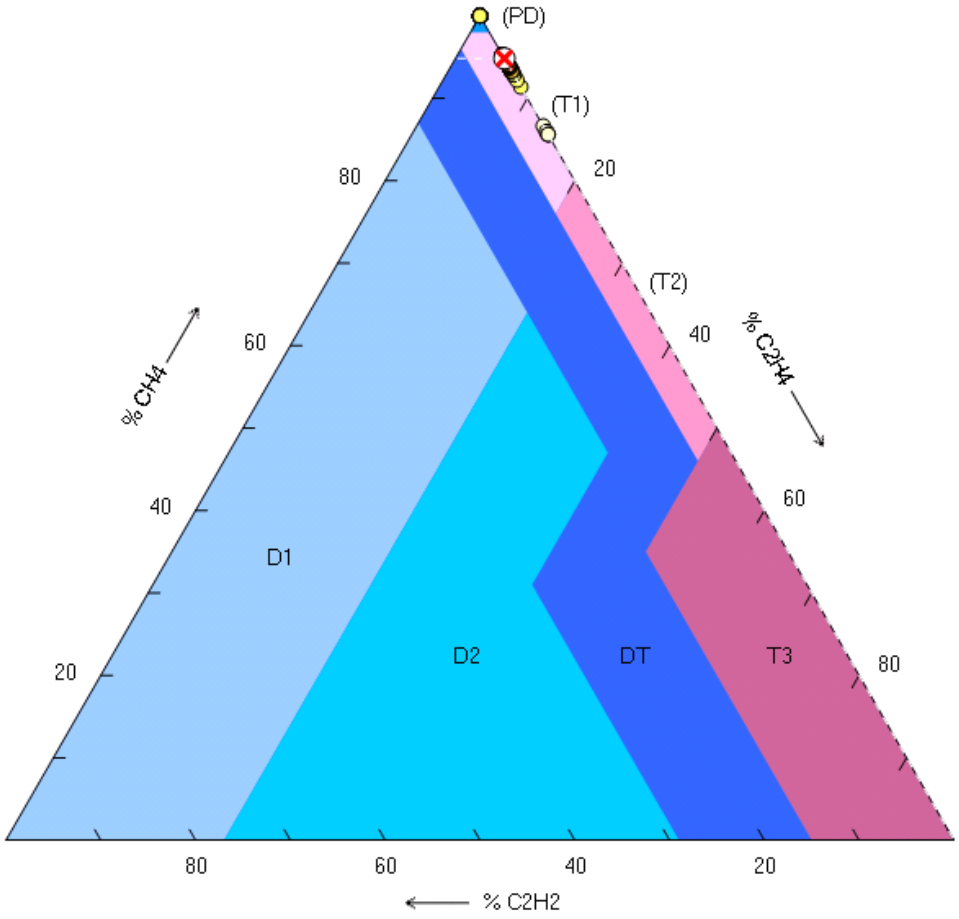

Fig. 135. The Duval Triangle method for fault condition analysis in CT4 during ageing process

Based on the guidelines given in [58], typical dissolved gas concentrations have been estimated for the complete life cycle of CT4. The obtained values are congruent with those presented in [72] based on IEC-60599 (Appendix A1) and are presented in Table 41.

Once again, the concentrations of CO and CO_2 are greater than those presented in the references summarized in Table 41, other concentrations are well within expected ranges of typical values Dissolved key gas concentration limits (ppm) as presented in [41, 58, 73] are compared to the maximum values registered during the accelerated ageing process in Table 42.

The gathered data indicate CO and CO_2 having concentrations greater than the maximum values considered for safe operation of the units. Even though, concentrations of both gases suggest

pre-failure condition, the unit continued operating up to 210,000 ageing hours. It can be questioned as the effect of only one stressing factor on the experimental work, and it might be possible that having other factors affecting the process would evolve in failure of the unit and possible permanent damage of the unit.

The progressive thermal stress applied to CT4 and the gas behavior during the complete experimentation process is observed in Fig. 166 in Appendix D of this dissertation.

Table 41. Typical Dissolved Gas Concentration Values for CT4

Dissolved Gas	**Typical Values for Instrument Transformers [72]**	**Typical Calculated Concentration (ppm) [58]**
Hydrogen	6-300	8.9
Methane	11-120	82.55
Ethane	7-130	22.05
Ethylene	3-40	4.75
Acetylene	1-5	0
Carbon Monoxide	250-1,100	1,708.15
Carbon Dioxide	800-4,000	27,963.3

Table 42. CT4 Maximum Dissolved Gas Concentrations and Standard Limits

Gas	Condition 1	Condition 2	Condition 3	Condition 4	Bureau of Reclamation	Pre-Failure Concentration	Max. Recorded Values CT4
H_2	100	101 - 700	701 – 1,800	>1,800	500	725	15.4
CH_4	120	121-400	401-1,000	>1,000	125	400	95
C_2H_2	35	36-50	51-80	>80	7	450	0
C_2H_4	50	51-100	101-200	>200	175	800	5.4
C_2H_6	65	66-100	101-150	>150	75	900	25
CO	350	351-570	571-1,400	>1,400	750	2,100	2,219.8
CO_2	2500	2,500-4,000	4,001 – 10,000	>10,000	10,000	50,000	32,354.5
TDCG	720	721-1,920	1,921-4,630	>4,630	-	5,380	2,353.3

4.7.5 Degree of Polymerization and Furanic Compound Analysis on CT4

The results obtained from the laboratory at different ageing stages during the process are presented in Table 43 and Fig. 136.

Table 43. CT4 Furanic Compound Concentration - Data Trend

Arrhenius Ageing (h)	HMF (ppb)	FOL (ppb)	2FAL (ppb)	2AF (ppb)	5M2F (ppb)	Total Furan Content (ppb)
0.03	0	0	3	0	0	3
254.07	0	0	184	0	0	184
1,538.34	0	0	159	0	0	159
10,030.02	0	0	194	0	0	194
30,070.57	0	0	456	3	0	459
60,058.57	0	0	1016	7	6	1029
90,179.60	0	0	1462	9	16	1487
120,093.72	27	0	1723	9	36	1795
150,109.52	41	1	2075	11	48	2176
180,196.97	50	0	2580	16	69	2715
210,066.31	50	0	2821	16	72	2959

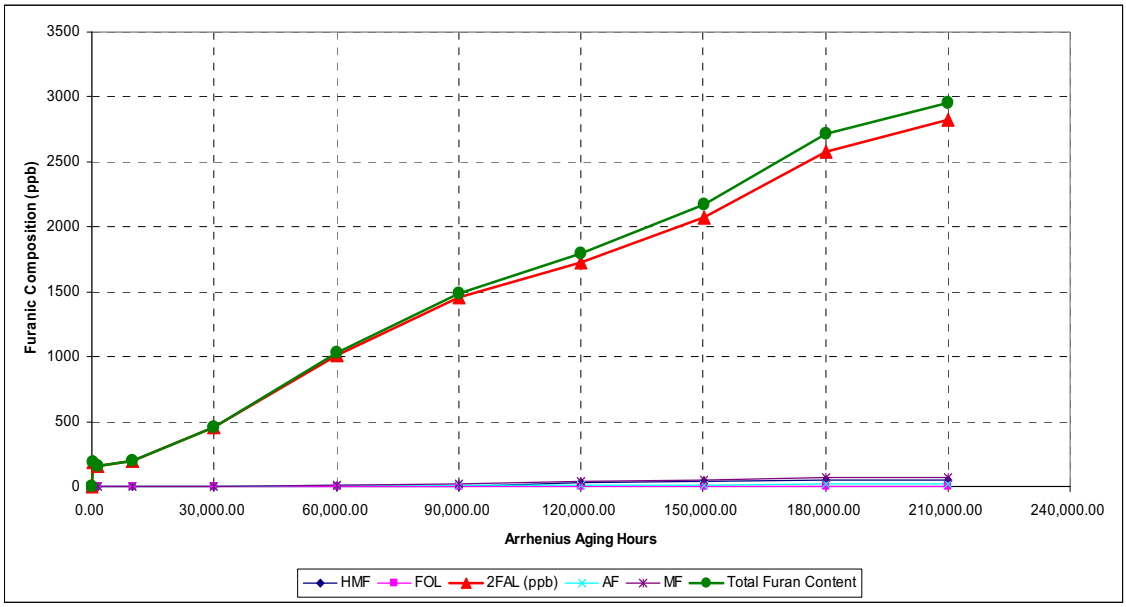

Fig. 136. Furanic Content Evolution during the ageing process of CT4

The Laboratory reported estimated values for DP, as shown in Table 44, DP was correlated to the estimated ageing is shown in Fig. 137.

DOBLE Laboratory estimated LOL to be 70%. This value also differs from the expected value when CT4 passed the 150,000 ageing hours, at 210,000 ageing hours the furanic composition was expected to be much higher.

Table 44. DP Estimated by DOBLE and % LOL Models for CT4

Arrhenius Ageing (h)	DOBLE Estimated DP	% LOL Emsley for DOBLE DP	% LOL General for DOBLE DP	% LOL Stebbins for DOBLE DP
0.03	1149	1%	5%	0%
254.07	639	18%	56%	23%
1,538.34	657	17%	54%	21%
10,030.02	632	18%	57%	24%
30,070.57	526	26%	67%	36%
60,058.57	427	36%	77%	50%
90,179.60	381	43%	82%	57%
120,093.72	361	46%	84%	61%
150,109.52	338	51%	86%	65%
180,196.97	311	57%	89%	71%
210,066.31	300	60%	90%	73%

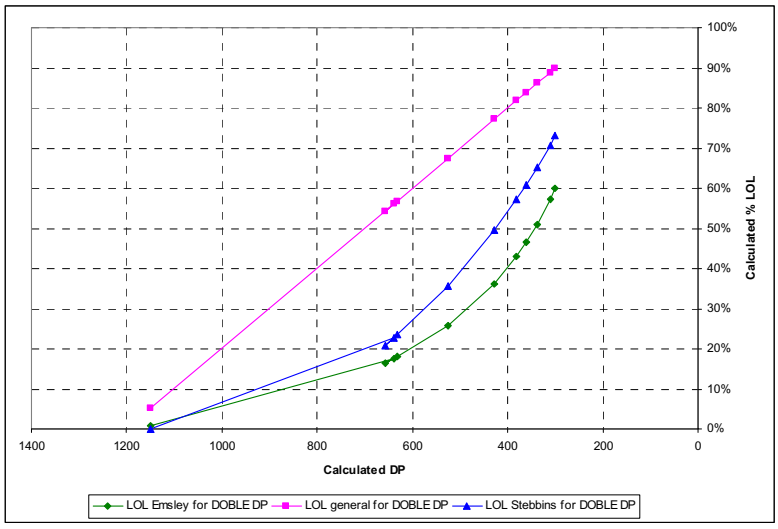

Fig. 137. DOBLE Estimated DP based on Furanic Concentration - Calculated % LOL for CT4

DePablo model as per (3.41) was used to calculate DP values and correlate with the estimated ageing of CT4 as shown in Table 45 and Fig. 138.

Table 45. DP Estimated by DePablo CIGRE and % LOL Models for CT4

Arrhenius Ageing	DePablo CIGRE Estimated DP	% LOL Emsley for DePablo DP	% LOL General for DePablo DP	% LOL Stebbins for DePablo DP
0.03	899.66	7%	30%	0%
254.07	879.68	7%	32%	2%
1,538.34	882.38	7%	32%	1%
10,030.02	878.60	7%	32%	2%
30,070.57	851.26	8%	35%	4%
60,058.57	798.18	10%	40%	8%
90,179.60	760.41	12%	44%	11%
120,093.72	739.92	12%	46%	13%
150,109.52	713.98	14%	49%	15%
180,196.97	679.78	15%	52%	19%
210,066.31	664.59	16%	54%	20%

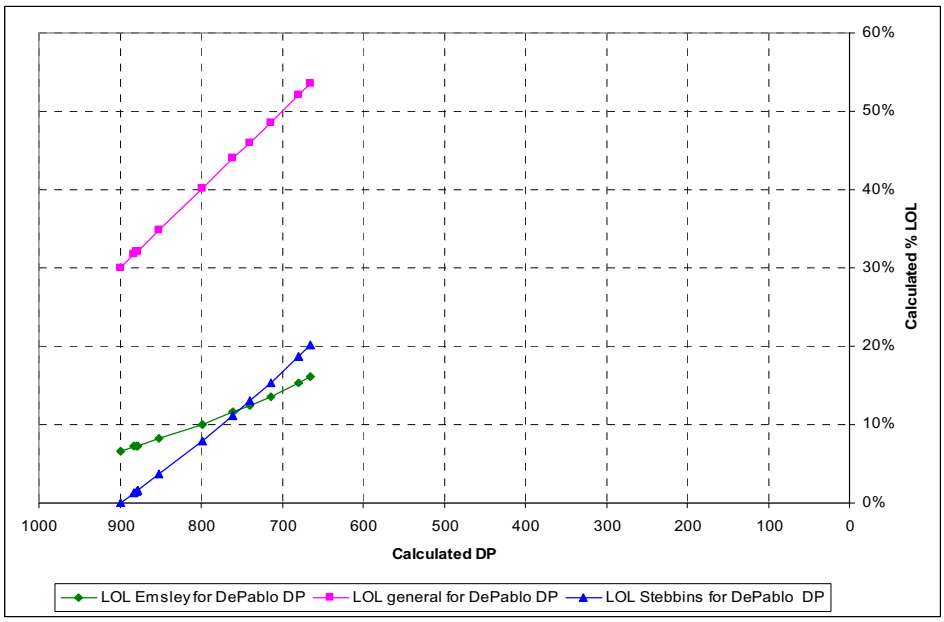

Fig. 138. DePablo CIGRE Estimated DP based on Furanic Concentration - Calculated % LOL for CT4

A great difference can be observed between the first two methods of estimating DP value. Applying DePablo's correlation, the furanic concentration values indicate still a strong DP characteristic even after such a long loading process and thus, a small % LOL. Because the initial DP value is less than 1200, the equation suggests a lower quality material from the beginning of the process. At first glance, DePablo's equation appears to be extremely conservative bearing in mind the long thermal stress applied to the unit. This has been observed in previous results as well.

Table 46 shows the estimated values of DP using Equation (3.48) as reported by the Transformer Maintenance Institute. The estimated DP values suggest close approach to the DP200 criterion and possible end-of-life at approximately 220,000 ageing hours as clearly visualized in Fig. 139. This result does not agree with DePablo's obtained values neither with DOBLE's estimates.

Table 46. DP Estimated by Stebbins / Myers and % LOL Models for CT4

Arrhenius Ageing	Stebbins/Myers Estimated DP	% LOL Emsley for Stebbins DP	% LOL General for Stebbins DP	% LOL Stebbins for Stebbins DP
0.03	804.97	10%	40%	7%
254.07	448.86	33%	75%	46%
1,538.34	461.49	32%	74%	44%
10,030.02	444.28	34%	76%	47%
30,070.57	370.34	45%	83%	59%
60,058.57	301.03	60%	90%	73%
90,179.60	269.55	69%	93%	80%
120,093.72	255.34	74%	94%	84%
150,109.52	239.25	80%	96%	88%
180,196.97	220.41	89%	98%	94%
210,066.31	212.68	93%	99%	96%

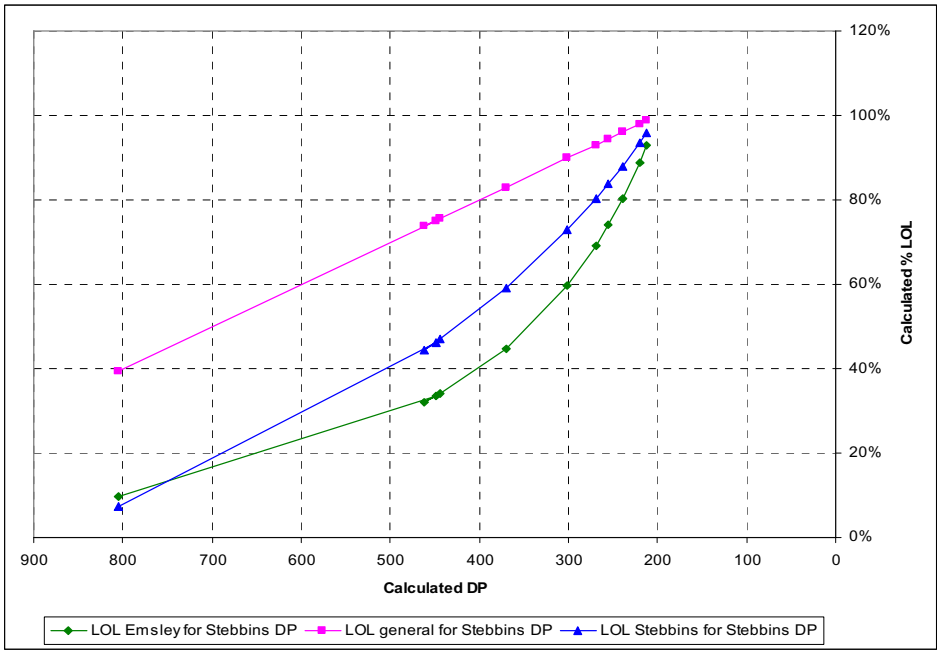

Fig. 139. Stebbins Estimated DP based on Furanic Concentration - Calculated % LOL for CT4

The estimated DP values using Chendong's expression (3.42) are presented in Table 47 with the corresponding percentages LOL calculated by the techniques presented in Chapter 3 and graphically presented in Fig. 140.

Table 47. DP Estimated by Chendong and % LOL Models for CT4

Arrhenius Ageing	Chendong Estimated DP	% LOL Emsley for Chendong DP	% LOL General for Chendong DP	% LOL Stebbins for Chendong DP
0.03	1152.25	1%	5%	0%
254.07	641.48	17%	56%	23%
1,538.34	659.60	16%	54%	21%
10,030.02	634.91	18%	57%	23%
30,070.57	528.87	25%	67%	35%
60,058.57	429.46	36%	77%	49%
90,179.60	384.30	42%	82%	57%
120,093.72	363.92	46%	84%	60%
150,109.52	340.85	50%	86%	65%
180,196.97	313.82	56%	89%	70%
210,066.31	302.74	59%	90%	72%

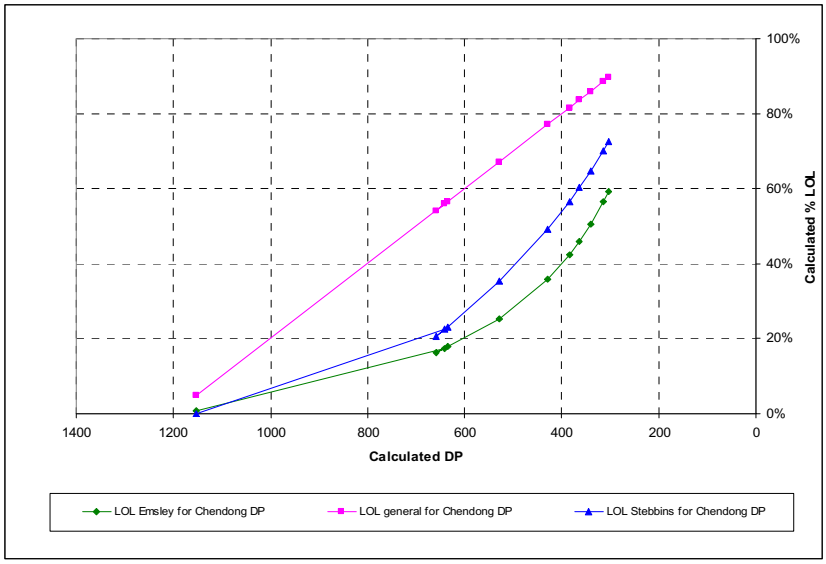

Fig. 140. Chendong Estimated DP based on Furanic Concentration - Calculated % LOL for CT4

The obtained DP values reflect almost similar values as the ones provided by DOBLE. The problem with using the Chendong equation is that it was empirically developed for thermally upgraded paper.

Another DP expression given by Pahlavanpour (3.44) using $DP_0 = 900$ is applied to the furanic concentration values and the resulting DP estimates are summarized in Table 48 and shown in Fig. 141.

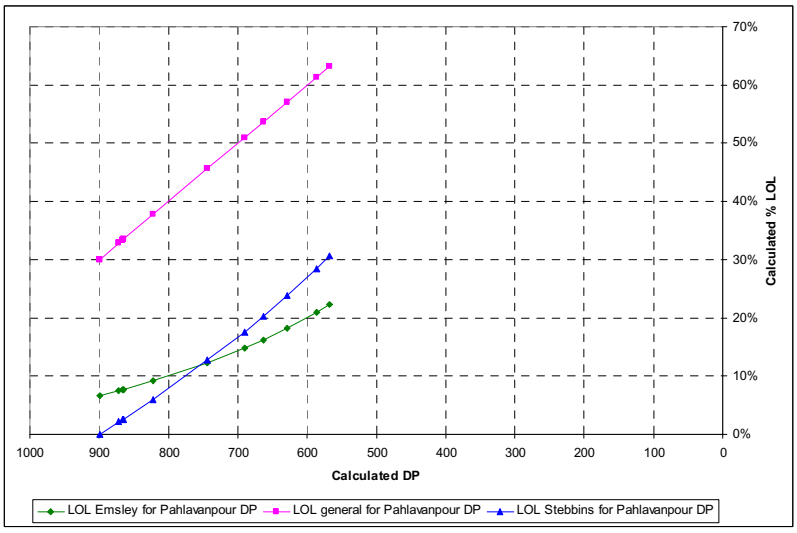

Fig. 141. Pahlavanpour Estimated DP based on Furanic Concentration - Calculated % LOL for CT4

Table 48. DP Estimated by Pahlavanpour and % LOL Models for CT4

Arrhenius Ageing	Pahlavanpour Estimated DP	LOL Emsley for Pahlavanpour DP	LOL general for Pahlavanpour DP	LOL Stebbins for Pahlavanpour DP
0.03	899.44	7%	30%	0%
254.07	866.92	8%	33%	2%
1,538.34	871.27	8%	33%	2%
10,030.02	865.19	8%	33%	3%
30,070.57	822.24	9%	38%	6%
60,058.57	743.37	12%	46%	13%
90,179.60	690.61	15%	51%	18%
120,093.72	663.07	16%	54%	20%
150,109.52	629.22	18%	57%	24%
180,196.97	586.29	21%	61%	28%
210,066.31	567.81	22%	63%	31%

By just visual inspection, it is not possible to define the most accurate result to estimate DP. All the models reviewed present different values which lead to a sparse probability of %LOL. One thing is clear from this experimental process and matches with the experimental process carried out on CT3, NIL is much higher than 150,000 hours. DP samples will not be taken from this unit and estimated DP will be based on the results obtained from CT3 dissection analysis.

CHAPTER 5

DATA ANALYSIS AND DISCUSSION

5.1 Life Data Analysis – Background

It is clear that patterns of change through time can take many forms, some meaningful, some not. The data obtained in this research work from all the tests carried out in the lab needs to be properly classified as meaningful or not because not all tests have shown characteristics of dependency with the ageing of the insulation system, thus, independent variables will not be considered to estimate the percentage loss-of-life of oil-immersed current transformers.

The aim in this chapter is to draw inferences capable of describing a relationship between the parameters recorded during the experimental stage and ageing of the experimental units, as a function of the thermal stress applied to the units and described by the Arrhenius equation, whether this relationship is linear or nonlinear. The patterns of data observed in Chapter 4 are visually inspected on basic characteristics as recommended from Stochastic Processes and Time Series Analysis theory; such characteristics are magnitude of change, shape of change, velocity of change, and direction of change.

The empirical and theoretical developments that define regression and correlation as statistical topics were presented by Sir Francis Galton in 1885. In 1895, Karl Pearson published the Pearson's product-moment correlation coefficient (r) [83].

Pearson's correlation coefficient is a dimensionless index described by the expression first developed in 1895.

$$r = \frac{\sum \left(X_i - \overline{X}\right)\left(Y_i - \overline{Y}\right)}{\left[\sum \left(X_i - \overline{X}\right)^2 \cdot \sum \left(Y_i - \overline{Y}\right)^2\right]^{1/2}} \tag{5.1}$$

The correlation expression (5.1) defines the departure of two random variables from independence. The denominator adjusts the scales of the variables to have equal units. Using the Cauchy-Schwarz corollary, it can be shown that this coefficient is limited in range from -1 to +1. Therefore, the correlation coefficient will suggest the strength and direction of a linear relationship between two random variables. In the event when the variables are independent, the correlation coefficient equals zero, but one should be aware that this statement is not always true because the coefficient only detects linear dependencies.

In order to properly measure the association between variables (ageing and test results) and their concomitant variation, the correlation coefficient value alone is only the starting point for further analysis and will help screening some of the data. As observed in Chapter 4, most of the variables describe nonlinear trends during the life of the CTs.

The tests carried out to determine functional parameters using the CT Analyzer described a steady linear function which indicates that these parameters will draw a very close to zero or zero correlation coefficient. Same argument can be made about dissolved in oil gases such as C_2H_2, C_2H_4, and H_2 which were not present during the test, were sporadically observed, or the rate of increase (magnitude of change) was a fluctuating value within the range of accuracy of the TM8 monitor.

Modeling of time series data is a complex procedure for the selection of a suitable probability model. The general approach to time series modeling described in [82] suggests in a first step to plot the series and perform a visual appreciation of the data scatter plot, trying to identify any trends, seasonal components, sharp changes in behavior, and any outlying observations. As any other practical

problem, in this experimental work, the starting point is the visual inspection of the gathered data. To assess the degree of dependence in the data and to select a model for the data, a correlation function is to be applied.

All gathered data during this experimental process were exported or converted into work datasheets stored in .xls Microsoft Excel files. Excel provides wide compatibility and very easy interface for data management, analysis, and graphics. By using the Data Analysis Toolbox – Correlation function in Excel, this first data screening stage was completed. A second and definitive stage was completed by the regression analysis of the time series data using the same Data Analysis Toolbox and the function regression. The results of the correlation and regression analysis applied to 1200:5, and 200:5 CTs data are presented independently herein.

5.2 Data Analysis – 1200:5 CTs

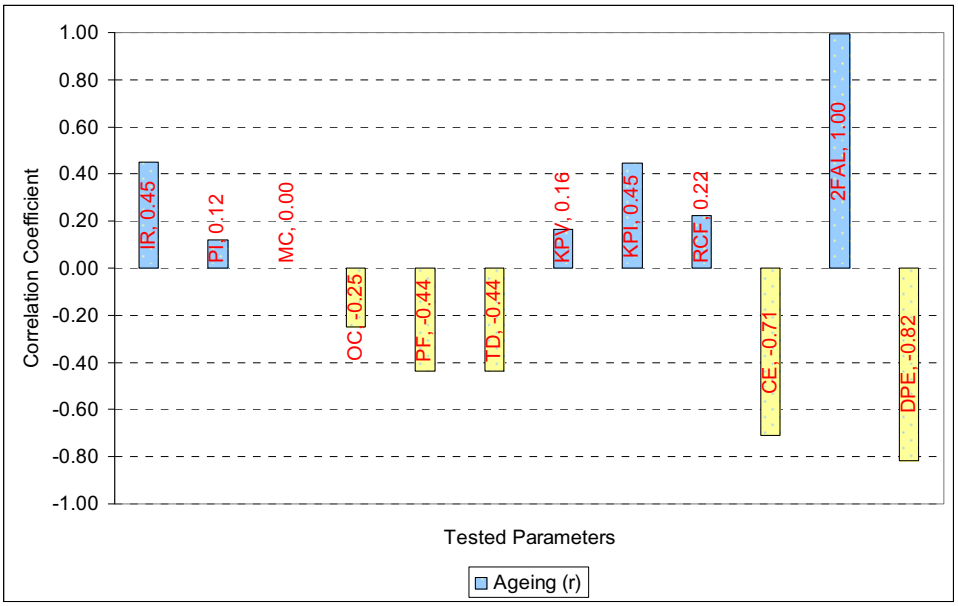

Fig. 142. 1200:5 CT Correlation Analysis of all Tested Parameters against Ageing of the CT

The analysis was based on the data presented in Chapter 4 summarizing the test results of the 1200:5 units and the measured independent variables were presented.

5.2.1 Correlation Analysis on 1200:5 CTs

The results of the correlation analysis are presented in Fig. 142. The data is provided in Table 63 of Appendix E.

Based on the information given by the correlation analysis and the figures presented in Chapter 4, it can be said that the functional parameters do not present any type of correlation with ageing of 1200:5 CTs and therefore, should not be considered for further regression analysis. The following data analysis was performed according to the type of test performed on the experimental unit. Complete results of the regression analysis of all tested variables can be found in Appendix E of this dissertation work. Linear regression analysis by using the "least squares" method was carried out to fit a line through the obtained through experimentation set of observations. The analysis suggests how ageing is affected by the values of the independent variables.

5.2.2 Regression Analysis on 1200:5 CTs

The results of the regression analysis on 1200:5 CT are summarized in Table 49.

The regression analysis indicated that the Insulation Resistance and the Polarization Index variables are not statistically significant to make an inference on Ageing of 1200:5 CTs at a 95% confidence level.

Table 49. Rgression Analysis Results for 1200:5 CT

Independent Variable	Denomination	Statistical Parameters					
		R^2	SS	MS	F	Significance F	p-value
IR	Insulation Resistance	0.20	3.59E+09	3.59E+09	1.02	0.37	0.37
PI	Polarization Index	0.01	2.59E+08	2.59E+08	0.06	0.82	0.82
MC	Moisture Content	0.00	1.19E+03	1.19E+03	2.71E-07	1.00	1.00
OC	Oil Conductivity	0.00	0.00E+00	0.00E+00	0.00E+00	1.00	#NUM!
PF	Power Factor @ 60Hz	0.19	3.36E+09	3.36E+09	0.94	0.39	0.39
TD	tan δ @ 60Hz	0.19	3.35E+09	3.35E+09	0.94	0.39	0.39
2FAL	2-Furaldehyde	0.99	2.31E+10	2.31E+10	783.09	1.91E-08	1.91E-08
DPE	Estimated Degree of Polymerization	0.67	1.56E+10	1.56E+10	14.16	0.01	0.01

Moisture content is not a linear function and the zero correlation value is not conclusive and could not be used to eliminate this variable from the regression analysis. Power Factor and Dissipation Factor (tanδ) describe similar patterns at different scales. The regression analysis at a 95% confidence level was performed for the variables recorded from the Frequency Domain Spectroscopy finding that none of them are statistically significant to make an inference of ageing on 1200:5 CTs.

Furanic compound concentration and specifically the concentration of 2-furaldehyde together with the estimated Degree of Polymerization values were brought to the regression analysis showing high level of correlation and nonlinearity. For the 2FAL concentration and the estimated DP, the regression analysis provided p-values below 0.05 and thus the variables are to be considered

statistically significant for a 95% confidence level. For completion of the regression analysis, and considering these variables to be time-dependent, an accurate function is to be identified based on previously reviewed methods on Chapter 3.

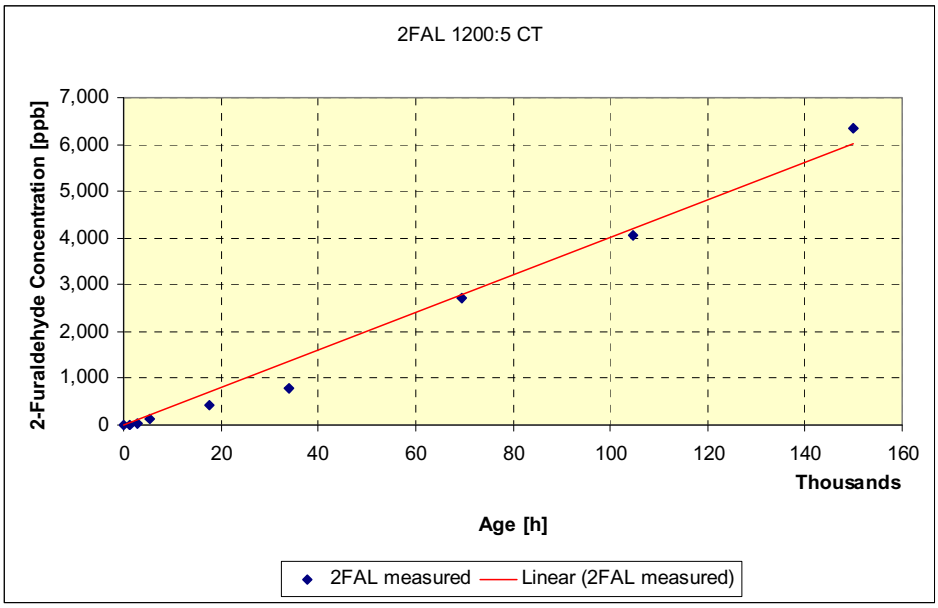

Fig. 143. Linear function to define Ageing in terms of 2FAL for 1200:5 CTs

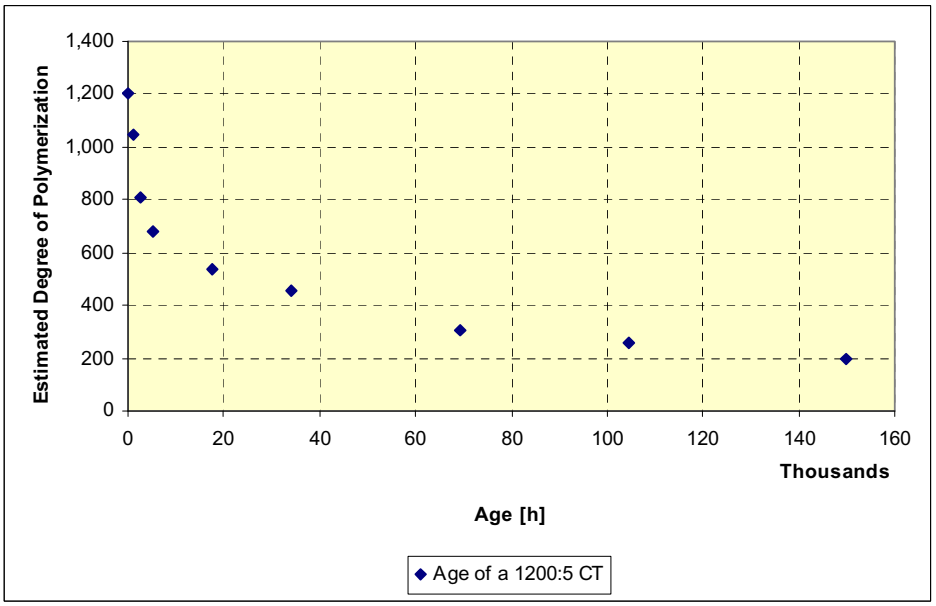

Fig. 144. Insulation Age in terms of estimated DP for 1200:5 CTs

A linear relationship between 2FAL compound evolution and the Arrhenius age of 1200:5 CTs has been identified to be an accurate fit as shown in Fig. 143, and is given by the expression:

$$Age_{1200:5CT} \approx 24.8756 \cdot \left(2FAL_{ppb}\right) \tag{5.2}$$

The analysis of the estimated DP values presented in Fig. 144 suggests a revision of the equation used to estimate DP as a function of 2FAL, and the approximation of these function using other models presented in Chapter 3.

Reviewing the data obtained in Chapter 4, where the furanic compound concentration was subjected to several estimation models to determine the DP value and, based on the results obtained after the dissection of CT1, we can conclude that the weakest value of DP reported from the Laboratory was found in the wrapping paper covering the core of the transformer DP=302 (see Table 33) and only two layers above the secondary winding wrapping registered a DP=426; therefore, the closest DP estimated value is the one given by Pahlavanpour's expression (3.45).

Since ageing was estimated in this research work based on the Arrhenius equation and as it was introduced in Section 3.4.2, DP must be expressed in terms of the thermal accelerated ageing effect. Using Equation (3.35), the value of the pre-exponential factor A of Equation (3.34) was determined for 1200:5 CTs to be: $A_{1200:5CT} = 8.37 \times 10^7$

The experimental work demonstrates that NIL (Normal Insulation Life) of 1200:5 CTs can be determined based on the criterion of DP=200. This results into an approximate value of 265,000 Arrhenius hours (~ 30.25 years) at a constant $F_{AA} = 1$ or, said it in terms of temperature, at a constant $HST = 95°C$. This NIL value is obtained by extrapolation of Equation (3.35).

Results of the data analysis are summarized in Table 50.

Table 50. Proposed Correlation between Arrhenius Age of 1200:5 CTs with 2FAL and DP

1200:5 CT - DP and FAL ANALYSIS								
DP_0	**DPt**	**A**	**E**	**R**	**T**	**AGE**	**2FAL measured**	**2FAL MODELED**
900	1,200.00	8.37E+07	111000	8.314	95	0.00		0.00
	1,100.00					0.00		0.00
	1,000.00					0.00		0.00
	900.00					0.00	2.00	0.00
	885.01					1,283.06	7.00	51.58
	867.99					2,793.27	47.00	112.29
	840.80					5,333.47	133.00	214.41
	731.47					17,453.65	411.00	701.64
	621.44					33,955.35	796.00	1,365.01
	469.83					69,357.48	2,723.00	2,788.17
	377.76					104,726.23	4,050.00	4,209.99
	302.01					149,990.53	6,331.00	6,029.62
	200.00					265,133.78		10,658.38

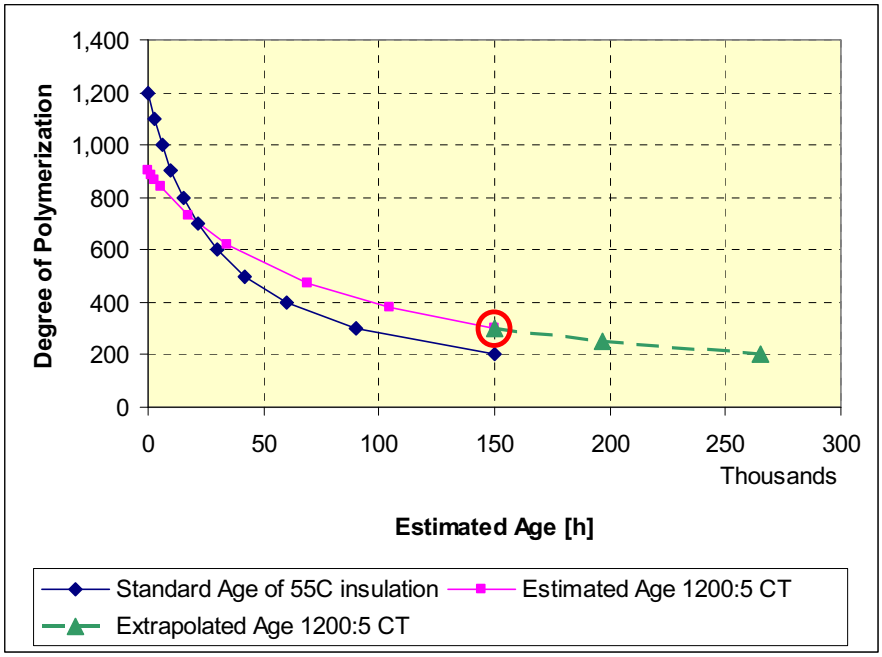

Fig. 145. Proposed Ageing functions for 1200:5 CTs based on revised 2FAL and DP expressions

Results are compared against standard values given for DP_0 and based on the DP_t=200 end-of-life criterion. The pre-exponential factor for 55°C temperature rise insulation in Equation (3.34) was found to be $A_{55°C} = 1.58 \times 10^8$. The data is presented in Fig. 145.

Failure of the unit was not reached and thus, the estimated percentage loss-of-life of this unit at the end of the experimental analysis was estimated to be 56.57% after 150,000 ageing hours.

5.3 Data Analysis – 200:5 CTs

The data analysis was performed based on the data gathered from the testing procedures applied to CT3 and CT4, previously presented in Chapter 4. Based on the outcome from the 1200:5 devices, the correlation analysis on the 200:5 units and the figures presented in Chapter 4, it can be said that functional parameters do not present any type of correlation with ageing of 200:5 CTs and, therefore, should not be considered for further regression analysis.

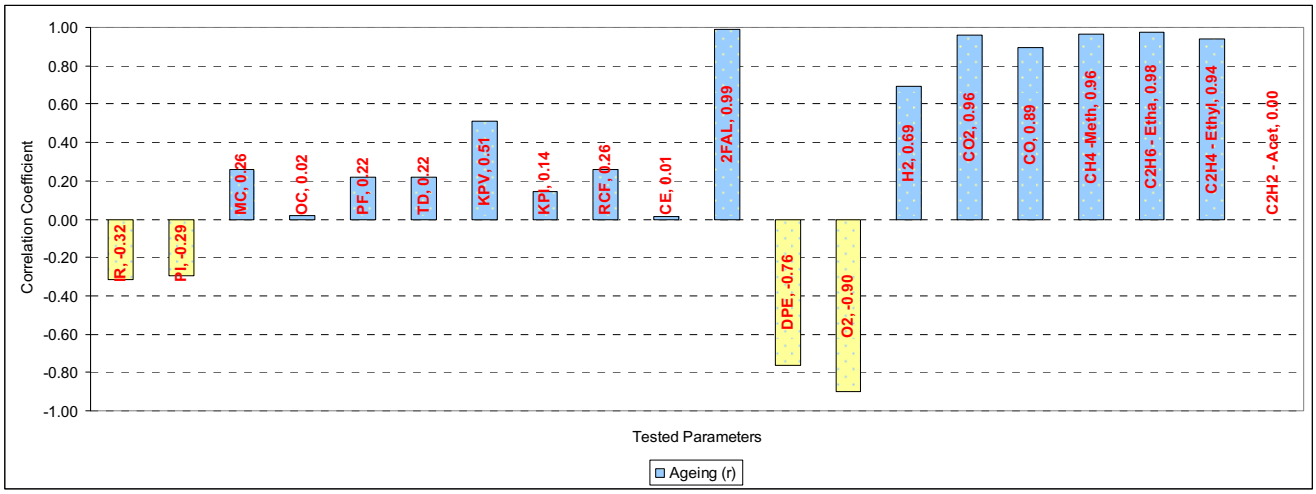

Fig. 146. 200:5 CT Correlation Analysis of all Tested Parameters against Ageing of the CT

5.3.1 Correlation Analysis on 200:5 CTs

The results of the correlation analysis are presented in Fig. 146. The data are provided in Table 64 of Appendix E.

5.3.2 Regression Analysis on 200:5 CTs

The results of the regression analysis on 200:5 CT are summarized in Table 51.

Table 51. Regression Analysis Results for 200:5 CTs

Independent Variable	Denomination	Statistical Parameters					
		R^2	SS	MS	F	Significance F	p-value
IR	Insulation Resistance	0.10	1.71E+10	1.71E+10	2.68	0.11	0.11
PI	Polarization Index	0.09	1.47E+10	1.47E+10	2.27	0.14	0.14
MC	Moisture Content	0.07	1.14E+10	1.14E+10	1.65	0.21	0.21
OC	Oil Conductivity	0.00	3.05E-05	3.05E-05	0.00	1.00	#NUM!
PF	Power Factor @ 60Hz	0.05	8.14E+09	8.14E+09	1.16	0.29	0.29
TD	tan δ @ 60Hz	0.05	8.24E+09	8.24E+09	1.17	0.29	0.29
2FAL	2-Furaldehyde	0.98	2.04E+11	2.04E+11	986.66	9.03E-20	9.03E-20
DPE	Estimated Degree of Polymerization	0.58	1.21E+11	1.21E+11	30.49	1.50E-05	1.50E-05
O_2	Oxygen	0.81	6.29E+10	6.29E+10	54.62	5.27E-06	5.27E-06
H_2	Hydrogen	0.48	3.76E+10	3.76E+10	12.13	4.04E-03	4.04E-03
CO_2	Carbon Dioxide	0.92	7.14E+10	7.14E+10	143.81	2.11E-08	2.11E-08
CO	Carbon Monoxide	0.80	6.22E+10	6.22E+10	51.83	6.96E-06	6.96E-06
CH_4	Methane	0.93	7.21E+10	7.21E+10	164.57	9.35E-09	9.35E-09
C_2H_6	Ethane	0.95	7.41E+10	7.41E+10	256.69	6.11E-10	6.11E-10
C_2H_4	Ethylene	0.89	6.89E+10	6.89E+10	100.29	1.77E-07	1.77E-07

Results obtained from the regression analysis indicate that Insulation Resistance and Polarization Index are not statistically significant to make an inference on Ageing of 200:5 CTs at a 95% confidence level.

Power Factor and Dissipation Factor (tan δ) describe similar patterns at different scales. The regression analysis at a 95% confidence level was performed for the variables recorded from the Frequency Domain Spectroscopy finding that none of them are statistically significant to make an inference of ageing on 200:5 CTs.

Previous experience from the analysis of 1200:5 units indicates that two variables are capable of providing a model for the ageing of CTs. Furanic compound concentration and specifically the concentration of 2-furaldehyde (2FAL) together with the estimated Degree of Polymerization values were brought to the regression analysis. The analysis indicates that the concentration of 2-furaldehyde compound as well as the estimated DP data is statistically significant at a 95% confidence level. Moreover, 2FAL draws a very linear expression similar to what was obtained for 1200:5 CTs, but with a different slope. The linear regression by least square method provided the expression correlating 2FAL and the Arrhenius age of 200:5 type of CTs.

A linear relationship between 2FAL compound evolution and the Arrhenius age of 200:5 CTs was identified to be an accurate fit as shown in Fig. 147 and given by the expression:

$$Age_{200:5CT} \approx 71.9424 \cdot \left(2FAL_{ppb}\right) \tag{5.2}$$

The estimated DP values as presented in Fig. 148 suggest a revision of the equation used to estimate DP as a function of 2FAL, and the approximation of these function using other models presented in Chapter 3.

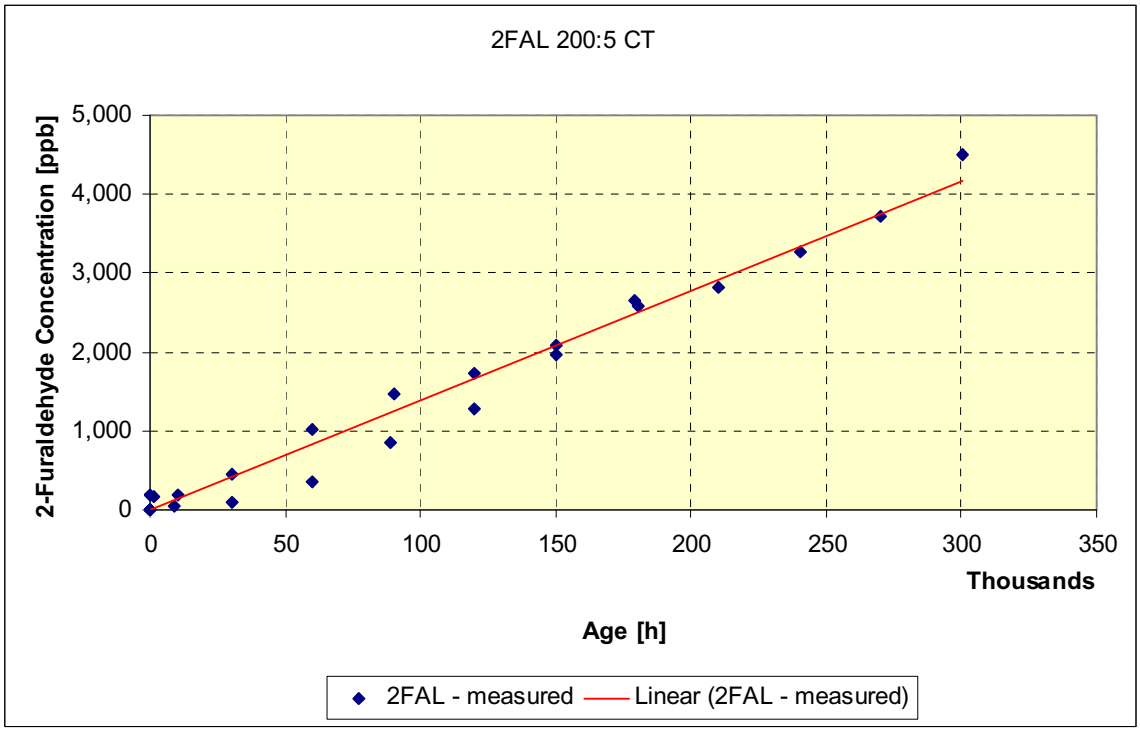

Fig. 147. Linear function to define Ageing in terms of 2FAL for 200:5 CTs

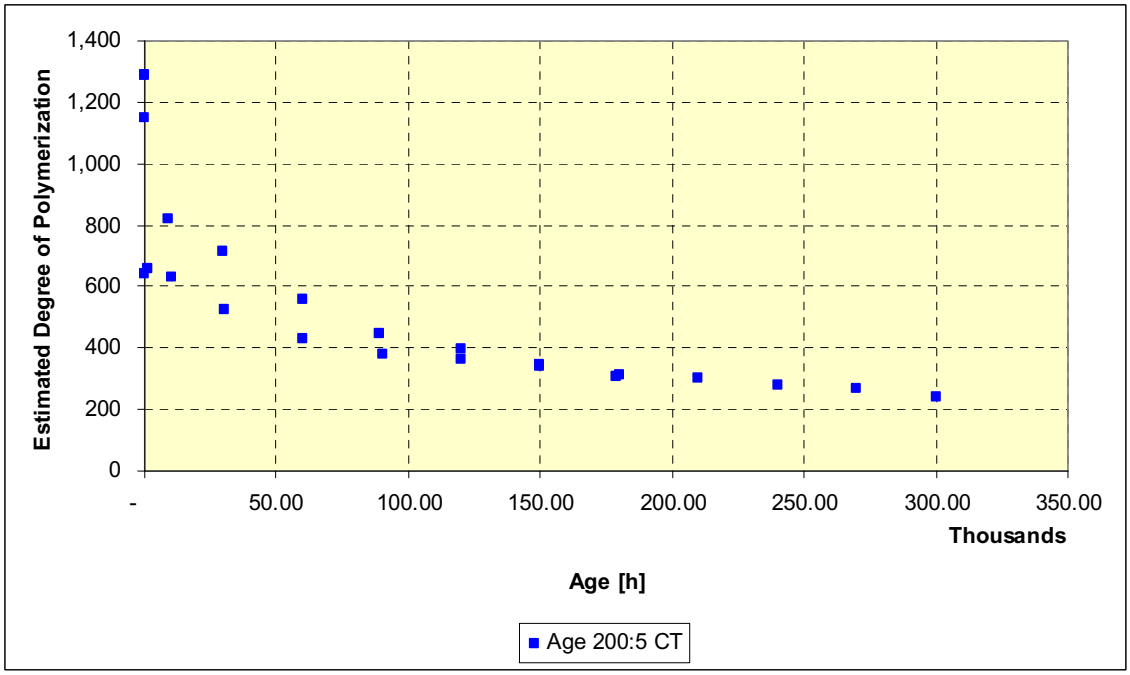

Fig. 148. Insulation Age in terms of estimated DP for 200:5 CTs

Reviewing the data obtained in Chapter 4, where the furanic compound concentration was subjected to several estimation models to determine the DP value and, based on the results obtained after the dissection of CT1, it can be said that the weakest value of DP reported from the Laboratory was found in the wrapping paper between the core and the secondary winding of the transformer DP=276 (seeTable 40). None of the previously reviewed models gave a close approximation to the estimation of DP based on the 2FAL concentration.

Similar to the analysis of 1200:5 CTs, ageing was estimated for CT3 and CT4 based on the Arrhenius equation that was introduced in Section 3.4.2, where DP must be expressed in terms of the thermal accelerated ageing effect. Therefore, by using Equation (3.35), the value of the pre-exponential factor A of Equation (3.34) was determined for 200:5 CTs to be: $A_{200:5CT} = 4.77 \times 10^7$

The experimental work demonstrated that NIL (Normal Insulation Life) of 200:5 CTs can be determined based on the criterion of DP=200 deriving into an approximate value above 450,000 Arrhenius hours (~ 51.4 years) at a constant $F_{AA} = 1$ or, said it in terms of temperature, at constant $HST = 95°C$.

Results are compared against standard values given for DP_0 and based on the DP_t=200 end-of-life criterion. The pre-exponential factor for 55°C temperature rise insulation in Equation (3.34) was found to be $A_{55°C} = 1.58 \times 10^8$. The data is presented in Fig. 149.

Failure of the unit was not reached and thus, the approximate loss-of-life of this unit at the end of the experimental analysis was estimated to be 64.6% at 300,000 ageing hours.

Results of the data analysis are summarized in Table 52.

Table 52. Proposed Correlation between Arrhenius Age of 200:5 CTs with 2FAL and DP

200:5 CT - DP and 2FAL ANALYSIS								
DP_0	DPt	A	E	R	T	AGE	2FAL - measured	2FAL MODELED
900.00	1,200.00	4.77E+07	111,000.00	8.31	95.00	0.00		0.00
	1,100.00					0.00		0.00
	1,000.00					0.00		0.00
	900.00					0.00		0.00
	900.00					0.03	3.00	0.00
	900.00					0.06	0.10	0.00
	900.00					0.60	0.10	0.01
	899.98					2.88	0.10	0.04
	898.28					254.23	184.00	3.53
	889.69					1,539.32	159.00	21.40
	841.18					9,285.33	42.00	129.07
	836.75					10,036.42	194.00	139.51
	733.93					30,045.09	100.00	417.63
	733.72					30,089.74	456.00	418.25
	619.72					60,051.19	358.00	834.71
	619.57					60,096.86	1,016.00	835.35
	538.65					89,073.74	845.00	1,238.12
	535.84					90,237.10	1,462.00	1,254.30
	472.44					120,162.20	1,279.00	1,670.25
	472.43					120,170.29	1,723.00	1,670.37
	422.40					150,127.47	1,966.00	2,086.77
	422.29					150,205.23	2,075.00	2,087.85
	383.03					179,209.08	2,651.00	2,491.01
	381.68					180,311.86	2,580.00	2,506.33
	348.42					210,200.25	2,821.00	2,921.78
	320.29					240,322.68	3,277.00	3,340.49
	296.48					270,285.28	3,711.00	3,756.97
	276.00					300,191.28	4,509.00	4,172.66
	200.00					464,719.19		6,459.60

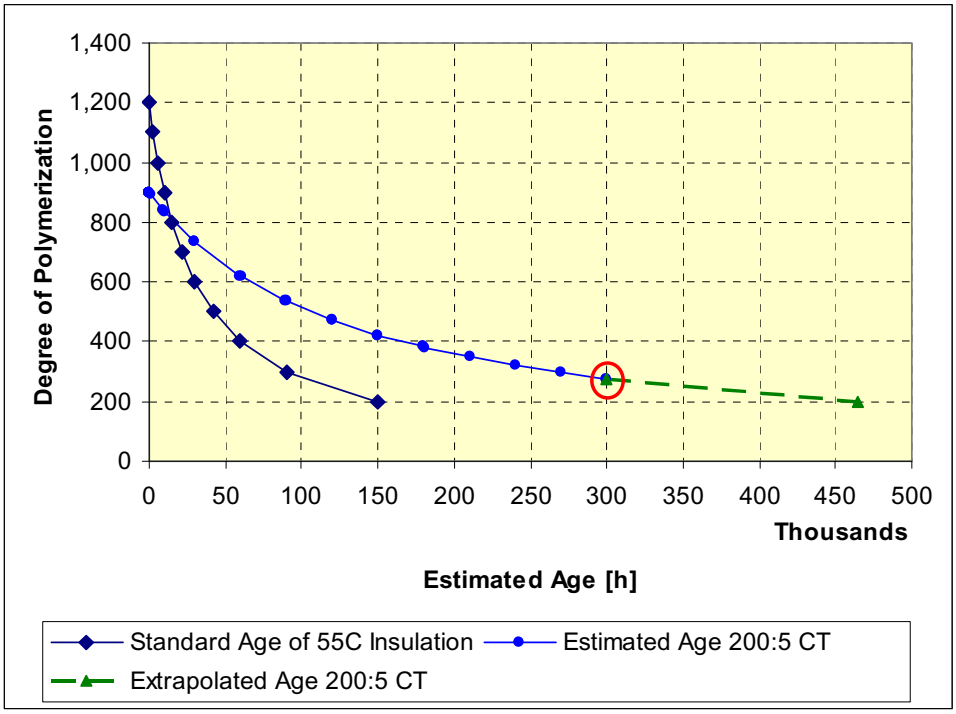

Fig. 149. Proposed Ageing functions for 200:5 CTs based on revised 2FAL and DP expressions

A final comparison of both types of CTs base of this study and the standard curve given for power transformers is presented in Fig. 150.

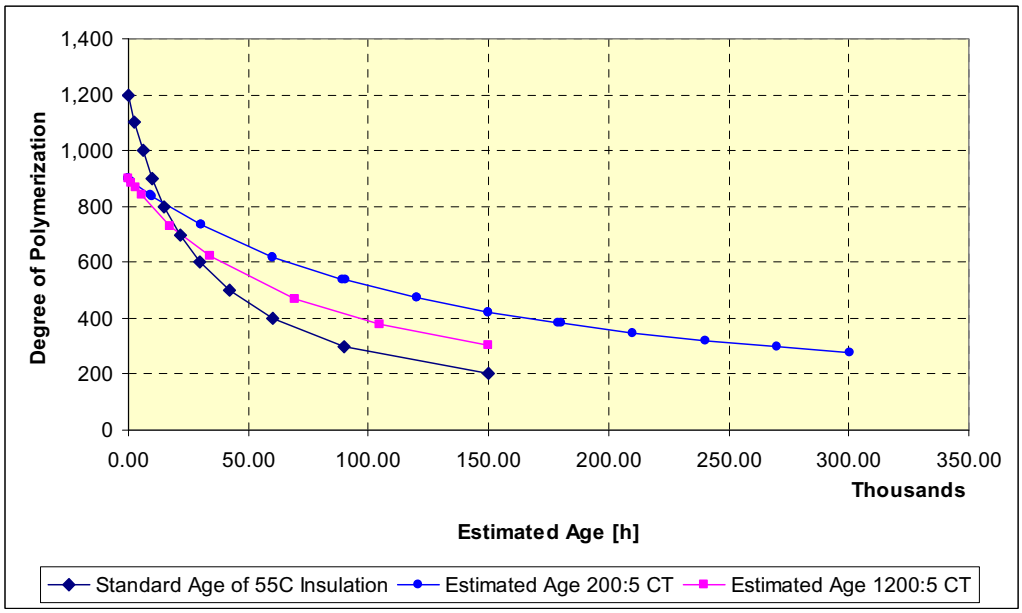

Fig. 150. CT life expectancy vs. Power Transformer life expectancy based on DP

Gases were not included in the analysis of 1200:5 CTs as the experiment aimed the rate of increase of the dissolved in oil gases due to the loading / thermal effect applied to the CTs. But for the 200:5 units, CT4 was exclusively dedicated to monitor the gas evolution during the thermal accelerated ageing process. The regression analysis is presented below starting with those gases which presence was recorded during the entire life of the unit:

In this specific type of current transformer, it was observed that almost all gases are statistically significant, considering that operating conditions do not allow ingress of any kind of contaminant from the outside, neither leaks of gases or oil, and of course, no changes of the liquid insulation during the service life of the unit. Gases are mainly considered to be fault indicators rather than ageing indicators, therefore it is important the use of engineering best practices and standards for the interpretation of gas concentration in oil. Nevertheless, this work provides expressions based on the experimental data gathered during the ageing process and obtained functions are graphically shown in Figures 151 to 153 with their corresponding empirical expressions:

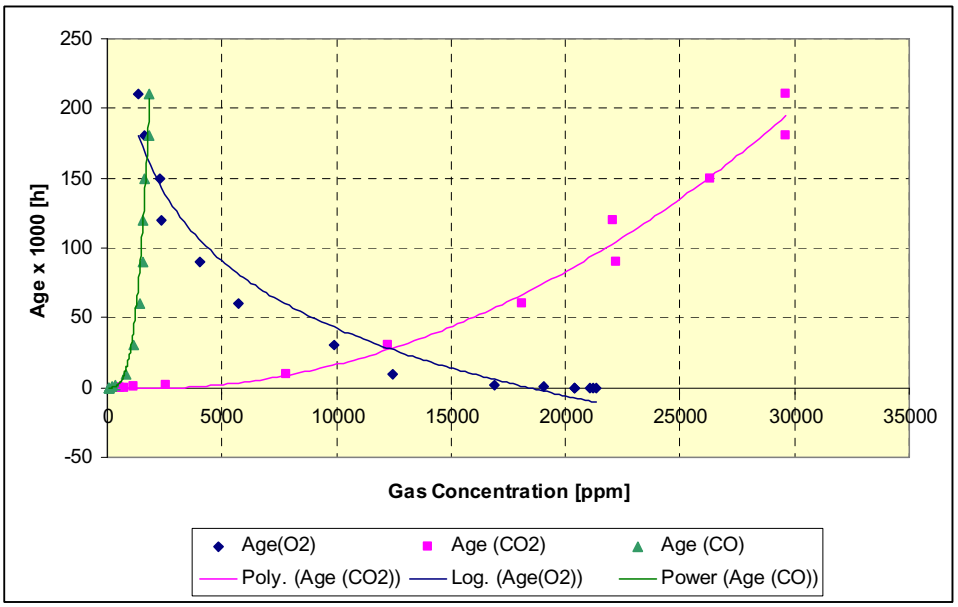

Fig. 151. Insulation Age in terms of O_2, CO, and CO_2 for 200:5 CTs

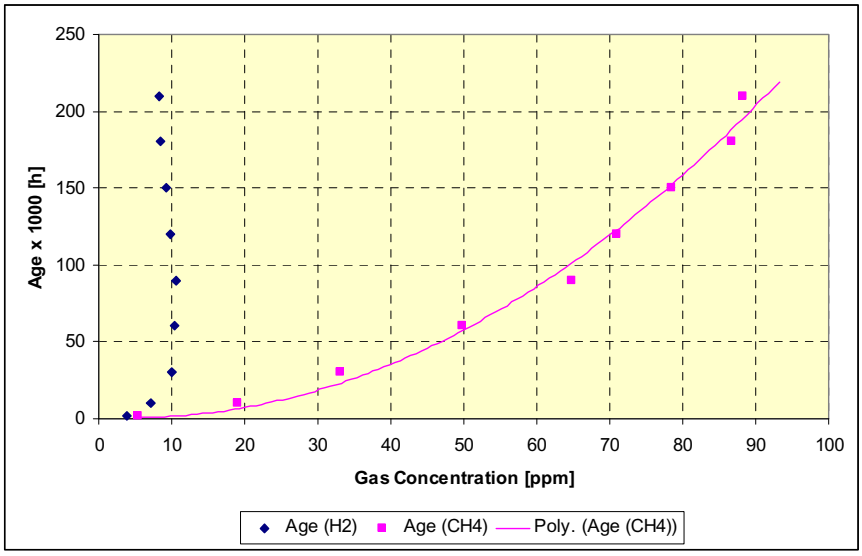

Fig. 152. Insulation Age in terms of H_2, and CH_4 for 200:5 CTs

$$Age_{200:5CT} \approx 0.0003 \cdot \left(CO_{2_{ppm}}\right)^2 - 0.8423 \cdot \left(CO_{2_{ppm}}\right) \tag{5.6}$$

$$Age_{200:5CT} \approx -69752 \ln\left(O_{2_{ppm}}\right) + 684839 \tag{5.7}$$

$$Age_{200:5CT} \approx 2 \times 10^{-6} \cdot \left(CO_{ppm}\right)^{3.349} \tag{5.8}$$

$$Age_{200:5CT} \approx 27.98 \cdot \left(CH_{4_{ppm}}\right)^2 - 273.57 \cdot \left(CH_{4_{ppm}}\right) + 1500 \tag{5.9}$$

The behavior of Methane as presented in Fig. 152, as well as of hydrogen, was observed only after approximately 1,500 hours. Both gases behave in very different ways. Hydrogen reached a concentration of 10ppm and remained within ± 2ppm during the entire life of the current transformer meaning that the gas must be used as a fault indicator and not for age related modeling.

$$Age_{200:5CT} \approx 14942 \cdot e^{0.1103 \cdot \left(C_2H_{6_{ppm}}\right)} \tag{5.10}$$

The behavior of Ethane (C_2H_6) as presented in Fig. 153, is observed only after approximately 30,000 hours; and Ethylene (C_2H_4) was observed only after approximately 60,000 hours. Ethane

presents a traceable path described by (5.10), but Ethylene does not provide values to be used for modeling Age of the current transformer. Ethylene reached a concentration of 4 ppm and remains within ± 1 ppm during the entire life of the current transformer meaning that the gas is to be used as a fault indicator mainly and not for ageing estimation.

Acetylene (C_2H_2) is not used for estimation of ageing of the unit as it was never observed during the entire experimental process. Acetylene is a clear fault indicator and its presence is not desirable, it will indicate possible internal arcing and/or partial discharges.

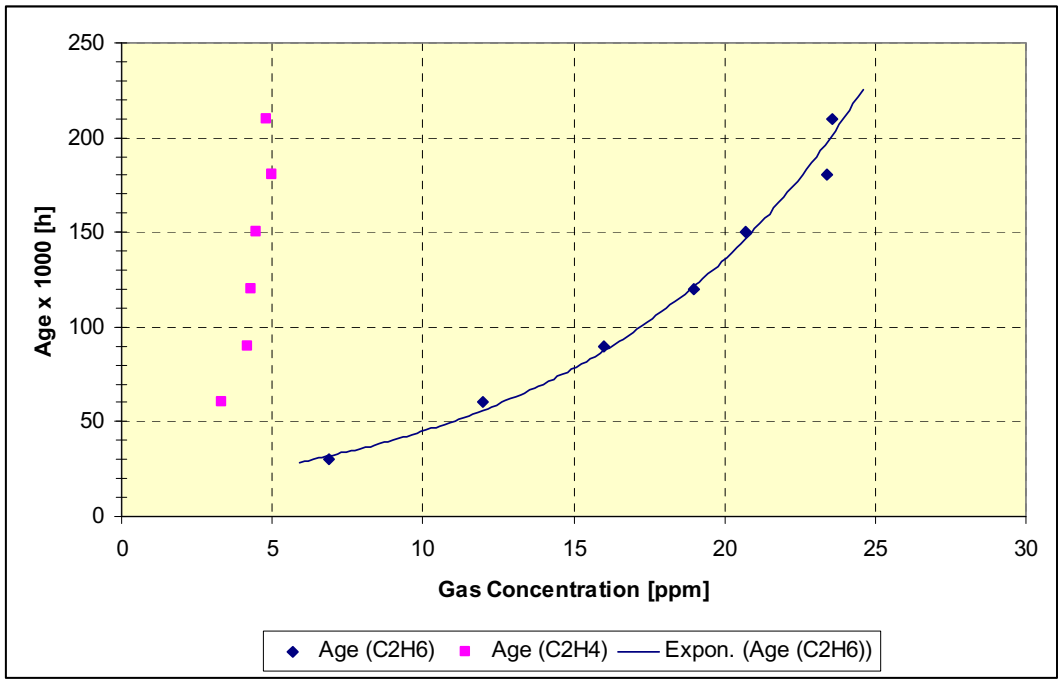

Fig. 153. Insulation Age in terms of C_2H_6 and C_2H_4 for 200:5 CTs

CHAPTER 6

CONCLUSIONS AND FUTURE WORK

High Voltage or Medium Voltage Oil-Immersed Current Transformers were successfully aged under thermal stress. The experimental setup installed to replicate the Pyrolysis aging factor on the combined liquid-solid insulation system delivered the expected levels of operation without compromising safety of the equipment or personnel working in this area. The interfaces created to monitor and acquire data from the embedded sensors provided accurate online information regarding the aging process of the Current Transformers when typical and non-typical profiles were applied.

The present research work has the following outcomes.

Thermal response to load was successfully modeled for each type of transformer based on existing IEEE models of Top-Oil Temperature (TOT) and Hot-Spot Temperature (HST) for Power Transformers. Thermal models to estimate the hottest-spot temperature (HST) were successfully tested under typical and non-typical load profiles which reached extreme conditions (3 p.u.) based on top-oil temperature measurement and ambient temperature. Under typical load profiles the calculated error was less than 5% as compared against measured values.

It was demonstrated that the Current Transformers of the 1200:5 ratio can be successfully operated by monitoring Top-Oil Temperature. The response time of TOT was found to be faster than that of HST which is good enough to monitor the operation of the unit under short-term overload. However, for over 24-hour overload operation, an HST sensor is recommended. The 200:5 Current Transformers can be supervised by monitoring Top-Oil Temperature, but the data need to be

converted into HST values in order to properly operate these devices and predict the Loss-of-Life at short-term overloads.

DC Tests carried out on both types of Current Transformers are not indicative of aging of the insulation system. Results obtained from the experimental work were considered not to be statistically significant within a 95% confidence level to define aging of the Current Transformer.

FDS (Frequency Domain Spectroscopy) is a powerful tool to provide condition assessment of the insulation system. Nevertheless, experimental work did not provide traceable data to model aging of the Current Transformer based on the results obtained through this work.

DGA (Dissolved Gas Analysis) monitoring device provided valuable data. In this work, rate of increase (or decrease) of dissolved in oil gases was evaluated for each specific gas component at different load and temperature levels. This information was used to estimate the risk of operation when calculating key ratios. The experimental work shows that the thermal effect leads to different fault conditions which may turn in to breakdown of the unit. DGA is demonstrated to be a great tool to recognize a fault condition during the operation of the Current Transformer and typical values for the experimental units used in this work have been provided. Interpretation of the data is shown to be better described by CIGRE Key Ratios and The Duval Triangle Methods. Carbon Gases provide a possible trend for ageing estimation

The most important tool to determine the age of Oil-Immersed Current Transformers by non-invasive techniques was demonstrated to be Furanic Compound Concentration. In particular, the concentration of the most abundant (as compared to other compounds) and stable compound 2-Furaldehyde (2FAL) was found to be the best indicator of ageing. This work provides the model to estimate the service age of the Current Transformer as a linear function of 2FAL concentration.

Recommendations for future work are given below.

The installation of external devices (e.g. temperature sensors, humidity sensors, and connection fittings) for future High/Medium Voltage Transformers to be tested must be performed in the factory and before the final drying procedure.

The use of fiber-optic sensors is recommended for different purposes: accurate temperature measurement of HST and TOT, and possible design of a fiber-optic 2-furaldehyde sensor to be installed in the tank totally immersed in the liquid insulation. Fiber sensors are electromagnetically passive so can operate in high and variable electric field environments. They are chemically and biologically inert since the transduction material, silica, is untouched by most chemical and many biological agents [87].

Based on this study, aging models and similar testing techniques could be applied to determine the life of pole-mounted distribution transformers, voltage transformers, and capacitive voltage transformers which have similar volumes of liquid and solid insulation.

To improve accuracy of the models which have been presented here, it is important to gather factory and field data. This is an extremely expensive task, if compared against work performed for power transformers by CIGRE or EPRI.

Further research is required using the DGA system in order to define a possible approach to %LOL Estimation

Aging estimation could be perfectly applied in future modeling of health indices for the instrument transformers.

REFERENCES

[1] IEEE Std C57.13-1993. IEEE Standard Requirements for Instrument Transformers

[2] M. Horning, J. Kelly, S. Myers, R. Stebbins, *Transformer Maintenance Guide,* 3rd ed. Transformer Maintenance Institute, 2004. ISBN 0-939320-02-9.

[3] IEEE Std C57.91-1995. *IEEE Guide for Loading Mineral-Oil-Immersed Transformers*

[4] CIGRE Task Force 15.01.09. *"Dielectric Response Methods for Diagnostics of Power Transformers."* IEEE Electrical Insulation Magazine. May/June 2003, Vol. 19, No. 3. pp. 12-18.

[5] W. J. McNutt, *"A Proposed Life Test Model for Power Transformers*." IEEE Transactions on Power Apparatus and Systems, Vol. Pas-96, No. 5. September/October 1977. pp. 1648 – 1656.

[6] C. T. Dervos, C. D. Paraskevas, P. D. Skafidas and N. Stefanou, *"Dielectric Spectrsocopy and Gas Chromatography Methods Applied on High-Voltage Transformer Oils."* International Conference on Dielectric Liquids, 2005.

[7] M. Kanno, N. Oota, T. Suzuki, T. Ishii, *"Changes in ECT and Dielectric Dissipation Factor of Insulating Oils Due to Aging in Oxygen."* IEEE Transactions on Dielectrics and Electrical Insulation. Vol. 8. No. 6. December 2001. pp. 1048 – 1053.

[8] P. Thomas, A. K. Shukla, *"Ageing Studies on Paper-Oil to Assess the Condition of Solid Insulation used in Power Transformers."* 2001 IEEE 7th International Conference on Solid Dielectrics, June, 2001, the Netherlands. pp. 69 – 72.

[9] S. Wolny, *"The Influence of Temperature and Dampness on the Value of the Main Time Constant of Paper-Oil Insulation Determined by using Deby's Model."* Physics and Chemistry of Solid State (Фізика і Хімія Твердого Тіла). Vol. 7, No. 3, 2006. pp. 572 – 576.

[10] R. Neimanis, L. Arvidsson, P. Werelius, *"Dielectric Spectroscopy Characteristics of Aged Transformer Oils."* Proceedings: Electrical Insulation Conference and Electrical Manufacturing and Coil Winding Technology Conference; EIC/EMCW, Indianapolis 2003. pp. 289 – 293.

[11] Z. Poniran, Z. Abdul-Malek, *"Life Assessment of Power Transformers via Paper Ageing Analysis."* XVth International Symposium on High Voltage Engineering, Slovenia, 2007. T7-15.

[12] A. N. Jahromi, R. Piercy, S. Cress, J. Service, and W. Fan, *"An Approach to Power Transformer Asset Management Using Health Index."* IEEE Electrical Insulation Magazine, March/April 2009 – Vol. 25, No. 2. pp.20 – 33.

[13] A. K. Jonscher, *Dielectric Relaxation in Solids*. Chelsea Dielectrics Press, London 1983. ISBN 0 9508711 09.

[14] T. J. Lewis, *"Ageing – A Perspective."* IEEE Electrical Insulation Magazine, July/August 2001 – Vol. 17, No. 4. pp. 6-16.

[15] A. K. Lokhanin, T. I. Morozova, G. Y. Shneider, V. V. Sokolov and V. M. Chornogotsky, *"Internal Insulation Failure Mechanisms of HV Equipment under Service Conditions."* Electricity Today, Issue 7, 2005. pp. 28 – 33.

[16] IEEE Std 100-1996. *The IEEE Standard Dictionary of Electrical and Electronics Terms*. Sixth Ed.

[17] Y. Du, M. Zahn, B.C. Lesieutre, A.V. Mamishev, S. R. Lindgren, *"Moisture Equilibrium in Transformer Paper-Oil Systems."* IEEE Electrical Insulation Magazine, January/February 1999 – Vol. 15, No. 1. pp.11-20.

[18] TJH2b. Analytical Services Incorporated. *"Oil Quality Testing."*

[19] MEGGER, *A Guide to Diagnostic Insulation Testing Above 1 kV*. MEG-489/2.5M/5.2006.

[20] G. Chen, M. Fu, X. Liu. *"Influence of AC ageing on space charge dynamics in LDPE."* XIIIth International Symposium on High Voltage Engineering, Netherlands 2003, Smit (ed.).

[21] M. Nagel, et al. *"Investigation of Transformer Insulation at High Frequencies and High Voltages"*. nagel@ieh.uni-karlsruhe.de

[22] Martin J. Heathcote, *J&P Transformer Book,* 13th ed. ELSEVIER. ISBN-13: 978-0-7506-8164-3.

[23] D. Susa, M. Lehtonen, H. Nordman, *"Dynamic Thermal Modeling of Power Transformers."* IEEE Transactions on Power Delivery, Vol. 20. No. 1, January 2005. pp. 197-204.

[24] D. Susa, M. Lehtonen, *"Dynamic Thermal Modeling of Power Transformers: Further Development – Part II."* IEEE Transactions on Power Delivery, Vol. 21. No. 4, October 2006. pp. 1971-1980.

[25] B.C. Lesieutre, W. H. Hagman, J. L. Kirtley, *"An Improved Transformer Top Oil temperature Model for Use in an Online Monitoring and Diagnostic System."* IEEE Transactions on Power Delivery, Vol. 12, No. 1, January 1997. pp. 249-256.

[26] D. J. Tylavsky, Q. He, J. Si, G. A. McCulla, and J.R. Hunt, *"Transformer Top-Oil Temperature Modeling and Simulation."* IEEE Transactions on Industry Applications, Vol. 46, No.5, September/October, 2000, pp. 1219-1225.

[27] Yong Liang, *"Simulation of Top Oil Temperature for Transformers."* M.S. Thesis and Final Report, PSERC Publication 01-21, Feb. 2001.

[28] G. Swift, T. S. Molinski and W. Lehn, *"A Fundamental Approach to Transformer Thermal Modeling – Part I : Theory and Equivalent Circuit ." IEEE Transactions on Power Delivery*, Vol. 16, No. 2, April 2001, pp. 171 – 175.

[29] G. Swift, T. S. Molinski, R. Bray, and R. Menzies, *"A fundamental Approach to Transformer Thermal Modeling – Part II: Field Verification."* IEEE Transactions on Power Delivery, Vol. 16, No. 2, April 2001, pp.176-180.

[30] W. Collet, S. M. Mahajan, *"Electromagnetic Modeling of a High Voltage Current Transformer."* 39th North American Power Symposium (NAPS 2007).

[31] A. E. Fitzgerald, C. Kingsley Jr., and S. D. Umans, *Electric Machinery,* 6th Edition. Boston. McGraw Hill, 2003.

[32] R. M. Rifaat, *"Considerations in Applying EMTP to Evaluate Current Transformer Performance under Transient and High Current Fault Conditions."* Presented at the International Conference on Power Systems Transients (IPST'05). Montreal, Canada. June 19 - 23, 2005. Paper No. IPST05 – 206.

[33] S. V. Kulkarni, S. A. Khaparde, *Transformer Engineering – Design and Practice*. Marcel Dekker, Inc. 2005. ISBN: 0-8247-5653-3.

[34] J. J. O'Dwyer, *"Breakdown in Solid Dielectrics."* IEEE Transactions on Electrical insulation Vol. EI-17, No. 6, December 1982. pp. 484-486.

[35] ASTM D 149 – 97a (2004), *Standard Test Method for Dielectric Breakdown Voltage and Dielectric Strength of Solid Electrical Insulating Materials at Commercial Power Frequencies*. ASTM Annual Book. Electrical Insulation (I). Vol. 10.01. 2007. pp. 15-25.

[36] Hikita M, Ieda M, Sawa G. *"Numerical Analysis of Steady State Thermal Breakdown."* Journal of Applied Physics. Vol. 54. Issue 4, April 1983. American Institute of Physics, 1983. pp. 2025-2029.

[37] R. C. Buehl, A. von Hippel, *"The Electrical Breakdown Strength of Ionic Crystals as a function of Temperature."* APS American Physical Society, Physical Review, Vol. 56, November 1, 1939. pp. 941-947.

[38] T. Leibfried, et al. *"Ageing and Moisture Analysis of Power Transformer Insulation Systems*." Submitted for publication: CIGRE Session, Paris, 2002.

[39] L. A. Dissado and J. C. Fithergill, *Electrical Degradation and Breakdown in Polymers,* Peter Peregrinus Ltd. 1992.

[40] International Electrical Testing Association. *Acceptance Testing Specifications –for Electrical Power Distribution Equipment and Systems*. 2003. ATS-2003.

[41] Paul Gill, *Electrical Power Equipment Maintenance and Testing.* Marcel Dekker, Inc., New York, Basel, 1998.

[42] S. Drennan. *Diagnostic Insulation Testing.* Megger Ltd. Available from: http://www.megger.com/common/documents/Diagnostic%20insulation%20testing%20by%20S%20Drennan.pdf.

[43] A. O. Reynolds. *The Lowdown on High-Voltage DC Testing.* AVO International, 1st Edition, 1988.

[44] M. Hanif. *"Principles and Applications of Insulation Testing with DC."* IEP-SAC Journal 2004-2005. pp. 57-63.

[45] International Standard IEC 156, *Insulating Liquids – Determination of the Breakdown Voltage at Power Frequency – Test Method*. Second Edition. IEC 1995.

[46] T. V. Oommen, T. A. Prevost, *"Cellulose Insulation in Oil-Filled Power Transformers: Part II – Maintaining Insulation Integrity Life."* IEEE Electrical Insulation Magazine, March/April 2006 – Vol. 22, No. 2. pp.5 – 14.

[47] W. S. Zaengl, *"Dielectric Spectroscopy in Time and Frequency Domain for HV Power Equipment, Part I: Theoretical Considerations."* IEEE Electrical Insulation Magazine – September/October 2003 – Vol. 19, No.5, pp. 5-19.

[48] ASTM D 150 – 98 (2004), *Standard Test Method for AC Loss Characteristics and Permittivity (Dielectric Constant) of Solid Electrical Insulation*. ASTM Annual Book. Electrical Insulation (I). Vol. 10.01. 2007. pp. 28-47.

[49] E. Kuffel, W. S. Zaengl, J. Kuffel, *High Voltage Engineering Fundamentals*, 2nd ed. ELSEVIER, 2001.

[50] W. P. Baker, *Electrical Insulation Measurements*, Chemical Publishing Co, N. Y., 1965.

[51] Working Group A2.30. *"Moisture Equilibrium and Moisture Migration within Transformer Insulation Systems."* CIGRE Report 349. June 2008.

[52] A. J. Kachler, I. Höhlein, *"Aging of Cellulose at Transformer Service Temperatures. Part 1: Influence of Type of Oil and Air on the Degree of Polymerization of Pressboard, Dissolved Gases, and Furanic Compounds in Oil."* IEEE Electrical Insulation Magazine. March/April 2005 – Vol. 21. No.2. pp. 15 – 21.

[53] I-U-Khan, Z. Wang, et al. *"Dissolved Gas Analysis of Alternative Fluids for Power Transformers."* DEIS September/October 2007 – Vol. 23, No.5. pp. 5-14.

[54] Tapan K. Saha, *"Review of Modern Diagnostic Techniques for Assessing Insulation Condition in Aged Transformers."* IEEE Transactions on Dielectrics and Electrical insulation. Vol. 10, No. 5. October 2003. pp. 903-917.

[55] IEEE Std. C57.104-1991, *Guide for the Interpretation of Gases Generated in Oil-Immersed Transformers."*

[56] *Guide to the Interpretation of Dissolved and Free Gasses Analysis*, IEC Std. 60599, IEC Publ. 60599, Mar. 1999.

[57] M. Duval, "*Dissolved Gas Analysis and the Duval Triangle."* AVO New Zeland / LORD

Consulting 2006 Conference Paper.

[58] M. Duval, *"Calculation of DGA Limit Values and Sampling Intervals in Transformers in Service."* IEEE Electrical Insulation Magazine. September/October 2008 – Vol.24, No.5. pp. 7-13.

[59] W. H. Tang et al, "*A Probabilistic Classifier for Transformer Dissolved Gas Analysis with a Particle Swarm Optimizer."* IEEE Transactions on Power Delivery, Vol 23, No. 2, April 2008.

[60] T. A. Prevost, T. V. Oommen, *"Cellulose Insulation in Oil-Filled Power Transformers: Part I – History and Development."* IEEE Electrical Insulation Magazine, January/February 2006 – Vol. 22, No. 1. pp. 28 – 35.

[61] T. S. R. Murthy, *"Assessment of Transformer Insulation Condition by Evaluation of Paper-Oil Systems."* 1996 IEEE Annual Report – Conference on Electrical Insulation and Dielectric Phenomena, San Francisco, October 20-23, 1996.

[62] Alfonso de Pablo, *"Furfural and Ageing: How are they Related."* IEE Power Division Colloquium Insulating Liquids, National Grid Leatherhead, UK, 1999.

[63] R. D. Stebbins, D. S. Myers, and A. B. Shkolnik, *"Furanic Compounds in Dielectric Liquid Samples: Review and Update of Diagnostic Interpretation and Estimation of Insulation Ageing."* Proceedings of the 7th International Conference on Properties and Applications of Dielectric materials. June 1-5, 2003, Nagoya.

[64] X. Chendong, *"Monitoring paper insulation ageing by measuring furfural content of oil*." Proceedings 7th Int. Symp. High Voltage Engineering, Aug. 26 – 30, 1991, pp.139-142.

[65] A. M. Emsley, G. C. Stevens, *"Review of Chemical Indicators of Degradation of Cellulosic Electrical Paper Insulation in Oil-filled Transformers."* IEE Proceedings Science Measurement technology, Vol. 141, No. 5, September 1994, pp. 324-334.

[66] M. Dong, Z. Yan, G. J. Zhang, *"Comprehensive Diagnostic and Ageing Assessment Method of Solid Insulation in Transformer."* IEEE 2003 Annual report Conference on Electrical Insulation and Dielectric Phenomena. 2003. pp. 137-140.

[67] ThermAsset2, *Fiber-optic Winding Temperature Controller – User's Manual*. Luxtron Corporation 2006.

[68] V. Sivan, D. Robalino, S. Mahajan, *"Measurement of Temperature Gradients inside a Medium Voltage Current Transformer."* 2007 39th North American Power Symposium. September 30 – October 02, 2007. New Mexico. NAPS'07.

[69] S. M. Mahajan, V. Sivan, D. M. Robalino, *"Thermal Modeling of an Oil-Immersed Current Transformer."* Submitted for review to IEEE Transactions on Power Delivery on April 27, 2009.

[70] IEC 354-1991, *Load Guide for Oil Immersed Power Transformers.*

[71] D. M. Robalino, S. M. Mahajan, *"Effects of Thermal Accelerated Ageing on Medium Voltage Oil-Immersed Current Transformers."* IEEE International Symposium on Electrical Insulation, June 2008, Vancouver, BC, Canada. pp. 470 – 473.

[72] M. Duval, A. DePablo, *"Interpretation of Gas-In-Oil Analysis Using New IEC Publication 60599 and IEC TC 10 Databases."* IEEE Electrical Insulation Magazine. March/April 2001 – Vol.17, No.2. p. 31-41.

[73] M. Wang, et al, *"Review of Condition Assessment of Power Transformers in Service."* IEEE Electrical Insulation Magazine. November/December 2002 – Vol.18, No.6. pp. 12-25.

[74] T.K. Saha, et al. *"Voltage Response Measurements for the Diagnosis of Insulation Condition in Power Transformer."* University of Queensland, Australia.

[75] *S1-1052 10kV Digital Insulation Tester – User Manual.* Megger, Inc.

[76] *DTS-60D Oil Dielectric Test Sets 0-60 kVac and 0-100 kVac.* Product brochure. High Voltage Inc.

[77] CT Analyzer. *The Revolution in Current Transformer Testing.* Omicron Electronics Corporation, USA.

[78] *IDAX-206 User's Manual.* Pax Diagnostics, 2006.

[79] ASTM D 202 – 97 (2002), *Standard Test Method for Sampling and Testing Untreated Paper Used for Electrical Insulation.* ASTM Annual Book. Electrical Insulation (I). Vol. 10.01. 2007. pp. 58-91.

[80] Проф. А. В. Лыков. *Теория Сушки*. Государственное Энергетическое Издательство, Москва, 1950. A. V. *Theory of Drying*, Moscow, 1950. (in Russian).

[81] Electric Utility Engineers of the Westinghouse Electric Corporation, *Electric Utility Engineering Reference Book – Distribution Systems.* Vol 3. Westinghouse Electric Corporation, 1965.

[82] P. J. Brockwell, R. A. Davis, *Introduction to Time Series and Forecasting*. 1996 Springer-Verlag New York Inc. ISBN 0-387-94719-1.

[83] J. L. Rodgers, W. A. Nicewander, *"Thirteen Ways to look at the Correlation Coefficient."* The American Statistician, February 1988, Vol. 42, No. 1. pp. 59-66.

[84] D. C. Montgomery, *Design and Analysis of Experiments.* 6th. Ed. John Wiley & Sons, Inc. 2005. ISBN -0-471-48735-X.

[85] I. A. Adejumobi, S. G. Oyagbinrin, *"Insulation Deterioration and its Effects on Power System."* Jornal of Engineering and Applied Sciences 2 (5): 870-873, 2007.

[86] M. A. Salam, H. Anis, A. El-Morshedy, R. Radwan, *High-Voltage Engineering Theory and Practice.* 2nd Edition, Marcel Dekker, Inc., New York, Basel. 2000.

[87] B. Culshaw, *"Optical Fiber Sensor Technologies: Opportunities and – Perhaps – Pitfalls."* Journal of Lightwave Technology, Vol. 22, No. 1. January 2004. pp. 39 – 50.

APPENDIX A

AGEING CHARTS FOR NON-THERMALLY UPGRADED PAPER INSULATION

A.1. Time durations in hours for continuous operation below/above rated HST

Table 53. Time durations in hours for continuous operation below/above rated HST based on NIL=150,000h for a 55°C temperature rise insulation system

Hot Spot temp °C	FAA	Overloading Time (NIL = 150k hours)										
		0.50	1.00	1.50	2.00	4.00	8.00	12.00	24.00	168.00	720.00	8,760.00
0	0.00	0.00	0.00	0.00	0.00	0.00	0.00	0.00	0.00	0.00	0.00	0.00
5	0.00	0.00	0.00	0.00	0.00	0.00	0.00	0.00	0.00	0.00	0.00	0.00
10	0.00	0.00	0.00	0.00	0.00	0.00	0.00	0.00	0.00	0.00	0.00	0.00
15	0.00	0.00	0.00	0.00	0.00	0.00	0.00	0.00	0.00	0.00	0.00	0.00
20	0.00	0.00	0.00	0.00	0.00	0.00	0.00	0.00	0.00	0.00	0.00	0.00
25	0.00	0.00	0.00	0.00	0.00	0.00	0.00	0.00	0.00	0.00	0.00	0.00
30	0.00	0.00	0.00	0.00	0.00	0.00	0.00	0.00	0.00	0.00	0.00	0.00
35	0.00	0.00	0.00	0.00	0.00	0.00	0.00	0.00	0.00	0.00	0.00	0.00
40	0.00	0.00	0.00	0.00	0.00	0.00	0.00	0.00	0.00	0.00	0.00	0.00
45	0.00	0.00	0.00	0.00	0.00	0.00	0.00	0.00	0.00	0.00	0.00	0.01
50	0.00	0.00	0.00	0.00	0.00	0.00	0.00	0.00	0.00	0.00	0.00	0.02
55	0.01	0.00	0.00	0.00	0.00	0.00	0.00	0.00	0.00	0.00	0.00	0.04
60	0.01	0.00	0.00	0.00	0.00	0.00	0.00	0.00	0.00	0.00	0.01	0.08
65	0.03	0.00	0.00	0.00	0.00	0.00	0.00	0.00	0.00	0.00	0.01	0.16
70	0.05	0.00	0.00	0.00	0.00	0.00	0.00	0.00	0.00	0.01	0.02	0.30
75	0.10	0.00	0.00	0.00	0.00	0.00	0.00	0.00	0.00	0.01	0.05	0.56
80	0.18	0.00	0.00	0.00	0.00	0.00	0.00	0.00	0.00	0.02	0.08	1.03
85	0.32	0.00	0.00	0.00	0.00	0.00	0.00	0.00	0.01	0.04	0.15	1.87
90	0.57	0.00	0.00	0.00	0.00	0.00	0.00	0.00	0.01	0.06	0.27	3.33
95	1.00	0.00	0.00	0.00	0.00	0.00	0.01	0.01	0.02	0.11	0.48	5.84
100	1.73	0.00	0.00	0.00	0.00	0.00	0.01	0.01	0.03	0.19	0.83	10.09
105	2.94	0.00	0.00	0.00	0.00	0.01	0.02	0.02	0.05	0.33	1.41	17.17
110	4.94	0.00	0.00	0.00	0.01	0.01	0.03	0.04	0.08	0.55	2.37	28.82
115	8.17	0.00	0.01	0.01	0.01	0.02	0.04	0.07	0.13	0.92	3.92	47.74
120	13.37	0.00	0.01	0.01	0.02	0.04	0.07	0.11	0.21	1.50	6.42	78.07
125	21.59	0.01	0.01	0.02	0.03	0.06	0.12	0.17	0.35	2.42	10.37	126.11
130	34.47	0.01	0.02	0.03	0.05	0.09	0.18	0.28	0.55	3.86	16.54	201.29
135	54.39	0.02	0.04	0.05	0.07	0.15	0.29	0.44	0.87	6.09	26.11	317.63
140	84.88	0.03	0.06	0.08	0.11	0.23	0.45	0.68	1.36	9.51	40.74	495.71
145	131.07	0.04	0.09	0.13	0.17	0.35	0.70	1.05	2.10	14.68	62.91	765.43
150	200.31	0.07	0.13	0.20	0.27	0.53	1.07	1.60	3.20	22.43	96.15	1,169.82
155	303.12	0.10	0.20	0.30	0.40	0.81	1.62	2.42	4.85	33.95	145.50	1,770.24
160	454.34	0.15	0.30	0.45	0.61	1.21	2.42	3.63	7.27	50.89	218.08	2,653.32
165	674.72	0.22	0.45	0.67	0.90	1.80	3.60	5.40	10.80	75.57	323.86	3,940.35
170	993.09	0.33	0.66	0.99	1.32	2.65	5.30	7.94	15.89	111.23	476.68	5,799.66
175	1,449.14	0.48	0.97	1.45	1.93	3.86	7.73	11.59	23.19	162.30	695.59	8,462.99
180	2,097.05	0.70	1.40	2.10	2.80	5.59	11.18	16.78	33.55	234.87	1,006.58	12,246.77

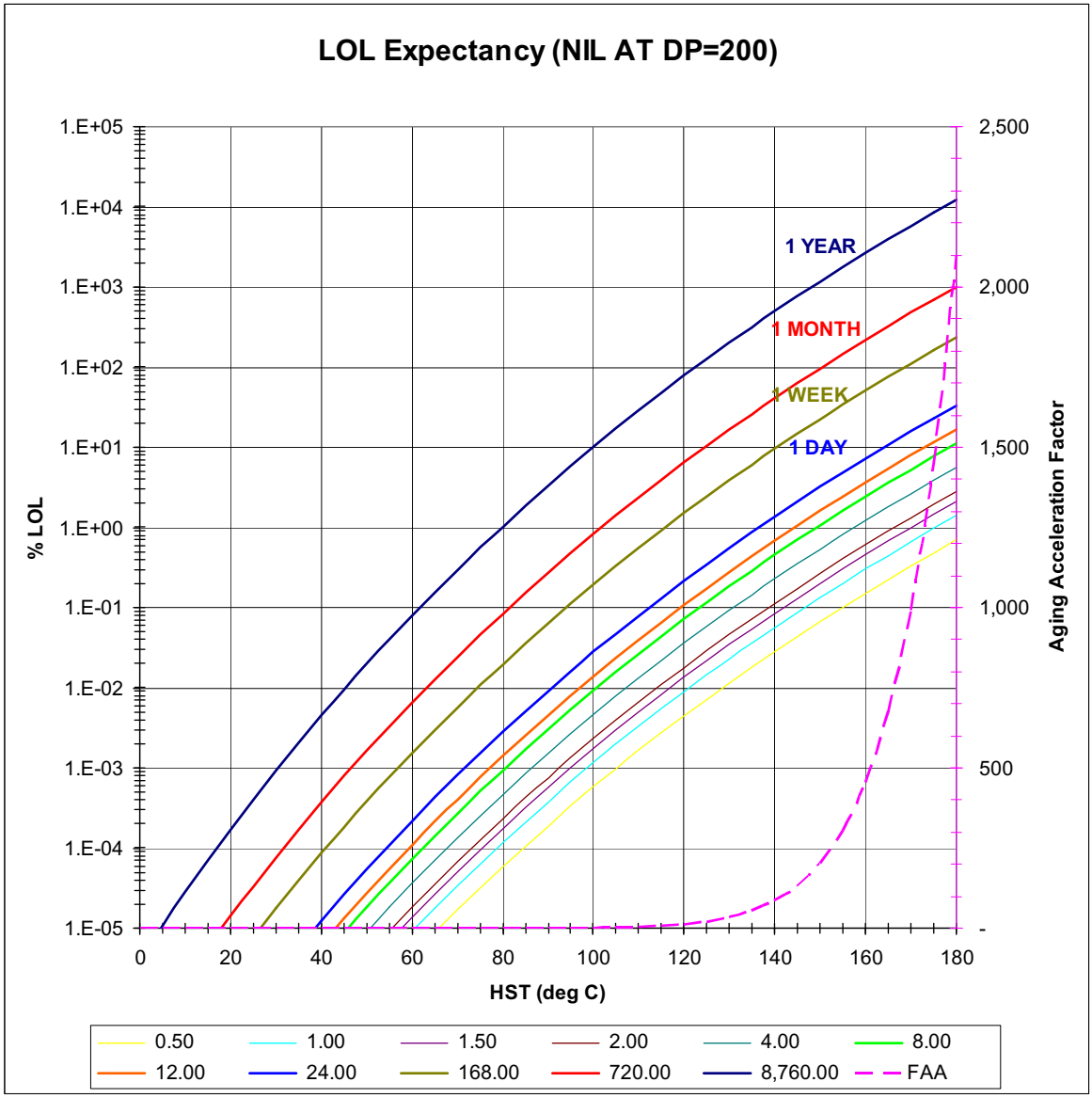

Fig. 154. Calculated LOL Expectancy for 55° C insulation systems for NIL=150,000h

APPENDIX B

TESTING EQUIPMENT SPECIFICATIONS

B. 1. Insulation Resistance MegOhmmeter (Megger)

The device used for Insulation Resistance, Polarization Index and Step Voltage testing is manufactured by Megger ®. The tester communicates via a serial port interface (RS-232) capable to deliver all testing data to an electronic file in the main data acquisition server.

A simplified block diagram of the device is shown below in Fig. 155. In this diagram, for a 10kV tester, the circuit components are C_1 = 15 nF; R_1 = 156 kΩ; and, R_2 = 110 kΩ.

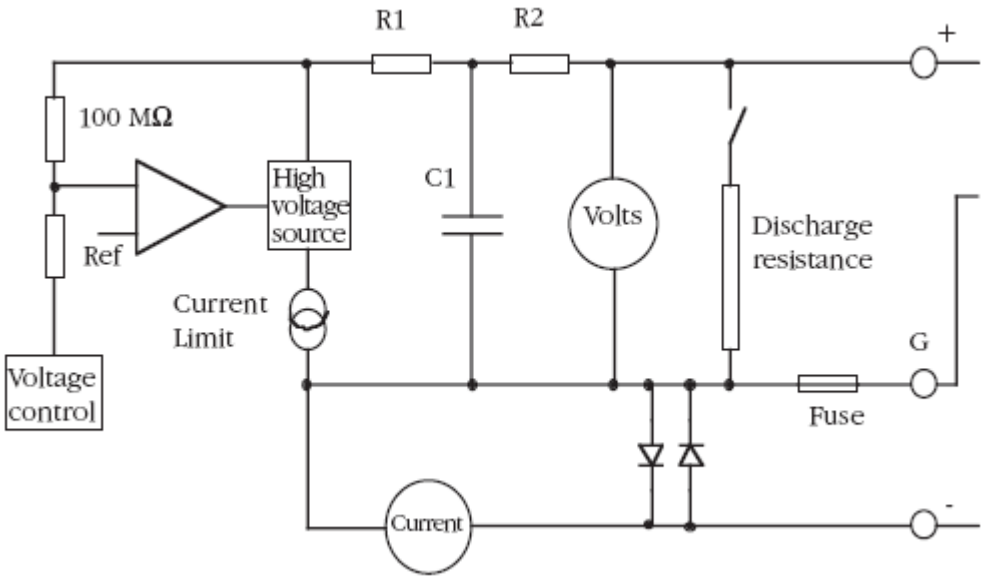

Fig. 155. Circuit Block Diagram - Digital Insulation Tester Megger ® [75]

The technical specifications for the S1-1052 unit are listed in Table 54.

Table 54. S1-1052 Megohmmeter - Technical Specifications [75]

Parameter	Description	Parameter	Description
Voltage input range	85-265 V rms, 50/60Hz, 60 VA	Current measurement range	0.01 nA to 5 mA
Battery life	4 hours continuous testing at 10 kV	Current measurement accuracy (23°C)	±5% ±0.2 nA at all voltages
Test voltages	250 V, 500 V, 1 kV, 2.5 kV, 5 kV, 10 kV ranges, adjustable in 10 V steps from 50 V to 1 kV, and 25 V steps from 1 kV to 10 kV	Data storage	Data stored: selected voltage, test time elapsed, voltage applied, leakage current, and insulation resistance. The PI, DAR, capacitance, time constant and DD values are also stored if available at the end of the test. Megger Download Manager may be used to transfer this data to a PC
Accuracy (23°C, 10 kV)	±5% @ 2 T½ ±20% @ 20 T½	Test regimes	Auto IR, PI, SV, DD DAR is calculated automatically if timers T1 and T2 are set
Guard	2% error guarding 500 k½ leakage with 100 M½ load	Interface	RS232: 38400 Baud, 8 data bits, 0 parity, 1 stop bit, no flow control. USB
Short circuit/charge current	5 mA @ 10 kV	Data output	Real time serial data output once per second of the test voltage, test current, and resistance
Capacitor charge time	<3 seconds per µF at 5mA to 10 kV	Voltage output accuracy (0°C to 30°C)	+4%, -0% ±10 V of nominal test voltage at 1 G½ load
Capacitor discharge time	<250 ms per µF to discharge from 10 kV to 50 V	Capacitance measurement (500 V minimum test voltage)	10 nF to 50 µF (dependent on test voltage)
		Capacitance measurement accuracy (23°C)	±5% ±5 nF

Fig. 156. DC Test carried out on CT2 using the Digital Insulation Tester

B. 2. Oil Dielectric Test Set DTS-60D (High Voltage, Inc)

The DTS Series of Oil/Liquid Dielectric AC test sets provide repeatable and accurate measurement of the breakdown voltage of insulating fluids used in transformers, circuit breakers, bushings, capacitors, etc. The technical specifications of the equipment are summarized in Table 55.

Table 55. DTS-60D Oil Dielectric Test Set - Technical Data [76]

Parameter	Description
Input	120V, 60Hz, 7Amps or 230V, 50/60Hz, 4Amps
Output	0 – 60 kV AC, 800 VA resistive load
Output Termination	Dual capacitively graded bushings with cradle contact mounting in test chamber
Testing Standards	ASTM D877, ASTM D1816, IEC 156
Gap Gauges	0.04” / 0.08” (1mm / 2mm)
Distortion	< 5%
Kilovolt Meter & Accuracy	3.5 Digit LED, Scaled 0 – 60 kV AC rms, 2% of full scale

B. 3. CT Analyzer (OMICRON)

OMICRON's CT Analyzer is an electronic multifunctional instrument designed to perform excitation, ratio, polarity and winding resistance tests on current transformers (CTs) as well as burden-impedance measurement.

The equipment provides automatic testing and calibration for all types of low leakage flux current transformers both on-site in the power system as well in the controlled environment of CT and switchgear manufacturers. The CT Analyzer allows an automatic assessment of test results clearly indicating whether the parameters of the CT under test match its specification.

Because of the patented (EP 1 398 644 A1) low voltage test method it is possible to test CTs with a knee point voltage up to 15 kV without stressing the insulation of the CT (max. 120 V test voltage). Testing of current transformers can be carried out to an extremely high level of accuracy. The accuracy level (0.02 % / 1 min.) makes the CT Analyzer the ideal tool for calibration and verification, not only for protection CTs but also for class 0.1 CTs for metering [77].

Table 56. CT Analyzer Technical Specifications

Parameter	Description
Generator / amplifier section	
Output current	0 ... 5 A rms (15 A peak)
Output voltage	0 ... 120 V
Output power	0 ... 400 VA (1500 VA peak)
Ratio accuracy for 0 VA up to rated power	
ratio 1 ... 2000	0.02 %
ratio 2000 ... 5000	0.03 %
ratio 5000 ... 10000	0.05 %
Phase measurement	
Resolution	0.1 min
Accuracy	1 min (for cos φ 0.8 ... 1)

The technical specifications of the equipment are summarized in Table 56.

A wide range of measurement functionalities are provided:

- Burden measurement
- CT Winding resistance measurement
- CT Excitation characteristic recording
- CT transient behavior measurement (IEC60044-6)
- CT ratio measurement with consideration of connected burden
- CT phase and polarity measurement
- Determination of accuracy limiting factor (ALF), instrument security factor (FS), secondary time constant (Ts), remanence factor (Kr), transient dimensioning factor (Ktd), knee point voltage/current, class, saturated and non saturated inductance
- Assessment according to defined standards: IEC60044-1, IEC60044-6, IEEE C57.13-1993

B. 4. IDAX – 206 Insulation Diagnostics (Megger)

IDAX-206 is an insulation diagnostic system for investigations/analysis of dielectric materials, normally insulators. The measurement method used is dielectric spectroscopy, i.e. measurement of the dielectric properties of the material as a function of the frequency, and in some cases also as a function of the voltage. By studying the dielectric material properties as functions of frequency it is possible to make a distinction between different types of phenomena. For example, it is possible to separate polarization loss from leakage currents.

The system applies a sinusoidal voltage with desired frequency over the sample. This voltage will generate a current in the sample. By accurately measuring the voltage and the current, the sample

impedance can be calculated. Depending upon the actual model of the sample, various parameters can be calculated from the impedance, such as capacitance, loss, resistance etc. This procedure can then be repeated at the specified frequencies and voltage levels and even more information on the sample can be revealed. The IDAX-206 uses three electrodes set-up, which allows for measurements of non-grounded as well as grounded objects with and without guard as it is shown in Fig. 157.

The voltage (and the current) is generated by a voltage source. There are currently two internal voltage sources available in the IDAX-206 system, which can deliver a maximum peak output of 10 V_{peak} or 200 V_{peak}, respectively. The voltage is measured by means of a voltmeter and the current is measured by an ammeter or electrometer which acts as a current-to-voltage converter. The analogue signals (voltages) are then converted to digital samples of the signals that are used in subsequent calculations.

The process described above returns calculated parameters of capacitance, power factor (PF), dissipation factor (tan δ), complex capacitance (C' and C") and complex permittivity ε' and ε". The inaccuracy of the system is defined by using capacitance and tan δ and represented in Fig. 158.

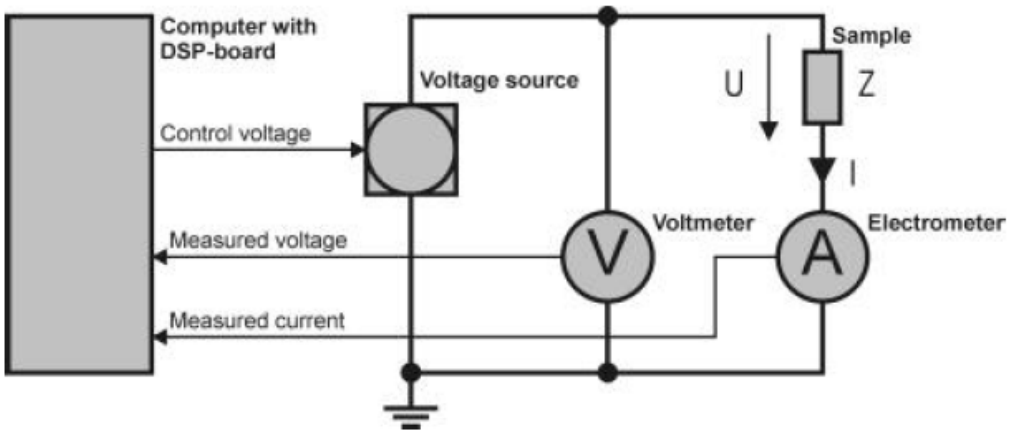

Fig. 157. IDAX-206 Measurement of Electrical impedance [78]

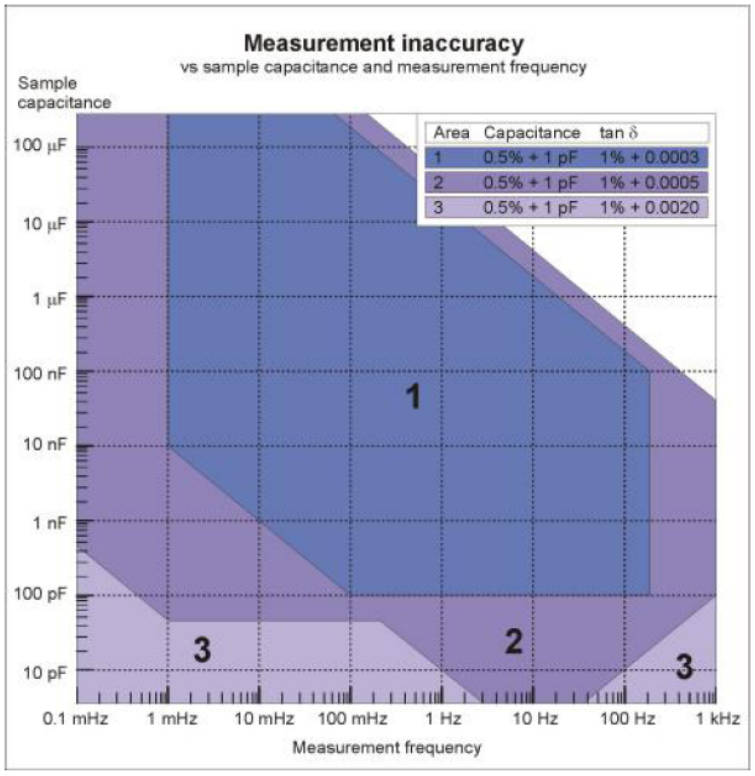

Fig. 158. Inaccuracies for different values of Capacitance and tan δ [78]

Table 57. IDAX-206 Technical Specifications

Parameter	Description
Output Current range:	10 V : 0 - 50 mApeak 200 V : 0 - 50 mApeak
Output Voltage range:	10 V : 0 - 10 Vpeak 200 V : 0 - 200 Vpeak
Accuracy in time base:	100 ppm* *Same time base is used for generation of voltages and in measurements.
Frequency range:	0.0001 Hz - 1 kHz
Power consumption:	Max. 250 VA
Communications	Interface: 16 cm (6.4") TFT Colour Monitor USB keyboard with PS2 trackball USB port for memory stick or accessory Analogue Video Port (EGA) Ethernet

Fig. 159. Dielectric Spectroscopy in the Frequency Domain using IDAX 206 and IDAX 300 on Oil-Immersed Current Transformers at AREVA T&D manufacturing facilities

B. 5. Online Transformer Monitor Model TM8 (SERVERON)

The Model TM8 offers a comprehensive DGA assessment. This assessment is provided through accurate and repeatable online measurements of the 8 critical fault gases and other key parameters. It correlates all 8 fault gases, moisture-in-oil, oil temperature and ambient temperature to transformer load. The device data supports IEEE and IEC diagnostic techniques for rapid warning and diagnosis of developing faults.

The installation of this device can not be considered as typical for oil immersed current transformer because the system is designed to be connected to power or distribution transformers

where the high voltage and low voltage terminals are placed in the same metallic enclosure. For bigger transformers, the price of the monitored unit is much higher than the price of acquisition of the TM8 monitor. The installation at TTU is unique and never used previously neither in the industry nor in research laboratories and it is shown in Fig. 160. The technical specifications of the TM8 monitor are summarized in Table 58.

Table 58. Online DGA Monitor TM8 Technical Specifications

DGA METHOD: LABORATORY GRADE GAS CHROMATOGRAPHY				
Gas		**Accuracy**[17]	**Repeatability**[18]	**Range**[19]
Hydrogen	H_2	±5% or ±3 ppm	<2%	3 – 3,000 ppm
Oxygen	O_2	±5% or +30/-0 ppm	<1%	30 – 25,000 ppm
Methane	CH_4	±5% or ±5 ppm	<1%	5 – 7,000 ppm
Carbon Monoxide	CO	±5% or ±5 ppm	<2%	5 – 10,000 ppm
Carbon Dioxide	CO_2	±5% or ±5 ppm	<1%	5 – 30,000 ppm
Ethylene	C_2H_4	±5% or ±3ppm	<1%	3 – 5,000 ppm
Ethane	C_2H_6	±5% or ±5 ppm	<1%	5 – 5,000 ppm
Acetylene	C_2H_2	±5% or ±1 ppm	<2%	1 – 3,000 ppm
Nitrogen	N_2	±10% or ±5,000 ppm	<20%	5,000 – 100,000 ppm
MOISTURE-IN-OIL AND OIL TEMPERATURE				
Parameter		**Accuracy**[20]		**Range**
Moisture-in-oil		±2%		0-100% RS
		<10% of reading for oil temp. >30°C		0-80 ppm [21]
		<18% of reading for oil temp. <30°C		0-80 ppm
Oil Temperature		±0.1°C (typ.)		-40°C to + 180°C

[17] Percent or PPM – whichever is greater
[18] At the calibration level
[19] Gas-in-oil
[20] Includes nonlinearity and repeatability
[21] Upper range limited to saturation

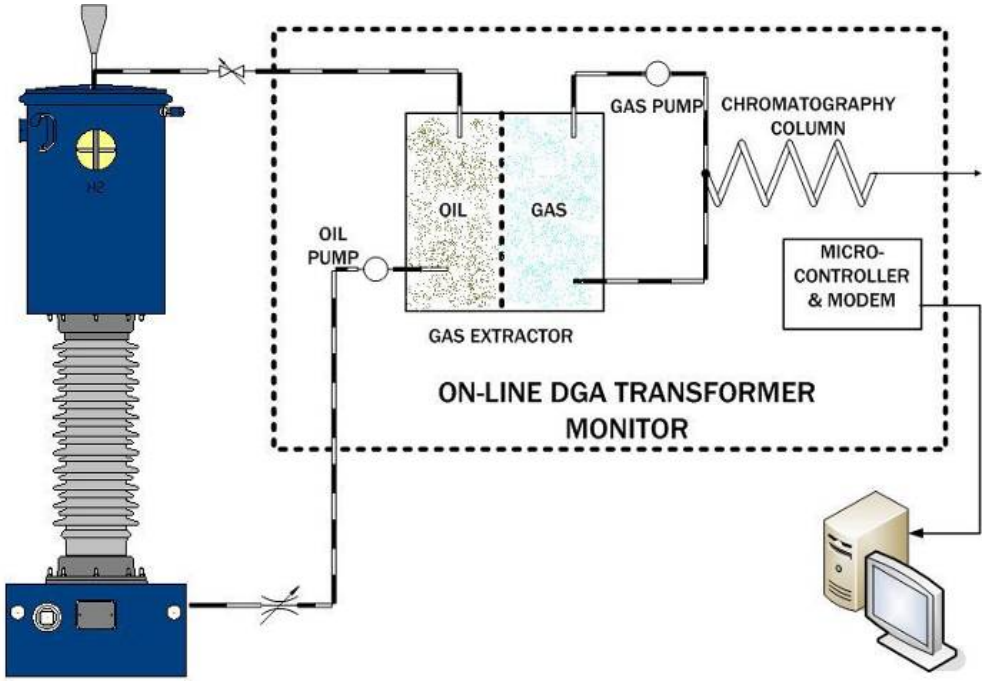

Fig. 160. DGA monitoring system attached to 69kV Oil-Immersed Current Transformer - Simplified Process Diagram

Fig. 161. DGA monitoring system - As installed in the HV/HC Lab CH-103

APPENDIX C

C.1. Thermal profile of the Ageing Process on CT1

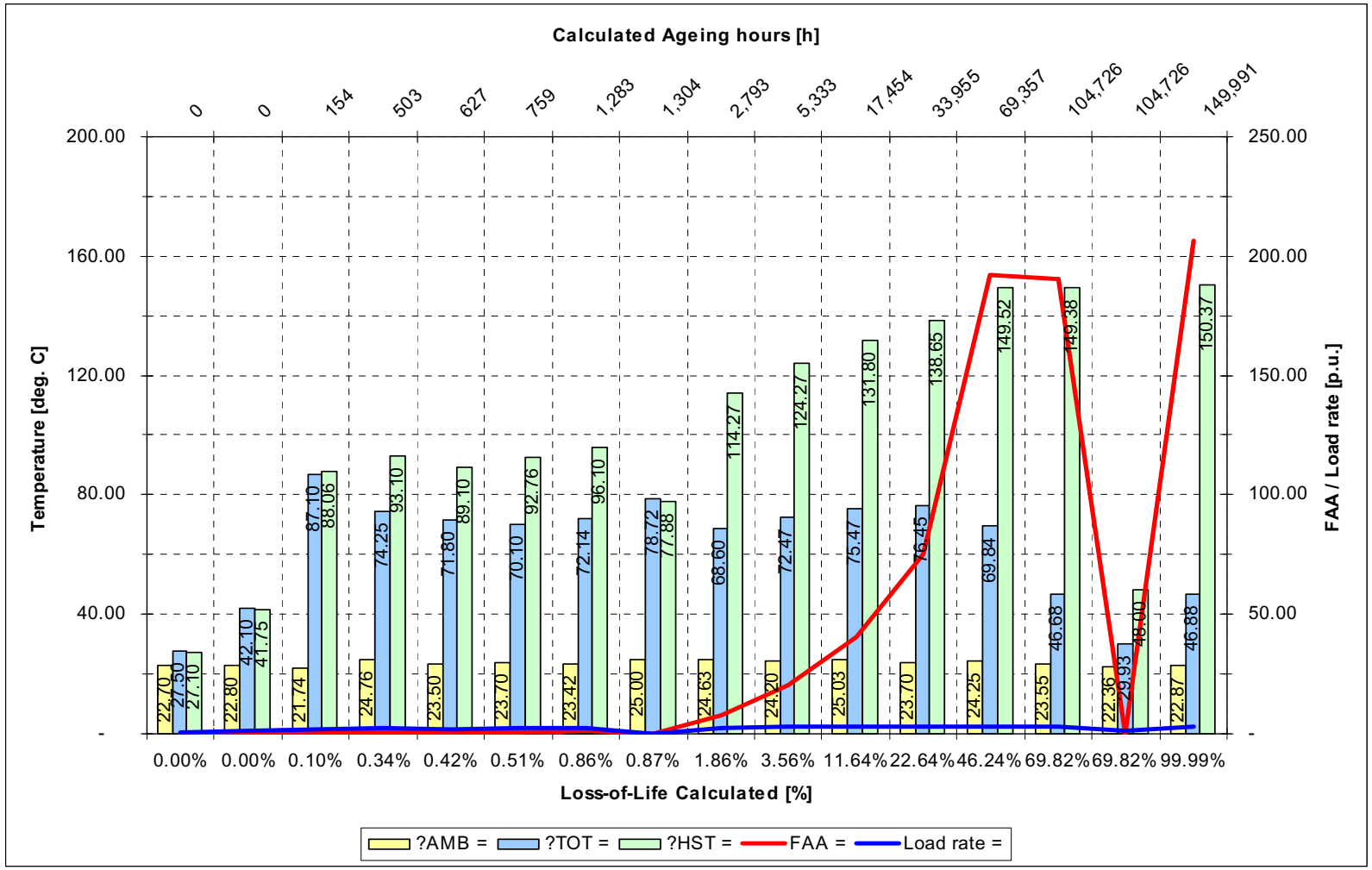

Fig. 162. Overall summary of the Accelerated Ageing Process applied on CT1 - Thermal Response

C.2. Thermal profile of the Ageing Process on CT3

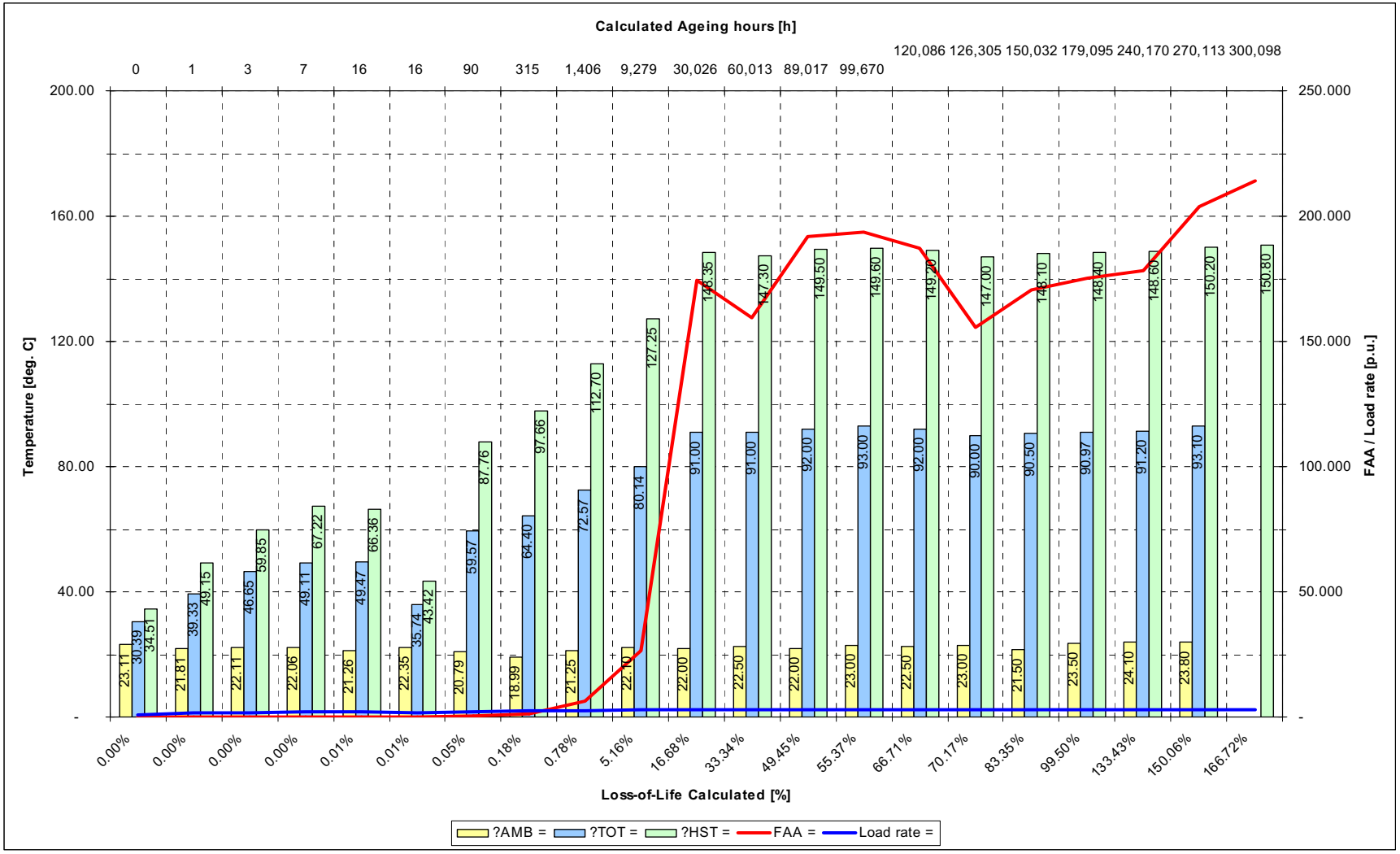

Fig. 163. Overall summary of the Accelerated Ageing Process applied on CT3 - Thermal Response

C.3. Thermal profile of the Ageing Process on CT4

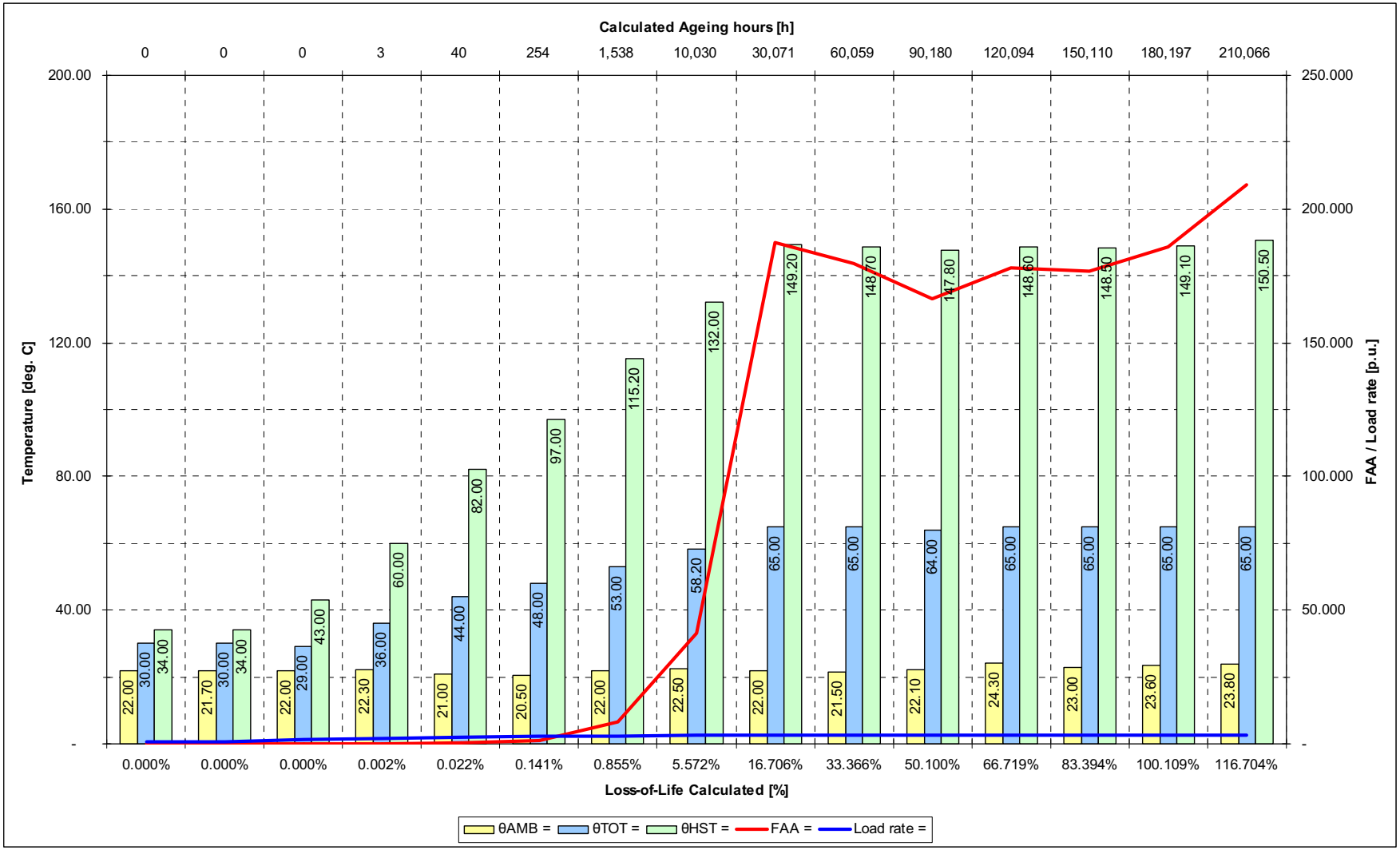

Fig. 164. Overall summary of the Accelerated Ageing Process applied on CT4 - Thermal Response CT

C.4. Functional Parameters – Data Trend of all CTs

Table 59. Functional Test Data of CT1 during Ageing Process

Ageing (h)	0.00	626.69	1,283.06	33,955.35	69,357.48	149,990.53
ANSI30 KP (V/V)	174.6	173.7	174.5	174.6	174.1	174.5
ANSI30 KP (I/mA)	67.39	65.7	67.37	67.32	67.19	67.63
Ratio	1200/4.9989	1200/5.0041	1200/5.0042	1200/5.0043	1200/5.0015	1200/5.0014
Deviation	-0.02%	0.08%	0.08%	0.09%	0.03%	0.03%
εc:	0.07%	0.09%	0.09%	0.09%	0.06%	0.06%
RCF	1.00023	0.99917	0.99916	0.99913	0.9997	0.99972
Phase (min)	2.23	0.73	0.75	0.73	1.67	1.63

Table 60. Functional Test Data of CT3 during Ageing Process

Ageing (h)	0.06	15.96	315.21	1,405.84	9,279.41	30,025.97	60,012.93	89,956.43	100,028.85	120,443.98	150,219.47	178,932.39
ANSI 30 KP (V/V)	194.4	195	195.1	195.3	195.3	195.4	195.5	195.4	195.5	195.3	195.6	195.4
ANSI 30 KP (I/mA)	65.44	65.44	65.62	65.89	65.77	65.38	65.67	65.32	65.49	65.4	65.3	65.41
Ratio	200 / 5.0017	200 / 4.9997	200 / 4.9995	200 / 4.9996	200 / 4.9996	200 / 4.9996	200 / 4.9996	200 / 4.9997	200 / 4.9996	200 / 4.9997	200 / 4.9996	200 / 4.9996
Deviation	0.03%	-0.01%	-0.01%	-0.01%	-0.01%	-0.01%	-0.01%	-0.01%	-0.01%	-0.01%	-0.01%	-0.01%
ε-c:	0.05%	0.05%	0.05%	0.05%	0.05%	0.05%	0.05%	0.05%	0.05%	0.05%	0.05%	0.05%
RCF	0.99966	1.00007	1.00009	1.00008	1.00009	1.00007	1.00008	1.00007	1.00007	1.00006	1.00007	1.00008
Phase (min)	1.18	1.56	1.55	1.56	1.53	1.56	1.57	1.53	1.54	1.51	1.53	1.55

Table 61. Functional Test Data of CT4 during ageing Process

Ageing (h)	0.03	0.26	0.47	254.07	1,538.34	10,030.02	30,070.57	60,058.57	90,179.60	120,093.72	150,109.5	180,196.9	210,066.3
ANSI30 KP (V/V)	194.1	194.3	194.1	194.5	195	194.8	195.2	195.2	195.2	195.3	195.1	195.2	195.1
ANSI30 KP (I/mA)	68.7	68.64	68.69	69.07	68.85	68.54	68.72	68.79	68.53	69.03	68.52	68.29	68.67
Ratio	200 / 5.0014	200 / 4.9990	200 / 4.9991	200 / 4.9991	200 / 4.9991	200 / 4.9992	200 / 4.9991	200 / 4.9991	200 / 4.9991	200 / 4.9991	200 / 4.9991	200 / 4.9991	200 / 4.9991
Deviation	0.03%	-0.02%	-0.02%	-0.02%	-0.02%	-0.02%	-0.02%	-0.02%	-0.02%	-0.02%	-0.02%	-0.02%	-0.02%
εc:	0.05%	0.06%	0.06%	0.06%	0.06%	0.06%	0.06%	0.06%	0.06%	0.06%	0.06%	0.06%	0.06%
RCF	0.99973	1.0002	1.00018	1.00019	1.00018	1.00017	1.00018	1.00019	1.00018	1.00019	1.00019	1.00019	1.00019
Phase (min)	1.42	1.91	1.91	1.91	1.89	1.89	1.91	1.93	1.89	1.88	1.93	1.89	1.91

APPENDIX D

D.1. DGA Recorded Data of the Ageing Process on CT1

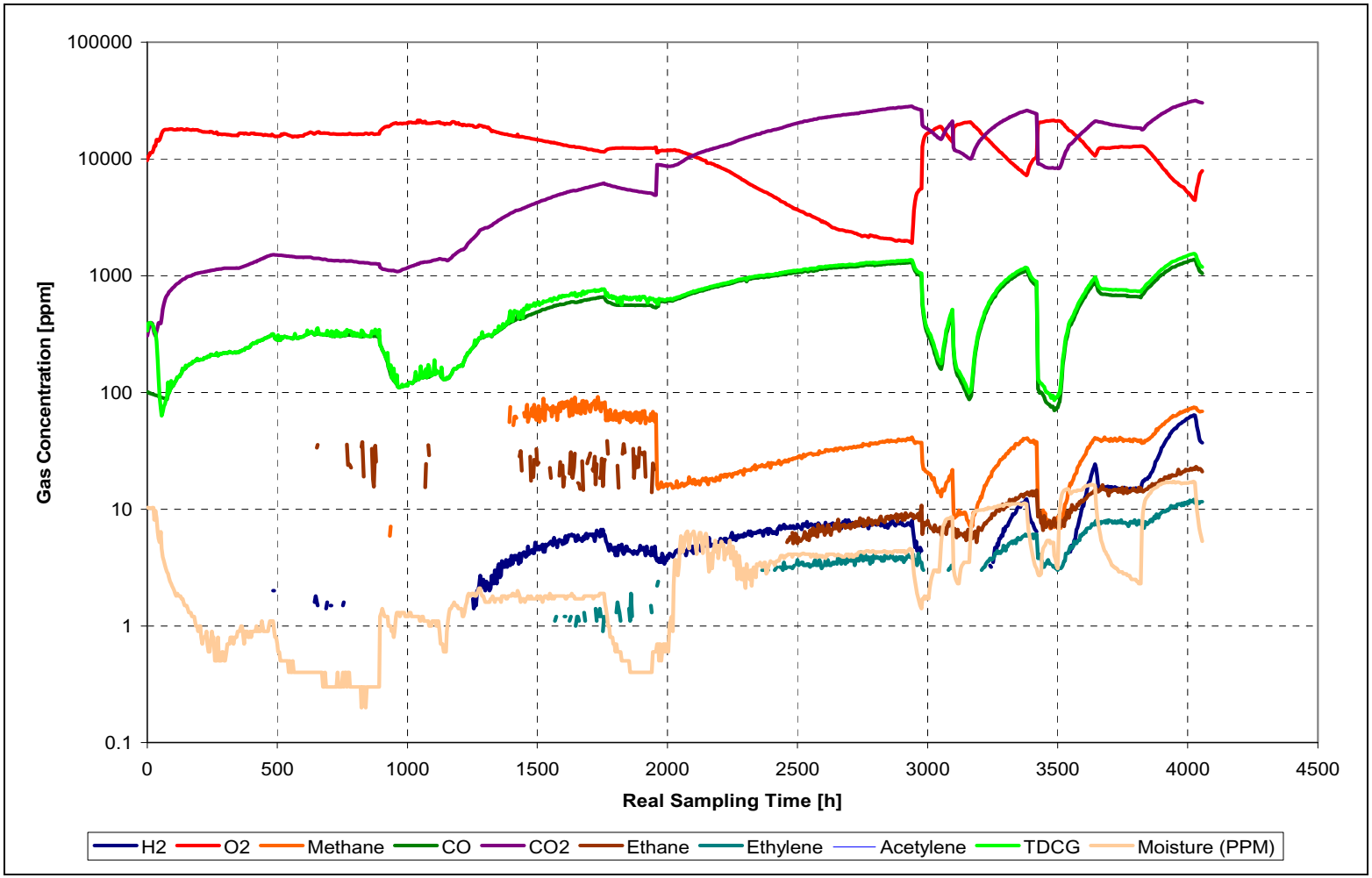

Fig. 165. Dynamic Gas Evolution in CT1 – Real Time Data

D.2. DGA Recorded Data of the Ageing Process on CT4

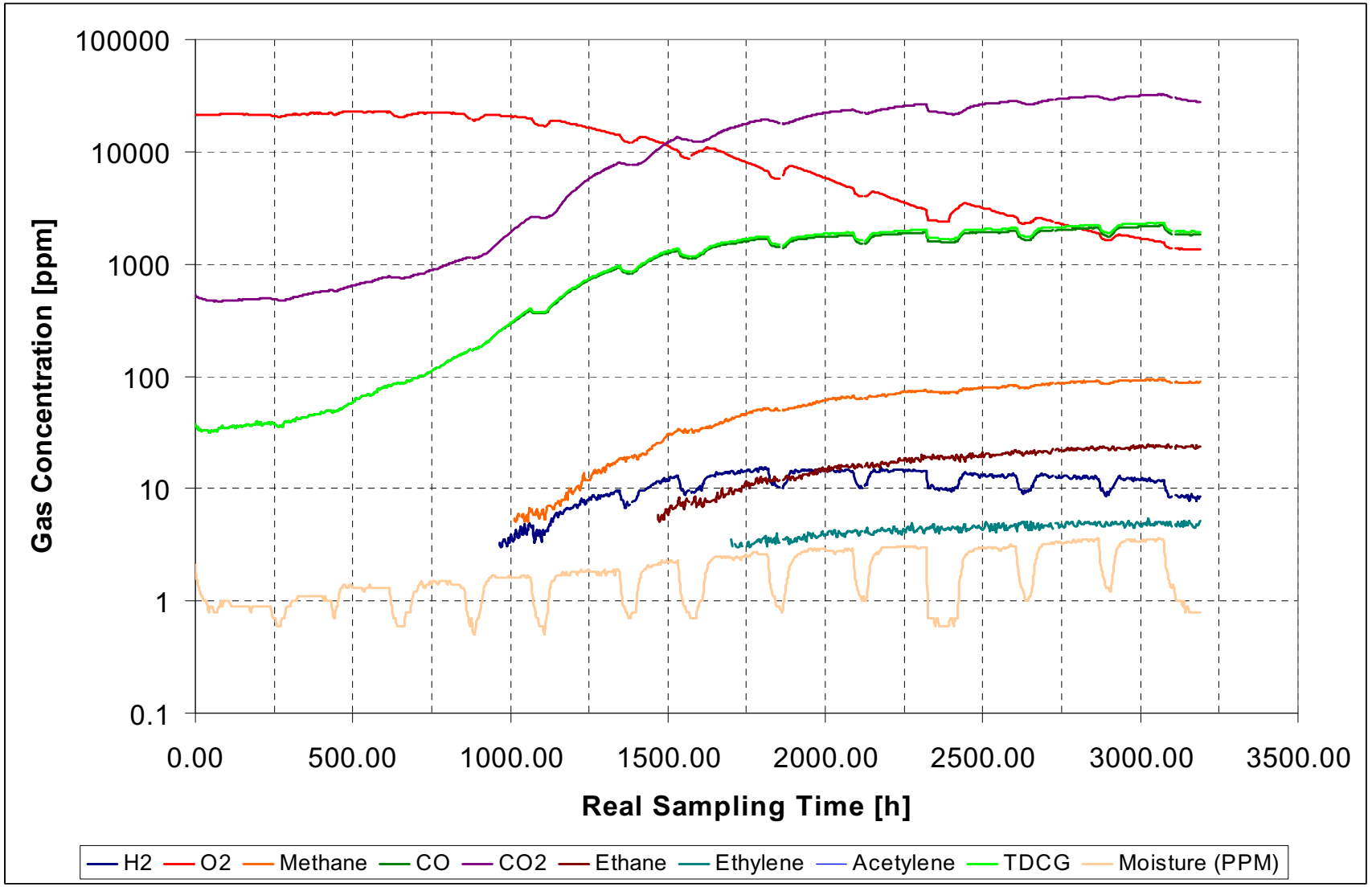

Fig. 166. Dynamic Gas Evolution in CT4 - Real Time Data

Table 62. DGA Log Book Data obtained from monitoring CT4

Ageing (h)	0.03	0.26	0.47	2.81	39.67	254.07	1,538.34	10,030.02	30,070.57	60,058.57	90,179.60	120,093.72	150,109.5	180,196.9	210,066.3
Oxygen	21100	21182.4	20390.2	21324.6	20372.2	19054	16890.6	12456.3	9885.9	5716.9	4008.6	2386.5	2317.6	1638.9	1373
Hydrogen	0	0	0	0	0	0	3.9	7.1	10	10.3	10.5	9.8	9.3	8.5	8.3
CO2	530	537.2	476.9	570.7	752.1	1127.5	2550.2	7783.2	12260.7	18079.2	22186.8	22103.1	26322.6	29604	29637.7
CO	37	37	35.7	47.9	86.8	174.5	364.6	837.8	1159.3	1417.2	1518.4	1570.6	1625.6	1790.7	1834.9
Methane	0	0	0	0	0	0	5.4	19.1	33.1	49.8	64.9	70.9	78.4	86.7	88.2
Ethane	0	0	0	0	0	0	0	0	6.9	12	16	19	20.7	23.4	23.6
Ethylene	0	0	0	0	0	0	0	0	0	3.3	4.2	4.3	4.5	5	4.8
Acetylene	0	0	0	0	0	0	0	0	0	0	0	0	0	0	0
KR#1	N/A	N/A	N/A	N/A	N/A	N/A	N/A	N/A	0.000	0.000	0.000	0.000	0.000	0.000	0.000
KR#2	N/A	N/A	N/A	N/A	N/A	N/A	0.722	0.372	0.302	0.207	0.162	0.138	0.119	0.098	0.094
KR#3	N/A	N/A	N/A	N/A	N/A	N/A	N/A	N/A	0.000	0.275	0.263	0.226	0.217	0.214	0.203
KR#4	14.324	14.519	13.359	11.914	8.665	6.461	6.995	9.290	10.576	12.757	14.612	14.073	16.193	16.532	16.152
KR#5	N/A	N/A	N/A	N/A	N/A	N/A	0.000	0.000	0.000	0.000	0.000	0.000	0.000	0.000	0.000
RR#1	0.000	0.000	0.000	0.000	0.000	0.000	1.385	2.690	3.310	4.835	6.181	7.235	8.430	10.200	10.627
RR#2	0.000	0.000	0.000	0.000	0.000	0.000	0.000	0.000	0.000	0.000	0.000	0.000	0.000	0.000	0.000
RR#3	0.000	0.000	0.000	0.000	0.000	0.000	0.000	0.000	0.000	0.275	0.263	0.226	0.217	0.214	0.203
KR#1 evaluation	N/A	N/A	N/A	N/A	N/A	N/A	N/A	N/A	OK	OK	OK	OK	OK	OK	OK
KR#2 evaluation	N/A	N/A	N/A	N/A	N/A	N/A	OK	OK	OK	OK	OK	OK	OK	OK	OK
KR#3 evaluation	N/A	N/A	N/A	N/A	N/A	N/A	N/A	N/A	OK	OK	OK	OK	OK	OK	OK
KR#4 evaluation	Overheating Cellulose	Overheating Cellulose	Overheating Cellulose	Overheating Cellulose	OK	OK	OK	OK	Overheating Cellulose	Overheating Cellulose	Overheating Cellulose	Overheating Cellulose	Overheating Cellulose	Overheating Cellulose	Overheating Cellulose
KR#5 evaluation	N/A	N/A	N/A	N/A	N/A	N/A	OK	OK	OK	OK	OK	OK	OK	OK	OK
RR - Case 0 - Normal	TRUE	TRUE	TRUE	TRUE	TRUE	TRUE	FALSE	FALSE	FALSE	FALSE	FALSE	FALSE	FALSE	FALSE	FALSE
RR - Case 1 - Low Energy Discharge	FALSE	FALSE	FALSE	FALSE	FALSE	FALSE	FALSE	FALSE	FALSE	FALSE	FALSE	FALSE	FALSE	FALSE	FALSE

RR - Case 2 - High Energy Discharge	FALSE	FALSE	FALSE	FALSE	FALSE	FALSE	FALSE	FALSE	FALSE	FALSE	FALSE	FALSE	FALSE	FALSE	FALSE
RR - Case 3 - Thermal Fault < 300C	FALSE	FALSE	FALSE	FALSE	FALSE	FALSE	Thermal Fault < 300	Thermal Fault < 300	Thermal Fault < 300	Thermal Fault < 300	Thermal Fault < 300	Thermal Fault < 300	Thermal Fault < 300	Thermal Fault < 300	Thermal Fault < 300
RR - Case 4 - Thermal Fault < 700C	FALSE	FALSE	FALSE	FALSE	FALSE	FALSE	FALSE	FALSE	FALSE	FALSE	FALSE	FALSE	FALSE	FALSE	FALSE
RR - Case 5 - Thermal Fault > 700C	FALSE	FALSE	FALSE	FALSE	FALSE	FALSE	FALSE	FALSE	FALSE	FALSE	FALSE	FALSE	FALSE	FALSE	FALSE

APPENDIX E

E.1. Correlation Analysis against Ageing for 1200:5 CTs

Table 63. 1200:5 CT - Results of the Correlation Analysis

	AGE	*IR*	*PI*	*MC*	*OC*	*PF*	*TD*	*KPV*	*KPI*	*RCF*	*CE*	*2FAL*	*DPE*
AGE	1.00												
IR	0.45	1.00											
PI	0.12	0.75	1.00										
MC	0.00	(0.73)	(0.57)	1.00									
OC	(0.25)	(0.38)	(0.81)	0.26	1.00								
PF	(0.44)	(0.56)	(0.15)	0.77	0.08	1.00							
TD	(0.44)	(0.56)	(0.15)	0.77	0.08	1.00	1.00						
KPV	0.16	0.47	0.79	(0.32)	(0.86)	(0.13)	(0.13)	1.00					
KPI	0.45	0.48	0.77	(0.27)	(0.96)	(0.21)	(0.21)	0.90	1.00				
RCF	0.22	0.82	0.71	(0.89)	(0.43)	(0.65)	(0.65)	0.30	0.42	1.00			
CE	(0.71)	(0.63)	(0.42)	0.51	0.40	0.65	0.65	(0.12)	(0.46)	(0.77)	1.00		
2FAL	**1.00**	0.43	(0.11)	0.08	0.37	(0.38)	(0.37)	(0.28)	0.59	0.16	(0.70)	1.00	
DPE	**(0.82)**	0.08	0.67	(0.28)	(0.80)	0.40	0.40	0.46	(0.12)	0.21	0.44	(0.78)	1.00

E.2. Correlation Analysis against Ageing for 200:5 CTs

Table 64. 200:5 CT – Results of the Correlation Analysis

	AGE	*IR*	*PI*	*MC*	*OC*	*PF*	*TD*	*KPV*	*KPI*	*RCF*	*CE*	*2FAL*	*DPE*	*O2*	*H2*	*CO2*	*CO*	*CH4 -Meth*	*C2H6 - Etha*	*C2H4 - Ethyl*	*C2H2 - Acet*
AGE	1.00																				
IR	-0.32	1.00																			
PI	-0.29	0.59	1.00																		
MC	0.26	-0.94	-0.65	1.00																	
OC	0.02	-0.41	-0.57	0.59	1.00																
PF	0.22	-0.50	-0.62	0.69	0.97	1.00															
TD	0.22	-0.50	-0.62	0.69	0.97	1.00	1.00														
KPV	0.51	-0.40	-0.45	0.56	0.40	0.57	0.57	1.00													
KPI	0.14	-0.03	-0.41	0.20	0.37	0.37	0.37	0.32	1.00												
RCF	0.26	-0.91	-0.45	0.80	0.51	0.54	0.54	0.31	0.00	1.00											
CE	0.01	-0.44	-0.33	0.32	0.52	0.43	0.43	-0.29	0.04	0.62	1.00										
2FAL	0.99	-0.35	-0.12	0.23	-0.13	0.09	0.09	0.43	-0.06	0.36	0.08	1.00									
DPE	-0.76	0.82	0.52	-0.73	-0.34	-0.54	-0.54	-0.70	-0.17	-0.84	-0.37	-0.75	1.00								
O2	-0.90	0.47	0.51	-0.78	-0.68	-0.79	-0.79	-0.88	-0.35	-0.39	-0.38	-0.90	0.90	1.00							
H2	0.69	-0.50	-0.70	0.87	0.88	0.93	0.93	0.94	0.39	0.39	0.40	0.59	-0.80	-0.93	1.00						
CO2	0.96	-0.40	-0.42	0.66	0.53	0.66	0.66	0.80	0.32	0.34	0.33	0.96	-0.85	-0.98	0.86	1.00					
CO	0.89	-0.47	-0.55	0.78	0.69	0.80	0.80	0.89	0.37	0.38	0.38	0.89	-0.89	-1.00	0.94	0.98	1.00				
CH4 - Meth	0.96	-0.39	-0.39	0.65	0.52	0.65	0.65	0.79	0.31	0.33	0.32	0.97	-0.85	-0.98	0.85	1.00	0.98	1.00			
C2H6 - Etha	0.98	-0.34	-0.28	0.57	0.42	0.57	0.57	0.74	0.27	0.30	0.28	0.98	-0.81	-0.95	0.79	0.98	0.94	0.99	1.00		
C2H4 - Ethyl	0.94	-0.32	-0.25	0.53	0.38	0.52	0.52	0.70	0.26	0.28	0.26	0.94	-0.78	-0.92	0.75	0.96	0.91	0.96	0.98	1.00	
C2H2 - Acet	#DIV/0!	#DIV/0!	#DIV/0!	#DIV/0!	#DIV/0!	#DIV/0!	#DIV/0!	#DIV/0!	#DIV/0!	#DIV/0!	#DIV/0!	#DIV/0!	#DIV/0!	#DIV/0!	#DIV/0!	#DIV/0!	#DIV/0!	#DIV/0!	#DIV/0!	#DIV/0!	1.00

E.3. Regression Analysis for 1200:5 CTs

E.3.1. Regression Analysis of DC Tests on 1200:5 CTs

Regression Statistics for Insulation Resistance 1200:5 CT	
Multiple R	0.451485406
R Square	0.203839072
Adjusted R Square	0.00479884
Standard Error	59198.83184
Observations	6

ANOVA

	Df	*SS*	*MS*	*F*	*Significance F*
Regression	1	3588994873	3588994873	1.0241099	0.368787074
Residual	4	14018006766	3504501691		
Total	5	17607001639			

	Coefficients	*Standard Error*	*t Stat*	*P-value*	*Lower 95%*	*Upper 95%*
Intercept	23341.19817	30721.85002	0.759758874	0.48971308	-61956.33193	108638.7283
IR	64.34389753	63.58198497	1.011983152	0.36878707	-112.1879934	240.8757885

Regression Statistics for Polarization Index 1200:5 CT	
Multiple R	0.121331355
R Square	0.014721298
Adjusted R Square	-0.231598378
Standard Error	65855.53076
Observations	6

ANOVA

	df	*SS*	*MS*	*F*	*Significance F*
Regression	1	259197913.8	259197913.8	0.05976501	0.818896045
Residual	4	17347803725	4336950931		
Total	5	17607001639			

	Coefficients	*Standard Error*	*t Stat*	*P-value*	*Lower 95%*	*Upper 95%*
Intercept	15322.10046	114517.212	0.133797358	0.90002448	-302628.6522	333272.8532
PI	14643.99204	59901.2641	0.244468831	0.81889604	-151668.5795	180956.5635

E.3.2. Regression Analysis of FDS Tests on 1200:5 CTs

Regression Statistics for Moisture Content 1200:5 CT	
Multiple R	0.000260455
R Square	6.78366E-08
Adjusted R Square	-0.249999915
Standard Error	66345.68645
Observations	6

ANOVA

	df	*SS*	*MS*	*F*	*Significance F*
Regression	1	1194.398388	1194.398388	2.7135E-07	0.999609318
Residual	4	17607000445	4401750111		
Total	5	17607001639			

	Coefficients	*Standard Error*	*t Stat*	*P-value*	*Lower 95%*	*Upper 95%*
Intercept	42498.63898	75803.50254	0.560642155	0.60495749	-167965.6246	252962.9026
MC	11.00895992	21134.13015	0.000520909	0.99960932	-58666.74325	58688.76117

Regression Statistics for Oil Conductivity 1200:5 CT	
Multiple R	0
R Square	0
Adjusted R Square	-0.2
Standard Error	59341.38798
Observations	6

ANOVA

	df	*SS*	*MS*	*F*	*Significance F*
Regression	1	0	0	0	1
Residual	5	17607001639	3521400328		
Total	6	17607001639			

	Coefficients	*Standard Error*	*t Stat*	*P-value*	*Lower 95%*	*Upper 95%*
Intercept	42535.519	24226.0202	1.755778236	0.13947998	-19739.44845	104810.4864
OC	0	0	65535	#NUM!	0	0

Regression Statistics for Power Factor 1200:5 CT	
Multiple R	0.436736069
R Square	0.190738394
Adjusted R Square	-0.011577007
Standard Error	59683.89737
Observations	6

ANOVA

	df	*SS*	*MS*	*F*	*Significance F*
Regression	1	3358331220	3358331220	0.94277743	0.386547064
Residual	4	14248670419	3562167605		
Total	5	17607001639			

	Coefficients	*Standard Error*	*t Stat*	*P-value*	*Lower 95%*	*Upper 95%*
Intercept	70392.96896	37640.85928	1.870121201	0.13481221	-34114.81053	174900.7484
PF	-30389.94541	31298.63024	-0.970967265	0.38654706	-117288.8741	56508.98331

Regression Statistics for tan-δ 1200:5 CT	
Multiple R	0.436239224
R Square	0.19030466
Adjusted R Square	-0.012119174
Standard Error	59699.88939
Observations	6

ANOVA

	df	*SS*	*MS*	*F*	*Significance F*
Regression	1	3350694469	3350694469	0.94012971	0.387150343
Residual	4	14256307170	3564076793		
Total	5	17607001639			

	Coefficients	*Standard Error*	*t Stat*	*P-value*	*Lower 95%*	*Upper 95%*
Intercept	70417.32729	37695.02493	1.868080136	0.13513089	-34240.84015	175075.4947
TD	-3037785.541	3133020.4	-0.96960286	0.38715034	-11736444.7	5660873.613

E.3.3. Regression Analysis of Furanic Concentration and Estimated DP on 1200:5 CTs

Regression Statistics for 2FAL Concentration 1200:5 CT	
Multiple R	0.99556028
R Square	0.991140271
Adjusted R Square	0.989874596
Standard Error	5431.703212
Observations	9

ANOVA

	df	*SS*	*MS*	*F*	*Significance F*
Regression	1	23103873732	23103873732	783.0919116	1.91164E-08
Residual	7	206523798.4	29503399.78		
Total	8	23310397531			

	Coefficients	*Standard Error*	*t Stat*	*P-value*	*Lower 95%*	*Upper 95%*
Intercept	4687.663779	2264.890334	2.069708943	0.077249938	-667.9508301	10043.27839
2FAL	23.63476345	0.844587969	27.98377944	1.91164E-08	21.63763025	25.63189664

Regression Statistics for Estimated DP 1200:5 CT	
Multiple R	0.818020803
R Square	0.669158034
Adjusted R Square	0.621894896
Standard Error	33192.20595
Observations	9

ANOVA

	df	*SS*	*MS*	*F*	*Significance F*
Regression	1	15598339781	15598339781	14.15813808	0.00704965
Residual	7	7712057749	1101722536		
Total	8	23310397531			

	Coefficients	*Standard Error*	*t Stat*	*P-value*	*Lower 95%*	*Upper 95%*
Intercept	119023.9016	23090.07374	5.1547649	0.001317053	64424.55331	173623.2499
DPE	-125.1042783	33.24827287	-3.762730136	0.00704965	-203.7239506	-46.484606

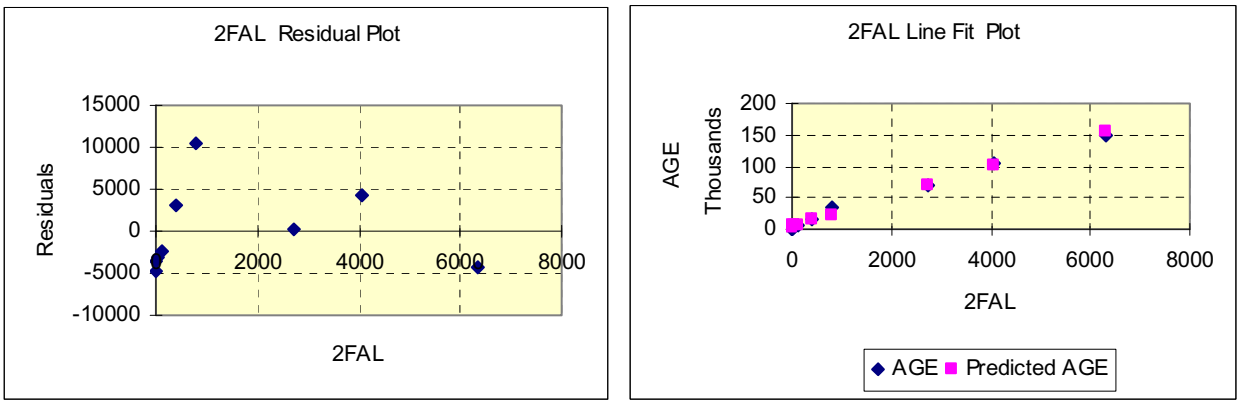

Fig. 167. a. Residual plot and b. Line Fit Plot for 2FAL of 1200:5 CT

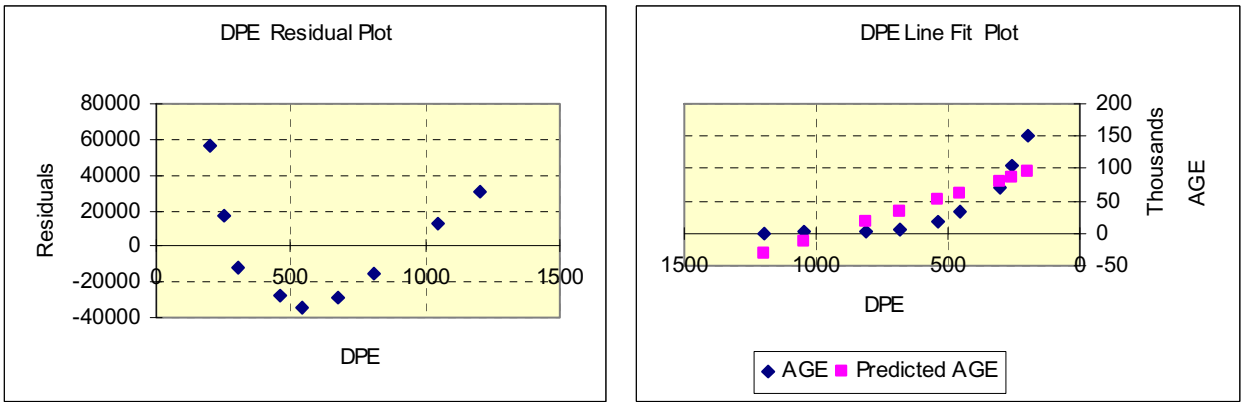

Fig. 168. a. Residual plot and b. Line Fit Plot for Estimated DP of 1200:5 CT

E.4. Regression Analysis for 200:5 CTs

E.4.1. Regression Analysis of DC Tests on 1200:5 CTs

Regression Statistics for Insulation Resistance 200:5 CTs	
Multiple R	0.31710926
R Square	0.10055828
Adjusted R Square	0.06308154
Standard Error	79872.7797
Observations	26

ANOVA

	df	*SS*	*MS*	*F*	*Significance F*
Regression	1	17118024808	17118024808	2.683218587	0.114456435
Residual	24	1.53112E+11	6379660939		
Total	25	1.7023E+11			

	Coefficients	*Standard Error*	*t Stat*	*P-value*	*Lower 95%*	*Upper 95%*
Intercept	87492.7128	18063.11667	4.843721842	6.17969E-05	50212.27252	124773.153
IR	-69.836183	42.63364556	-1.638053292	0.114456435	-157.8277026	18.15533569

Regression Statistics for Polarization Index 200:5 CT	
Multiple R	0.294017
R Square	0.086446
Adjusted R Square	0.048381
Standard Error	80496.96
Observations	26

ANOVA

	df	*SS*	*MS*	*F*	*Significance F*
Regression	1	14715644826	14715644826	2.271017	0.144864175
Residual	24	1.55514E+11	6479760105		
Total	25	1.7023E+11			

	Coefficients	*Standard Error*	*t Stat*	*P-value*	*Lower 95%*	*Upper 95%*
Intercept	224058.6	101632.194	2.204602179	0.037313	14300.01875	433817.094
PI	-85620.4	56815.51423	-1.506989356	0.144864	-202881.8325	31641.0821

E.4.2. Regression Analysis of FDS Tests on 200:5 CTs

Regression Statistics for Moisture Content 200:5 CT	
Multiple R	0.258594084
R Square	0.0668709
Adjusted R Square	0.02630007
Standard Error	83036.97095
Observations	25

ANOVA

	df	*SS*	*MS*	*F*	*Significance F*
Regression	1	11364917079	11364917079	1.648250721	0.211980724
Residual	23	1.58588E+11	6895138545		
Total	24	1.69953E+11			

	Coefficients	*Standard Error*	*t Stat*	*P-value*	*Lower 95%*	*Upper 95%*
Intercept	-26510.98904	78591.10354	-0.337328118	0.738928663	-189089.0726	136067.0945
MC	32612.46899	25402.24158	1.283842171	0.211980724	-19936.07108	85161.00907

Regression Statistics for Oil Conductivity 200:5 CT	
Multiple R	1.34002E-08
R Square	1.79565E-16
Adjusted R Square	-0.041666667
Standard Error	84150.93177
Observations	25

ANOVA

	df	*SS*	*MS*	*F*	*Significance F*
Regression	1	3.05E-05	3.05176E-05	0	1
Residual	24	1.7E+11	7081379318		
Total	25	1.7E+11			

	Coefficients	*Standard Error*	*t Stat*	*P-value*	*Lower 95%*	*Upper 95%*
Intercept	72109.1172	16830.19	4.284510919	0.00025619	37373.32003	106844.9144
OC	0	0	65535	#NUM!	0	0

Regression Statistics Power Factor 200:5 CT	
Multiple R	0.21890596
R Square	0.047919819
Adjusted R Square	0.006525029
Standard Error	83875.93882
Observations	25

ANOVA

	df	*SS*	*MS*	*F*	*Significance F*
Regression	1	8144122027	8.14E+09	1.157629229	0.293114988
Residual	23	1.61809E+11	7.04E+09		
Total	24	1.69953E+11			

	Coefficients	*Standard Error*	*t Stat*	*P-value*	*Lower 95%*	*Upper 95%*
Intercept	17824.96554	53168.85918	0.335252	0.740473611	-92163.19902	127813.1301
PF	122151.5564	113530.9477	1.075932	0.293114988	-112705.1012	357008.214

Regression Statistics tan-δ 200:5 CT	
Multiple R	0.220205675
R Square	0.048490539
Adjusted R Square	0.007120563
Standard Error	83850.79553
Observations	25

ANOVA

	df	*SS*	*MS*	*F*	*Significance F*
Regression	1	8241117677	8241117677	1.172119095	0.290186522
Residual	23	1.61712E+11	7030955911		
Total	24	1.69953E+11			

	Coefficients	*Standard Error*	*t Stat*	*P-value*	*Lower 95%*	*Upper 95%*
Intercept	17624.13741	53046.46207	0.332239639	0.742717222	-92110.82943	127359.1042
TD	12271391.84	11334645.81	1.082644491	0.290186522	-11176109.33	35718893.02

E.4.3. Regression Analysis of Furanic Concentration and Estimated DP on 200:5 CTs

Regression Statistics for 2FAL of 200:5 CT	
Multiple R	0.989034306
R Square	0.978188858
Adjusted R Square	0.977197442
Standard Error	14361.56277
Observations	24

ANOVA

	df	*SS*	*MS*	*F*	*Significance F*
Regression	1	2.03503E+11	2.03503E+11	986.6587647	9.02909E-20
Residual	22	4537598673	206254485.2		
Total	23	2.0804E+11			

	Coefficients	*Standard Error*	*t Stat*	*P-value*	*Lower 95%*	*Upper 95%*
Intercept	5267.71486	4112.38844	1.280938057	0.213554586	-3260.856732	13796.28645
2FAL	69.21705289	2.203584023	31.41112486	9.02909E-20	64.64709935	73.78700643

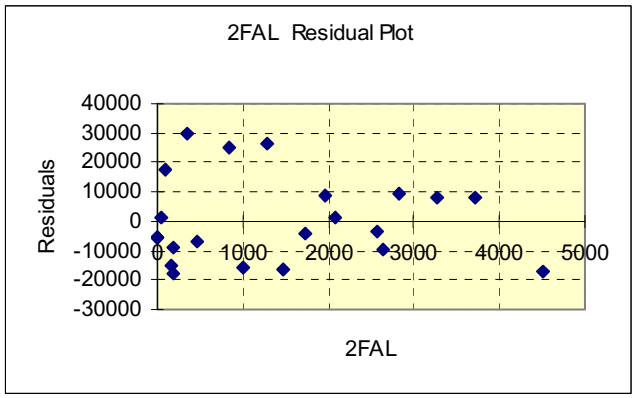

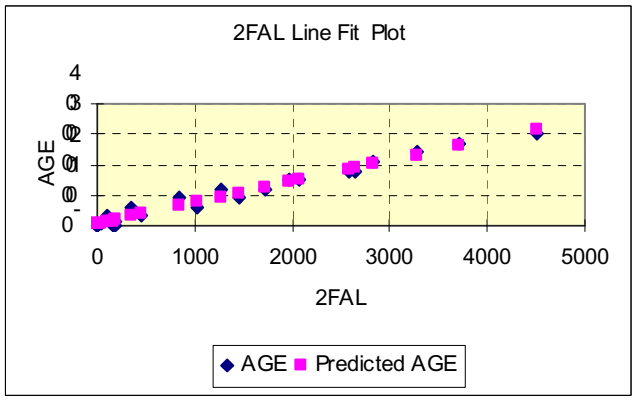

Fig. 169. a. Residual Plot and b. Line Fit Plot for 2FAL concentration data of 200:5 CTs

Regression Statistics for DPE of 200:5 CT	
Multiple R	0.762154
R Square	0.580879
Adjusted R Square	0.561828
Standard Error	62955.26
Observations	24

ANOVA

	df	*SS*	*MS*	*F*	*Significance F*
Regression	1	1.20846E+11	1.20846E+11	30.49085	1.50391E-05
Residual	22	87194024379	3963364744		
Total	23	2.0804E+11			

	Coefficients	*Standard Error*	*t Stat*	*P-value*	*Lower 95%*	*Upper 95%*
Intercept	218618.3	25678.38182	8.513709339	2.07E-08	165364.5749	271871.983
DPE	-211.047	38.22032463	-5.521852271	1.5E-05	-290.3110879	-131.782885

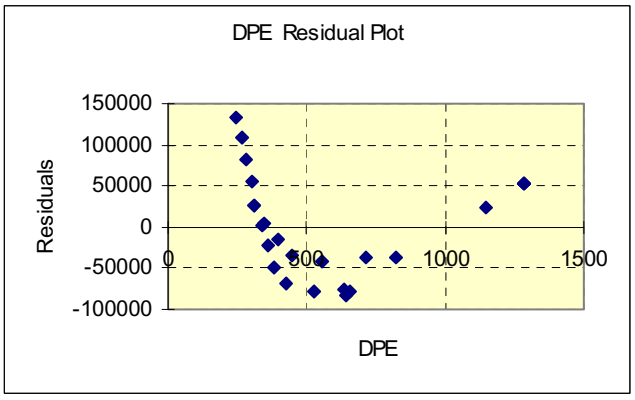

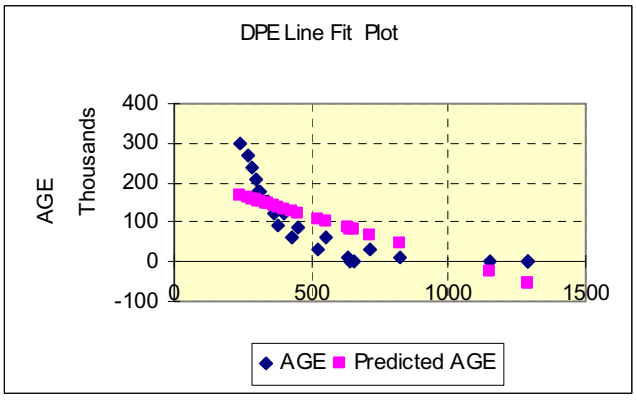

Fig. 170. a. Residual Plot and b. Line Fit Plot for Estimated DP data of 200:5 CTs

E.4.4. Regression Analysis of DGA data on 200:5 CTs

Regression Statistics for O_2 of 200:5 CT	
Multiple R	0.89874599
R Square	0.807744355
Adjusted R Square	0.792955459
Standard Error	33927.64116
Observations	15

ANOVA

	df	*SS*	*MS*	*F*	*Significance F*
Regression	1	62870297475	62870297475	54.61830055	5.26662E-06
Residual	13	14964102855	1151084835		
Total	14	77834400330			

	Coefficients	*Standard Error*	*t Stat*	*P-value*	*Lower 95%*	*Upper 95%*
Intercept	152877.0986	15671.45445	9.755131477	2.39707E-07	119020.9797	186733.2
O2	-7.998522742	1.08228264	-7.390419511	5.26662E-06	-10.33665223	-5.66039

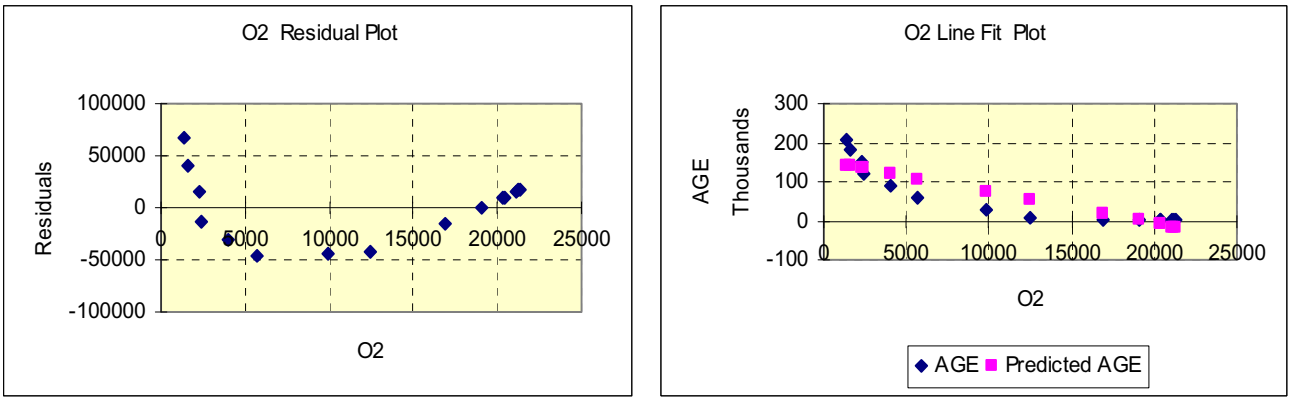

Fig. 171. a. Residual Plot and b. Line Fit Plot for Oxygen Concentration data of 200:5 CTs

Regression Statistics for CO_2 of 200:5 CTs	
Multiple R	0.957652905
R Square	0.917099087
Adjusted R Square	0.910722093
Standard Error	22278.9015
Observations	15

ANOVA

	df	*SS*	*MS*	*F*	*Significance F*
Regression	1	71381857455	71381857455	143.8137127	2.10605E-08
Residual	13	6452542875	496349451.9		
Total	14	77834400330			

	Coefficients	*Standard Error*	*t Stat*	*P-value*	*Lower 95%*	*Upper 95%*
Intercept	-13638.5978	8223.867222	-1.65841658	0.121152918	-31405.18274	4127.98715
CO2	6.057806481	0.505144055	11.99223552	2.10605E-08	4.966509099	7.14910386

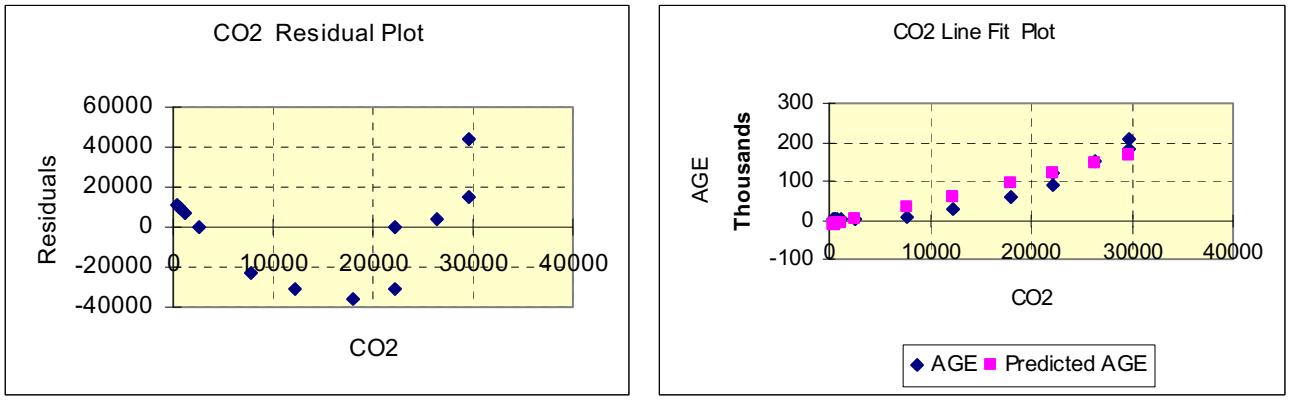

Fig. 172. a. Residual Plot and b. Line Fit Plot for Carbon Dioxide Concentration data of 200:5 CTs

Regression Statistics for CO of 200:5 CTs	
Multiple R	0.894130703
R Square	0.799469714
Adjusted R Square	0.784044307
Standard Error	34650.0689
Observations	15

ANOVA

	df	*SS*	*MS*	*F*	*Significance F*
Regression	1	62226245754	62226245754	51.82811273	6.95628E-06
Residual	13	15608154576	1200627275		
Total	14	77834400330			

	Coefficients	*Standard Error*	*t Stat*	*P-value*	*Lower 95%*	*Upper 95%*
Intercept	-18104.9235	13726.69657	-1.31895707	0.209945541	-47759.64851	11549.80143
CO	89.66460226	12.45484505	7.199174448	6.95628E-06	62.75754544	116.5716591

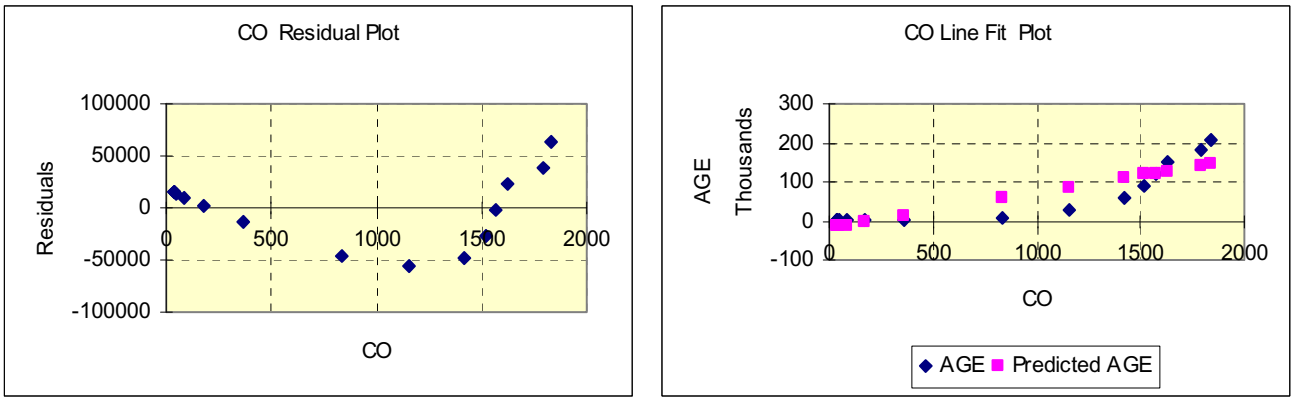

Fig. 173. a. Residual Plot and b. Line Fit Plot for Carbon Monoxide Concentration data of 200:5 CTs

Regression Statistics for H_2 of 200:5 CTs	
Multiple R	0.69478305
R Square	0.48272349
Adjusted R Square	0.44293299
Standard Error	55651.323
Observations	15

ANOVA

	df	*SS*	*MS*	*F*	*Significance F*
Regression	1	37572493520	37572493520	12.1316265	0.004043389
Residual	13	40261906810	3097069755		
Total	14	77834400330			

	Coefficients	*Standard Error*	*t Stat*	*P-value*	*Lower 95%*	*Upper 95%*
Intercept	-825.987137	21922.69258	-0.037677267	0.970517441	-48187.08496	46535.11
H2	11132.9567	3196.32554	3.48304845	0.004043389	4227.715219	18038.2

Regression Statistics for CH_4 of 200:5 CTs	
Multiple R	0.962698718
R Square	0.926788821
Adjusted R Square	0.921157192
Standard Error	20936.43902
Observations	15

ANOVA

	df	*SS*	*MS*	*F*	*Significance F*
Regression	1	72136052103	72136052103	164.5685101	9.346E-09
Residual	13	5698348226	438334478.9		
Total	14	77834400330			

	Coefficients	*Standard Error*	*t Stat*	*P-value*	*Lower 95%*	*Upper 95%*
Intercept	-9023.983902	7455.515839	-1.210376867	0.247682159	-25130.64661	7082.679
CH4 -Meth	1989.930893	155.1188677	12.82842586	9.346E-09	1654.816954	2325.045

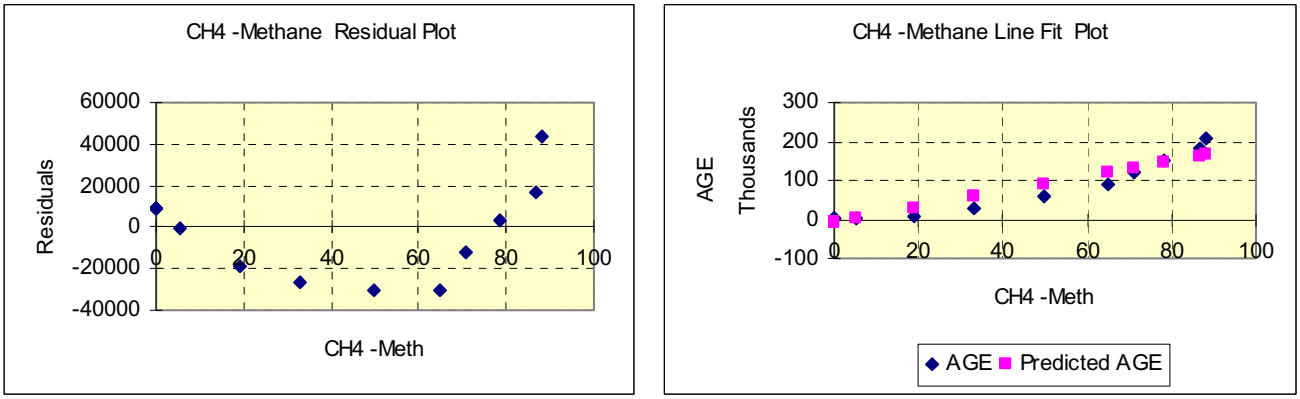

Fig. 174. a. Residual Plot and b. Line Fit Plot for Methane Concentration data of 200:5 CTs

Regression Statistics for C_2H_6 of 200:5 CTs	
Multiple R	0.97560038
R Square	0.9517961
Adjusted R Square	0.94808811
Standard Error	16988.5059
Observations	15

ANOVA

	df	*SS*	*MS*	*F*	*Significance F*
Regression	1	74082478995	74082478995	256.687745	6.10845E-10
Residual	13	3751921335	288609333.4		
Total	14	77834400330			

	Coefficients	*Standard Error*	*t Stat*	*P-value*	*Lower 95%*	*Upper 95%*
Intercept	-3080.38245	5764.505393	-0.534370643	0.602104656	-15533.8392	9373.074
C2H6 - Etha	7391.83114	461.3701257	16.02147762	6.10845E-10	6395.101585	8388.561

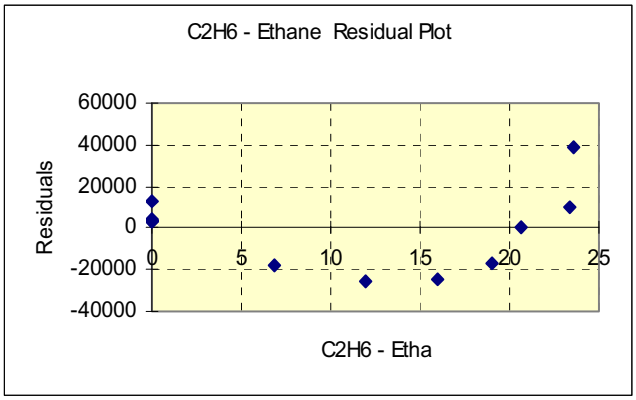

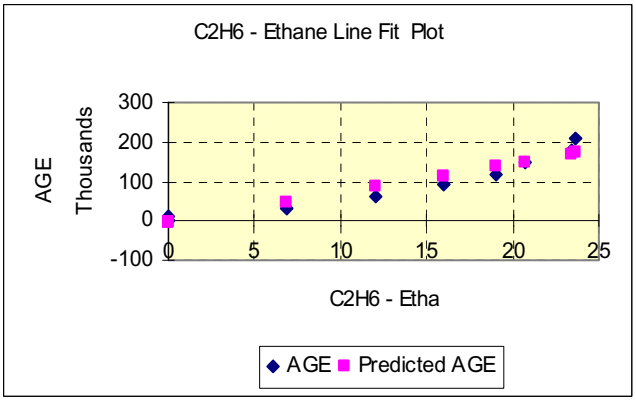

Fig. 175. a. Residual Plot and b. Line Fit Plot for Ethane Concentration data of 200:5 CTs

Regression Statistics for C_2H_4 of 200:5 CTs	
Multiple R	0.940879043
R Square	0.885253374
Adjusted R Square	0.876426711
Standard Error	26211.02939
Observations	15

ANOVA

	df	*SS*	*MS*	*F*	*Significance F*
Regression	1	68903165526	68903165526	100.2930918	1.76895E-07
Residual	13	8931234803	687018061.8		
Total	14	77834400330			

	Coefficients	*Standard Error*	*t Stat*	*P-value*	*Lower 95%*	*Upper 95%*
Intercept	2211.285368	8692.521482	0.254389405	0.803174315	-16567.76555	20990.3363
C2H4 - Ethyl	31397.38121	3135.147053	10.01464387	1.76895E-07	24624.30779	38170.4546

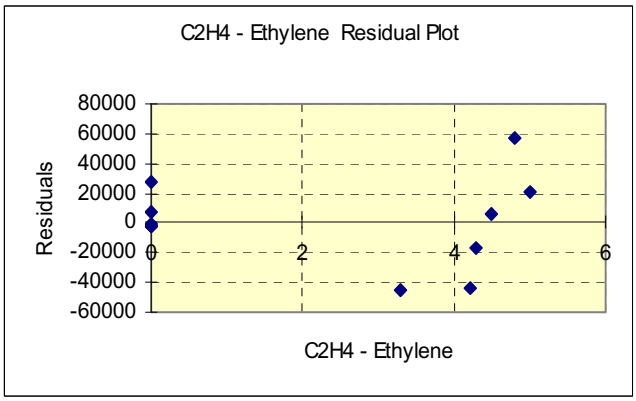

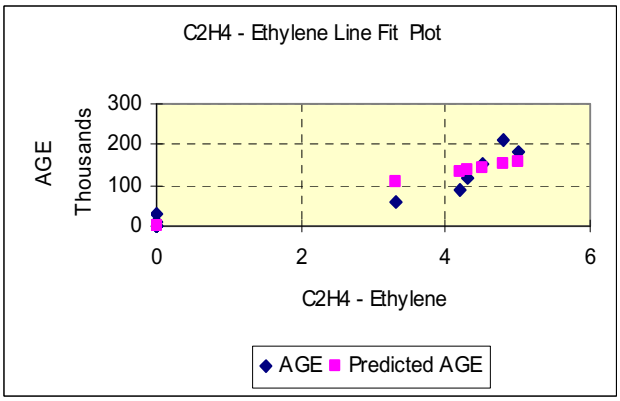

Fig. 176. a. Residual Plot and b. Line Fit Plot for Ethylene Concentration data of 200:5 CTs

VITA

Diego M. Robalino Vanegas was born in Quito, Ecuador, on May 23, 1970. He received his Bachelor's and Master of Science Degree in Electrical Engineering from the Kriviy Rig Technical University, Ukraine, in 1996. He received the degree of Project Management Specialist from Universidad San Francisco de Quito in 2004. Since 1996, he exercised electrical engineering practice in Ecuador as independent contractor for local utilities and worked as Academic Planning Director for "Escuela Politecnica Javeriana del Ecuador." Since 1998, he worked for IISA del Ecuador as Operations Manager supervising all maintenance and construction operation for the Oil & Gas industry. From 2001, he was hired as Project Electrical Engineer for the Major Projects Division of EnCana and AEC Ecuador developing the Oil & Gas Industry in the Ecuadorian rain forest. He was responsible for the overall design, construction, commissioning, and start-up of complex electromechanical projects, including Oil Batteries, Storage Facilities, Water Injection Systems, Wellpad Electrification, HV/MV/LV Distribution, and Power Generation Systems. Mr. Robalino is a Registered Professional Electrical Engineer in Ecuador (CIEEPI), certified Project Management Professional with the PMI and member of international professional societies (IEEE, SHPE, ASTM, PMI). He entered Tennessee Technological University in August 2006. Together with other graduate students form the Electrical and Computer Engineering (ECE) Department, he founded the first Graduate Electrical and Computer Engineering Student Association (GECESA) at Tennessee Technological University and served as Vice-President from 2008 to 2009. Diego is a candidate for the Doctor of Philosophy Degree in Engineering.